

ANGEWANDTE CHEMIE

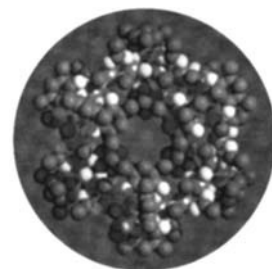
A Journal of the
Gesellschaft
Deutscher Chemiker

International Edition in English

1997
36/24
Page 2699–2914

COVER PICTURE

The cover picture might resemble a Christmas decoration, as one can expect at this time of the year, but is in fact a space-filling model of the structure of an octadecairon(III) complex that shows idealized D_{3d} symmetry. Cyclic molecules have always fascinated chemists—see for example the Highlight on p. 348 in issue 4 of this year—and there are many molecular counterparts of everyday ring-shaped objects. Multinuclear macrocyclic transition metal complexes can have interesting characteristics. Antiferromagnetic interactions occur between the 18 high-spin iron(III) centers in the molecular 18-wheeler shown in the cover picture. More on the largest known ring-shaped iron(III) compound is reported by S. J. Lippard et al. on p. 2774 ff (computer graphics: Felice Frankel, Massachusetts Institute of Technology).

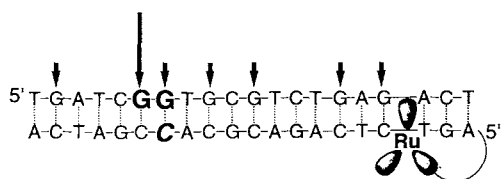


REVIEWS

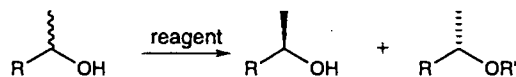
Electron transfer between intercalators bound to DNA are remarkably efficient and point to the double helix as a unique matrix which facilitates chemistry from a distance. When the stacked DNA bases not only mediate electron transfer but also serve as reactants, selective oxidative damage at guanine bases (see below) and repair of lesions in thymine dimers may be promoted from a remote site.

R. E. Holmlin, P. J. Dandliker,
J. K. Barton * 2715–2730

Charge Transfer through the DNA Base
Stack



Selectivities that begin to rival those obtained by traditional enzymatic methods are achieved in some recently developed nonenzymatic techniques for the kinetic resolution of secondary alcohols (see scheme below). The most promising approaches are surveyed.



P. Somfai * 2731–2733

Nonenzymatic Kinetic Resolution of Secondary Alcohols

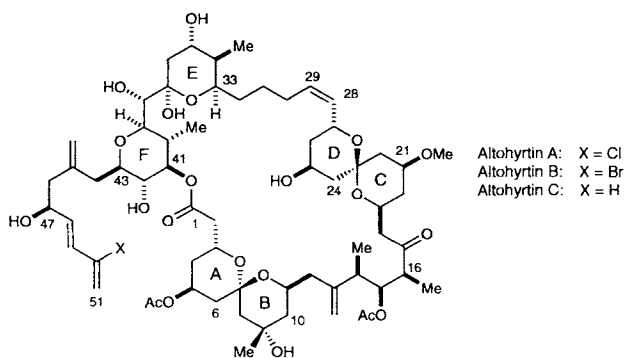
For the development of molecule-based switching devices, cobalt and manganese complexes of 1,2-benzoquinone ligands are of great interest. These compounds have electronically labile ground states, which leads to phenomena such as mixed valency, spin crossover, and valence tautomerism. Recently, the electronic behavior of these complexes was investigated carefully, and there are indications that complexes that show such characteristics can also be obtained with other metals.

P. Gülich,* A. Dei 2734–2736

Valence Tautomeric Interconversion in Transition Metal 1,2-Benzoquinone Complexes

COMMUNICATIONS

The first total synthesis of a spongipyran macrolide, altohyrtin C (spongistatin 2; see picture below), has been realized. The spongipyrans derived from marine sponges are among the most potent cytotoxic compounds yet isolated, and exhibit subnanomolar activities against a variety of human cancer cell lines. While the structures proposed for the independently isolated altohyrtins and spongistatins are largely homologous, they differ significantly with regard to internal stereochemical relationships. This discrepancy has been resolved by the total synthesis, which verifies the altohyrtin structural assignment and establishes the identity of altohyrtin C and the independently isolated spongistatin 2.



D. A. Evans,* P. J. Coleman,
L. C. Dias 2738–2741

Enantioselective Synthesis of Altohyrtin C (Spongistatin 2): Synthesis of the AB- and CD-Spiroketal Subunits

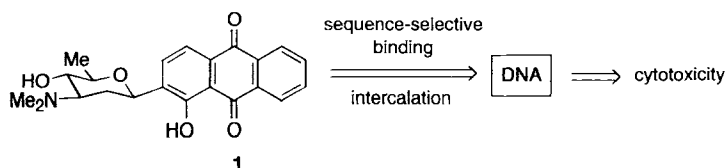
D. A. Evans,* B. W. Trotter, B. Côté,
P. J. Coleman 2741–2744

Enantioselective Synthesis of Altohyrtin C (Spongistatin 2): Synthesis of the EF-Bis(pyran) Subunit

D. A. Evans,* B. W. Trotter, B. Côté,
P. J. Coleman, L. C. Dias,
A. N. Tyler 2744–2747

Enantioselective Synthesis of Altohyrtin C (Spongistatin 2): Fragment Assembly and Revision of the Spongistatin 2 Stereochemical Assignment

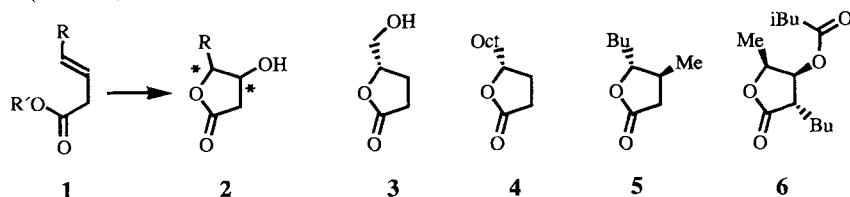
Intercalation and sequence selectivity characterize the binding of the anthraquinone-carbohydrate hybrid **1** to DNA. Important for this binding and for the cytotoxicity of **1** is the hybrid structure, which is based on that of several natural antitumor antibiotics. The enantiomer of **1** is about six times less cytotoxic because of its distinctly reduced intercalation potential.



K. Toshima,* H. Ouchi, Y. Okazaki,
T. Kano, M. Moriguchi, A. Asai,
S. Matsumura 2748–2750

Artificial Anthraquinone-Carbohydrate Hybrids: Design, Synthesis, DNA Binding, and Cytotoxicity

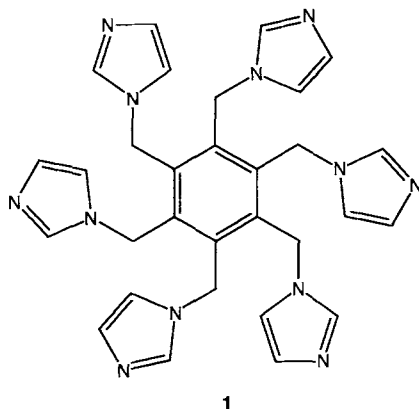
Deconjugated esters 1 and AD mix α or AD mix β give cis-configured γ -alkyl- β -hydroxy- γ -lactones **2**. They are versatile precursors for γ -chiral butenolides and γ -chiral butyrolactones of moderate to high enantiomeric purity, as shown through their conversion into the natural products **3** (92% ee), **4** (95% ee), **5** (97% ee), and **6** (78% ee).



C. Harcken, R. Brückner* . 2750–2752

Synthesis of Optically Active Butenolides and γ -Lactones by the Sharpless Asymmetric Dihydroxylation of β,γ -Unsaturated Carboxylic Esters

The new ligand hexakis(imidazol-1-ylmethyl)benzene (hkimb, 1) forms a heavily hydrated coordination polymer with CdF_2 of composition $\text{Cd}(\text{hkimb})\text{F}_2 \cdot 14\text{H}_2\text{O}$. A unique aspect of the structure is that the water assembles itself into two independent and different hydrogen-bonded 2D networks, which interweave throughout the 3D α -Po-related coordination polymer network.

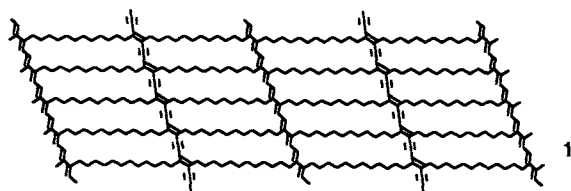


B. F. Hoskins, R. Robson,*

D. A. Slizys 2752–2755

A Hexaimidazole Ligand Binding Six Octahedral Metal Ions To Give an Infinite 3D α -Po-Like Network Through Which Two Independent 2D Hydrogen-Bonded Networks Interweave

Fused parallelogrammic rings sharing all sides are seen in the structure of **1** (shown below). This atomic cloth was prepared by photopolymerizing alkate-trayne molecules that were vapor-deposited and laid flat on graphite. The structural fit between the atomic cloth and the substrate, observed by scanning tunneling microscopy, enables one to determine the unit mesh.

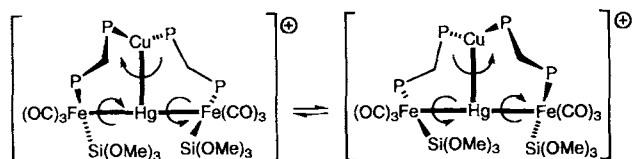


T. Takami,* H. Ozaki,* M. Kasuga,
T. Tsuchiya, Y. Mazaki, D. Fukushi,
A. Ogawa, M. Uda,

M. Aono 2755–2757

Periodic Structure of a Single Sheet of a Clothlike Macromolecule (Atomic Cloth) Studied by Scanning Tunneling Microscopy

A ten-membered heterometallic ring complex with a T-shaped CuHgFe_2 framework is the result of a bonding Cu – Hg interaction (Cu – Hg 2.668(6) Å). In solution this complex exhibits a motion comparable to a “molecular torsion pendulum” (shown schematically below), which generates an average mirror plane containing the four metal atoms; in the solid state only a C_2 axis is present.



M. Beynard, U. Bodensieck,
P. Braunstein,* M. Knorr, M. Strampfer,
C. Strohmann 2758–2761

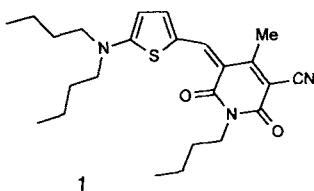
Conformation Control in Polymetallic Mesocycles by Metal–Metal Bonding: The First Example of an Hg – Cu Interaction

Theoretical computations give new insights into the energetic, geometric, and magnetic properties of highly reactive *o*-benzyne. Comparisons with experimental NMR data for the species trapped in a hemiacerand agree best for the geometry optimized at the Becke3LYP/6-311 + G** density functional level, which has more acetylenic (cyclohexa-3,5-dienyne) than cumulenic character.

H. Jiao, P. von R. Schleyer,* B. R. Beno, K. N. Houk,* R. Warmuth* 2761–2764

Theoretical Studies of the Structure, Aromaticity, and Magnetic Properties of *o*-Benzyne

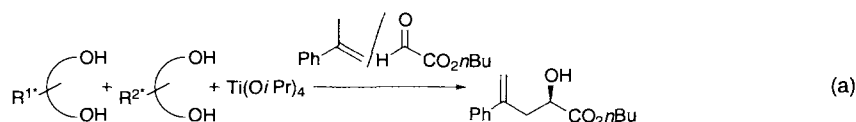
By tuning the donor–acceptor strength in heterocyclic methine dyes such as **1**, the cyanine limit was accessible. Despite almost vanishing second-order polarizabilities (β) this new class of chromophores sets a new hallmark for photorefractive applications. With a dye content of only 20% complete diffraction of the readout beam is achieved at a wavelength of 790 nm and a field strength of 68 V μm^{-1} .



F. Würthner,* R. Wortmann,* R. Matschiner, K. Lukaszuk, K. Meerholz,* Y. DeNardin, R. Bittner, C. Bräuchle, R. Sens 2765–2768

Merocyanine Dyes in the Cyanine Limit: A New Class of Chromophores for Photorefractive Materials

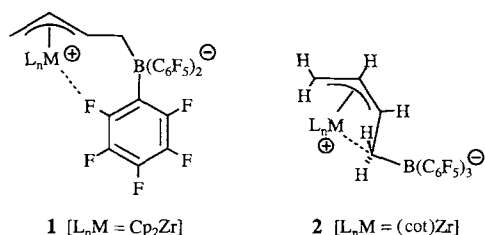
“Smart” self-assembly of several chiral diols and an achiral pre-catalyst results in the formation of a highly enantioselective catalyst for the carbonyl–ene reaction (a). The assembly is not influenced by the order of addition of the components and always results in the exclusive formation of a single catalyst, as shown by NMR spectroscopy studies.



K. Mikami,* S. Matsukawa, T. Volk, M. Terada 2768–2771

Self-Assembly of Several Components into a Highly Enantioselective Ti Catalyst for Carbonyl–Ene Reactions

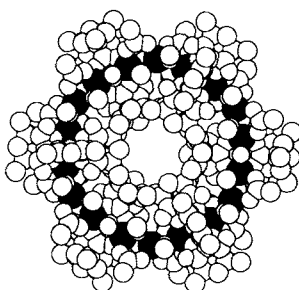
The type of intramolecular stabilization of zirconium borate betaines is governed by the location of the substituents in the allyl unit: *E* configuration results in Zr...F coordination (**1**), whereas *Z* configuration favors the formation of an internal Zr...CH2[B] ion pair (**2**).



J. Karl, G. Erker,* R. Fröhlich, F. Zippel, F. Bickelhaupt, M. Schreuder Goedheijt, O. S. Akkerman, P. Binger, J. Stannek 2771–2774

Noncovalent Interactions in Organometallic Compounds: Formation of an Intramolecular Metal–Carbon Ion Pair in Zirconium Borate Betaines

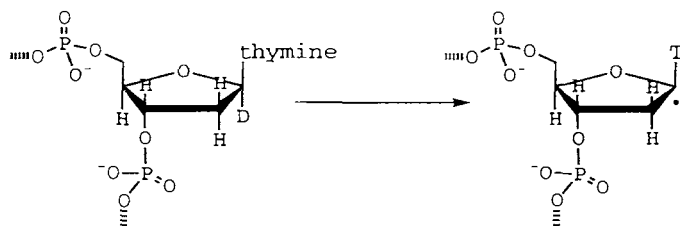
D_{3d} symmetry characterizes complex **1** (see structure on the right). This circular molecular contains 18 high-spin, antiferromagnetically coupled iron(III) centers. Isolated as the double salt **1** · 6Et₄N(NO₃) · 15CH₃OH · 6Et₂O · 24H₂O it is the largest cyclic ferric cluster yet reported.



S. P. Watton, P. Fuhrmann, L. E. Pence, A. Caneschi, A. Cornia, G. L. Abbati, S. J. Lippard* 2774–2776

A Cyclic Octadecairon(III) Complex, the Molecular 18-Wheeler

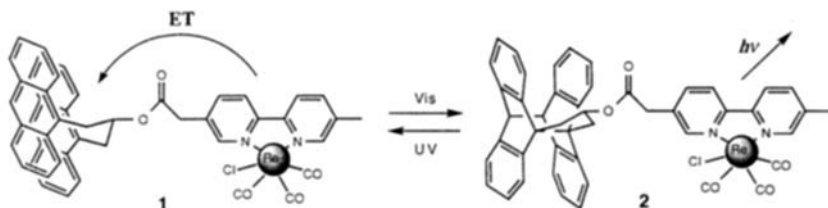
C-1'H and not C-2'H is the initial site of oxidative cleavage of DNA with the chemical nuclease $[\text{Cu}(\text{phen})_2]^+/\text{H}_2\text{O}_2$. This is the result of experiments with DNA containing C-1'-deuterated thymidine groups (the first step of the reaction sequence is shown below). If C-2'H is extracted in the first step, a one-electron oxidation and H/D migration should take place; there is no evidence of this.



O. Zelenko, J. Gallagher,
D. S. Sigman* 2776–2778

Scission of DNA with Bis(1,10-phenanthroline)copper without Intramolecular Hydrogen Migration

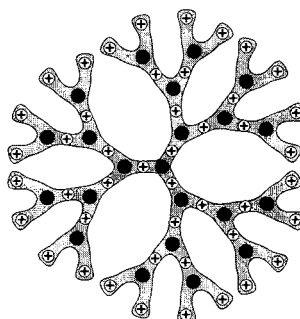
A markedly different emission behavior is exhibited by the two rhenium complexes **1** and **2**. These can be interconverted photochemically; the forward reaction (cyclization to the "closed" form) is triggered by visible light, and the reverse reaction by UV light. Therefore, this is a photoswitchable molecular system in which the anthracene groups function as the switching unit and the complexed rhenium as the detector.



A. Beyeler, P. Belser,*
L. DeCola 2779–2781

Rhenium Complexes with a Photochemically Variable Anthracene Subunit: A Molecular Switch

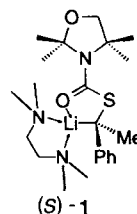
Forty-five cationic sites are present in the dendrimer shown schematically on the right, which was obtained by an efficient convergent synthesis. The key step in the reaction sequence for generation growth is the high-yielding Menshutkin reaction



P. R. Ashton, K. Shibata, A. N. Shipway,
J. F. Stoddart* 2781–2783

Polycationic Dendrimers

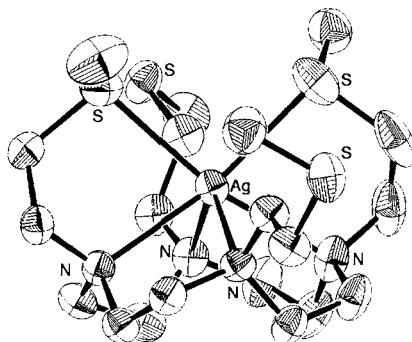
Configurationally stable even at 0°C, the lithiated benzyl thiocarbamate (**S**)-**1** can be substituted by most electrophilic reagents with inversion of configuration. It is the first enantiomerically pure α -thiocarbanyllithium whose outstanding configurational stability allows synthetic use.



D. Hoppe,* B. Kaiser, O. Stratmann,
R. Fröhlich 2784–2786

A Highly Enantiomerically Enriched α -Thiocarbanyllithium Derivative with Unusual Configurational Stability

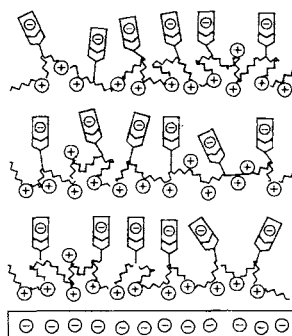
The highest known binding constant for the silver(I) complex with a cyclen-derived ligand was recently measured ($\lg K = 19.63$; crystal structure shown on the right). This ligand is preorganized in the metal-free form. It contains four nitrogen and four sulfur atoms, but the soft silver(I) ion prefers coordination through the nitrogen atoms and binds to only two sulfur atoms in the solid state. The chelating ligand was designed for in vivo therapeutic application of the β -emitting radio-nuclide ^{111}Ag .



T. Gyr, H. R. Mäcke,*
M. Hennig 2786–2788

A Highly Stable Silver(I) Complex of a Macrocycle Derived from Tetraazatetra-thiacyclen

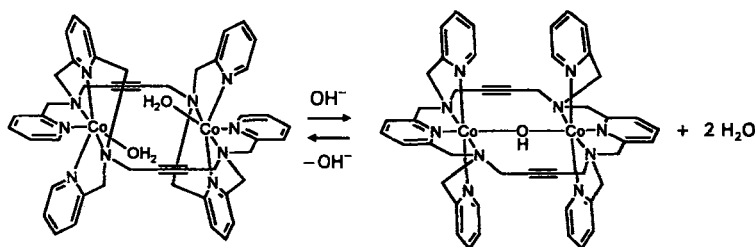
Alternating physisorption and chemical activation characterizes the method presented here for assembling thin, defined organic multilayers (shown schematically on the right). A variety of structures are suitable for the new process, with which even noncentrosymmetric films can be obtained.



A. Laschewsky,* B. Mayer,
E. Wischerhoff, X. Arys, A. Jonas,
M. Kauranen, A. Persoons .. 2788–2791

A New Technique for Assembling Thin, Defined Multilayers

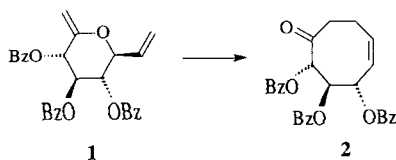
Trigonal prismatic at pH 4, octahedral at pH 6.5! A simple change of pH reversibly switches the coordination geometry of a macrocyclic dicobalt(II) complex. The structural change is induced by bridging of the metal ions by a hydroxide ion (see below).



C. Wendelstorf, R. Krämer* 2791–2793

Interchangeable Coordination Geometries: pH-Controlled Change of Trigonal-Prismatic to Octahedral Metal Coordination in a Dinuclear Cobalt(II) Complex

Loss of the carbohydrate structure accompanies the sigmatropic rearrangement of the doubly unsaturated saccharide derivative **1**. In this way, a highly functionalized eight-membered carbocycle (**2**) is obtained in a simple reaction sequence from D-glucose.

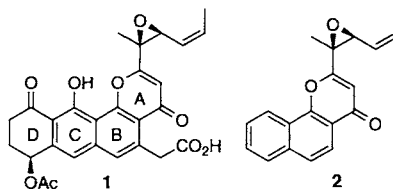


B. Werschkun, J. Thiem* ... 2793–2794

From D-Glucose to a New Chiral Cyclo-octenone

With a 5'-Gpu-3' sequence selectivity

ity that is very similar to that of the natural antitumor antibiotic kapurimycin A₃ (**1**), the ABC ring analogue **2** effectively cleaves DNA by guanine alkylation. Essential for cleavage activity are the reactive alkenyl epoxide group in the side chain and the strong intercalation of the aromatic units of **1** and **2** in the DNA duplex; this was made clear by the significantly lower activity of an AB ring analogue.

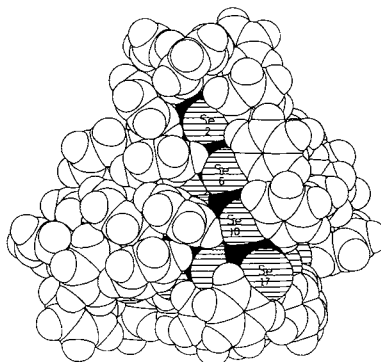


K. Nakatani,* A. Okamoto,
I. Saito* 2794–2797

Synthesis of an ABC Ring Analogue of Kapurimycin A₃ as an Effective DNA Alkylating Agent

Clusters with and without cavities

are formed in the reaction of [CdCl₂(PPh₃)₂] with PhSeSiMe₃. Depending on the organic solvent used, [Cd₁₀Se₄(SePh)₁₂(PPh₃)₄] or [Cd₁₆(SePh)₃₂(PPh₃)₂] (depicted on the right; the cluster is almost completely covered with phenyl rings) crystallizes. The clusters are composed of fused adamantanoid Cd–Se cages.



S. Behrens, M. Bettenhausen,
A. Eichhöfer, D. Fenske* .. 2797–2799

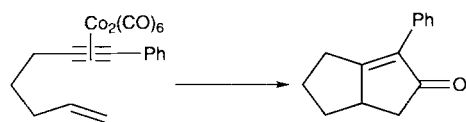
Synthesis and Crystal Structure of [Cd₁₀Se₄(SePh)₁₂(PPh₃)₄] and [Cd₁₆(SePh)₃₂(PPh₃)₂]

The use of different donor ligands as chemical scissors allows fragments to be "cut out" from the solid-state structure of BaI₂, which results in the barium compounds given in the title. According to X-ray structural analyses these compounds exhibit different dimensionalities.

K. M. Fromm* 2799–2801

Structural Evolution from the Solid State to the Molecule for BaI₂: Synthesis and Crystal Structures of [BaI₂(μ₂-OH₂)₂]_{3/∞}, [BaI₂(μ₂-OH₂)(OC₃H₆)₂]_{2/∞}, [BaI₂(thf)₃]_{1/∞}, and [BaI₂(thf)₅] · THF

Two economical and practical sets of conditions have been developed for the Pauson–Khand reaction on the basis that primary amines accelerate this reaction. One method employs more than three equivalents of cyclohexylamine in 1,2-dichloroethane at 83°C, whereas the other requires a mixed solvent of 1,4-dioxane and 2 m aqueous NH₃ (1/3 v/v) at 100°C. Under these conditions, for instance, the cyclization shown below is complete in 5 or 15 minutes, respectively, and the product is isolated in 99 or 93% yield, respectively.



T. Sugihara,* M. Yamada, H. Ban,
M. Yamaguchi,* C. Kaneko 2801–2804

Rate Enhancement of the Pauson–Khand Reaction by Primary Amines

[Pd₂(dba)₃] in the presence of trifurylphosphane catalyzes the stepwise reaction of CH₂(ZnI)₂ with different electrophiles [Eq. (a)]. The homologous Zn₂ compound CH₃CH(ZnI)₂ reacts in the first step analogously with cinnamyl chloride; however, stoichiometric amounts of CuCN/LiCN are required for the coupling with allyl bromide in the second step

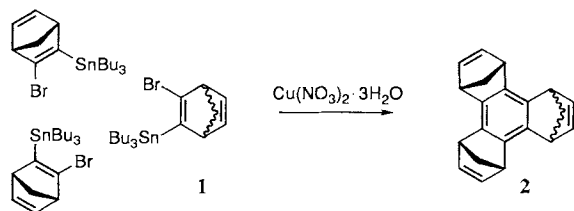
K. Utimoto,* N. Toda, T. Mizuno,
M. Kobata, S. Matsubara ... 2804–2805

Stepwise Reaction of Bis(iodozincio)methane with Two Different Electrophiles



RX = PhCH=CHCH₂Cl, *n*-C₈H₁₇C≡CCH₂Br, C₂H₅C≡CCH(*n*-C₅H₁₁)Br
EX = DCl/D₂O, CH₂=CHCH₂Br, PhCOCl

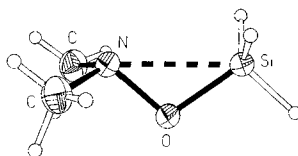
Up to 80% yields of cyclotrimers, including **2** depicted below, can be achieved by reaction of bromo(stannyl)alkenes such as **1** with $\text{Cu}(\text{NO}_3)_2 \cdot 3\text{H}_2\text{O}$ at room temperature in THF. This route, a definite improvement over previously reported methods, makes such molecules available in sufficient quantity for study, for example, as precursors of fullerene fragments.



R. Durr, S. Cossu, V. Lucchini,
O. DeLucchi* 2805–2807

Trisannulated Benzenes by Cyclotrimerization of Bromostannylalkenes

Strongly compressed Si-O-N angles are observed in $\text{H}_3\text{SiONMe}_2$ (crystal structure shown on the right) and $\text{H}_2\text{Si}(\text{ONMe}_2)_2$ with respect to the Si-O-C angle in isoelectronic SiOC compounds. This is due to weak donor-acceptor bonds between the Si and N atoms. The resulting partial hypercoordination at silicon explains the unique chemical behavior of hydroxylaminosilanes.



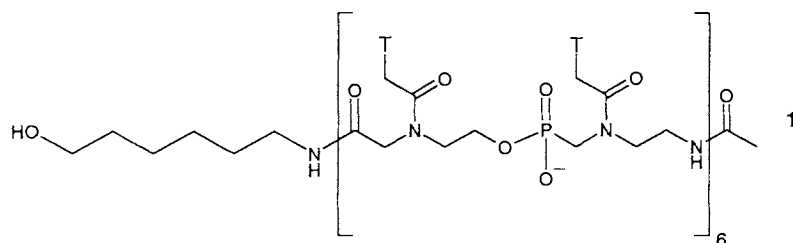
N. W. Mitzel,* U. Losehand 2807–2809

β -Donor Bonds in Compounds Containing SiON Fragments

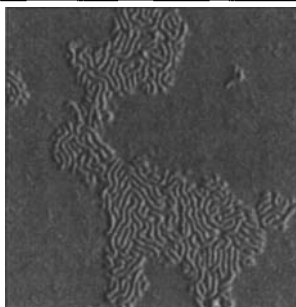
A winning combination! PHONA–PNA co-oligomers such as **1** ($\text{T} = 1$ -thymine) unite the outstanding binding properties of PNAs with the improved physical properties of PHONAs—in particular, their excellent water solubility.

A. Peyman,* E. Uhlmann, K. Wagner,
S. Augustin, C. Weiser, D. W. Will,
G. Breipohl 2809–2812

PHONA–PNA Co-Oligomers: Nucleic Acid Mimetics with Interesting Properties



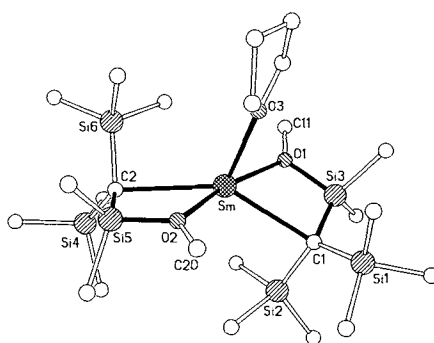
A two-dimensional labyrinth is formed by self-organization of cylindrical brushlike polymacromonomers. Single "brush molecules" can be visualized by atomic force microscopy within a monolayer (see picture on the right). This represents a first step towards the production of well-defined nanostructured surfaces with molecular resolution.



P. Dziezok, S. S. Sheiko, K. Fischer,
M. Schmidt,* M. Müller 2812–2815

Cylindrical Molecular Brushes

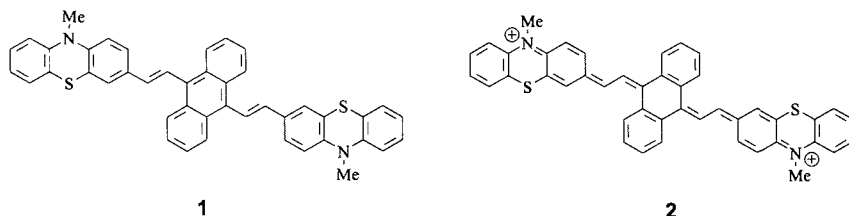
The first $\text{Sm}^{\text{II}}-\text{C}$ σ bonds to be verified by X-ray structure analysis are 2.787(5) and 2.845(5) Å in length. These distances were obtained for a samarium(II) complex in which two $\text{C}(\text{SiMe}_3)_2(\text{SiMe}_2\text{OMe})$ ligands are each bound to the samarium center through the carbanionic carbon center and the oxygen atom of the methoxy group (see structure depicted on the right). This compound reacts with benzophenone to give the corresponding samarium(III) ketal radical anion complex.



W. Clegg, C. Eaborn, K. Izod,*
P. N. O'Shaughnessy,
J. D. Smith 2815–2817

The First Structurally Authenticated σ -Bonded Organosamarium(II) Derivative and Its Reaction with Benzophenone

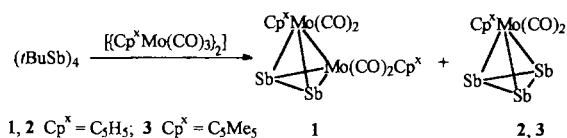
A structural change between a benzoid (1) and a quinoid (2) is possible upon the transfer of two electrons. This finding is supported by cyclic voltammetric and spectroscopic data, and is in agreement with quantum-mechanical calculations on the semiempirical level.



A. Knorr, J. Daub* 2817–2819

Structural Reorganization of Anthracene-Bridged Stilbenoids by Oxidation and Reduction

A suitable antimony source for complexes with substituent-free Sb_n ligands is the four-membered ring $(tBuSb)_4$, which reacts with $[(Cp^xMo(CO)_3)_2]$ to yield the tetrahedranes **1** and **2**, and with $[(C_5Me_5(CO)_3Mo)_2]$ to give **3**. Compounds **2** and **3** are the first complexes to contain the *cyclo*- Sb_3 ligand. In the crystal they are linked through close $Sb \cdots Sb$ interactions.

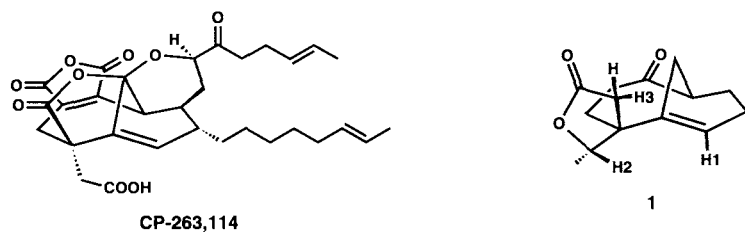


H. J. Breunig,* R. Rösler,

E. Lork 2819–2821

Complexes with Sb_2 and *cyclo*- Sb_3 Ligands: The Tetrahedranes $[(C_5H_5(CO)_2Mo)_2Sb_2]$, $[C_5H_5(CO)_2MoSb_3]$, and $[C_5Me_5(CO)_2MoSb_3]$

A Rh-catalyzed generation of a carbenoid and its intramolecular trapping, followed by a divinylcyclopropane rearrangement and a radical cyclization, are the crucial reactions in a new strategy for constructing the bicyclo[4.3.1]dec-1(9),4-diene-10-one framework of the natural products in the title. The resulting model compound **1** differs from this target core only in the configuration of the quaternary center.

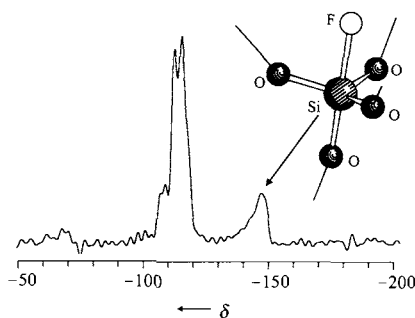


K. C. Nicolaou,* M. H. D. Postema,

N. D. Miller, G. Yang 2821–2823

A Novel Approach to the CP-225,917 and CP-263,114 Core

With fluoride as a mineralizing agent, the high-silica zeolites nonasil and ZSM-5 were obtained by hydrothermal syntheses. ^{29}Si NMR spectroscopy showed that five-coordinate silicon exists in the form of $SiO_{4/2}F^-$ in the zeolite frameworks (see the $^{29}Si\{^{19}F\}$ CPMAS NMR spectrum of nonasil on the right). In ZSM-5 at room temperature the fluoride ion undergoes a dynamic exchange between different silicon atoms, which is frozen out at 140 K.

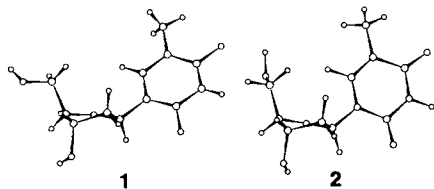


H. Koller,* A. Wölker, H. Eckert,

C. Panz, P. Behrens 2823–2825

Five-Coordinate Silicon in Zeolites: Probing $SiO_{4/2}F^-$ Sites in Nonasil and ZSM-5 with ^{29}Si Solid-State NMR Spectroscopy

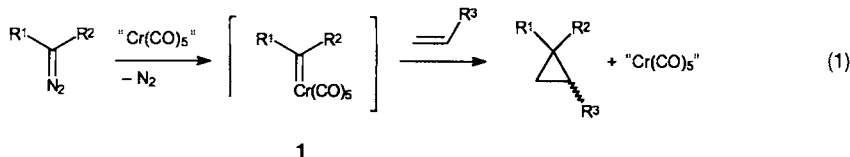
Large differences in the electrostatic properties of nucleosides can have surprisingly small effects on DNA replication. Size and shape appear to be more important, as structural studies of difluorotoluene deoxynucleoside **1**, an isostere of thymidine (**2**), prove. The two nucleosides have virtually the same aromatic ring, almost identical sugar puckers, and very similar glycosidic angles (see the structural formulas). Hydrogen-bonding capacity is apparently not crucial for templating in DNA replication.



K. M. Guckian, E. T. Kool* 2825–2828

Highly Precise Shape Mimicry by a Difluorotoluene Deoxynucleoside, a Replication-Competent Substitute for Thymidine

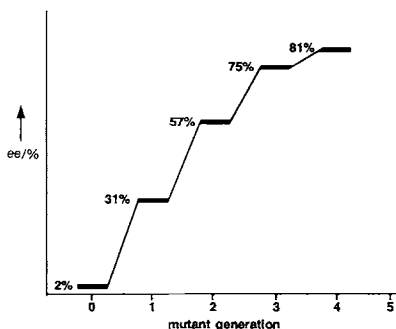
A new catalytic route to cyclopropanes from alkenes and diazoalkanes is provided by pentacarbonyl(η^2 -*cis*-cyclooctene)chromium(0), which generates the catalyst "Cr(CO)₅". The reactions (1) are characterized by a pronounced chemoselectivity of the participating carbene complex intermediates **1** and allow the unambiguous discrimination of diversely substituted olefins.



J. Pfeiffer, K. H. Dötz* 2828–2830

[2+1] Cycloadditions of Diazoalkanes to Enol Ethers Catalyzed by Chromium Complexes—The First Direct Spectroscopic Observation of a Carbene Complex Intermediate

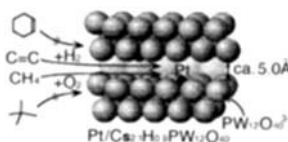
Evolution in the test tube: With the help of the error-prone polymerase chain reaction as a method for random mutagenesis, an efficient gene-expression system, and a screening test for the rapid identification of enantioselective catalysts, it is possible to increase sequentially the *ee* value of an unselective lipase-catalyzed ester hydrolysis (see picture on the right).



M. T. Reetz,* A. Zonta, K. Schimossek, K. Liebeton, K. E. Jaeger* . 2830–2832

Creation of Enantioselective Biocatalysts for Organic Chemistry by In Vitro Evolution

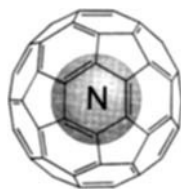
Preferentially smaller molecules are oxidized and hydrogenated in the presence of the ultramicroporous (pore diameter < 5.9 Å), platinum-containing (0.5 wt%) heteropolyoxometalate compound Pt/Cs_{2.1}H_{0.9}PW₁₂O₄₀, according to studies with methane/2,2-dimethylpropane and ethene/cyclohexene (shown schematically on the right).



Y. Yoshinaga, K. Seki, T. Nakato, T. Okuhara* 2833–2835

Shape-Selective Hydrogenation and Oxidation over a Platinum-Containing Ultramicroporous Heteropolyoxometallic Compound

The concave inner face of C₆₀ is so inert with respect to the formation of covalent bonds, that even atomic nitrogen in the quartet ground state is stable as an encapsulated guest (shown on the right). Semiempirical calculations and ESR investigations offer an explanation for this unprecedented behavior.



H. Mauser, N. van Eikema Hommes, T. Clark, A. Hirsch,* B. Pietzak, A. Weidinger, L. Dunsch . . . 2835–2838

Stabilization of Atomic Nitrogen Inside C₆₀

* Author to whom correspondence should be addressed

CORRIGENDUM

In the communication by **C. Mioskowski et al.** in issue number 21, pp. 2342–2344, the chloroacetals (entries 21 and 22 in Table 1) prepared by chlorination of the corresponding acetals are not stable as mentioned in the paper, but rearrange spontaneously into the corresponding 2-chloroethyl esters (reference: H. Gross, J. Freiberg, B. Costisella, *Chem. Ber.* **1968**, *101*, 1250–1256).

SERVICE

| | |
|----------------|--------|
| • Events | 2713 |
| • Keywords | 2840 |
| • Author Index | 2841 |
| • Preview | 2842 |
| • Indexes | 2843ff |

German versions of all reviews, communications, and highlights in this issue appear in the second December issue of *Angewandte Chemie*. The appropriate page numbers can be found at the end of each article and are also induced in the Author Index on p. 2841.

All the Tables of Contents from 1995 onwards may be found on the WWW under:
<http://www.wiley-vch.de/home/angewandte>

In order to expand the editorial teams of the renowned journals *Angewandte Chemie* and *Chemistry – A European Journal* we are looking for an

Editorial Assistant

WILEY-VCH, is a successful and expanding international publishing company within the Wiley group.

This permanent full-time post will be based in Weinheim, a historic town near Heidelberg in the southwest of Germany.

English should be your native language, and you should have good communication skills and a sound working knowledge of German. Other requirements are a B.Sc. in chemistry, experience with PCs, and a keen eye for detail.

The work will primarily involve assisting the editors in their daily work: routine PC file management (e-mail, diskettes), copyediting, proofreading, coordination of free-lance work and contact with authors.

If you enjoy the challenge of using the full range of your skills to produce high-quality work to tight schedules within a motivated team, please send full career details to:

WILEY-VCH Verlag GmbH
Human Resources
P.O. Box 10 11 61
69451 Weinheim
Germany
Tel.: +49 (0) 6201 606-0

 **WILEY-VCH**

ANGEWANDTE CHEMIE

A Journal of the
Gesellschaft
Deutscher Chemiker

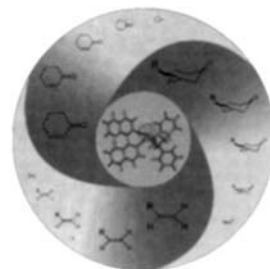
International Edition in English

1997
36/23
Page 2537–2698

The editorial staff and the publishers thank all readers, authors, referees, and advertisers for their interest and support over the past year, and wish them all a happy new year.

COVER PICTURE

The cover picture shows schematically the catalytic formation of single enantiomers of 3-alkylcyclohexanones starting from cyclohexenones and the appropriate substituted alkenes. The alkenes are initially transformed into organozinc reagents that then add to the enone in a completely stereocontrolled, copper-catalyzed reaction. In the inner circle is a molecular model of a novel phosphoramidite that has been used as chiral ligand (the copper ion is indicated by a dotted sphere) in this 1,4-addition. Since several functionalized organozinc reagents are readily accessible from alkenes, this reaction and also the combined 1,4-addition/aldol reaction provide access to a variety of highly enantiomerically pure cyclohexanones. More about this method, which is also applicable to dienones, is reported by B. L. Feringa et al. on page 2620 ff. The authors thank Dr. J. Esch for the design of this picture.



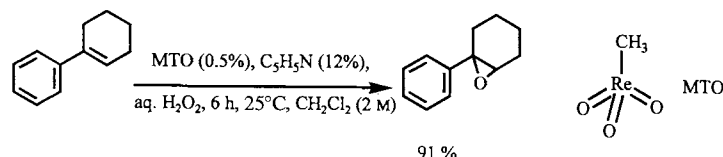
REVIEW

Contents

A *terra incognita* with a huge potential for chemical synthesis is opened by activation of organic substrates by one-electron transfer: Reactions of radical cations can be extremely selective when proper control over the primary and secondary reactions is attained. An analysis that combines the observed reactivity patterns of numerous instructive examples with thermodynamic and kinetic data leads to a useful categorization of radical cation reactivity and reveals the principles governing their mode of action. This should facilitate the directed planning of synthetic transformations with these intermediates.

M. Schmittel,* A. Burghart 2550–2589
Understanding Reactivity Patterns of
Radical Cations

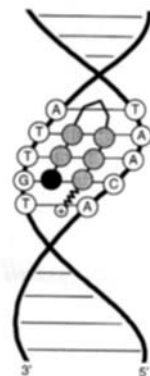
Simply by adding pyridine ligands and using aqueous hydrogen peroxide as stoichiometric oxidant the methyltrioxorhenium (MTO)-catalyzed epoxidation becomes a simple, chemoselective, and highly efficient reaction, as exemplified below. A wide variety of functional groups is tolerated, and the epoxides are obtained in high yield in a short time with low catalyst loading.



A. Gansäuer * 2591–2592

A Novel Methyltrioxorhenium (MTO)-Catalyzed Epoxidation of Olefins: An Impressive Example of Simplicity, Selectivity, and Efficiency

Interference with the transcription of specific genes in vivo can be achieved with artificial, low molecular weight pyrrole-imidazole polyamides, as shown by recent studies by Gottesfeld, Dervan et al. This is possible because these ligands are capable of binding with high affinity and specificity to predetermined DNA sequences in the minor groove of double-stranded DNA (see schematic representation on the right; gray: pyrrole, black: imidazole units).

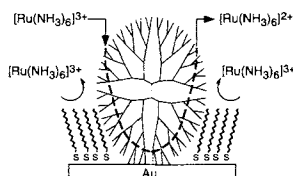


K. Weisz * 2592–2594

Polyamides as Artificial Regulators of Gene Expression

COMMUNICATIONS

Behavior as single-molecule gates for certain ions is demonstrated by dendrimers confined on surfaces and within thiol monolayers (see picture). The permeability depends on the chemical state of the dendrimer and the charge on the ion. These composite structures are models of biological membranes in that mass transfer occurs through the interior of the dendrimer in analogy to ion motion through membrane proteins.

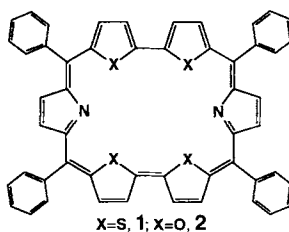


M. Zhao, H. Tokuhisa,

R. M. Crooks * 2596–2598

Molecule-Sized Gates Based on Surface-Confined Dendrimers

The remarkably simple synthesis of tetrathia- and tetraoxarubryns **1** and **2** is achieved by the routes presented here. Spectroscopic, ^1H NMR, and electrochemical data suggest that **1**, **2**, and their protonated derivatives are aromatic 26π electron systems, and the protonated derivatives form stable complexes in solution with anions such as F^- , N_3^- , and adenosine 5'-monophosphate.



A. Srinivasan, V. M. Reddy,

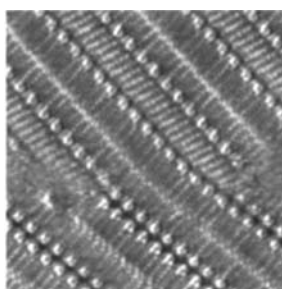
S. J. Narayanan, B. Sridevi,

S. K. Pushpan, M. Ravikumar,

T. K. Chandrashekar 2598–2601

Tetrathia- and Tetraoxarubryns: Aromatic, Core-Modified, Expanded Porphyrins

The photopolymerization of a monolayer physisorbed on graphite and containing diacetylene derivatives comprising a isophthalic acid head group and a decyl group as nonpolar tail was studied by scanning tunneling microscopy (STM). The submolecularly resolved STM image on the right depicts a domain boundary between an unpolymerized monolayer (lower domain) and a polymerized monolayer (upper domain).



P. C. M. Grim, S. De Feyter,

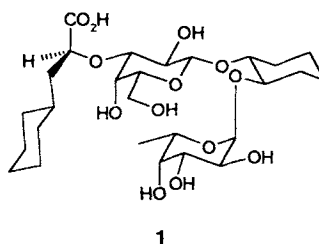
A. Gesquière, P. Vanoppen, M. Rücker,

S. Valiyaveetil, G. Moessner, K. Müllen,

F. C. De Schryver * 2601–2603

Submolecularly Resolved Polymerization of Diacetylene Molecules on the Graphite Surface Observed with Scanning Tunneling Microscopy

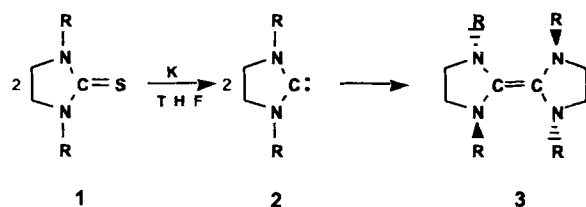
For the rational design of drugs that inhibit the interaction between E-selectin and sialyl Lewis^X, structural information on bound inhibitors is required. The bioactive conformation of the potent sialyl Lewis^X mimic **1** was therefore determined by transfer NOE NMR spectroscopic methods.



W. Jahnke,* H. C. Kolb,
M. J. J. Blommers, J. L. Magnani,
B. Ernst 2603–2607

Comparison of the Bioactive Conformations of Sialyl Lewis^X and a Potent Sialyl Lewis^X Mimic

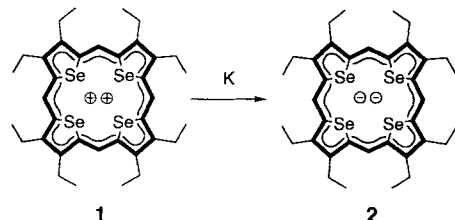
Two *tert*-butyl groups at the nitrogen atoms of the cyclic carbene **2**, which is accessible from **1** by reduction with potassium, provide sufficient stability to enable it to be stored indefinitely under exclusion of air and moisture. In contrast, sterically less shielded carbenes of type **2** (R = Me, Et, *i*Pr) dimerize slowly at room temperature to olefins **3**.



M. K. Denk,* A. Thadani, K. Hatano,
A. J. Lough 2607–2609

Steric Stabilization of Nucleophilic Carbenes

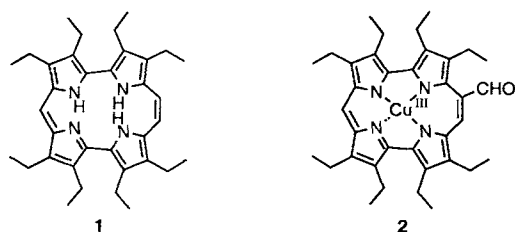
The electronic “umpolung” of the title compound **1** to the dianion **2** is achieved by the uptake of four electrons from potassium in THF. Although the ring skeleton of the 18π **1** deviates significantly from planarity because of the steric requirements of the four selenium atoms, the new macrocycle fulfils the NMR criteria for aromaticity.



E. Vogel,* C. Fröde, A. Breihan,
H. Schmickler, J. Lex* 2609–2612

Octaethyltetraselenaporphyrin Dication

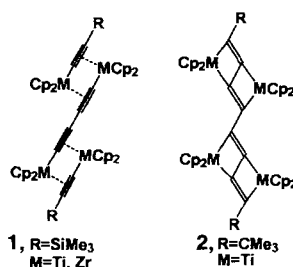
The most stable of the three possible structural isomers of corrole is, according to theory, isocorrole, for which the title compound **1** is a model compound. The reductive McMurry coupling of the corresponding α,ω -tetrapyrroledialdehyde affords an entry to **1**. The isocorrole derivative **1** has, like corrole, the propensity to stabilize metals in high oxidation states. This is exemplified by the Cu^{III} complex **2**, which has been isolated as an intermediate in the synthesis of 9-formyloctaethylisocorrole.



E. Vogel,* B. Binsack, Y. Hellwig,
C. Erben, A. Heger, J. Lex,
Y.-D. Wu* 2612–2615

Contracted Porphyrins:
Octaethylisocorrole

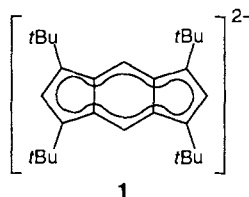
Cleavage or complexation of octatetraynes occur in the reaction with four titanocene or zirconocene units, depending on the groups R attached to the tetrayne. The structures of the products **1** and **2** have been unequivocally proven by spectroscopy and X-ray structure analysis.



P.-M. Pellny, N. Peulecke, V. V. Burlakov, A. Tillack, W. Baumann, A. Spannenberg, R. Kempe, U. Rosenthal * .. 2615–2617

Twofold C–C Single Bond Activation and Cleavage in the Reaction of Octatetraynes with Titanocene and Zirconocene Complexes

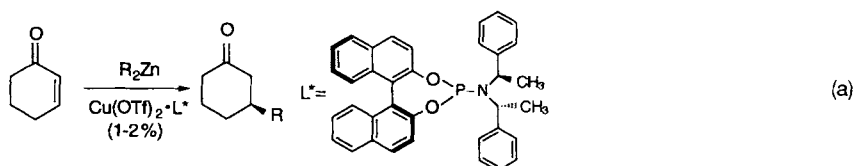
Reduction of the formally antiaromatic compound 1,3,5,7-tetra-*tert*-butyl-*s*-indacene to the dianion **1** is achieved with lithium or potassium. Both salts were characterized by NMR spectroscopy and X-ray crystallography, which revealed that the polycyclic hydrocarbon framework exhibits a delocalized π -electron system, as does the neutral compound. The results of density functional theory calculations are in agreement with the experimental findings.



D. R. Cary, J. C. Green, D. O'Hare * 2618–2620

Synthetic, Structural, and Bonding Studies of Indacene Dianions

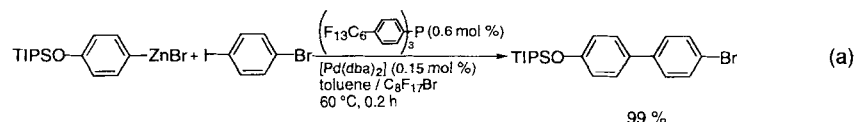
Complete stereocontrol with the added advantage of functional-group tolerance in copper-catalyzed 1,4-additions of organozinc reagents to enones has been achieved for the first time with the chiral phosphoramidite L* as ligand in the copper complex [Eq. (a), Tf = trifluoromethanesulfonate]. The zinc enolate intermediate of the reaction can be trapped with aldehydes.



B. L. Feringa,* M. Pineschi, L. A. Arnold, R. Imbos, A. H. M. de Vries 2620–2623

Highly Enantioselective Catalytic Conjugate Addition and Tandem Conjugate Addition–Aldol Reactions of Organozinc Reagents

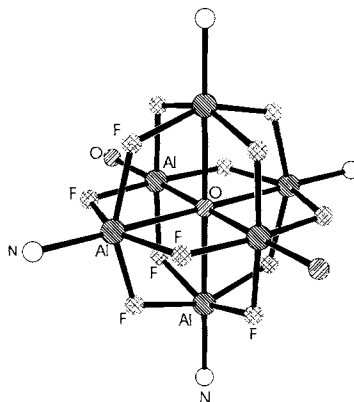
A remarkable selectivity for iodide is characteristic of the Pd⁰ catalyst obtained from (F₁₃C₆H₄)₃P and [Pd(dba)₂] in the cross-coupling of organozinc bromides with aryl iodides in a biphasic perfluorinated solvent [Eq. (a)]. In general, this method provides C–C coupled products in high yields and requires only a small amount of catalyst (0.15 mol %), which can be separated by simple phase separation and reused several times; dba = dibenzylideneacetone, TIPS = *i*Pr₃Si.



B. Betzemeier, P. Knochel * 2623–2624

Palladium-Catalyzed Cross-Coupling of Organozinc Bromides with Aryl Iodides in Perfluorinated Solvents

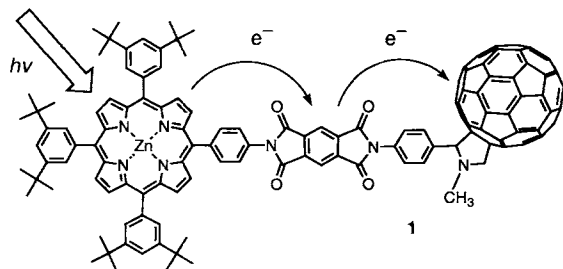
Depending on the size of the substituents R and R', the recrystallization of $(2,6\text{-R}_2\text{C}_6\text{H}_3)[\text{Si}(\text{R}')\text{Me}_2]\text{-NaAlF}_2\cdot\text{THF}$ either leads back to the starting products, or to larger clusters. The corners of these clusters are occupied by aluminum atoms, the edges by fluorine atoms (a partial view of a cluster in the crystal is depicted on the right). An oxygen atom is located at the center of the tetrakis-hexahedron surrounded by six aluminum atoms. In molecular compounds this type of structure was only known for d- and f-block elements until now.



S. D. Waezsada, F.-Q. Liu, C. E. Barnes,
H. W. Roesky,* M. L. Montero,
I. Usón 2625–2626

Synthesis and Structure of Aluminum-
Fluorine-Oxygen Clusters

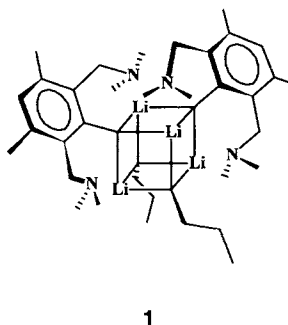
A model for the reaction center of photosynthesis is the porphyrin-imide- C_{60} triad **1**. The C_{60} unit accelerates quenching of the excited singlet state of the porphyrin group. Thus, electron transfer can proceed either by a two-step process through the imide spacer with formation of a long-lived intermediate with separated charge or directly through space.



H. Imahori,* K. Yamada, M. Hasegawa,
S. Taniguchi, T. Okada,*
Y. Sakata* 2626–2629

A Sequential Photoinduced Electron
Relay Accelerated by Fullerene in a
Porphyrin-Pyromellitimide- C_{60} Triad

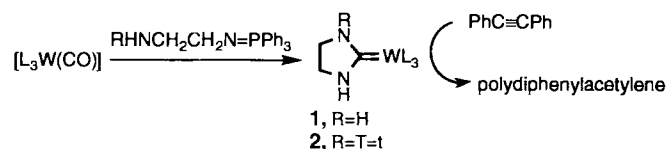
With natural abundance of ^{15}N in the sample, scalar $^6\text{Li},^{15}\text{N}$ spin-spin couplings across coordinative Li-N bonds were detected for the tetrameric organolithium compound **1** in solution and in the solid state. The coupling constants of 3.6 and 4.2 Hz correlate with the Li-N distances determined in the crystal structure analysis.



D. Hüls, H. Günther,* G. van Koten,
P. Wijkens,
J. T. B. H. Jastrzebski 2629–2631

Detection of Scalar $^6\text{Li},^{15}\text{N}$ Coupling
across Coordinative Li-N Bonds

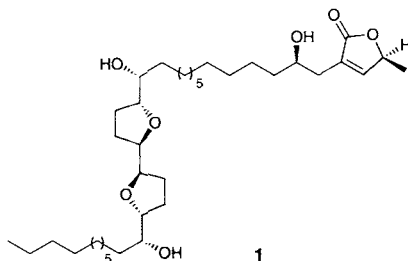
Only alkyne and carbene ligands surround the tungsten atom in complexes **1** and **2**. Complex **1**, which has been characterized by X-ray crystallography, catalyzes the polymerization of diphenylacetylene (see below). $\text{L} = \text{PhC}\equiv\text{CPh}$.



R.-Z. Ku, D.-Y. Chen, G.-H. Lee,
S.-M. Peng, S.-T. Liu* 2631–2632

Novel Alkyne Carbene Tungsten
Complexes

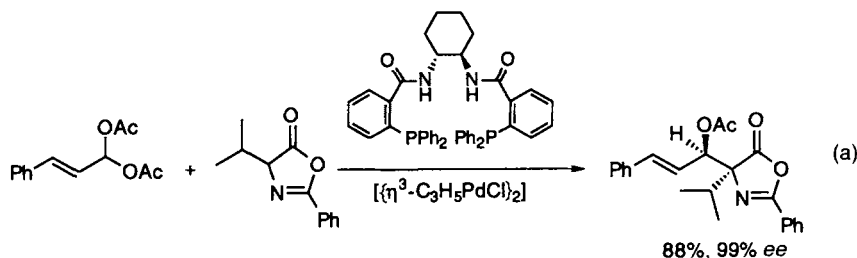
Thirty of the thirty-five carbon atoms of the acetogenin (+)-parviflorin (**3**, also named squamocin E) in this highly convergent synthesis derive from one building block, the readily accessible alcohol **1**. The remaining five have their origin in an alkyne obtained from lactic acid. The key step of this general strategy to bis(tetrahydrofuran) acetogenins is a Ru-catalyzed Alder–ene coupling of the alkyne with a bis(tetrahydrofuran) made from two units of **1**.



B. M. Trost,* T. L. Calkins,
C. G. Bochet 2632–2635


A Convergent Synthesis of
(+)-Parviflorin, (+)-Squamocin K, and
(+)-5*S*-Hydroxyparviflorin

The synthesis of modified peptides depends to a large extent on α -alkylated amino acids. Such amino acids can be prepared in a novel asymmetric synthesis with readily available azlactones: the allylic alkylations of a variety of azlactones catalyzed by palladium proceeds with excellent diastereo- and enantioselectivities [Eq. (a)].



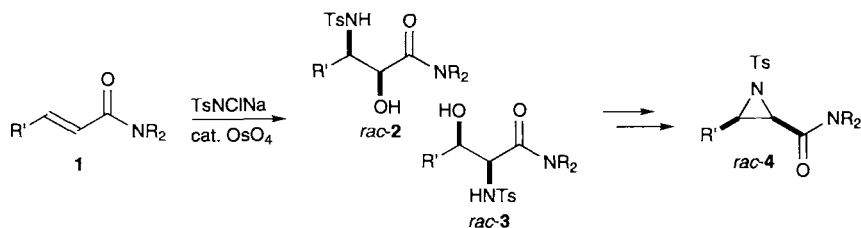
B. M. Trost,* X. Ariza 2635–2637

Catalytic Asymmetric Alkylation of
Nucleophiles: Asymmetric Synthesis of
 α -Alkylated Amino Acids

 **In the absence of external ligands** α,β -unsaturated amides represent one of the few olefin classes which exhibit excellent rates and yields in osmium-catalyzed aminohydroxylation. The scope of the reaction was examined, and a one-pot method for the conversion of the hydroxysulfonamides **2** and **3** into the corresponding aziridines **4** developed. Ts = *p*-MeC₆H₄SO₂.

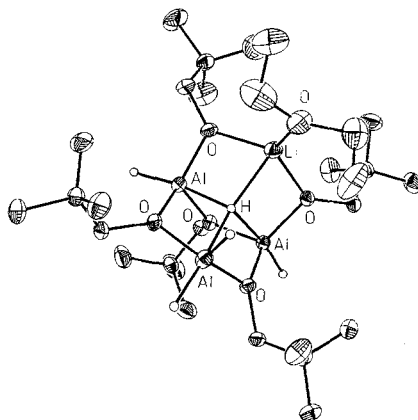
A. E. Rubin,
K. B. Sharpless* 2637–2640

A Highly Efficient Aminohydroxylation
Process



O- and/or H-bridged aluminum centers are found in the multinuclear alanes presented here. A peculiarity is the cage compound **1** (crystal structure shown on the right), in which *all* Al atoms are pentacoordinated. This is the first molecular compound with a tetracoordinated hydride ion.

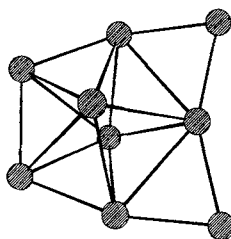
Li[(*t*BuCH₂O)₅Al₃H₃] · Et₂O **1**



H. Nöth,* A. Schlegel, J. Knizek,
H. Schwenk 2640–2643

Di-, Tri-, and Tetranuclear
Alkoxyaluminum Hydrides

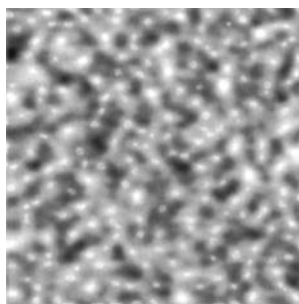
A doubly edge-bridged pentagonal bipyramid of gallium atoms (depicted on the right) occurs in the gallium cluster $[\text{R}_6\text{Ga}_9]^-$ (**1**). Anion **1**, like the electron-precise $[(\text{RGa})_4\text{I}_3]^-$, which has a heterocubane framework, is accessible from "GaI" and $\text{RLi}(\text{thf})_3$. $\text{R} = \text{Si}(\text{SiMe}_3)_3$.



W. Köstler, G. Linti * 2644–2646

Synthesis and Structure of a Tetragallane $[\text{R}_4\text{Ga}_4\text{I}_3]^-$ and a Polyhedral Nonagallane $[\text{R}_6\text{Ga}_2]^-$

No periodic structures can be observed in the topographical scanning tunneling microscopy image of the fracture surface of a Ba/Si/O/C glass (see picture). The results reveal the enormous potential of this young method for the determination of characteristic structural elements in solids without translational symmetry.



W. Raberg, V. Lansmann, M. Jansen,*
K. Wandelt * 2646–2648

Atomically Resolved Structure of Fracture Surfaces of a Ba/Si/O/C Glass with Atomic Force Microscopy

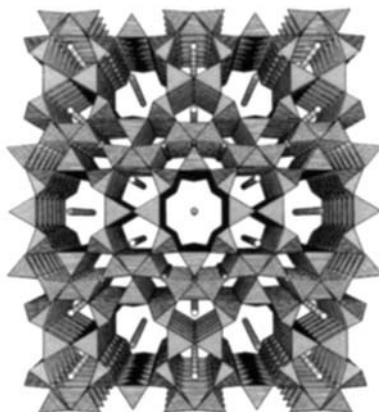
Extremely effective cooperative effects operate during the formation of chiral stacks of C_3 -symmetrical molecules in alkane solvents (a molecule is depicted on the right). The sergeants-and-soldiers principle as well as chiral solvation lead to a preferred helical sense in the columnar aggregates. The amplification of chirality in dynamic systems shows the precision in aggregation.



A. R. A. Palmans, J. A. J. M. Vekemans,
E. E. Havinga,
E. W. Meijer * 2648–2651

Sergeants-and-Soldiers Principle in Chiral Columnar Stacks of Disc-Shaped Molecules with C_3 Symmetry

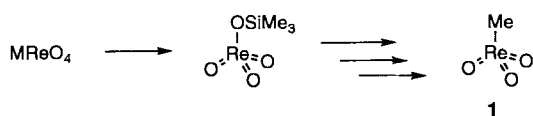
A synthetic access to novel nitridozeolites has been opened by the formal exchange of oxygen for nitrogen in microporous oxozeolites. $\text{Ba}_2\text{Nd}_7\text{Si}_{11}\text{N}_{23}$ is the first example of a network structure containing corner-sharing SiN_4 tetrahedra with wide channels. In sharp contrast to conventional oxidic zeolites, this nitridozeolite is stable up to 1600 °C.



H. Huppertz,
W. Schnick * 2651–2652

$\text{Ba}_2\text{Nd}_7\text{Si}_{11}\text{N}_{23}$ —A Nitridosilicate with a Zeolite-Analogous Si–N Structure

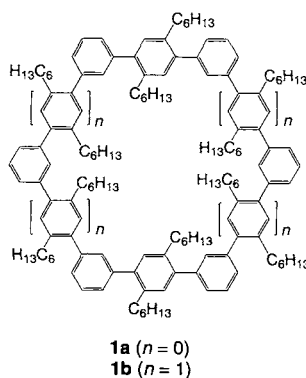
Methyltrioxorhenium in an Erlenmeyer flask: An in situ activation with chloroalkylsilanes converts readily available perrhenates into organorhenium(VII) oxides (as depicted below), which are valuable and diverse homogenous catalysts. Reaction intermediates are trimethylsilyl perrhenate, dirhenium heptoxide, and chlorotrioxorhenium. The application of methyltrioxorhenium CH_3ReO_3 (**1**) in industrial processes might become feasible, particularly since the catalyst can be recycled.



W. A. Herrmann,* R. M. Kratzer,
R. W. Fischer 2652–2654

Alkylrhenium Oxides from Perrhenates: A New, Economical Access to Organometallic Oxide Catalysts

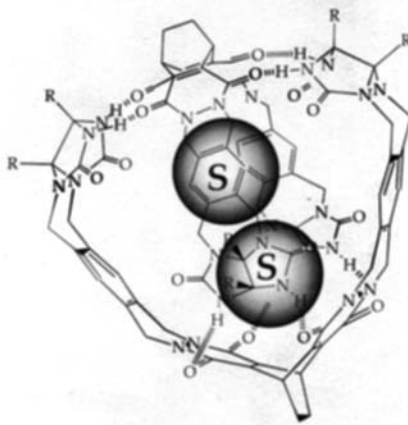
Suzuki cross-coupling has again proved itself as the method of choice for the formation of complex hydrocarbons. Macrocycles **1** could be synthesized from preformed oligophenylene modules. The crystal structure of **1a** shows that each macrocycle contains a chloroform molecule, which is fixed in its position through a CH- π interaction.



V. Hensel, K. Lützow, J. Jacob,
K. Gessler, W. Saenger,
A.-D. Schlüter * 2654–2656

Repetitive Construction of Macrocylic
Oligophenylenes

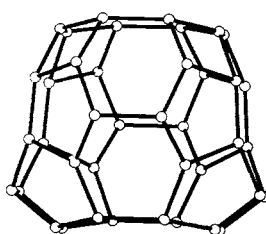
The solvent is the template! Reaction intermediates recognize solvent molecules S and encapsulate them (shown schematically on the right). The formation of covalent bonds could often proceed via noncovalently preassembled building blocks.



Y. Tokunaga, D. M. Rudkevich,
J. Rebek, Jr. * 2656–2659

Solvation and the Synthesis of Self-
Assembled Capsules

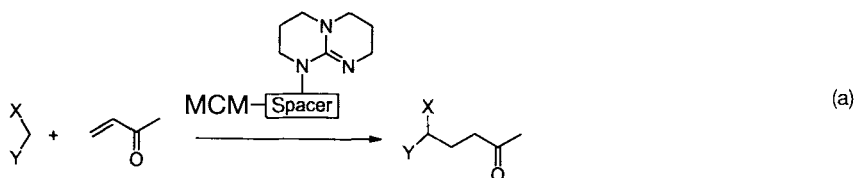
Hydrothermal syntheses in fluoride medium readily yield very open materials, as the example of ITQ-3 demonstrates. This new polymorph of silica with the formula $[\text{SiO}_2]_{64}$ has a framework characterized by a low density (16.3 SiO_4 tetrahedra per 1000 \AA^3), a very large void volume ($0.23 \text{ cm}^3 \text{ g}^{-1}$), and a two-dimensional system of straight channels whose intersection defines a large cage (picture on the right).



M. A. Camblor,* A. Corma, P. Lightfoot,
L. A. Villaescusa,
P. A. Wright * 2659–2661

Synthesis and Structure of ITQ-3, the First
Pure Silica Polymorph with a Two-Dimen-
sional System of Straight Eight-Ring
Channels

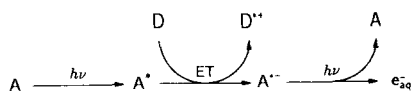
Michael additions, Knoevenagel condensations, and epoxidation of enones with H_2O_2 can be catalyzed under mild conditions with a new mesoporous base. Equation (a) shows the principle for a Michael addition ($\text{X} = \text{CN}$, $\text{Y} = \text{CO}_2\text{Et}$); the catalyst is obtained by immobilization of a guanidine base in MCM-41.



Y. V. Subba Rao, D. E. De Vos,
P. A. Jacobs * 2661–2663

1,5,7-Triazabicyclo[4.4.0]dec-5-ene
Immobilized in MCM-41: A Strongly
Basic Porous Catalyst

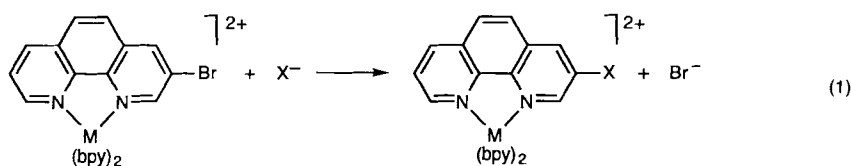
With quite high efficiency the route described here leads to solvated electrons (see below). In this pathway the second photon of a two-photon ionization is absorbed by a radical ion. The studies were conducted with the anthraquinone-1,5-disulfonate/methionine (A/D) system in water. Analogous results were obtained with triethylamine or sulfite ions in place of methionine.



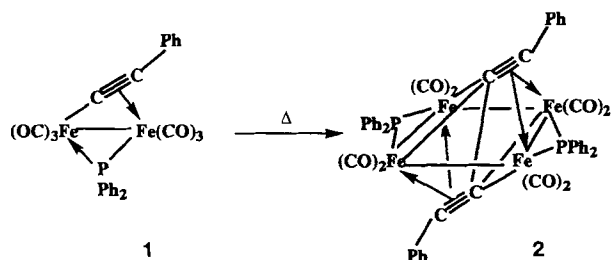
V. Zubarev, M. Goez * 2664–2666

Absorption/Electron Transfer/Absorp-
tion—An Efficient Pathway to Hydrated
Electrons in Laser Flash Photolysis

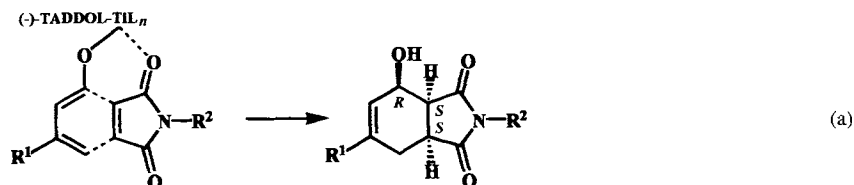
The increased electrophilicity of the complexed phenanthroline ring and the resonance stabilization of the "anionic" addition intermediate account for the unprecedented reactivity of the Ru^{II} and Os^{II} coordination compounds shown in reaction (1). bpy = 2,2'-bipyridine; M = Ru, Os; X = SCH₃, OCH₃, F.



An unprecedented coordination mode for a diyne ligand is present in the Fe₄ complex **2**, which is accessible by thermolysis of the alkyne complex **1** in toluene at 373 K. In **2** the $\mu_4\text{-}\eta^2$ acetylide ligands on each Fe₄ face are linked together by a C–C bond through the plane of four metal atoms.

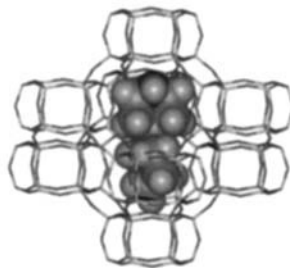


The key to success in asymmetric Diels–Alder cycloadditions may be the preorganization of the reactants through combined covalent and coordinative bonds (dative O–Ti interactions). Even reactions with the difficult, monodentate, C_{2v}-symmetric maleimide dienophiles give the desired adducts in high yields and respectable enantioselectivities [Eq. (a)]. R¹ = H, CH₃; R² = CH₃, PhCH₂, *p*-BrC₆H₄CH₂, (*R*)-PhCH₂(CH₃).



A high-spin ground state characterizes the cubane complex, which was obtained from copper(II) acetate monohydrate and the bridging ligand 2-(4-hydroxysalicylidenamino)ethanol. In the crystal these cubane clusters are arranged to give a channel structure (depicted on the right), which is attributed to a hydrogen-bonding network formed between hydroxyl groups and water molecules.

About four hours reaction time is all that is needed to synthesize the Chabazitic cobalt aluminophosphate (DAF-5) with 4-piperidinopiperidine as template. The template was designed with computer modeling techniques (resulting model shown on the right), after the desired properties of the microporous material had been identified. The work demonstrates the viability of such an approach for the synthesis of new microporous solids.



D. Tzalis, Y. Tor * 2666–2668

The Organic Chemistry of Coordination Compounds: Unprecedented Substitution Reactions of Functionalized Polypyridine Complexes

J. E. Davies, M. J. Mays,* P. R. Raithby, K. Sarveswaran 2668–2669

The Linking of Two Acetylide Units through a Plane of Four Iron Atoms

H. Bienaymé * 2670–2673

Enantioselective Diels–Alder Cycloaddition by Preorganization on a Chiral Lewis Acid Template

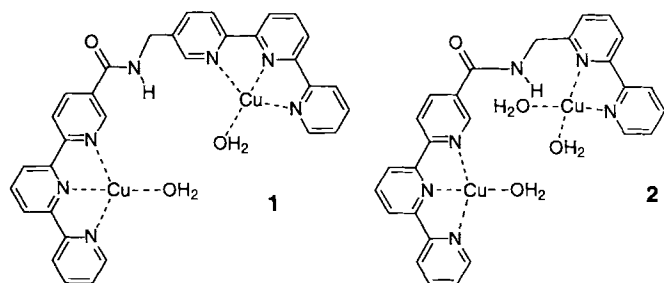
H. Oshio,* Y. Saito, T. Ito 2673–2675

Cluster Assembly by Hydrogen Bonds: Channel Structure of Cu₄L₄ Cubanes

D. W. Lewis,* G. Sankar, J. Wyles, J. M. Thomas,* C. R. A. Catlow,* D. J. Willock 2675–2677

Synthesis of a Small-Pore Microporous Material Using a Computationally Designed Template

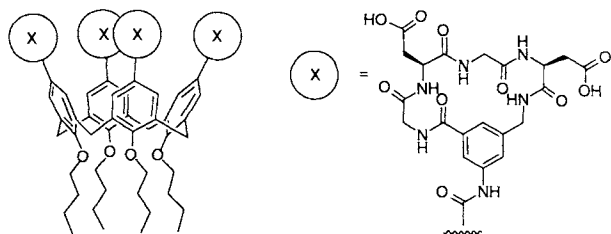
Two characteristics that never before appeared together are combined in complexes **1** and **2**, which show high activity and high selectivity in the hydrolysis of cyclic nucleoside 2',3'-monophosphates as model compounds for RNA. In the case of **1** the regioselectivity is exceptional, and, in the case of **2**, the base selectivity.



S. Liu, Z. Luo,
A. D. Hamilton * 2678–2680

Rapid and Highly Selective Cleavage of Ribonucleoside 2',3'-Cyclic Monophosphates by Dinuclear Cu^{II} Complexes

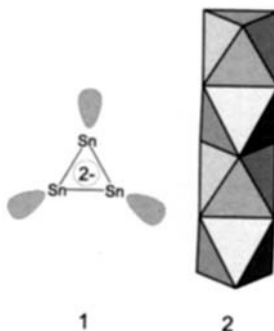
Four constrained cyclic peptides containing the sequence Gly-Asp-Gly-Asp are linked to a central calixarene scaffold (see diagram below) to form a large surface area for interaction with proteins. These antibody mimics not only bind strongly to the surface of cytochrome c but also disrupt its interaction with reducing agents.



Y. Hamuro, M. C. Calama, H. S. Park,
A. D. Hamilton * 2680–2683

A Calixarene with Four Peptide Loops: An Antibody Mimic for Recognition of Protein Surfaces

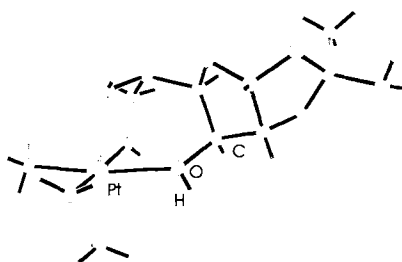
Molecular wires 2 are formed by the stacking of Sn₃²⁻ triangles **1** in BaSn₃. The balanced interplay of interactions between localized and delocalized structural components is responsible for the superconductivity of **2**. The “fingerprint” in the band structure of this superconductor is discussed with the help of partial electron density (PED) introduced here as well as the electron localization function (ELF).



T. F. Fässler,*
C. Kronseder 2683–2686

BaSn₃: A Superconductor at the Border of Zintl Phases and Intermetallic Compounds. Real-Space Analysis of Band Structures

In the first carbohydrate complexes of platinum(II), 1,2-*O*-isopropylidene- α -D-glucos- and - α -D-allofuranose are coordinated to the trimethylplatinum cation only by three OH groups. These are also the only complexes of platinum that contain neutral carbohydrate ligands without anchor groups. The structure of the glucofuranose complex cation [PtMe₃(C₉H₁₆O₆)]⁺ is depicted on the right.



D. Steinborn,* H. Junicke,
C. Bruhn 2686–2688

Carbohydrates Coordinated to Platinum(IV) through Hydroxyl Groups: A New Class of Platinum Complexes with Bioactive Ligands

| | |
|--|--|
| Principles and Practice of Heterogeneous Catalysis • J. M. Thomas, W. J. Thomas | <i>J. R. Anderson, M. Boudart</i> 2689 |
| Handbook of Heterogeneous Catalysis • G. Ertl, H. Knözinger, J. Weitkamp | <i>M. A. Vannice</i> 2690 |
| Encyclopedia of Molecular Biology and Molecular Medicine • R. A. Meyers | <i>H. Kubinyi</i> 2691 |
| A Lifetime of Synergy with Theory and Experiment • A. Streitwieser | <i>J. J. Wolff</i> 2692 |
| Synthetic Methods of Organometallic and Inorganic Chemistry. Vol 6. Lanthanides and Actinides • F. T. Edelmann | <i>W. J. Evans</i> 2693 |
| Inorganic and Organometallic Reaction Mechanisms • J. D. Atwood | <i>A. Grohmann</i> 2694 |
| Handbook of Microscopy. Applications in Materials Science, Solid-State Physics and Chemistry • S. Amelincks, D. van Dyck, J. van Landuyt, G. van Tendeloo | <i>R. Ramlua</i> 2694 |

German versions of all reviews, communications, and highlights in this issue appear in the first December issue of *Angewandte Chemie*. The appropriate page numbers can be found at the end of each article and are also included in the Author Index on p. 2697.

All the Tables of Contents from 1995 onwards may be found on the WWW under:
<http://www.wiley-vch.de/home/angewandte>

SERVICES

| | |
|-----------------------|-------------|
| • Keywords | 2696 |
| • Author Index | 2697 |
| • Preview | 2698 |

ANGEWANDTE CHEMIE

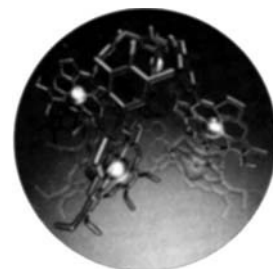
A Journal of the
Gesellschaft
Deutscher Chemiker

International Edition in English

1997
36/22
Pages 2389–2534

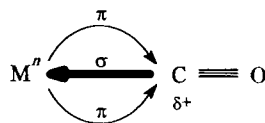
COVER PICTURE

The cover picture shows a stick model of an aggregated calix[4]arenoporphyrin derived from crystal-structure coordinates (oxygen atoms of one molecule are represented in red, and nickel atoms as glass balls; the second molecule is depicted by fainter sticks). Aggregation of two molecules to give a cogwheel arrangement is clearly a dominant structural phenomenon. Combination of calix[4]arenes, which possess strong ion-bonding properties, with porphyrins, which are pH-dependent photoactive chromophores, can potentially lead to new molecular receptors for the development of efficient sensors. Calix[4]arenoporphyrins may also serve as potential models for biological systems such as the tetrapyrrole units in the light-harvesting component of bacterial LH2. More about this supramolecular array is reported by K. M. Smith and co-workers on pages 2497–2500. The graphic was generated by Philippe Schmitt, University of Oxford, UK, with the programs POV-Ray 3.0 and POV-Chem.



REVIEWS

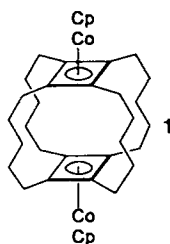
Predominantly σ -bonded CO ligands are encountered in homoleptic carbonyl cations of electron-rich metals (Groups 8–12; see diagram on the right). As a result of the severely reduced π -back-bonding, the cations, which can all be generated in superacid media and form exclusively as thermally stable compounds with $[\text{Sb}_2\text{F}_{11}]^-$, are impressive examples of a new class of coordination compounds of CO with unprecedented spectroscopic properties.



H. Willner,* F. Aubke* 2402–2425

Homoleptic Metal Carbonyl Cations of the Electron-Rich Metals: Their Generation in Superacid Media Together with Their Spectroscopic and Structural Characterization

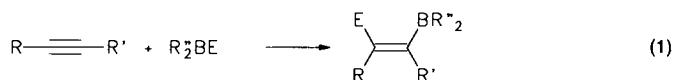
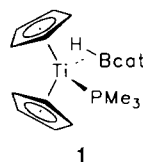
Amazing advances in the synthesis of small-ring cyclophanes are presented here. Carbene addition can be used much more selectively for cyclopropanations than before. In the presence of transition metal complexes, cyclodienes dimerize to cyclobutadieno-superphanes such as **1**. Theoretical investigations and X-ray crystal structure analyses support the obtained results.



R. Gleiter,* M. Merger 2426–2439

Phanes with Three- and Four-Membered Rings as Building Elements

Boryl metal complexes are not old hat, as demonstrated by the great interest in this class of compounds in recent years. Today, the importance of these complexes lies mainly in their role as intermediates in borylations catalyzed by transition metals [Eq. (1)], for which there are numerous synthetic applications. With regard to new types of structures, the combination metal complex/borane continues to produce many novelties, for example σ complexes of type 1.

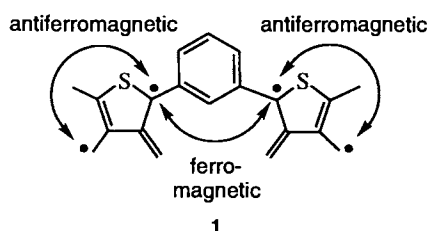


$E = H, BR_2, SiR_3, \dots$

H. Wadepohl* 2441–2444

Boryl Metal Complexes, Boron Complexes, and Catalytic (Hydro)boration

The toolbox for spin coupling is now well equipped, since nearly all possible topologies of organic tri- and tetradicals are known, which can be applied as building blocks for the synthesis of practically useful polyradical materials. High-spin polyradicals could be useful as organic ferromagnets, whereas several low-spin polyradicals are suggested to support electric conductivity. An example of the latter is the derivative of the singlet tetradical 1, in which both ferromagnetic and anti-ferromagnetic coupling operate.

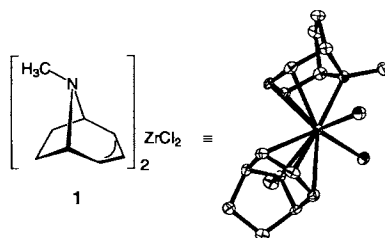


W. M. Nau* 2445–2448

Organic Tri- and Tetradicals with High-Spin or Low-Spin States

COMMUNICATIONS

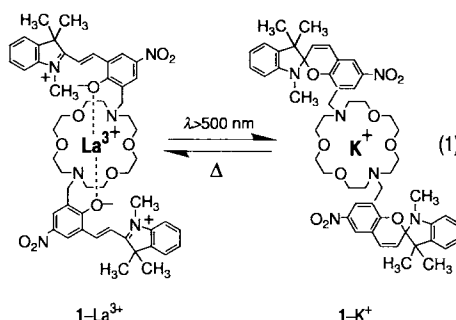
Isoelectronic to cyclopentadienyl but less symmetrical: the tropidynyl (trop) ligand. Therefore, in the stable complexes $[(trop)_2ZrCl_2]$ (1) and $[(trop)_2ZrMe_2]$, the two trop ligands are rotated by 77 and 88° with respect to one another. Preliminary investigations show that 1 catalyzes the polymerization of ethylene.



G. G. Lavoie,
R. G. Bergman* 2450–2452

Synthesis, Structural Characterization, and Reactivity of Novel Zirconium(IV) Complexes Containing the Tropidynyl Ligand

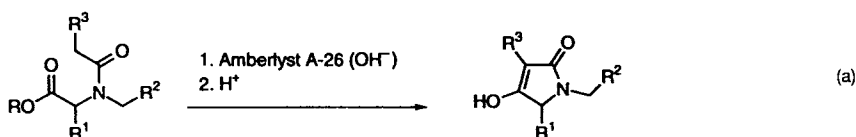
The transition between the merocyanine and spiropyran forms switches the selectivity of the bis(spiropyran) azacrown ether 1 from La^{3+} to K^+ [Eq. (1)]. Thus, 1 offers much greater possibilities for selectivity control between multi- and monovalent metal ions than the corresponding unsubstituted azacrown ether.



K. Kimura,* T. Utsumi, T. Teranishi,
M. Yokoyama, H. Sakamoto,
M. Okamoto, R. Arakawa,
H. Moriguchi, Y. Miyaji 2452–2454

High La^{III} Affinity of a Bis(spirobenzopyran) Azacrown Ether and Photoinduced Switching of its Ion Selectivity between Multivalent and Monovalent Metal Ions

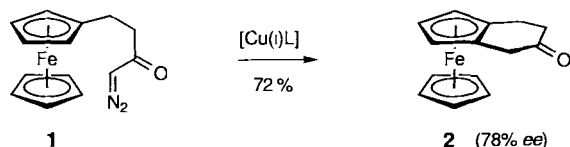
By temporary immobilization on a quaternary ammonium resin (Amberlyst 26-A, OH^- form), the acidic 2,4-pyrrolidinediones (tetramic acids) could be purified immediately after being synthesized by a Dieckmann condensation of amide esters that was catalyzed by this resin [Eq. (a)]. $R^1 = H$, alkyl, benzyl; $R^2 =$ phenyl, aryl; $R^3 = CN$, $o-O_2NC_6H_4$, $P(O)(OEt)_2$.



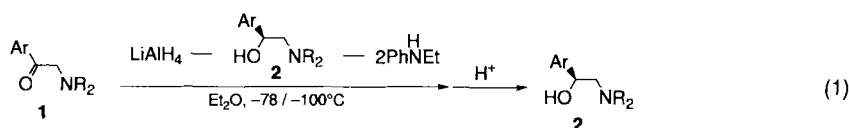
B. A. Kulkarni,
A. Ganesan* 2454–2455

Ion-Exchange Resins for Combinatorial Synthesis: 2,4-Pyrrolidinediones by Dieckmann Condensation

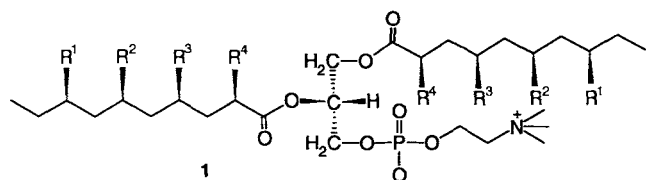
Not only significant enantioselectivities, but also chemical yields that are clearly higher than with achiral catalysts are seen for the asymmetric variant of the transition metal catalyzed cyclization of diazoketones such as **1**. The carbene chemistry known for the functionalization of benzene derivatives has now been transferred to ferrocene for the first time.



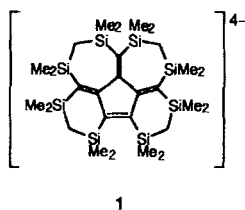
The product triggers the enantioselectivity. This concept is exemplified by the reduction of α -amino ketones with lithium aluminum hydride shown in Equation (1). By first modifying the reducing agent with product alcohols as chiral ligands, yields of 65–93% and *ee* values of 69–90% *ee* are obtained.



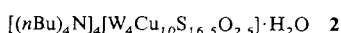
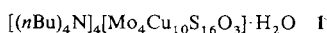
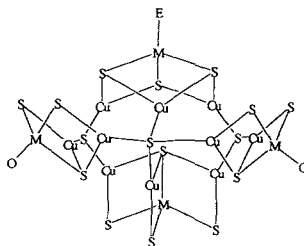
The number of methyl groups on the acyl groups of phosphatidylcholines **1** (R^1 – R^4 = H, CH_3) determines their surfactant characteristics. Differential calorimetric investigations show that little or even no branching leads to ordered gel phases. The behavior of the compounds at the water–air interface is also determined by these structural factors.



Orange crystals of the tetralithium salt of the tetraanion **1** were isolated from the reduction of the neutral octasilyl-substituted trimethylenecyclopentene compound with lithium in THF. The tetraanion **1** is the first example of an eight-center, twelve-electron π system.



Self-assembly with incorporation of sulfur ligands into the systems $[\text{MS}_n\text{O}_{4-n}]^{2-}/\text{Cu}^+$ ($M = \text{Mo}, \text{W}$; $n = 3, 4$) leads to the synthesis of salts **1** and **2**. The framework of their anions is shown schematically on the right. It consists of one cubane-like $\text{Cu}_3\text{MS}_3\text{E}$ fragment, one trigonal-prismatic Cu_3MS_4 fragment, and two butterfly-type $\text{Cu}_2\text{MS}_3\text{O}$ fragments that are bridged by one μ_4 -S and two μ_3 -S atoms. Clusters such as **1** and **2** are of interest inter alia as models for the active centers of some enzymes.



S. Siegel, H. G. Schmalz* 2456–2458

Insertion of Carbenoids into Cp–H Bonds of Ferrocenes: An Enantioselective-Catalytic Entry to Planar-Chiral Ferrocenes

T. Shibata, T. Takahashi, T. Konishi, K. Soai* 2458–2460

Asymmetric Self-Replication of Chiral 1,2-Amino Alcohols by Highly Enantioselective Autoinductive Reduction

M. Morr,* J. Fortkamp, S. R  he 2460–2462

Chiral Methyl-Branched Surfactants and Phospholipids: Synthesis and Properties

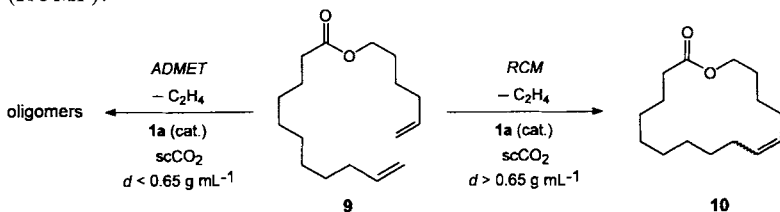
A. Sekiguchi,* T. Matsuo, C. Kabuto 2462–2464

A Supercharged Anion with a Silyl-Substituted Eight-Center, Twelve-Electron π System: Synthesis and Characterization of the Tetralithium Salt of an Octasilyl-Substituted Trimethylenecyclopentene Tetraanion

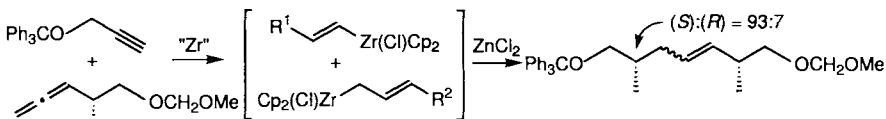
J. Guo, X.-T. Wu,* W.-J. Zhang, T.-L. Sheng, Q. Huang, P. Lin, Q.-M. Wang, J.-X. Lu 2464–2466

Tetradecanuclear Molybdenum (Tungsten)/Copper/Sulfur Heterobimetallic Clusters $[(n\text{Bu})_4\text{N}]_4[\text{M}_4\text{Cu}_{10}\text{S}_{16}\text{O}_2\text{E}] \cdot \text{H}_2\text{O}$, ($M = \text{Mo}, \text{E} = \text{O}$; $M = \text{W}, \text{E} = 1/2\text{O} + 1/2\text{S}$)

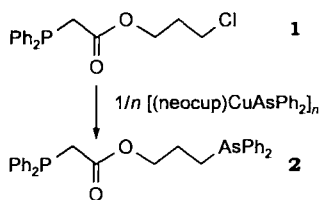
The product distribution can be controlled by varying the density of the reaction medium when olefin metatheses of acyclic dienes are carried out in supercritical CO₂ (scCO₂), as shown below. Substrates with NH groups, which are generally not tolerated in conventional solvents, are compatible with Ru-based metathesis catalysts in scCO₂. Avoidance of potentially hazardous organic solvents, simple isolation of the products, and the recovery of the catalysts in active form are additional practical advantages associated with using compressed CO₂ as reaction medium for ring-closing metathesis (RCM) and ring-opening metathesis polymerization (ROMP).



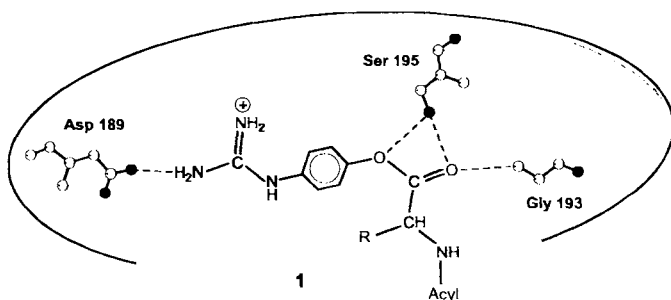
The α -adduct is the sole product of the coupling of vinyl- and allylzirconium compounds with ZnCl₂ (see below), provided no Mg^{II} salts are present. The zirconium compounds are formed in situ from alkynes and allenes, and the overall reaction opens a new preparative route to the vitamin E side chain through asymmetric induction in the 1,5-position. R¹ = CH₂OCPh₃, R² = CHMeCH₂OCH₂OMe, "Zr" = [Cp₂Zr(H)Cl].



Use of bipyridine, phenanthroline, or neocuproine as the co-ligand results in fine-tuning of the reactivity of copper(I) pnictogenide complexes with respect to organohalides. This therefore allows the selective synthesis of functionalized phosphanes (1) and arsanes as well as mixed phosphanyl arsanes (2).



Cationic specificity determinants of substrate mimetics 1 bind optimally to the binding site of highly specific proteases that normally determines their primary specificity. This designed imitation not only allows trypsin-catalyzed nonspecific and irreversible peptide-bond formation, but now also the use of thrombin and especially the cysteine protease clostripain, which acts as the most efficient peptide ligase.



A. Fürstner,* D. Koch, K. Langemann, W. Leitner,* C. Six 2466–2469

Olefin Metathesis in Compressed Carbon Dioxide

K. Suzuki,* T. Imai, S. Yamanoi, M. Chino, T. Matsumoto 2469–2471

Unusual Regioselectivity in the Reductive Coupling of Alkynes and Allenes by Hydrozirconation and Zinca-Claisen Rearrangement

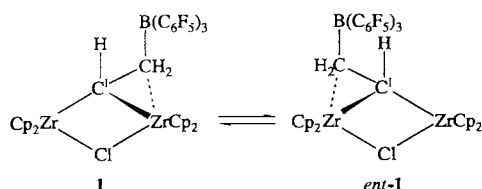
C. Meyer, H. Grützmacher,* H. Pritzkow 2471–2473

Copper Pnictogenides as Selective Reagents: A New Access to Functionalized Phosphanes and Arsanes

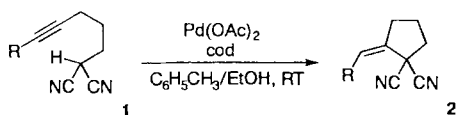
F. Bordusa, D. Ullmann, C. Elsner, H. D. Jakubke* 2473–2475

Substrate Mimetic Mediated Peptide Synthesis: An Irreversible Ligation Strategy That Is Independent of Substrate Specificity

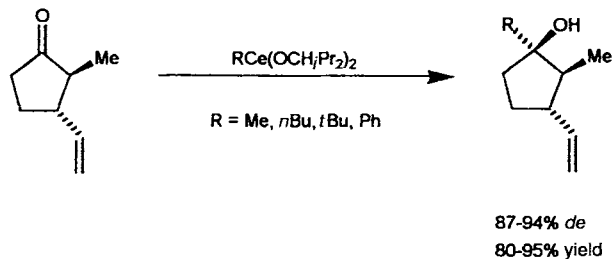
An intramolecular ion-pair interaction stabilizes the unusual, distorted coordination geometry of C¹ in **1**. In the course of the topomerization **1** \rightleftharpoons *ent*-**1**, which was followed by NMR spectroscopy, the internal Zr \cdots CH₂ ion pair must be cleaved. The rearrangement pathway probably proceeds via a species with "normal" tetrahedral coordination geometry at C¹.



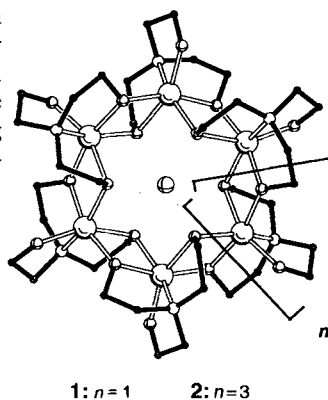
A [(cod)Pd⁰] species is the catalyst for the title reaction. ϵ -Alkynyl malononitriles **1** cyclize selectively in the process to give (*Z*)-alkylenecyclopentanes **2** in good to very good yields. Phosphanepalladium complexes are significantly less effective in this reaction than alkenepalladium compounds. cod = 1,5-cyclooctadiene.



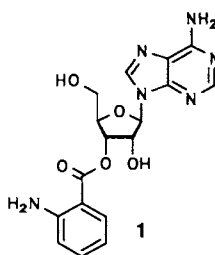
Low basicity and high nucleophilicity are the important characteristics of organocerium reagents that make them suitable for reactions with readily enolizable substrates such as the cyclopentanone derivative shown below. The organocerium compounds presented here add to such carbonyl substrates in a highly selective fashion and afford the corresponding alcohol in excellent yields; increasing the steric hindrance of the reagent leads to higher diastereoselectivity.



The type of bait determines the prey: In a pond with triethanolamine ligands and iron(III) ions, six- (**1**) or eight-membered (**2**) iron coronates can be captured, depending upon whether sodium or cesium ions are used as the bait. This finding is especially interesting in connection with a possible combinatorial approach in supramolecular chemistry.



Anthraniloyladenine **1** binds specifically to the elongation factor Tu of the bacterial protein biosynthesis. The structure and binding features in the molecular recognition of **1**, which acts as a mimetic of charged tRNA, could be inferred from detailed NMR investigations.



J. Schottek, G. Erker,*
R. Fröhlich 2475–2477

Stabilization of a C_{2v}-Distorted Methane Derivative in an Organometallic Framework

N. Tsukada, Y. Yamamoto* ... 2477–2480

Intramolecular Hydrocarbonation of ϵ -Alkynyl Malononitriles Catalyzed by Palladium Olefin Complexes

C. Alcaraz, U. Groth* 2480–2482

Ligand Effects in Diastereoselective Additions of Organocerium Reagents to Carbonyl Substrates

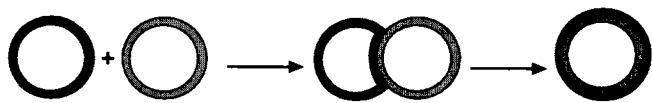
R. W. Saalfrank,* I. Bernt, E. Uller,
F. Hampel 2482–2485

Template-Mediated Self Assembly of Six- and Eight-Membered Iron Coronates

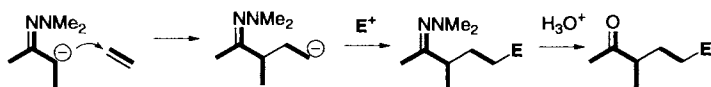
S. Limmer,* M. Vogtherr, B. Nawrot,
R. Hillenbrand, M. Sprinzl ... 2485–2489

Specific Recognition of a Minimal Model of Aminoacylated tRNA by the Elongation Factor Tu of Bacterial Protein Biosynthesis

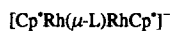
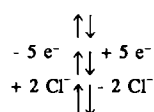
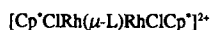
Two giant vesicles of opposite charge are seen by phase-contrast microscopy to “snap together” when brought into contact with each other. One of the vesicles then bursts, thereby surrounding the other with a layer of opposite charge (shown schematically below). The process can be repeated to construct alternating layers.



An olefinic analogue of the aldol reaction makes possible the ready synthesis of ketones by coupling the three components: zinc hydrazone, olefin (e. g. ethylene or styrene), and electrophile E^+ (see below). Fine-tuning the electronic properties of the carbometalated hydrazone is decisive for the success of this reaction.



Electron-reservoir behavior, the formation of Rh^I/Rh^{II} mixed-valent species, and the separation of redox processes and thus “communication” between individual reaction centers were established in a first systematic study of the ligand-mediated coupling of two equivalent “chemical” redox (ECE) reaction centers (E = electron transfer, C = chemical step (here dissociation of chloride); see scheme on the right, $Cp^* = C_5Me_5$, L = multidentate ligand).



F. M. Menger,* J. S. Keiper . . . 2489–2491

Electrostatic Layering of Giant Vesicles

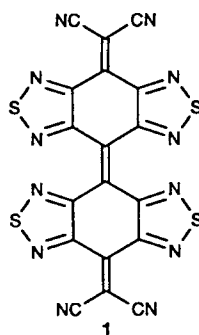
K. Kubota, E. Nakamura* . . . 2491–2493

Addition of Azaenolates to Simple, Unactivated Olefins

W. Kaim,* R. Reinhardt, J. Fiedler 2493–2495

Ligand-Mediated Coupling of Organo-metallic Reaction Centers

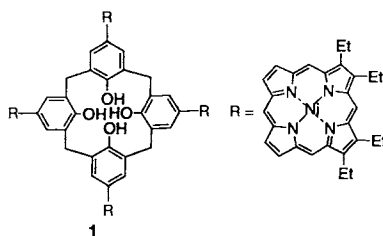
Reversible machano- and thermochromic behavior are features of the title bis(tricyclic) olefin. These characteristics are a consequence of the different properties of the interconvertible folded and twisted conformers. Despite the severe molecular deformation the conductive charge-transfer complexes and stable salts of the radical anion could be isolated due to their strong electron affinity.



T. Suzuki,* T. Fukushima, T. Miyashi, T. Tsuji 2495–2497

Isolation and X-ray Structural Determination of Both Folded and Twisted Conformers of Bis{4*H*,8*H*-4-(dicyanomethylene)-benzo[1,2-*c*:4,5-*c'*]bis[1,2,5]thiadiazol-8-ylidene}, an Overcrowded Ethylene with High Electron Affinity

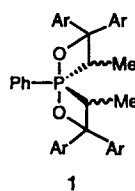
All four porphyrin units on the same side—that is the surprising conformation adopted by calixarene **1**. A “cogwheel” dimeric structure was identified for the compound in the solid state, in which π - π aggregation is the dominating structural feature.



R. G. Khoury, L. Jaquinod, K. Aoyagi, M. M. Olmstead, A. J. Fisher, K. M. Smith* 2497–2500

A Calix[4]arenoporphyrin

A distorted tetragonal-pyramidal structure is adopted by the *trans-trans* diastereomer of the spirophosphorane **1**. In contrast, the *cis-trans* isomer displays a distorted trigonal-bipyramidal structure. These two as well as the *cis-cis* diastereomer were synthesized as stable crystals by taking advantage of electronic and steric effects of the methyl groups in the 3- and 7-positions. Interestingly, thermolysis of **1** gave two molar equivalents of $Ar_2C=CHMe$. $Ar = 4-ClC_6H_4$.

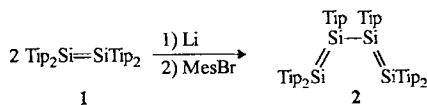


T. Kawashima,* Rei Okazaki, Renji Okazaki* 2500–2502

Synthesis, Structure, and Double Olefin Extrusion of All Three Diastereomers of 2,2,6,6-Tetrakis(4-chlorophenyl)-3,7-dimethyl-4-phenyl-1,5-dioxo-4 λ^5 -phosphaspiro[3.3]heptane

The first tetrasilabuta-1,3-diene (2)

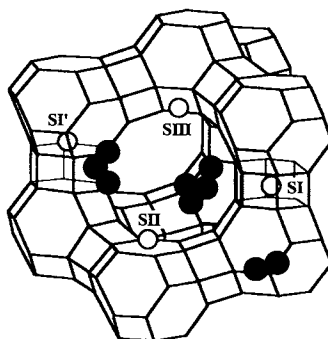
was obtained as reddish-brown crystals simply and unexpectedly by lithiation of disilene **1**, partial bromination with an aryl bromide, and intermolecular cleavage of lithium bromide. The conjugation between the two Si–Si double bonds of **2** was demonstrated by electron spectroscopy and X-ray crystallography. Mes = 2,4,6-Me₃C₆H₂, Tip = 2,4,6-*i*Pr₃C₆H₂.



M. Weidenbruch,* S. Willms, W. Saak,
G. Henkel 2503–2504

Hexaaryltetrasilabuta-1,3-diene:
A Molecule with Conjugated Si–Si Double Bonds

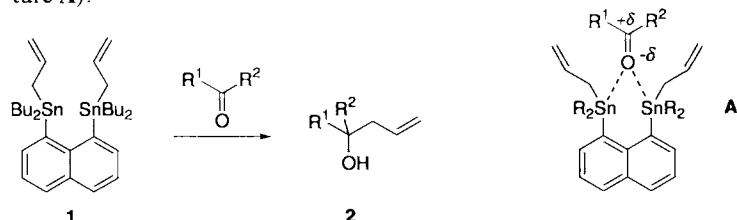
An increase in the basicity of the zeolite host, which is determined by the oxide guest component, was observed for the first time with a zeolite impregnated with cesium hydroxide (a section of the structure is shown on the right; ○ cations, ● guest component). The application of such materials as basic solid-state catalysts could be of interest for the chemical industry.



M. Hunger,* U. Schenk, B. Burger,
J. Weitkamp 2504–2506

Synergism between the Guest Compound
and the Host Framework in Zeolite CsNaY
after Impregnation with Cesium Hydroxide

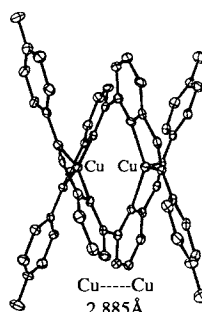
A large variety of carbonyl substrates can be allylated with **1** under neutral conditions. In the case of dicarbonyl compounds, products **2** form chemoselectively. The driving force of this reaction is ascribed to the latent Lewis acidity, which is induced by chelation of neutral, bidentate bis(stannane)s on the carbonyl group (structure **A**).



N. Asao, P. Liu,
K. Maruoka* 2507–2509

1,8-Bis(allylstannyl)naphthalene Derivatives as Neutral Allylation Agents: Rate Acceleration by Chelation-Induced Lewis Acidity

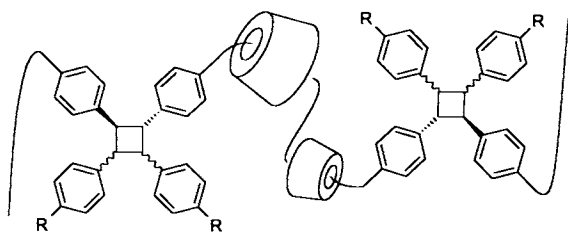
The isolation of a mononuclear key intermediate and the measurement of stability constants gave insight into the stepwise formation of helicates (depicted on the right) consisting of copper(I) ions and oligopyridine ligands. A positive cooperativity for cation binding is not mandatory for helicate formation.



R. Ziessel,* A. Harriman,* J. Suffert,
M. T. Youinou, A. De Cian,
J. Fischer 2509–2511

Copper(I) Helicates Containing Bridging
But Nonchelating Polypyridine Fragments

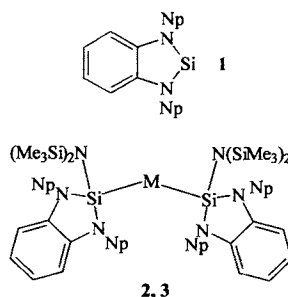
The additional inclusion of stilbene monomers within cyclodextrin rings strung on a stilbene polymer leads to a supramolecular stabilization of the molecular necklace. This assembly can be transformed into a polyrotaxane (see drawing below) by photochemical formation of tetraphenylcyclobutane blocking groups.



W. Herrmann, M. Schneider,
G. Wenz* 2511–2514

Photochemical Synthesis of Polyrotaxanes
from Stilbene Polymers and Cyclodextrins

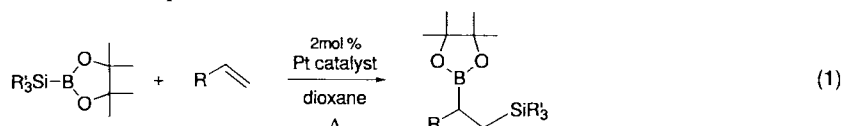
The first insertion of a silylene into a M–N bond was observed in the presented transformations of the thermally stable silylene **1**, Np = neopentyl, with metal(II) bis(silyl)amides. Bis(silyl)metal(II) compounds **2** and **3** were obtained for M = Sn and Pb, respectively, whereas a colorless azadisilagermole was formed for M = Ge. Noteworthy is the very long Sn–Si bond of 2.712(2) Å in **2**.



B. Gehrhus, P. B. Hitchcock,
M. F. Lappert* 2514–2516

New Reactions of a Silylene: Insertion into
M–N Bonds of $M[N(SiMe_3)_2]_2$ (M = Ge,
Sn, or Pb)

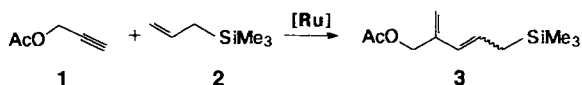
2-Boryl-1-silylalkanes form regioselectively upon addition of a B–Si bond to the C–C double bond of simple terminal alkenes in the presence of a (triphenylphosphane)platinum complex as catalyst [Eq. (1)]. At the B–C bond, homologation by one C atom is possible.



M. Suginome, H. Nakamura,
Y. Ito* 2516–2518

Platinum-Catalyzed Regioselective Silabo-
ration of Alkenes

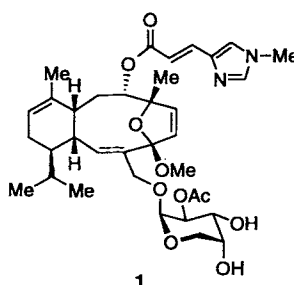
No special functional groups are required for a new method of selective C–C coupling of monosubstituted alkynes such as **1** with alkenes like **2**. This crossed yne–ene metathesis also proceeds with atom economy, and provides easy access to such interesting synthetic building blocks as the 1,3-substituted diene **3**.



R. Stragies, M. Schuster,
S. Blechert* 2518–2520

A Crossed Yne–Ene Metathesis Showing
Atom Economy

Taxol-like activity is exhibited by eleutherobin (**1**), one of the most promising antitumor agents isolated from nature in recent years. The first total synthesis of this compound also provided a route to two biologically active analogues, thus enabling the first structure–activity relationships within the eleutherobin family to be established.



K. C. Nicolaou,* F. van Delft,
T. Ohshima, D. Vourloumis, J. Xu,
S. Hosokawa, J. Pfefferkorn,
S. Kim, T. Li 2520–2524

Total Synthesis of Eleutherobin

* Author to whom correspondence should be addressed

BOOKS

Concepts in Chemistry – A Contemporary Challenge • D. H. Rouvray

Fuzzy Logic in Chemistry • D. H. Rouvray

An Introduction to Polymer Science • H.-G. Elias

Alkyl Polyglycosides. Technology, Properties and Applications •
K. Hill, W. von Rybinski, G. Stoll

Enzymes. A Practical Introduction to Structure, Mechanism and Data Analysis •
R. A. Copeland

I. Hargittai 2525

F. Ehrentreich 2524

M. Soucek 2526

H.-D. Dörfler 2527

J. Rétey 2527

| | |
|--|--|
| Organic and Bio-organic Mechanisms · M. Page, A. Williams | <i>M. Kalesse</i> 2528 |
| Fundamental Toxicology for Chemists · J. H. Duffus, H. G. J. Worth | <i>J. Döhmer, D. Lenoir</i> 2529 |
| Handbook of Downstream Processing · E. Goldberg | <i>E. Ehlers</i> 2529 |
| Molecular Chemistry of the Transition Elements. An Introductory Course · F. Mathey, A. Sevin | <i>L. H. Gade</i> 2530 |

German versions of all reviews, communications, and highlights in this issue appear in the December issue of *Angewandte Chemie*. The appropriate page numbers can be found at the end of each article and are also included in the Author Index on p. 2533.

All the Tables of Contents from 1995 onwards may be
found on the WWW under:
<http://www.wiley-vch.de/home/angewandte>

SERVICES

| | |
|----------------|-------|
| ● Sources | A-101 |
| ● Events | 2448 |
| ● Keywords | 2532 |
| ● Author Index | 2533 |
| ● Preview | 2534 |

The following reviews will appear in future issues:

Charge Transfer through the DNA Base Stack
J. K. Barton

Catabolic Pathways and Their Biocatalysts: Bacterial Degradation of Quinoline and Derivatives
S. Fetzner, B. Tshisuaka, F. Lings, R. Kappl, J. Hüttermann

Aerogels—Airy Materials: Chemistry - Structure - Properties
U. Schubert, N. Hüsing

A New Model for Aluminophosphate Formation: Transformation of a Linear Aluminophosphate to Chain, Layer, and Framework Structural Types
G. A. Ozin

Supramolecular Electrochemistry
L. Echegoyen, P. L. Boulas M. Gómez-Kaifer

Four- π -Electron Four-Membered λ^5 -Phosphorus Heterocycles: Electronic Isomers of Heterocyclobutadienes
G. Bertrand

C₃ Symmetry in Asymmetric Catalysis and Chiral Recognition
C. Moberg

Commercial, Synthetic Non-Nutritive Sweeteners
D. J. Ager, D. P. Pantaleone

α -Heterosubstituted 1-Alkenyllithium Reagents: Carbanions and Carbenoids for C–C Bond Formation
M. Braun

Lithistid Sponges: Star Performers or Hosts to the Stars
C. A. Bewley, D. J. Faulkner

Electroluminescent Conjugated Polymers—Seeing Polymers in A New Light
A. Kraft, A. C. Grimsdale, A. B. Holmes

Protein Folding: A Perspective from Theory & Experiment
C. M. Dobson, A. Šali, M. Karplus

Vicinal Diamines: Biological and Chemical Interest, Methods of Preparation
D. Lucet, T. Le Gall, C. Mioskowski

Cationic Liposomes for Gene Therapy
A. D. Miller

Ligand Design for Electrochemically Controlling Transition Metal Stoichiometric and Catalytic Reactivity
A. M. Allgeier, C. A. Mirkin

Chemical Applications of ZEKE Spectroscopy
K. Müller-Dethlefs, E. W. Schlag

Moderne Varianten der Mannich-Reaktion
M. Arend, B. Westermann, N. Risch

ANGEWANDTE CHEMIE

A Journal of the
Gesellschaft
Deutscher Chemiker

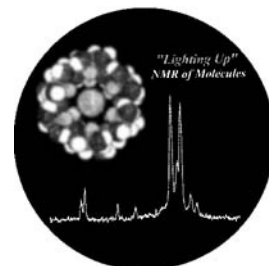
International Edition in English

1997
36/21

Pages 2257–2388

COVER PICTURE

The cover picture shows at the top left corner a space-filling model of an α -cyclodextrin molecule containing a xenon atom in its hydrophobic pocket. By application of optical pumping, a large nuclear-spin polarization of the xenon atom can be achieved, which can be transferred by cross-relaxation to ^1H nuclei near xenon binding sites. This process, dubbed “spin polarization induced nuclear overhauser effect” (SPINOE), permits selective enhancement of NMR signals for protons in the interior of the pocket. A section of a SPINOE NMR spectrum of dehydrated α -cyclodextrin after introduction of laser-polarized xenon is shown at the bottom. Read more about this promising method in the contribution from A. Pines et al. on pages 2368–2370.

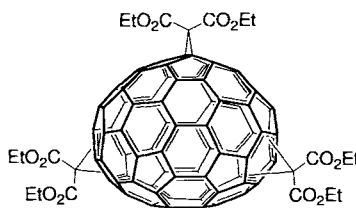


REVIEWS

Contents

The chemistry of higher fullerenes is no longer on the sidelines. Seven years

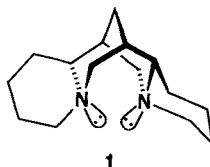
after fullerenes became available on a preparative scale, the functionalization of the higher homologues of buckminsterfullerene C_{60} —in particular C_{70} , but also C_{76} , C_{78} (a tris-adduct is shown on the right as an example), and C_{84} —has made considerable progress. It has now been reviewed for the first time under particular consideration of the aspects of chirality and some emerging reactivity principles.



C. Thilgen, A. Herrmann,
F. Diederich* 2268–2280

The Covalent Chemistry of Higher Fullerenes: C_{70} and Beyond

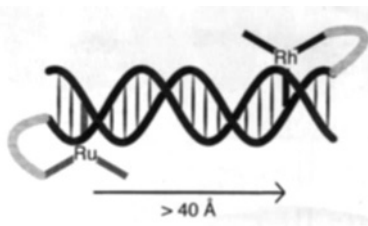
No longer on the list of exotic synthons! “Chiral carbanions”, that is. enantiomerically enriched lithium carbanion pairs, have for some time played an important role in asymmetric synthesis. The trick lies in using chiral ligands such as the lupine alkaloid (–)-sparteine **1**, which has gained a reputation for its exceptional efficiency and wide applicability.



D. Hoppe,* T. Hense 2282–2316

Enantioselective Synthesis with
Lithium/(–)-Sparteine Carbanion Pairs

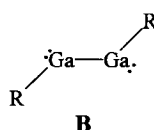
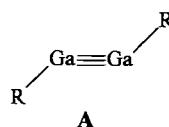
Electron transfer over distances of more than 40 Å through a DNA double strand (see schematic representation on the right) still stimulates controversy about mechanism but seems to be proven experimentally. Biochemical processes such as repair of photodimer damage can be initiated by DNA electron transfer. The dependence of electron transport on how nearly perfect a DNA base stack is suggests that conductivity can be used to quantify stacking quality or to recognize a DNA single strand.



U. Diederichsen* 2317–2319

Charge Transfer in DNA: A Controversy

Which formula gives the best representation for the bonding in the “gallyne” **1** (Mes* = 2,4,6-*i*Pr₃C₆H₂) recently reported by Robinson et al., **A** or **B**? Is there a Ga–Ga triple bond, although the classical criteria are not met?

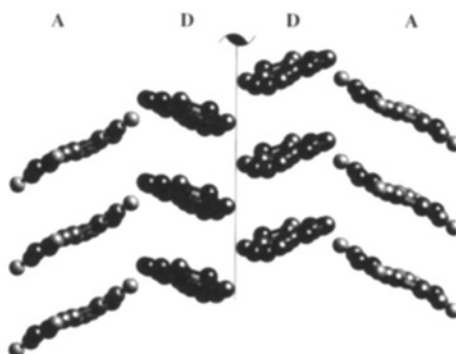


K. W. Klinkhammer* 2320–2322

How Can One Recognize a Triple Bond between Main Group Elements?

COMMUNICATIONS

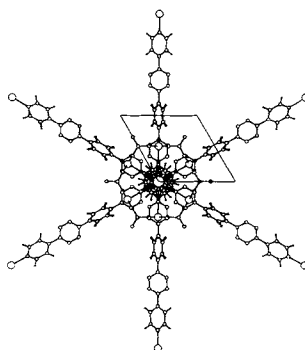
Pairs of stacks of organic donors **D** in the salt [(DT-TTF)₂][Au(mnt)₂] (DT-TTF = dithiophene-tetrathiafulvalene, mnt = maleonitriledithiolate) form a classical ladder structure due to three close S···S interactions (see picture). Below 225 K the double stack of donor molecules forms a spin ladder with two legs, which arises through localization of unpaired electrons in the (DT-TTF)₂ dimers.



C. Rovira,* J. Veciana, E. Ribera, J. Tarrés, E. Canadell, R. Rousseau, M. Mas, E. Molins, M. Almeida, R. T. Henriques, J. Morgado, J.-P. Schoeffel, J. P. Pouget ... 2324–2326

An Organic Spin-Ladder Molecular Material

A helical staircase structure is observed for the layers made from chains of alternating Ag^I centers and pytz ligands in [Ag(pytz)(NO₃)]_∞ (pytz = 3,6-di-(4-pyridyl)-1,2,4,5-tetrazine). Decisive for the formation of this array—a view of the structure along the helical axis is shown on the right—is the anionic ligand NO₃[−], as shown by the comparison with the analogous PF₆[−] and BF₄[−] compounds. These two show parallel chains of alternating Ag^I ions and pytz ligands held in pairs through weak Ag–Ag contacts and π–π interactions between adjacent pytz ligands.



M. A. Withersby, A. J. Blake, N. R. Champness, P. Hubberstey,* W. S. Li, M. Schröder* 2327–2329

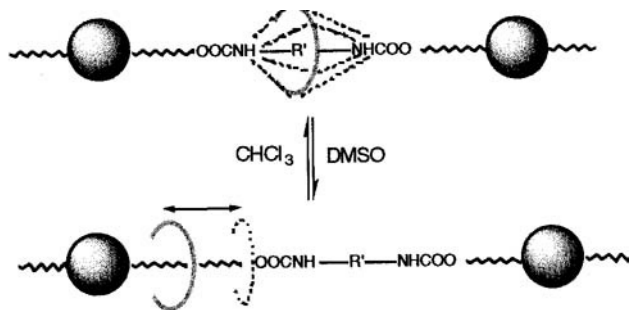
Anion Control in Bipyridylsilver(I) Networks: A Helical Polymeric Array

The use of high magnetic field and high frequency in an unconventional spectrometer has provided very informative EPR spectra of a manganese(III) octahedral complex for the first time. The parameters of the spin Hamiltonian operator are in fair agreement with those calculated with ligand-field theory. High-frequency EPR is thus a powerful tool for the structural investigation of complexes that contain metal ions with integer spins.

A.-L. Barra, D. Gatteschi,* R. Sessoli, G. L. Abbati, A. Cornia, A. C. Fabretti, M. G. Uytterhoeven 2329–2331

Electronic Structure of Manganese(III) Compounds from High-Frequency EPR Spectra

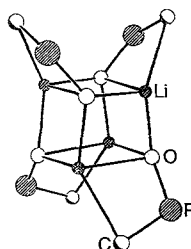
Localized at the NH group in chloroform, but forced away from the NH group in DMSO: This describes the behavior of the cyclic units in poly(urethane/crown ether rotaxane)s. The dependency on the solvent results in different microstructures (shown schematically below).



C. Gong, H. W. Gibson* 2331–2333

Controlling Microstructure in Polymeric Molecular Shuttles: Solvent-Induced Localization of Macrocycles in Poly(urethane/crown ether) Rotaxanes

A cubane-like tetrameric structure with Li–C bonds and two stereogenic centers per monomeric unit results from lithiation of $\text{Ph}_2\text{P}(\text{O})\text{CH}_2\text{C}(\text{H})\text{MeEt}$ in toluene. Retention of the Li–C bonds on dissolution in $[\text{D}_8]\text{THF}$ is confirmed by ^{13}C NMR spectroscopy. The central framework of this lithiated phosphane oxide is shown on the right.



J. E. Davies, R. P. Davies, L. Dunbar, P. R. Raithby, M. G. Russell, R. Snaith,* S. Warren, A. E. H. Wheatley 2334–2335

The First Lithiated Phosphane Oxide with Li–C Bonds: Synthesis and Structure of $\{[\text{Ph}_2\text{P}(\text{O})\text{CHLiC}(\text{H})\text{MeEt}]_4\}$

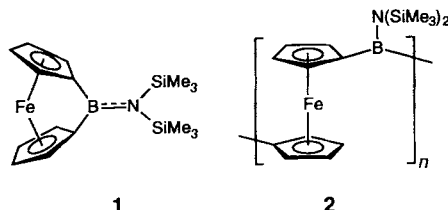
Two independent and interpenetrating two-dimensional networks, whose outstanding structural features are the polyrotaxane columns of the unprecedented type shown on the right, are found in the coordination polymer $[\text{Zn}(\text{bix})_2(\text{NO}_3)_2] \cdot 4.5 \text{H}_2\text{O}$. This compound is only the third example of a 2-D rotaxane; the other two were just recently reported.



B. F. Hoskins, R. Robson, D. A. Slizys* 2336–2338

The Structure of $[\text{Zn}(\text{bix})_2(\text{NO}_3)_2] \cdot 4.5 \text{H}_2\text{O}$ (bix = 1,4-Bis(imidazol-1-yl)methyl)-benzene): A New Type of Two-Dimensional Polyrotaxane

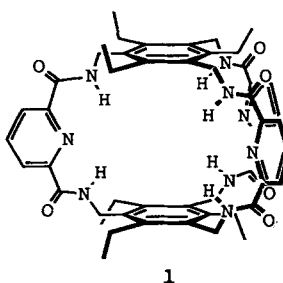
A new record tilt angle $[32.4(2)^\circ]$ is present between the planes of the cyclopentadienyl ligands in the [1]boraferrocenophane **1**. This compound is the first [1]ferrocenophane containing a first row element in the bridge. Ring-opening polymerization of **1** leads to cyclic oligomers and insoluble polymer **2**.



H. Braunschweig,* R. Dirk, M. Müller, P. Nguyen, R. Resendes, D. P. Gates, I. Manners* 2338–2340

Incorporation of a First Row Element into the Bridge of a Strained Metallocenophane: Synthesis of a Boron-Bridged [1]Ferrocenophane

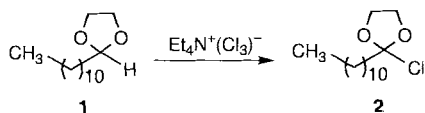
A combination of geometric and electrostatic complementarity explains why nitrate is bound only slightly less strongly than acetate within the bicyclic cyclophane **1**, although nitrate is a significantly weaker base. The crystal structure of the acetate complex of **1** depicts the binding of the anion in the host's cavity, as in the case of the analogous chloride complex.



A. P. Bisson, V. M. Lynch, M. K. C. Monahan, E. V. Anslyn* 2340–2342

Recognition of Anions through NH– π Hydrogen Bonds in a Bicyclic Cyclophane—Selectivity for Nitrate

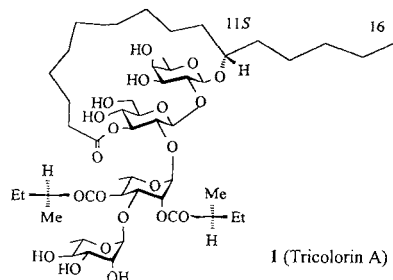
Applicable to a broad range of substrates and convenient to handle, the titel compound oxidizes saturated alcohols to aldehydes or ketones; in the case of allyl alcohols, chlorination at the double bond is preferred. Especially interesting is the reaction of acetal **1**, since other reagents provide α -halogenated acetals and not product **2**.



T. Schlama, K. Gabriel, V. Gouverneur, C. Mioskowski* 2342–2344

Tetraethylammonium Trichloride: A Versatile Reagent for Chlorinations and Oxidations

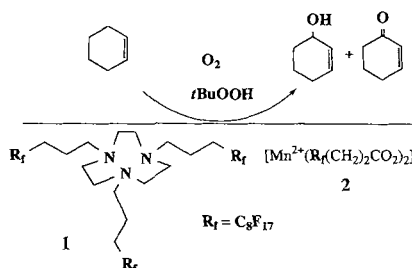
A regioselective macrolactonization and a one-pot synthesis are the key steps in the first total synthesis of tricolorin A (**1**), the principal component of a plant used in traditional Mexican agriculture for weed control. The synthesis of this macrolactone tetrasaccharide, which starts from D-(+)-mannitol, contains 45 steps with a longest linear sequence of 20 steps (overall yield 0.65%).



S. F. Lu, Q. O'yang, Z. W. Guo, B. Yu,* Y. Z. Hui* 2344–2346

The First Total Synthesis of Tricolorin A

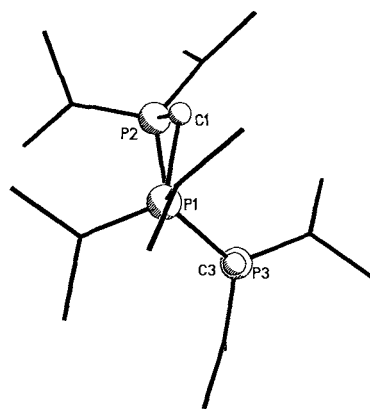
An autoxidation mechanism was involved in the oxidation of alkanes and alkenes with *t*BuOOH and O₂ under conditions of fluorous biphasic catalysis. The catalytically active complexes are soluble in perfluoroheptane and form in situ from ligand **1** and the Mn²⁺ complex **2** with polyfluorinated carboxylate ligands (fluoroponytails).



J. M. Vincent, A. Rabion, V. K. Yachandra, R. H. Fish* 2346–2349

Fluorous Biphasic Catalysis: Complexation of 1,4,7-[C₈F₁₇(CH₂)₃]₃-1,4,7-Triazacyclononane with [M(C₈F₁₇(CH₂)₂CO₂)₂] (M = Mn, Co) To Provide Perfluoroheptane-Soluble Catalysts for Alkane and Alkene Functionalization in the Presence of *t*-BuOOH and O₂

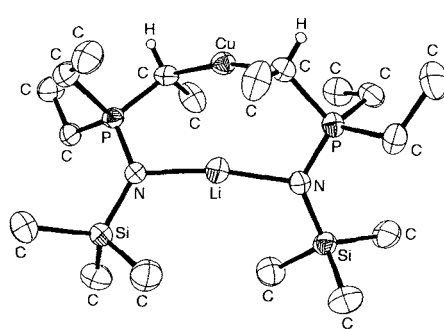
Three neighboring charge carriers are found in close proximity in the six-membered ring of the title compound. In the solid state the trication contains two PC units that lie in a plane, and a third unit attached slanted at an angle above the plane (a side view is depicted on the right).



E. Gorbunowa, G. Heckmann, E. Fluck,* M. Westerhausen, R. Janoschek 2349–2350

A 1,3,5-Triphosphantrium Ion

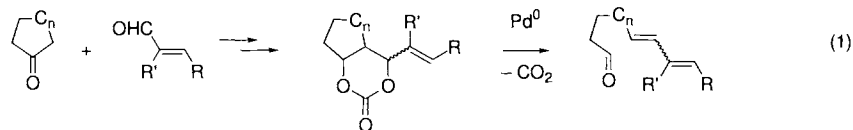
A nearly linear coordination geometry is exhibited by the two metal atoms in the lithium cuprate that is obtained from the title anion after reaction with CuI. The puckered eight-membered ring in this compound is depicted on the right; reaction of the carbanion with ZnCl₂ instead of CuI results in a 24-membered macrocycle.



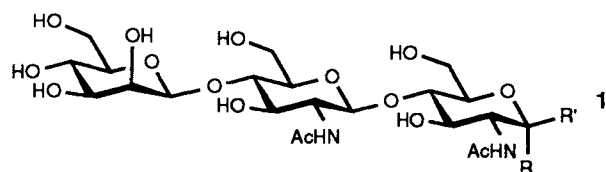
A. Müller, B. Neumüller, K. Dehnicke* 2350–2352

[CH(Me)P(Et)₂NSiMe₃][−]—A Carbanion That Functions as a Bridging Ligand

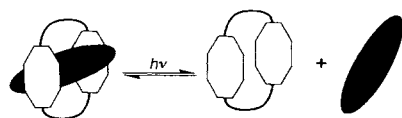
Excellent diastereoselectivity is observed for the conversion of cyclic vinyl-substituted carbonates into unsaturated open-chain carbonyl compounds [Eq. (1)]. Decisive for the success of this ring opening is a Pd^0 complex as the catalyst. C_n = complex, also cyclic substituted carbon chains with $n = 0, 1, 2, 4, 8$; R, R' = H, Me.



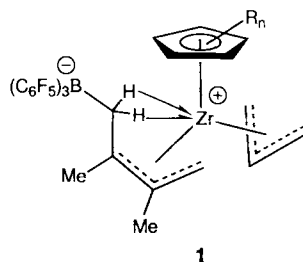
A highly stereo- and regioselective linkage for the β -1,4-mannoside bond of trisaccharide **1** (R/R' = H/OH) is achieved with a redesigned recombinant biocatalyst: a suitably modified yeast enzyme (ALG1) was expressed in *E. coli*; the enzyme was then immobilized on a Ni^{II} affinity column.



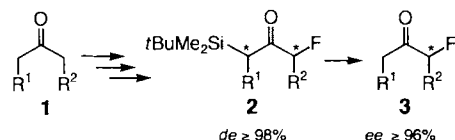
Careful balancing of the energy levels permits photoseparation of a closely coupled inclusion complex (see schematic representation below). Diffusive charge recombination gives rise to strong fluorescence upon optical excitation of the transitory (uncomplexed) guest molecule.



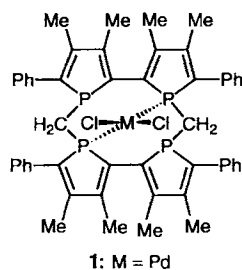
The zwitterionic allyl complex 1 ($\text{R}_n = 1,3\text{-(SiMe}_3)_2$) is a new catalyst type for the polymerization of ethene under mild conditions. The propensity of these and similar zwitterionic complexes for C–H activation and rearrangements is very sensitive to steric conditions. The reactions provide evidence for a new, surprisingly facile catalyst-deactivation mechanism.



Practically enantiopure α -fluoroketones 3 are accessible for the first time starting from simple ketones **1**. Key steps in this new method are the asymmetric electrophilic α -fluorination of α -silylketone enolates with NF reagents and subsequent racemization-free removal of the silyl auxiliary group.



No precipitation of palladium occurs when complex **1** is employed in Stille and Heck reactions, even at high temperature. This complex also remains fully active even after more than 48 h. The use of the title compound as a complex ligand is the first application of such phosphole macrocycles.



1: M = Pd

H. Harayama, T. Kuroki, M. Kimura, S. Tanaka, Y. Tamaru* 2352–2354

Synthesis of Doubly Unsaturated Aldehydes and Ketones by a Novel β -Decarboxylation

G. M. Watt, L. Revers, M. C. Webberley, I. B. H. Wilson, S. L. Flitsch* 2354–2356

Efficient Enzymatic Synthesis of the Core Trisaccharide of N-Glycans with a Recombinant β -Mannosyltransferase

A. C. Benniston,* A. Harriman,* D. S. Yufit 2356–2358

Artificial Phototropism: Reversible Photoseparation of Self-Assembled Interlocking Conjugates

G. J. Pindado, M. Thornton-Pett, M. Bouwkamp, A. Meetsma, B. Hessen,* M. Bochmann* 2358–2361

Novel Zwitterionic Diallylzirconium Complexes: Synthesis, Structure, Polymerization Activity, and Deactivation Pathways

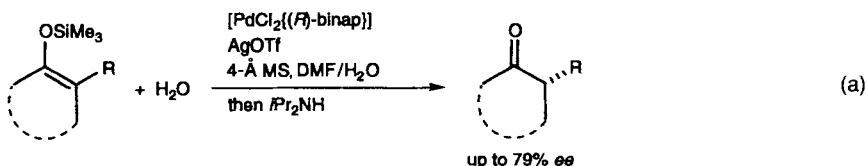
D. Enders,* M. Potthoff, G. Raabe, J. Runsink 2362–2364

Regio- and Enantioselective Synthesis of α -Fluoroketones by Electrophilic Fluorination of α -Silylketone Enolates with *N*-Fluorobenzosulfonimide

F. Mercier, F. Laporte, L. Ricard, F. Mathey,* M. Schröder, M. Regitz 2364–2366

The Use of a Ten-Membered Tetraphosphole Macrocycle To Increase the Lifetime of a Palladium Catalyst

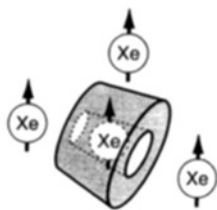
Addition of amine is required to convert the chiral cationic palladium complex obtained from a silver salt and $[\text{PdCl}_2\{(\text{R})\text{-binap}\}]$ into an efficient asymmetric catalyst for the protonation of cyclic silyl enol ethers with water [Eq. (a)]. The effect of the amine is most likely based on selective deactivation of an initially formed Pd–binap complex. The “surviving” Pd species cause a reaction that is slower but proceeds with enhanced enantioselectivity.



M. Sugiura, T. Nakai* 2366–2368

Asymmetric Catalytic Protonation of Silyl Enol Ethers with Chiral Palladium Complexes

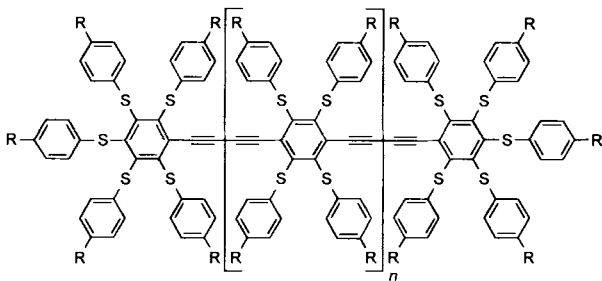
“Lighting up” the nuclear magnetic resonance of molecules with laser-polarized xenon could be a valuable new source of structural information. The ^1H NMR signals of protons near the xenon binding site in α -cyclodextrin (shown schematically on the right) are selectively enhanced through couplings that are sensitive to ^{129}Xe – ^1H internuclear distances.



Y. Q. Song, B. M. Goodson, R. E. Taylor, D. D. Laws, G. Navon, A. Pines* 2368–2370

Selective Enhancement of NMR Signals for α -Cyclodextrin with Laser-Polarized Xenon

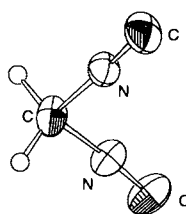
More positive reduction potentials with increasing molecular length characterize the title compounds (see drawing below, $n = 0, 1$). Their physical and chemical properties, in particular the facile reduction that was investigated with cyclic voltammetry, make them promising candidates for the development of molecular electronic and photonic devices.



M. Mayor, J. M. Lehn,* K. M. Fromm, D. Fenske 2370–2372

Reducible Nanoscale Molecular Rods Based on Diacetylene-Linked Poly(phenylthio)-Substituted Benzenes

Unstable even in solution is how Neidlein described diisocyanomethane, which has been known for over 30 years. Now this compound, the only geminal diisocyanide known (crystal structure depicted on the right), has been isolated by fractional condensation. The compound can be stabilized by coordination to transition metal complex fragments.



J. Buschmann, T. Bartolmäs, D. Lentz,* P. Luger, I. Neubert, M. Röttger 2372–2374

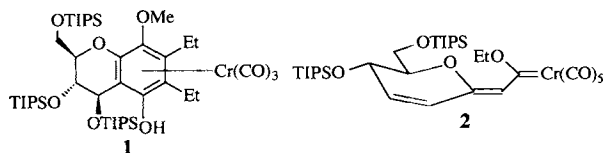
Synthesis, Structure, and Coordination Chemistry of Diisocyanomethane

Without an oxidant like O_2 , Fe/H-ZSM-5 catalysts are able to convert methane selectively into benzene, toluene, and naphthalene. Methane is activated on iron oxide clusters, and the primary product ethylene undergoes subsequent oligomerization and cyclization reactions on Brønsted acidic sites to form the aromatic products.

B. M. Weckhuysen, D. Wang, M. P. Rosynek, J. H. Lunsford* 2374–2376

Catalytic Conversion of Methane into Aromatic Hydrocarbons over Iron Oxide Loaded ZSM-5 Zeolites

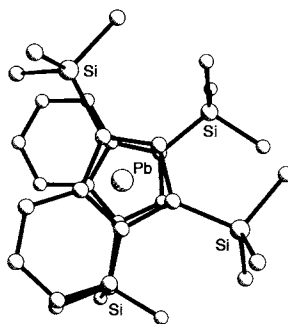
New opportunities in the functionalization of carbohydrates arise from carbene complex modified glycals. They undergo a chromium-induced benzannulation to give benzoglycals **1** and allow a C₂-homologization to **2** with retention of the metal–carbene bond by a diastereoselective insertion of yno! ethers.



K. H. Dötz,* R. Ehlenz,
D. Paetsch 2376–2378

Carbene Complex Modified Glycals:
Synthesis and Reactivity

Where are all the bis(π-indenyl) complexes of the “post-transition elements”? The first example of this type of complex with a Group 14 element has now been synthesized and characterized. [Pb{1,3-(SiMe₃)₂C₉H₅}₂] is unstable in solution, but forms thermally stable crystals that reveal a sandwich geometry with nearly parallel, η⁵-coordinated C₅ rings of the indenyl ligand (see structure on the right).



J. S. Overby, T. P. Hanusa,*
P. D. Boyle 2378–2379

Stabilization of the (π-Indenyl)–Lead Bond: The First Structurally Authenticated Bis(η⁵-indenyl) Complex of a Post-Transition Element, [Pb{1,3-(SiMe₃)₂C₉H₅}₂]

Not only pinacolate intermediates appear in McMurry reactions of aliphatic ketones R₂CO (R = Me, Et, *i*Pr) with MCl₄/Li(Hg) (M = Ti, U) [Eq. (1)]. Rather, carbenoid species must also be considered. This conclusion was drawn from an exact analysis of the reaction products as well as control experiments with pinacol derivatives. 2 R₂CO + [Ti[•]] → metallopinacolate or carbenoid? → R₂C=CR₂ (1)

C. Villiers,*
M. Ephritikhine* 2380–2382

New Insights into the Mechanism of the McMurry Reaction

* Author to whom correspondence should be addressed

BOOKS

Contents

Episodes from the History of the Rare Earth Elements • C. H. Evans

R. Anwander 2383

The History of the Faraday Society • L. E. Sutton, M. M. Davis

Lord Dainton 2384

Table of Isotopes • R. B. Firestone, V. S. Shirley

G. Herrmann 2384

German versions of all reviews, communications, and highlights in this issue appear in the first November issue of *Angewandte Chemie*. The appropriate page numbers can be found at the end of each article and are also included in the Author Index on p. 2387.

SERVICES

| | |
|----------------|------|
| • Events | 2322 |
| • Keywords | 2386 |
| • Author Index | 2387 |
| • Preview | 2388 |

All the Tables of Contents from 1995 onwards may be found on the WWW under:
<http://www.wiley-vch.de/home/angewandte>

ANGEWANDTE CHEMIE

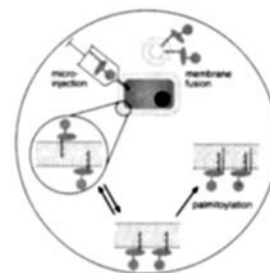
A Journal of the
Gesellschaft
Deutscher Chemiker

International Edition in English

1997
36/20
Pages 2137–2256

COVER PICTURE

The cover picture shows a model for the selective incorporation and localization of lipopeptides and lipid-modified proteins in the plasma membrane of cells. The lipopeptides were introduced into the cell by microinjection or membrane fusion. According to this model, peptides and proteins which contain S-farnesylated cysteine residues can diffuse freely between different subcellular membranes until they are additionally S-acylated in a membrane compartment. The now doubly lipid-modified peptide/protein can no longer be transferred between different membranes and is localized in the membrane where S-acylation takes place, here the plasma membrane. More on this proposed mechanism and how it was approached by a combination of techniques from organic synthesis, biophysics, and cell biology can be found on pages 2238 ff in the contribution from the groups of Waldmann, Wittinghofer, and Silviu.



REVIEWS

Contents

The first growth factors revealed to be involuntary helpers of cancer were hormones. Synthetic modification of the decapeptide hormone LHRH gave about 5000 analogues, which are superagonists or antagonists. After the sequence determination of the human LHRH receptor and models derived from it, characterization of the substances and a search for new lead structures by high-throughput screening have become possible. The first peptidomimetics and the growing understanding of the three-dimensional structure of the receptor raises hopes of a new generation of clinically active LHRH antagonists.

B. Kutscher,* M. Bernd, T. Beckers,
E. E. Polymeropoulos,
J. Engel 2148–2161

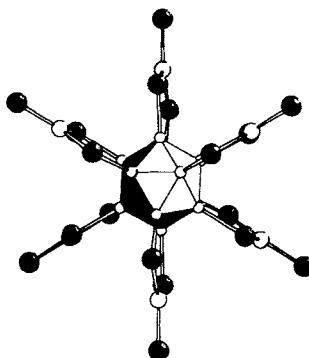
Chemistry and Molecular Biology in the
Search for New LHRH Antagonists

An important role in organometallic chemistry is predicted for N-heterocyclic carbenes, which are no longer laboratory curiosities but have developed into an industrially interesting class of compounds. They are readily accessible from azolium salts, can combine with a large variety of metals in different oxidation states, and form highly active and stable catalysts.

W. A. Herrmann,*
C. Köcher 2162–2187

N-Heterocyclic Carbenes

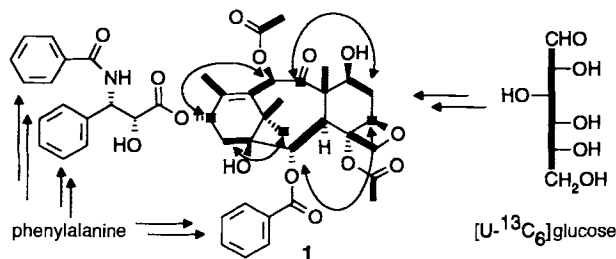
Among the diverse range of polyhedra seen for structures of boron clusters, the icosahedron is of particular importance. An unusual icosahedral boron cluster, in which both *closo*-borate and selenoborate substructures are present, was recently synthesized by Krebs et al. from cesium selenide, boron, and selenium (see schematic representation on the right, $\circ = \text{B}$, $\bullet = \text{Se}$).



L. Wesemann* 2189–2190

The Direct Synthesis of a *closo*-Borate from Elemental Boron

Taxol, a true “evergreen” in natural product chemistry! Owing to the limited supply of this successful antitumor agent in the bark of yew trees, alternative sources are being sought. Crucial information on its unusual and complex biosynthesis (shown below) has been obtained, and some enzymes responsible have been identified. The long-term goal is the efficient, biotechnological production of taxol (**1**) by fungi or plant tissue cultures.

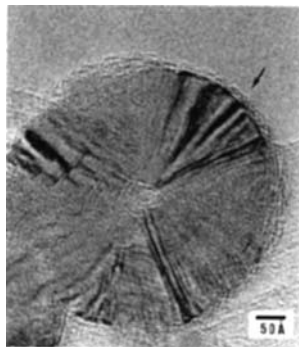


J. Rohr* 2190–2195

Biosynthesis of Taxol

COMMUNICATIONS

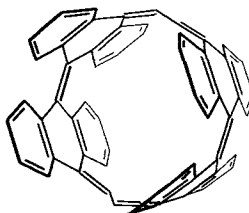
A combination of biotechnology and material science enables the immobilization of DNA on carbon nanotubes. After labeling with the heavy atoms platinum and iodine, the double-stranded DNA can be visualized by high-resolution transmission electron microscopy. In the picture the arrow highlights the DNA layer.



S. C. Tsang, Z. Guo, Y. K. Chen,
M. L. H. Green, H. A. O. Hill,
T. W. Hambley, P. J. Sadler* .. 2198–2200

Immobilization of Platinated and Iodinated
Oligonucleotides on Carbon Nanotubes

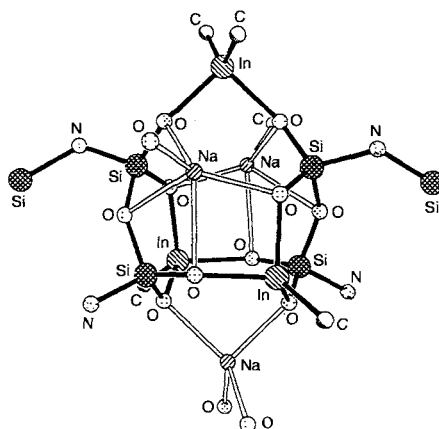
A substructure of a (5,5)-armchair nanotube was obtained by metathesis reactions with tetrahydrodianthracene. The C–C bonds in the product are all unsaturated and form a fully conjugated, beltlike system. A set of molecular building blocks can be used to synthesize other sections of nanotubes as well.



S. Kammermeier, P. G. Jones,
R. Herges* 2200–2202

Beltlike Aromatic Hydrocarbons by
Metathesis Reaction with Tetrahydro-
dianthracene

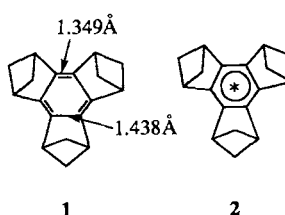
Small variations in the reaction conditions and the choice of starting materials lead to a diverse range of novel indium siloxane structures. These compounds can serve as model compounds for zeolites. The framework of one of the indium siloxanes is depicted on the right.



A. Voigt, M. G. Walawalkar,
R. Murugavel, H. W. Roesky,*
E. Parisini, P. Lubini 2203–2205

Organic-Soluble Neutral and Ionic Indium Siloxane Cages: Potential Precursors for Indium-Containing Silicates

Why does the benzene nucleus have a structure similar to cyclohexatriene in the ground state **1**, and a virtually D_{6h} -symmetrical structure in the $\pi \rightarrow \pi^*$ excited state **2**? A simple model based on the distortive propensity of the π electrons in the ground state and their opposite tendency in the excited state predicts this behavior, and more.



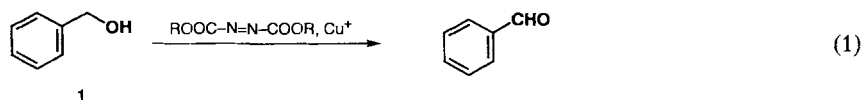
A. Shurki, S. Shaik* 2205–2208

The Distortive Tendency of Benzene π Electrons: How Is It Related to Structural Observables?

The aerobic copper-catalyzed oxidation of alcohols such as **1** [Eq. (1)] functions even in the absence of oxygen. Non-benzylic and secondary alcohols are further suitable substrates. A key role in this reaction is played by azocarboxylates, which not only serve as complex ligands but also as hydride acceptors; bulky R groups such as *tert*-butyl are particularly suitable.

I. E. Markó,* M. Tsukazaki, P. R. Giles,
S. M. Brown, C. J. Urch 2208–2210

Anaerobic Copper-Catalyzed Oxidation of Alcohols to Aldehydes and Ketones



Why are there so few exceptions to the fact that $\rho_R/\rho_F = \lambda$ is positive? A straightforward theoretical basis is provided for the interpretation of the dediazotiation of benzenediazonium ions, one of the most prominent examples of the few reactions for which the reaction constants ρ_R and ρ_F [Eq. (1)] have opposite signs. The results support the model that describes C–N bonding as synergistic N \rightarrow C σ dative and C \rightarrow N π backdative bonding. The analysis furnishes details about the electronic structure that cannot be deduced from physical–organic studies alone.

R. Glaser,* C. J. Horan,
H. Zollinger* 2210–2213

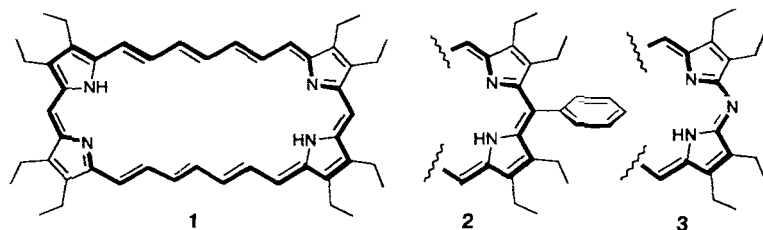
Electron-Density Relaxation and Oppositely Signed Reaction Constants in Dual Substituent Parameter Relationships in Dediazotiation Reactions

$$\lg(k_X/k_0) = \sigma_F \rho_F + \sigma_R \rho_R \quad (1)$$

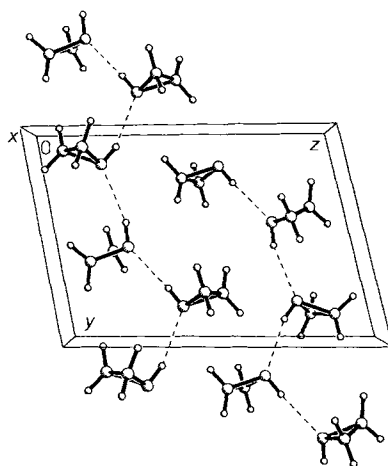
The incorporation of pyrrole units was the key to stabilizing the largest annulene from Sondheimer et al., [30]annulene. Of the new aromatic [30]porphyrins **1–3**, the 16-phenyl derivative **2** is the most stable.

C. Eickmeier, B. Franck* 2213–2215

Hexavinyllogous Porphyrins with Aromatic 30 π -Electron Systems



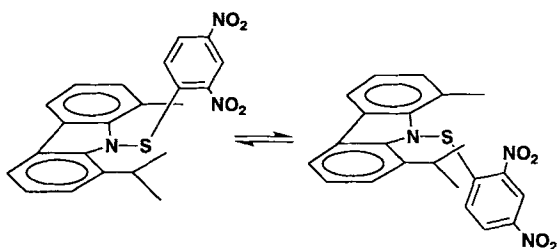
The simplest nitrogen heterocycle, aziridine, a very toxic and potentially explosive liquid at room temperature, forms endless chains with an ABCABC motif by hydrogen bonding in the solid state. The results of the crystal structure analysis at 145 K do not suggest any deformations of the molecular skeleton on going from the gas phase to the solid state.



N. W. Mitzel,* J. Riede,
C. Kiener 2215–2216

The Crystal Structure of Aziridine

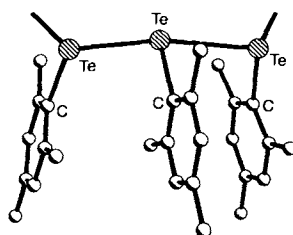
Optical activity due only to restricted rotation about the S–N bond in a sulfenamide is demonstrated for the first time. Selective inversion recovery experiments were utilized to measure the rate of interconversion of the enantiomers (shown below) that were separated by using HPLC.



M. B. D. Blanca, E. Maimon,
D. Kost* 2216–2219

The Chiral S–N Axis in Sulfenamides: Enantiomeric Resolution, Direct Demonstration of Optical Activity, and Kinetics of Interconversion

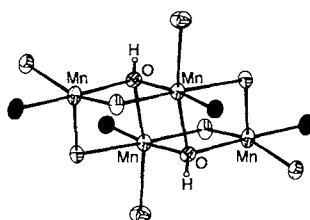
The first stable derivative of the hypothetical Te_3^{4-} ion—the triiodide-analogous $[\text{Mes}_3\text{Te}_3]^+$ ion (partial structure depicted on the right; Mes = 2,4,6-trimethylphenyl)—is obtained by addition of the nucleophile Mes_2Te to the iodine-like electrophilic ion $[\text{Mes}_3\text{Te}_2]^+$. This reaction provides the first experimental proof of the close relationship between the formation of hypervalent nonclassical Te_3 units and that of triiodide from I_2 and I^- .



J. Jeske, W. W. du Mont,*
P. G. Jones 2219–2221

Synthesis of a Triiodide-Like Pentamesityl-tritellurium Cation by Addition of Dimesityltelluride to the Remarkably Electrophilic Trimesitylditelluronium Ion

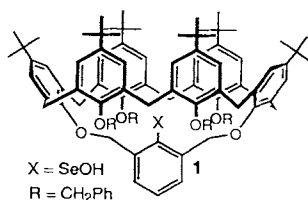
Two molecules of water inserted between two dinuclear Mn_2^{II} species as μ_3 -hydroxo bridges are evident in the manganese–oxygen core of $[\{\text{Mn}_2^{\text{II}}(\text{L})(\text{OH})(\text{thf})\}_2] \cdot 2\text{THF}$ (structure shown on the right). This discrete complex is thus an appealing functional model of the Mn_4 core of the oxygen-evolving center in photosystem II at an early *S* state. LH_3 = 1,5-bis(3,5-dinitrosalicylideneamino)pentan-3-ol; solid unmarked ellipsoids: N; open unmarked ellipsoids: O.



L. Stelzig, B. Donnadieu,
J. P. Tuchagues* 2221–2222

The First Di- μ_3 -hydroxo-Bridged Tetramanganese(II) Complex

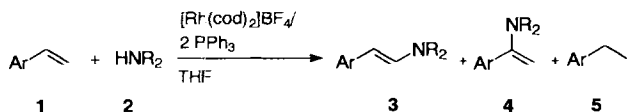
The deep cavity in the calix[6]arene framework provides a sterically shielded environment for the SeOH group of the selenenic acid **1**. Thanks to this shielding the compound is extraordinarily stable—no decomposition was observed even after heating at 120 °C for 5 h in $\text{CDCl}_2\text{CDCl}_2$ —although the functional group is still reactive.



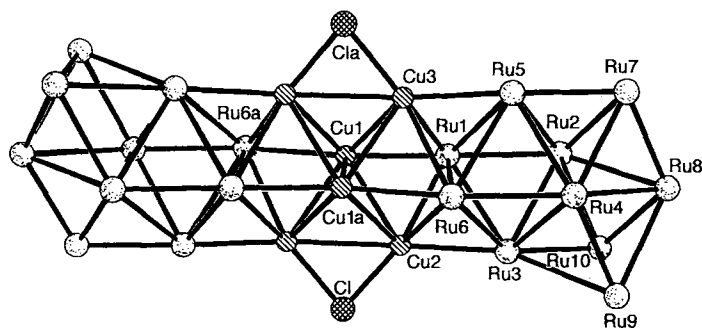
T. Saiki, K. Goto,
R. Okazaki* 2223–2224

Isolation and X-ray Crystallographic Analysis of a Stable Selenenic Acid

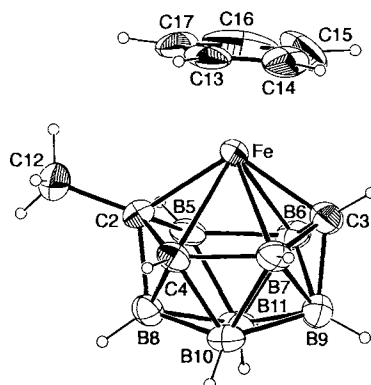
Not the Markovnikov product 4, but the anti-Markovnikov product **3** is obtained by the oxidative amination of styrenes **1** with secondary amines **2**. The oxidant in this rhodium-catalyzed reaction is the olefin itself, which is reduced to the ethylarene **5**. Ar = aryl, R = alkyl, aryl.



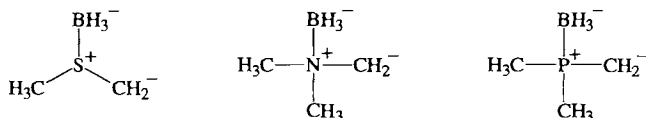
A precursor for Cu/Ru mixed-metal catalysts? This is one of the potential applications of the title cluster (structure of the $\text{Ru}_{20}\text{Cu}_6\text{Cl}_2$ framework shown below), which can be isolated as the $n\text{Bu}_4\text{N}^+$ salt from the reaction of $[(\text{Ph}_3\text{P})_2\text{N}]_2[\text{Ru}_{10}\text{H}_2(\text{CO})_{25}]$ with $n\text{Bu}_4\text{NOH}/\text{H}_2\text{O}$, $[\text{Cu}(\text{MeCN})_4]$, and $(\text{Ph}_3\text{P})_2\text{NCl}$.



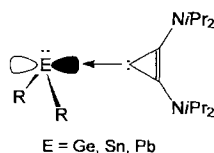
A cationic ferratricarbadeboranyl analogue of the ferrocenium cation was synthesized and structurally characterized (structure shown on the right). Cytotoxicity and topoisomerase II inhibition studies of the AsF_6^- and SbF_6^- salts strongly suggest that tricarbadeboranyl analogues of other metallocene antitumor agents will exhibit significant and selective anticancer activities.



Borane complexation at the heteroatom increases the gas-phase C–H acidities of dimethyl sulfide, trimethylamine, and trimethylphosphane by up to 20 kcal mol^{-1} . Deprotonation of the volatile Lewis acid–base complexes in the gas phase produces dipole-stabilized carbanions (see below) that do not rearrange to the more stable borate isomers. The complexation also enhances the reactivity of pendant methyl and ethyl groups toward substitution and elimination reactions.



Not germa-, stanna-, and plumbaethenes, but ylidic carbene adducts (depicted on the right) are obtained with bis(diisopropylamino)cyclopropenylenes. The first main group metal complexes with this nucleophilic carbene are interesting alternatives to the intensively studied imidazol-2-ylidenes.



M. Beller,* M. Eichberger,
H. Trauthwein 2225–2227

Anti-Markovnikov Functionalization of
Olefins: Rhodium-Catalyzed Oxidative
Aminations of Styrenes

M. A. Beswick, J. Lewis,
P. R. Raithby,*
M. C. Ramirez de Arellano ... 2227–2228

$[\text{Ru}_{20}\text{H}_4\text{Cu}_6\text{Cl}_2(\text{CO})_{48}]^{4-}$: A New High
Nuclearity Copper–Ruthenium Cluster

M. D. Wasczak, C. Lee,
I. H. Hall,* P. J. Carroll,
L. G. Sneddon* 2228–2230

Cationic Metallocene Antitumor Agents:
Synthesis, Structure, and Antineoplastic
Activity of $[1-(\eta^5\text{-C}_5\text{H}_5)\text{Fe-2-Me-2,3,4-}$
 $\text{C}_3\text{B}_7\text{H}_9]^+[\text{X}]^-$ Salts ($\text{X}^- = \text{AsF}_6^-, \text{SbF}_6^-$)

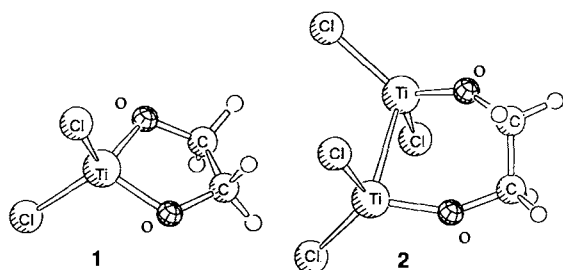
J. Ren, D. B. Workman,
R. R. Squires* 2230–2232

Enhanced α -CH Acidity and Reactivity of
Lewis Acid–Base Complexes in the Gas
Phase

H. Schumann,* M. Glanz, F. Girgsdies,
F. E. Hahn, M. Tamm,*
A. Grzegorzewski 2232–2234

Cyclopropenylidene Adducts of Divalent
Germanium, Tin, and Lead

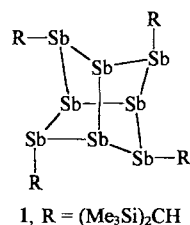
A nucleophilic rather than a radical mechanism was recently proposed for the McMurry reaction. Quantum chemical density functional calculations support this hypothesis. An intramolecular and an intermolecular pathway for the C–C coupling step are discussed, and the pinacolate complexes **1** and **2** are identified as central intermediates.



M. Stahl, U. Pidun,
G. Frenking* 2234–2237

On the Mechanism of the McMurry Reaction

The reaction of RSbCl_2 with magnesium in tetrahydrofuran provides, in addition to Sb_4R_4 and Sb_3R_3 , the title compound **1**. The X-ray structure analysis of the yellow crystals of **1** shows that the Sb_8 cage corresponds to the P_8 section of the structure of Hittorf's phosphorus and is structurally related to realgar (As_4S_4).



H. J. Breunig,* R. Rösler,
E. Lork 2237–2238

Sb_8R_4 , $\text{R} = (\text{Me}_3\text{Si})_2\text{CH}$ —A Polycyclic Organostibane

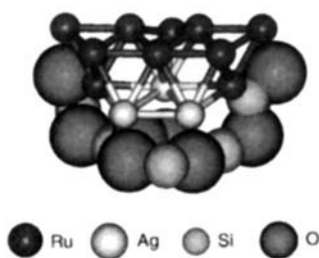
Very small regions determine where lipoproteins accumulate in the cell. S-Farnesylated and S-palmitoylated N-Ras lipopeptides **1** accumulate specifically in the plasma membrane, as determined by investigations on fibroblast cells with fluorescence microscopy. (In the structure below the shaded circle symbolizes a fluorescent label.) Peptides that were only S-farnesylated do not accumulate in the plasma membrane.

1

H. Waldmann,* M. Schelhaas, E. Nägele,
J. Kuhlmann, A. Wittinghofer,*
H. Schroeder, J. R. Silvius* ... 2238–2241

Chemoenzymatic Synthesis of Fluorescent N-Ras Lipopeptides and Their Use in Membrane Localization Studies In Vivo

A new hydrogenation catalyst is formed by thermolysis of the anionic carbonyl cluster $[\text{Ag}_3\text{Ru}_{10}\text{C}_2(\text{CO})_{28}\text{Cl}]^{2-}$ anchored to the mesoporous silicate MCM-41. The cluster was isolated and characterized in MCM-41 both before and after thermal treatment. The picture on the right shows a model, based in particular on EXAFS analysis, of the active bimetallic particle. The distribution of the Ag/Ru particles in the MCM-41 cavities was determined by electron microscopy.



D. S. Shephard, T. Maschmeyer,
B. F. G. Johnson,* J. M. Thomas,*
G. Sankar, D. Ozkaya, W. Zhou,
R. D. Oldroyd, R. G. Bell ... 2242–2245

Bimetallic Nanoparticle Catalysts Anchored Inside Mesoporous Silica

* Author to whom correspondence should be addressed

| | |
|---|---------------------------------|
| The Chemistry of Ceramics · H. Yanagida, K. Kuomoto, M. Miyayama | <i>R. Riedel</i> 2247 |
| CVD of Nonmetals · W. S. Rees Jr. | <i>R. A. Fischer</i> 2247 |
| Introduction to glass science and technology · J. E. Shelby | <i>U. Schubert</i> 2248 |
| Chemistry of Powder Production · Y. Arai | <i>R. Riedel</i> 2249 |
| Hydrocarbon Resins · R. Mildenberg, M. Zander, G. Collin | <i>R. Mülhaupt</i> 2249 |
| Chemometrics in Environmental Analysis · J. W. Einax, H. W. Zwanziger, S. Geiss | <i>C. Zwiener</i> 2250 |
| Inorganic Chemistry. An Industrial and Environmental Perspective · T. W. Swaddle | <i>S. Hasenzahl</i> 2250 |
| NMR Data Processing · J. C. Hoch, A. S. Stern | <i>C. Griesinger</i> 2251 |
| Handbook of Palladium-Catalyzed Reactions · J.-L. Malleron, J.-C. Fiaud, J.-Y. Lagros | <i>U. Kazmaier</i> 2252 |
| Database of Palladium Chemistry. Reactions, Catalytic Cycles and Chemical Parameters on CD-ROM · J.-L. Malleron, A. Juin | <i>F. Zumpe</i> 2252 |
| Protein and Peptide Analysis by Mass Spectrometry · J. R. Chapman | <i>J. W. Metzger</i> 2253 |

German versions of all reviews, communications, and highlights in this issue appear in the second October issue of *Angewandte Chemie*. The appropriate page numbers can be found at the end of each article and are also included in the Author Index on p. 2255.

All the Tables of Contents from 1995 onwards may be found on the WWW under:
<http://www.wiley-vch.de/home/angewandte>

SERVICES

| | |
|----------------|------|
| ● Events | 2195 |
| ● Keywords | 2254 |
| ● Author Index | 2255 |
| ● Preview | 2256 |

ANGEWANDTE CHEMIE

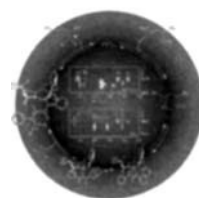
A Journal of the
Gesellschaft
Deutscher Chemiker

International Edition in English

1997
36/19
Pages 2025–2136

COVER PICTURE

The cover picture shows the mechanism of Pd-catalyzed allylic alkylation with phosphinoaryldihydrooxazole ligands. In the center are two sections of 2D NMR spectra that characterize the primary olefin–Pd⁰ complex and prove the nuclear constellation as well as the constitution of the η^2 -olefin–Pd complex shown on the left (E = CO₂Me). More about this mechanism and details of the structure determination based on NMR spectroscopy are reported by H. Steinhagen, M. Regglin, and G. Helmchen on pp. 2108ff.



REVIEW

Contents

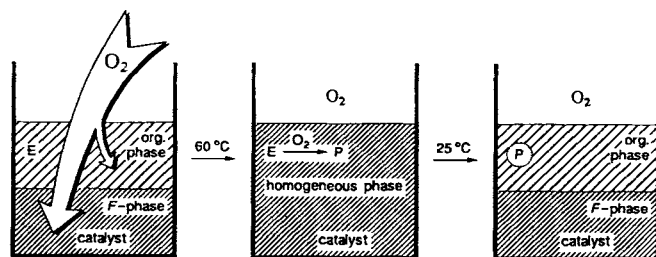
Tailor-made polymers and complex compounds of low molecular weight are accessible for olefin metathesis with modern Ru- and Mo-alkylidene complexes. Ring-closing and ring-opening metatheses, selective cross-metathesis of alkenes, and stereoselective olefin metatheses, which proceed “waste-free” and atom economically, are just a few of the reactions that have joined the arsenal of methods in organic chemistry, or will do so soon. New generations of catalysts make this over 40-year-old reaction principle feasible, even for the future.

M. Schuster, S. Blechert* 2036–2055

Olefin Metathesis in Organic Chemistry

HIGHLIGHTS

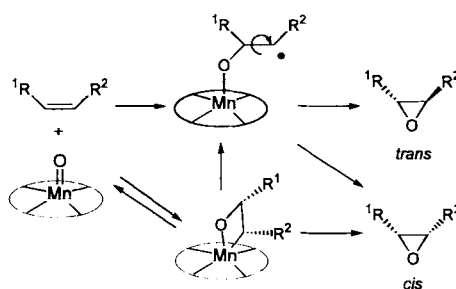
Something new is afoot in chemistry: FBS! The principle of reactions in fluorous biphasic systems (FBS) is shown below for an oxidation (E = starting material, P = product). A large number of publications on this new technique have appeared within a very short time.



B. Cornils* 2057–2059

Fluorous Biphasic Systems—The New Phase-Separation and Immobilization Technique

Radicals or manganooxetanes – what are the intermediates in the Jacobsen–Katsuki epoxidation (see scheme on the right)? Recent investigations have shown that the mechanism of the epoxidation is strongly dependent on the substituents of the alkene and on the reaction conditions.

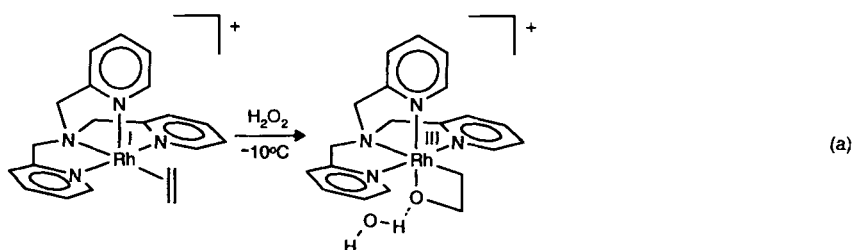


T. Linker* 2060–2062

The Jacobsen–Katsuki Epoxidation and Its Controversial Mechanism

COMMUNICATIONS

Stable unsubstituted 1,2-oxarhodacyclobutanes (2-rhodaoxetanes) are obtained upon oxidation of $[\text{Rh}^{\text{I}}(\text{ethene})\text{'N}_4]^+$ complexes [Eq. (a)]. Similar oxidation of $[\text{Rh}^{\text{I}}(\text{cod})\text{'N}_3]^+$ complexes results in oxarhodatetracyclodecanes via a proposed oxarhodacyclobutane intermediate (cod = (Z,Z)-1,5-cyclooctadiene; 'N_4 ' and 'N_3 ' = tetra- and tridentate ligands). The mechanistically interesting formation of these oxarhodacyclobutanes gives insight into the catalytic oxidation of olefins with late transition metal complexes.



B. de Bruin, M. J. Boerakker, J. J. M. Donners, B. E. C. Christiaans, P. P. J. Schlebos, R. de Gelder, J. M. M. Smits, A. L. Spek, A. W. Gal* 2064–2067

Oxidation of $\text{Rh}^{\text{I}}(\text{olefin})$ Fragments to 2-Rhoda(III)oxetanes

Four- and five-component pseudorotaxanes, which self-assemble by the threading of dibenzylammonium ions through macrocyclic polyethers, behave as anion receptors. The preorganization of the positively charged recognition sites in these superstructures induces the complexation of a PF_6^- ion in the solid state. This anion is partially encapsulated in the four-component, triple-stranded pseudorotaxane, but is completely enveloped within the larger binding pocket of the five-component, quadruple-stranded pseudorotaxane (see picture on the right).



M. C. T. Fyfe, P. T. Glink, S. Menzer, J. F. Stoddart,* A. J. P. White, D. J. Williams* 2068–2070

Anion-Assisted Self-Assembly

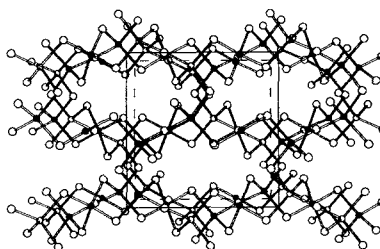
Two large and five small rings interlock to give the [7]catenane depicted on the right. Every potential π -donor and π -acceptor recognition site within this molecule is utilized. Only the application of high pressure (12 kbar) made possible the efficient assembly of this exotic molecular compound, for which a solid-state structure was obtained by X-ray crystallography.



D. B. Amabilino, P. R. Ashton,
S. E. Boyd, J. Y. Lee, S. Menzer,
J. F. Stoddart,*
D. J. Williams* 2070–2072

The Five-Stage Self-Assembly of a
Branched Heptacatenane

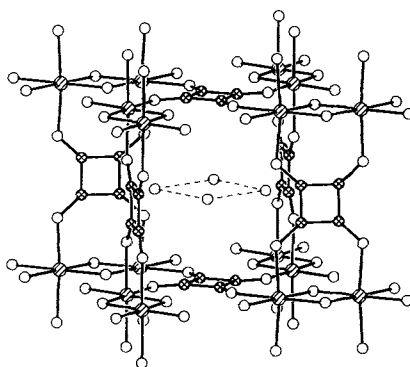
The first non-oxide, direct analogues of aluminosilicate zeolites are materials with the anionic partial structure $[\text{Cu}_n\text{Zn}_m-\text{Cl}_{2m}]^{n-}$. Varying the templating alkylammonium counterion results in different framework structures: $[\text{HNMMe}_3][\text{CuZn}_5\text{Cl}_{12}]$ adopts the known sodalite structure, whereas $[\text{H}_2\text{NEt}_2][\text{CuZn}_5\text{Cl}_{12}]$ exhibits a novel three-dimensional channel structure with eleven- and eight-ring channels (the latter is depicted on the right). Controlled addition of methanol or water results in formation of colloidal particles that are implicated as intermediates in the construction of open frameworks.



J. D. Martin,*
K. B. Greenwood 2072–2075

Halozeotypes: a New Generation of Zeo-
lite-Type Materials

Square apertures and windows are characteristic structural motifs of the title compounds. Compound **1** (see picture) has large cavities and clathrates the rare cyclic water tetramer at the intersection of the channels. The tetramers are interlinked by hydrogen bonding to form a water layer.



K.-J. Lin,* K.-H. Lii 2076–2077

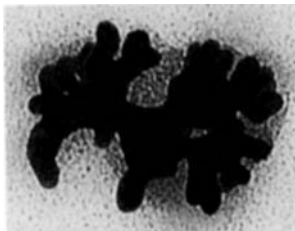
Binuclear Vanadium(III) Squarates with
Layered and Framework Structures: Hy-
drothermal Synthesis and Structures of
 $[\{\text{V}(\text{OH})(\text{C}_4\text{O}_4)(\text{H}_2\text{O})\}_2]$ and
 $[\{\text{V}(\text{OH})(\text{C}_4\text{O}_4)\}_2] \cdot 4\text{H}_2\text{O}$

Chemical bonds in highly fluxional molecules—are such descriptions useful? Results of fully quantum-mechanical calculations together with a novel analysis of the electron localization function (ELF) of the protonated methane molecule CH_5^+ give a positive answer to this question. The concept of three-center, two-electron bonding is impressively supported by this method.

D. Marx,* A. Savin 2077–2080

Topological Bifurcation Analysis: Elec-
tronic Structure of CH_5^+

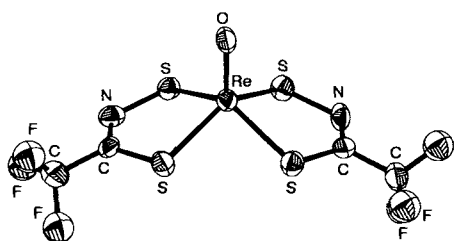
Nuggets and threads form upon reduction of gold salts under various reaction conditions in nanometer-sized polymer gel particles (see picture on the right). Due to their structure and resulting elasticity, these microgels create a local reaction environment that, as with biomineralization, favors the production of ordered nanostructures. Thus, size and shape control are not restricted to living organisms, but are also possible in synthetic colloid systems.



M. Antonietti,* F. Gröhn, J. Hartmann,
L. Bronstein 2080–2083

Nonclassical Shapes of Noble-Metal
Colloids by Synthesis in Microgel Nano-
reactors

In the presence of oxidants such as amine oxides, nitriles add to $[\text{ReS}_4]^-$ ions to give bicyclic adducts (structure of the CF_3CN adduct on the right). This reaction provides a new model for the activation of unsaturated nitrogen compounds by metal sulfides, which are known to be good catalysts for the hydrogenation of such substrates.



J. T. Goodman,
T. B. Rauchfuss* 2083–2085

Addition of Nitriles to Metal Sulfides:
Possible Insight into the Metal Sulfide
Catalyzed Hydrogenation of Nitriles and
Dinitrogen

Bovine serum albumin and chicken-egg lysozyme can be cleaved with high specificity into two fragments by the method shown below. A pyrene-L-phenylalanine conjugate was used as the probe (shown schematically over the first arrow), which binds with site specificity to the protein and produces the cleavage upon irradiation with visible light in the presence of a Co^{III} compound.

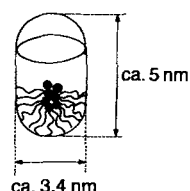
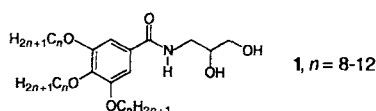


C. V. Kumar,*

A. Buranaprapuk 2085–2087

Site-Specific Photocleavage of Proteins

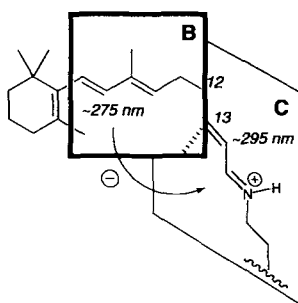
Inverted micelles and the absence of solvent molecules characterize the thermotropic cubic mesophases that are formed from triple-chain *N*-(dihydroxypropyl)benzamides of type 1. X-ray crystallographic findings reveal a micelle built up from approximately 44 molecules (depicted on the right).



K. Borisch, S. Diele, P. Göring, H. Kresse, C. Tschierske* 2087–2089

Design of Thermotropic Liquid Crystals with Micellar Cubic Mesophases: Amphiphilic *N*-(2,3-Dihydroxypropyl)benzamides

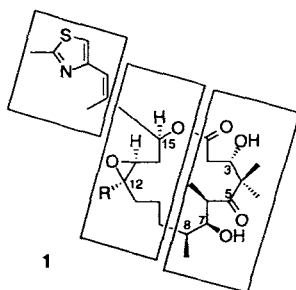
Insight into the visual transduction process: Details on the structure of the retinal chromophore in rhodopsin are crucial to understanding the visual transduction process on a molecular structural level. Exciton-coupled circular dichroism (CD) spectra of opsin-bound 11,12-dihydroretinals exhibit negative bisignate couplets, which indicate that the B and C planes are oriented as shown on the right.



Q. Tan, J. Lou, B. Borhan, E. Karnaukhova, N. Berova, K. Nakanishi* 2089–2093

Absolute Sense of Twist of the C12–C13 Bond of the Retinal Chromophore in Bovine Rhodopsin Based on Exciton-Coupled CD Spectra of 11,12-Dihydroretinal Analogues

Ahead! Epothilone B (1, R = Me) displayed better antitumor activity than paclitaxel (Taxol), as shown by in vivo studies with resistant mouse tumor models. The “acyl sector” C1–C8 in the epothilones is very sensitive to modification. The other two sectors (see structure on the right) can be varied to a certain extent; however, none of the analogues examined thus far have surpassed the parent compound.



D.-S. Su, A. Balog, D. Meng, P. Bertinato, S. J. Danishefsky,* Y.-H. Zheng, T.-C. Chou, L. He, S. B. Horwitz 2093–2096

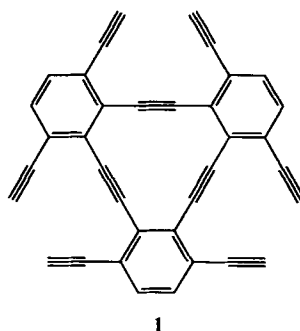
Structure–Activity Relationships of the Epothilones and the First In Vivo Comparison with Paclitaxel

A library of epothilone A and B analogues, which was constructed by solid-phase combinatorial synthesis using SMART Microreactors and solution chemistry, was screened in two different tubulin binding assays. Selected compounds were subjected to cytotoxicity studies against a number of cell lines, including Taxol-resistant cells. Important structure–activity relationships emerged from these studies, which sets the stage for further discoveries and developments in the anticancer field.

K. C. Nicolaou,* D. Vourloumis, T. Li, J. Pastor, N. Winssinger, Y. He, S. Ninkovic, F. Sarabia, H. Vallberg, F. Roschangar, N. P. King, M. R. V. Finlay, P. Giannakakou, P. Verdier-Pinard, E. Hamel .. 2097–2103

Designed Epothilones: Combinatorial Synthesis, Tubulin Assembly Properties, and Cytotoxic Action against Taxol-Resistant Tumor Cells

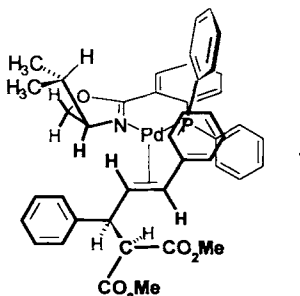
The largest subunit of the carbon allotrope “graphyne”, title compound **1**, is also a potential precursor to circular [6]phenylene, antikekulene. Single and double CpCo-catalyzed cycloisomerization provided the respective angular [3]- and [5]phenylenes. Their spectroscopic data indicate that they harbor superdelocalization.



C. Eickmeier, H. Junga, A. J. Matzger,
F. Scherhag, M. Shim,
K. P. C. Vollhardt* 2103–2108

5,6,11,12,17,18-Hexadehydro-
1,4,7,10,13,16-hexaethynyltribenzo[*a,e,i*]-
cyclododecene: Synthesis and CpCo-Cata-
lyzed Cycloisomerization to the First
Superdelocalized Oligophenylenes

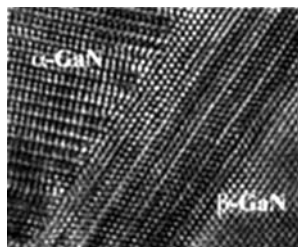
Under the 2D NMR spectroscopic magnifying glass: The intermediacy of **1** in the Pd-catalyzed allylic substitution was investigated and proven. Characterization of this Pd⁰ complex, which is primarily formed in the catalytic cycle, shows that attack of the nucleophile malonate at the double bond of the allyl ligand is preferred *trans* to the P atom.



H. Steinhagen, M. Reggelin,*
G. Helmchen* 2108–2110

Palladium-Catalyzed Allylic Alkylation
with Phosphinoaryldihydrooxazole Lig-
ands: First Evidence and NMR Spectro-
scopic Structure Determination of a
Primary Olefin–Pd⁰ Complex

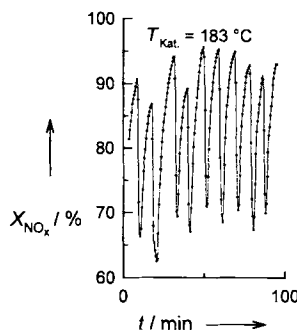
The production of single-phase GaN, which is important for the realization of optoelectronic devices, is intricately by the existence of two polytypes (α -GaN hexagonal, β -GaN cubic, metastable). Both the orientation of the interface between the cubic matrix and the polytypic hexagonal inclusion and the influence of the specific nature of the interface on the stability of the transformed polytype are of fundamental importance for the phase transformation of β - to α -GaN.



A. Trampert,* O. Brandt,
K. H. Ploog 2111–2112

Phase Transformations and Phase Stability
in Epitaxial β -GaN Films

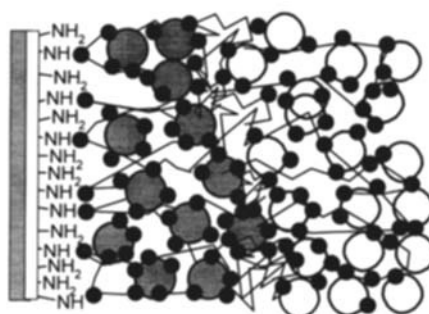
Platinum, vanadium, and water are required for the occurrence of oscillations in diesel exhaust gas upon reduction of NO_x with propene on zeolites (see example on the right; *X* = conversion). Results of experiments with temperature-programmed reduction suggest that the oscillations originate from redox reactions.



Y. Traa, M. Breuninger, B. Burger,
J. Weitkamp* 2113–2114

Oscillation of NO_x Concentration in the
Selective Catalytic Reduction of Nitrogen
Oxides on Platinum-Containing Zeolite
Catalysts

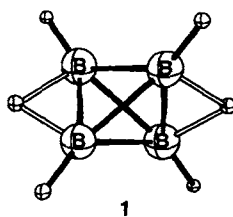
A Velcro-like thin-film composite in which dendrimers act as burrs and a reactive anhydride copolymer acts like wool (see schematic representation on the right) can be readily prepared from commercially available reagents. Films that are 10–50 nm thick and contain alternating layers of both components were synthesized on glass, silicon, and gold-coated silicon wafers.



Y. Liu, M. L. Bruening, D. E. Bergbreiter,*
R. M. Crooks* 2114–2116

Multilayer Dendrimer–Polyanhydride
Composite Films on Glass, Silicon, and
Gold Wafers

The reaction of RBBR_2 and Na/K alloy or the two-step reaction of B_4R_4 and Na/K alloy with subsequent action of HCl results in the tetraborane $\text{B}_4\text{H}_2\text{R}_4$ ($\text{R} = t\text{Bu}$). A tetrahedral B_4 structure **1** with two hydrogen-bridged opposite edges (D_{2d} symmetry) is deduced from NMR data for $\text{B}_4\text{H}_2\text{R}_4$ as well as from ab initio calculations for the parent molecule B_4H_6 and for $\text{B}_4\text{H}_2\text{Me}_4$. Upon reaction with lithium in tetrahydropyran (L), a bridging H atom on $\text{B}_4\text{H}_2\text{R}_4$ can be replaced by the group LiL_2 . $(\text{L}_2\text{Li})\text{B}_4\text{HR}_4$ was characterized by a crystal structure analysis.



A. Neu, T. Mennekes, U. Englert,
P. Paetzold,* M. Hofmann,
P. von R. Schleyer 2117–2119

Tetra-tert-butyltetraborane(6) $\text{B}_4\text{H}_2t\text{Bu}_4$:
A Derivative in the Series B_4H_{n+2}

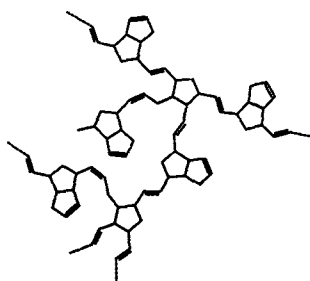
New application for a chiral auxiliary: *N*-acyl imides like **1**, which is formed in an enantioselective aldol reaction, can be converted into thioesters and decarboxylated to give **2** ($\text{TES} = \text{Et}_3\text{Si}$). The oxazolidinone auxiliary is thus removed under mild conditions in a one-pot reaction, which is a key step in the elegant synthesis of the title compound.



D. A. Evans,* D. H. B. Ripin,
J. S. Johnson,
E. A. Shaughnessy 2119–2121

A New Strategy for Extending *N*-Acyl
Imides as Chiral Auxiliaries for Aldol
and Diels–Alder Reactions: Application
to an Enantioselective Synthesis of
 α -Himachalene

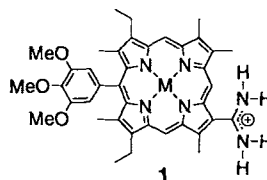
$[\text{Ru}(p\text{-cymene})\text{Cl}_2(\text{PCy}_3)]$ was identified as a latent, very tolerant, one-component catalyst for the bulk polymerization of dicyclopentadiene (DCPD). The robustness of this catalyst in combination with the interesting properties of filled or unfilled poly(DCPD) allows the preparation of novel thermosets (structure shown on the right).



A. Hafner,* A. Mühlebach,
P. A. van der Schaaf 2121–2124

One-Component Catalysts for Thermal and
Photoinduced Ring Opening Metathesis
Polymerization

An unusually slow electron transfer takes place in the porphyrinato complex **1** ($\text{M} = \text{Ni}, \text{Zn}$). The rate of this proton-coupled electron transfer is influenced by a salt bridge in which benzoate ions are bound to the amidinium group, even in solvents with a high dielectric constant, such as DMSO.



Y. Deng, J. A. Roberts, S.-M. Peng,
C. K. Chang,
D. G. Nocera* 2124–2127

The Amidinium–Carboxylate Salt Bridge
as a Proton-Coupled Interface to Electron
Transfer Pathways

* Author to whom correspondence should be addressed

BOOKS

| | | |
|--|--|------|
| Medical Chemistry: Today and Tomorrow · M. Yamakazi | <i>H. Waldmann</i> | 2129 |
| Basic Principles of Membrane Technology · M. Mulder | <i>U. Kragl</i> | 2129 |
| An Introduction to Enzyme and Coenzyme Chemistry · T. Bugg | <i>W.-P. Kuhl, K.-H. van Pée</i> | 2130 |
| NMR of Polymers · F. A. Bovey, P. A. Mireau | <i>B. Blümich</i> | 2131 |
| Introduction to Medicinal Chemistry. How Drugs Act and Why · A. Gringauz | <i>G. Müller</i> | 2131 |
| Spectra Interpretation of Organic Compounds · E. Pretsch, J. T. Clerc | <i>L. Ernst</i> | 2131 |

German versions of all reviews, communications, and highlights in this issue appear in the first October issue of *Angewandte Chemie*. The appropriate page numbers can be found at the end of each article and are also included in the Author Index on p. 2135.

SERVICES

| | |
|----------------|------|
| • Corrigendum | 2127 |
| • Keywords | 2134 |
| • Author Index | 2135 |
| • Preview | 2136 |

All the Tables of Contents from 1995 onwards may be found on the WWW under:
<http://www.wiley-vch.de/home/angewandte>

ANGEWANDTE CHEMIE

A Journal of the
Gesellschaft
Deutscher Chemiker

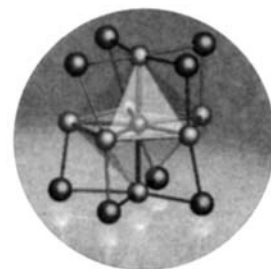
International Edition in English

1997
36/18

Pages 1915–2024

COVER PICTURE

The cover picture shows the ball-and-stick model of a $[\{\text{RhBi}_7\}\text{Br}_8]$ cluster from the structure of one of the first ternary subhalides of bismuth, Bi_7RhBr_8 . The seven bismuth atoms (blue) surround the central rhodium atom (yellow) forming a regular pentagonal bipyramid. The two apical bismuth atoms are each in an approximate square-planar environment of four bromine atoms. The squares are staggered and thus the $\{\text{RhBi}_7\}$ bipyramid is surrounded by a distorted square antiprism of bromine atoms. On closer analysis, this apparently unfavorable atomic arrangement emerges as an exceptional solution to the need to satisfy the electronic requirements of all participating atoms. More about this as yet unique molecular cluster is discussed by M. Ruck on pages 1971 ff. The graphics were generated by M. Ruck and G. Baum with the program POV-Ray.



REVIEWS

Contents

“Being isolated in those pre-fax and pre-e-mail days in Australia was a great advantage, as it allowed time to discuss and to think things through. We had outspoken and informed local critics, the freedom and resources to pursue our own ideas, and were given full credit for our efforts. Those of us who have senior roles in science need to do everything possible to ensure that comparable opportunities and environments remain available to young scientists.” With this provocative exhortation P. C. Doherty ended his Nobel Lecture.

P. C. Doherty* 1926–1936

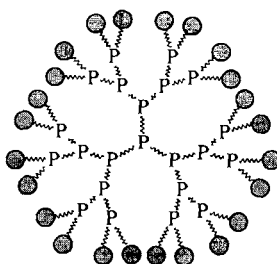
Cell-Mediated Immunity in Virus Infections (Nobel Lecture)

In the complex balance between virus and host the T cells and the properties of the virus play an important role. The unexpected discovery of the MHC-restricted T cell recognition (MHC = major histocompatibility complex) prompted many important investigations, which have led to a detailed understanding on a molecular level of T cell recognition of virus-infected target cells. As a result of these findings the immunological specificity as well as the immunological memory, and above all, pathogenesis of infectious diseases and of autoimmunity can be better understood.

R. M. Zinkernagel* 1938–1949

Cellular Immune Recognition and the Biological Role of Major Transplantation Antigens (Nobel Lecture)

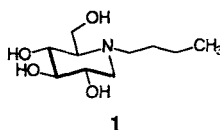
The allure of cascade molecules has long since reached main group chemistry. Dendrimers constructed from silicon- and phosphorus-based building blocks (see schematic representation on the right) not only are among the largest cascade molecules ever synthesized, but also offer unique possibilities for binding functional groups at the surface or in the interior. This property may open new perspectives for the design of catalysts and synthetic reagents.



D. Gudat* 1951–1955

Inorganic Cauliflower: Functional Main Group Element Dendrimers Constructed from Phosphorus- and Silicon-Based Building Blocks

Great advances have been made in the treatment of Tay–Sachs disease, one of a group of inherited diseases in which the degradation of sphingolipids is impaired. In the animal model, application of compound 1 was successful in inhibiting the biosynthesis of nondegradable enzyme substrates and in this way reducing the extent of the disease.

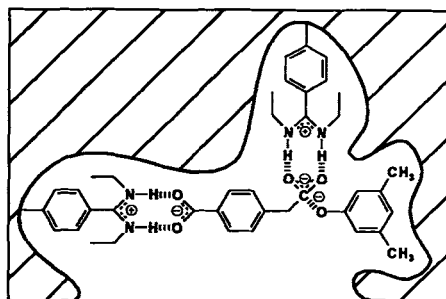


T. Kolter* 1955–1959

A Chemical Concept for the Treatment of Tay–Sachs Disease

COMMUNICATIONS

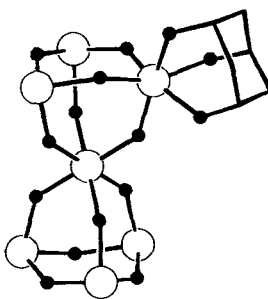
Functions similar to those of catalytic antibodies are shown by molecularly imprinted polymers, when the cavities in the polymer not only have the correct form but also contain catalytically active groups. Polymers have now been prepared by imprinting with a transition state analogue of alkaline ester hydrolysis (see picture). These “artificial enzymes” combine strong catalytic activity with typical enzyme properties such as Michaelis–Menten kinetics, competitive inhibition, turnover, and substrate selectivity.



G. Wulff,* T. Gross,
R. Schönfeld 1962–1964

Enzyme Models Based on Molecularly Imprinted Polymers with Strong Esterase Activity

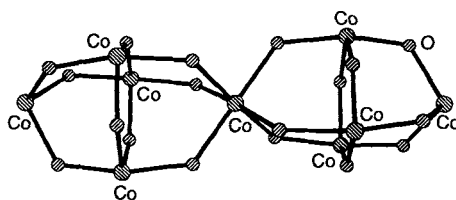
Only corner-sharing between the seven TaO_6 octahedra is observed in the neutral complex $[\text{H}_{-11}\text{Ta}_7\text{O}_{12}(\text{tdci})_6]$ ($\text{tdci} = 1,3,5$ -trideoxy-1,3,5-tris(dimethylamino)-*cis*-inositol). The structure on the right (only one tdci ligand is illustrated) depicts the Ta_7O_{30} double adamantane core. In contrast to previously described structures of polyoxometalate ions, which have a predominantly edge-shared framework, this compound has an unusually open structure.



K. Hegetschweiler,* T. Raber,
G. J. Reiss, W. Frank, M. Wörle,
A. Currao, R. Nesper,
T. Kradolfer 1964–1966

A Polyoxo–Polyolato Complex of Tantalum(v) with a Double Adamantane-Like $[\text{Ta}_7\text{O}_{12}]^{11+}$ Core

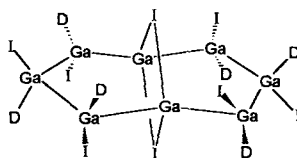
Avoidance of a metal–metal bond is a significant factor favoring the formation of the nonanuclear cobalt complex $[\text{Co}_9(\text{chp})_{18}]$ (framework depicted on the right; $\text{chp} = 6$ -chloro-2-pyridonate). The complex is homoleptic, which is unusual for 3d-complexes of pyridonates, and this contrasts with the similar, but heteroleptic, nickel double adamantane frameworks also reported.



E. K. Brechin, S. G. Harris, S. Parsons,
R. E. P. Winpenny* 1967–1969

Clusters from Vertex- and Face-Sharing Adamantane-Like Units: A New Topology for Multinuclear Complexes

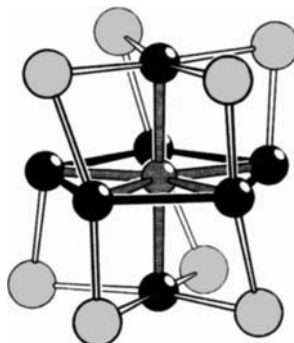
Merely the illusion of a Ga–Ga bond is given between the doubly I-bridged atoms of the nearly planar eight-membered ring in $\text{Ga}_8\text{I}_8 \cdot 6\text{PET}_3$ (shown on the right). This finding is remarkable, since the corresponding Al^{I} halides have four-membered Al rings. D = PET_3 .



C. U. Doriat, M. Friesen, E. Baum,
A. Ecker, H. Schnöckel* 1969–1971

Synthesis, Structure, and Oxidation of
Donor-Stabilized Gallium(I) Iodide:
 $\text{Ga}_8\text{I}_8 \cdot 6\text{PET}_3$

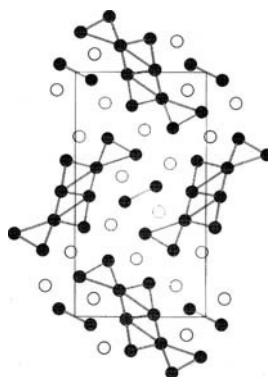
A unique type of cluster, the $[\{\text{RhBi}_7\}\text{Br}_8]$ molecule, is the building block from which the halogen-rich bismuth subbromide Bi_7RhBr_8 is constructed. The Bi atoms are arranged as a pentagonal bipyramid around the central Rh atom, and they, in turn, are surrounded by the Br atoms as a square antiprism (shown on the right; Rh = dark gray, Bi = black, Br = pale gray). In contrast to Bi_7RhBr_8 , the metal-rich bismuth subiodides known to date are not composed of discrete molecules.



M. Ruck* 1971–1973

Bi_7RhBr_8 : A Subbromide with Molecular
 $[\{\text{RhBi}_7\}\text{Br}_8]$ Clusters

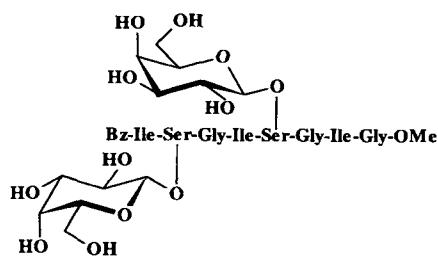
Condensed double chains of edge-sharing scandium octahedra are contained in Sc_2Te . These structural units are augmented by more loosely bound pyramidal and zigzag scandium aggregates. On the right is a projection of these chains together with tellurium (the open circles). The metal array may be viewed as the result of the dissociation of the metal frameworks in electron-rich chalcogenides.



P. A. Maggard,
J. D. Corbett* 1974–1976

Sc_2Te : A Novel Example of Condensed
Metal Polyhedra in a Metal-Rich but
Relatively Electron-Poor Compound

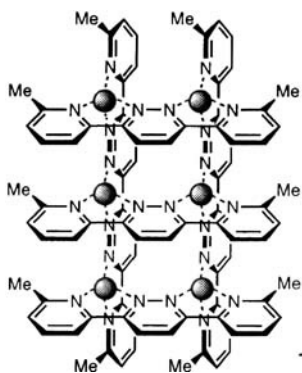
Glycopeptide libraries in which both the carbohydrate part and the peptide part have been varied can be generated by stereoselective glycosylation of free hydroxy groups of support-bound peptides with glycosyl trichloroacetimidates. The use of temporary *t*Bu protecting groups enabled the stereoselective synthesis of a model library of four glycopeptides (one is depicted on the right) that each have two different glycosyl groups.



A. Schleyer, M. Meldal,* M. Renil,
H. Paulsen, K. Bock 1976–1978

Direct Solid-Phase Glycosylations of Peptide
Templates on a Novel PEG-Based
Resin

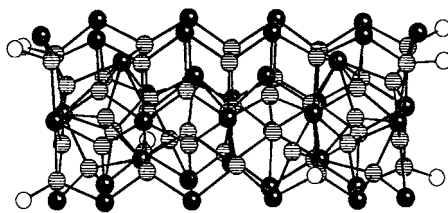
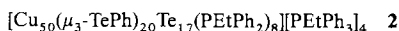
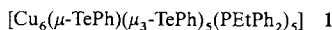
A significantly larger variety of ligand combinations is possible for rectangular $[m \times n]$ grids (such as the first complex of this type, $[2 \times 3]$ grid 1) than for symmetric square $[n \times n]$ grids. The product distribution $[2 \times 3]:[2 \times 2]:[3 \times 3]$ for the reaction of tri- and ditopic ligands with Ag^{I} ions in a 2:3:6 ratio is 90:8:2! The spheres represent the Ag^{I} ions.



P. N. W. Baxter, J.-M. Lehn,*
B. O. Kneisel, D. Fenske 1978–1981

Multicomponent Self-Assembly: Preferential
Generation of a Rectangular $[2 \times 3]$ G
Grid by Mixed-Ligand Recognition

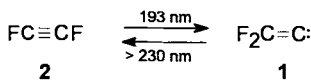
Photolytic cleavage of TePh_2 from the phosphane-stabilized, hexanuclear cluster **1** results in the mixed telluride–telluroate cluster **2** in good yields (the structure of the anion in **2** is shown on the right; dark spheres represent Te atoms, hashed spheres Cu atoms, and white spheres P atoms).



J. F. Corrigan, D. Fenske* ... 1981–1983

New Copper Telluride Clusters by Light-Induced Telluroate–Telluride Conversions

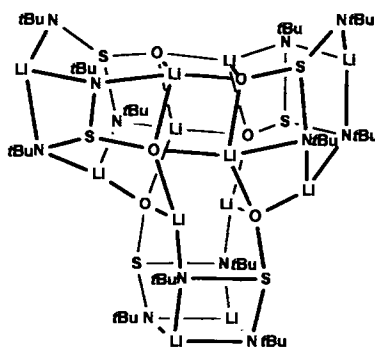
An alkyne–vinylidene isomerization is also possible with the difluoro compounds **1** and **2**! Irradiation of **2** ($\lambda = 193 \text{ nm}$) in an Ar matrix yields **1** exclusively. The IR spectrum agrees with results of novel ab initio calculations, which also suggest that **1**—in sharp contrast to the vinylidenes $\text{RHC}=\text{C}—$ is protected against isomerization into **2** by a kinetic barrier. Irradiation with light with $\lambda > 230 \text{ nm}$ converts **1** back into **2**. Already at 35–42 K **1** adds CO and N_2 to yield F_2CCCCO and F_2CCNN , respectively.



J. Breidung, H. Bürger,* C. Kötting, R. Kopitzky, W. Sander,* M. Senzlober, W. Thiel,* H. Willner* ... 1983–1985

Difluorovinylidene, $\text{F}_2\text{C}=\text{C:}$

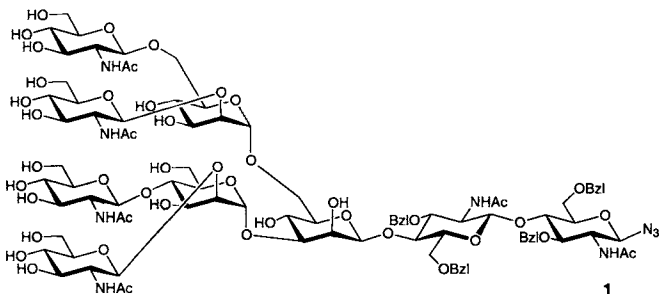
Depending on the type of substituent on the nitrogen atom, the two thirty-six atom clusters of main group elements formed on treating RNSO with $\text{LiNH}t\text{Bu}$ adopt different structures ($\text{R} = t\text{Bu}, \text{SiMe}_3$). For instance, the compound depicted on the right can be described as an aggregate of three hexagonal prisms.



J. K. Brask, T. Chivers,* M. Parvez, G. Schatte ... 1986–1988

Self-Assembly of Thirty-Six Atom Clusters ($\text{Li}_{12}\text{S}_6\text{O}_6\text{N}_{12}$) Containing Diazasulfite Anions

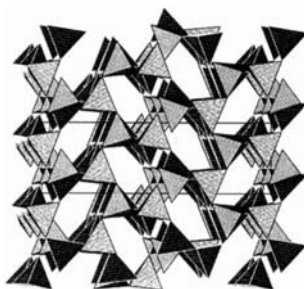
Double regioselective glycosylation is the key to the generally applicable strategy by which two triantennary octasaccharides and the tetraantennary nonasaccharide **1** are available. A modular system of oligosaccharide building blocks is the basis of an efficient synthesis of complex *N*-glycans with the desired number of branches in unexpectedly high yields.



C. Unverzagt* ... 1989–1992

A Modular System for the Synthesis of Complex *N*-Glycans

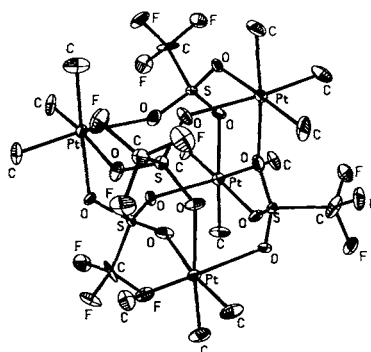
Starting from a diphosphazene as a molecular precursor, single-phase HP_4N_7 could be synthesized for the first time. The structure was determined from powder-diffraction investigations with synchrotron radiation. A section of the crystal structure is shown on the right.



S. Horstmann, E. Irran, W. Schnick* ... 1992–1994

Phosphorus(v) Nitride Imide HP_4N_7 : Synthesis from a Molecular Precursor and Structure Determination with Synchrotron Powder Diffraction

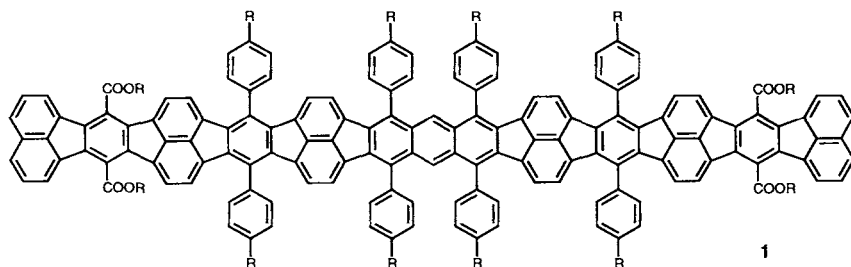
Depending on the donor strength of the base, tri-, di-, or mono-nuclear complexes are formed on reaction of the tetranuclear complex $[\{\text{Me}_3\text{Pt}(\text{O}_3\text{SCF}_3)\}_4]$ (structure depicted on the right) with Lewis bases. These complexes of different nuclearity offer a rich synthetic potential because of their precisely tunable properties.



S. Schlecht, J. Magull, D. Fenske, K. Dehnicke* 1994–1995

Trimethylplatinum Triflate: A Versatile Building Block in Coordination Chemistry

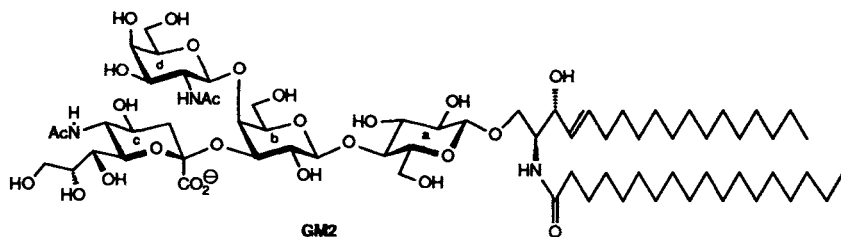
The exceptionally long (4.5 nm) monodisperse polycyclic aromatic hydrocarbon **1** contains 29 condensed five- and six-membered rings. Since the dodecyl chains make this extended, flat (tabular) molecule unusually soluble in common organic solvents, it can be readily characterized. Compound **1** can be reduced to the octaanion within a relatively small potential range, and the tetracation that forms on oxidation is stable for several seconds.



B. Schlicke, A.-D. Schlüter,* P. Hauser, J. Heinze 1996–1998

Polycyclic Aromatic Hydrocarbons in the Nanometer Range

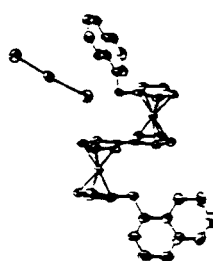
A target antigen for cancer immunotherapy, ganglioside GM2, is expressed on the cell surface of several human cancer types. An efficient chemical synthesis can now make available ample amounts of a structurally well-defined synthetic GM2, free of biological contaminants. This greatly facilitates the systematic construction of safe and efficient GM2 cancer vaccines.



J. C. Castro-Palomino, G. Ritter,* S. R. Fortunato,* S. Reinhardt, L. J. Old, R. R. Schmidt* 1998–2001

Efficient Synthesis of Ganglioside GM2 for Use in Cancer Vaccines

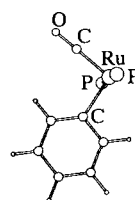
Extreme sensitivity to changes in the lattice is observed for electron-transfer rates in the $\text{Fe}^{\text{II}}/\text{Fe}^{\text{III}}$ title compound, as shown by Mössbauer spectroscopic investigations of the two crystallographic phases in which the compound can be isolated. The structure of the cation and anion in the monoclinic phase $P2_1/n$ is shown on the right.



T.-Y. Dong,* X.-Q. Lai, Z.-W. Lin, K.-J. Lin 2002–2004

Effects of Environment on Intramolecular Electron Transfer in Mixed-Valence 1',1'''-Dinaphthylmethyl(biferrocenium) Triiodide: Structural and ^{57}Fe Mössbauer Characteristics

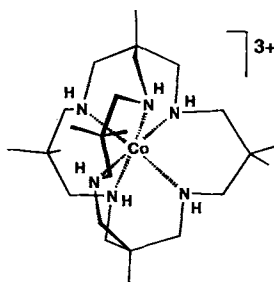
A nonplanar arrangement of four ligands is intrinsic to the title compound in solution and in the crystal. There is no interaction between the Ru center and the counterion $[3,5-(\text{CF}_3)_2\text{C}_6\text{H}_3]_4\text{B}^-$. Density functional theory calculations of the model complex $[\text{Ru}(\text{Ph})(\text{CO})(\text{PH}_3)_2]^+$ provided the structure shown on the right, which shows no *ortho*-CH...Ru interaction.



D. Huang, W. E. Streib, O. Eisenstein,* K. G. Caulton* 2004–2006

$[\text{Ru}(\text{Ph})(\text{CO})(\text{P}t\text{Bu}_2\text{Me})_2]^+$: A Unique 14-Electron Ru^{II} Complex with Two Agostic Interactions

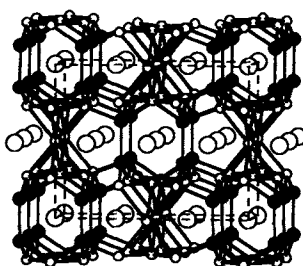
The structure of the exciting blue form of a new hexa-aminecobalt(III) cage compound (Lewis structure shown on the right) was not known, while that of the more usual yellow conformer was determined experimentally. A combination of molecular-mechanics calculations and the simulation of spectroscopic and electrochemical properties can be used to determine the structure, and to interpret the unprecedentedly low ligand field and high redox potential.



P. Comba,*
A. F. Sickmüller 2006–2008

Solution Structures of a Pair of Stable Hexaaminecobalt(III/II) Conformers

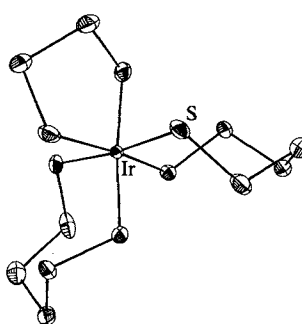
A variant of the BaAl_4 structure, the $\alpha\text{-La}_3\text{Al}_{11}$ structural type is observed upon crystallization of the new ternary intermetallic phase $\text{Ln}_3\text{Au}_2\text{Al}_9$ ($\text{Ln} = \text{Dy}$ and Tb). Calculations of the electronic structure were used to investigate the characteristics of Au and Al atoms within the framework. The gray atoms in the picture of the structure prefer heteronuclear Au–Al contacts over homonuclear Al–Al and Au–Au contacts.



K. J. Nordell, G. J. Miller* ... 2008–2010

$\text{Ln}_3\text{Au}_2\text{Al}_9$ ($\text{Ln} = \text{Dy}, \text{Tb}$): Heteronuclear versus Homonuclear Bonding in Inter-metallic Phases

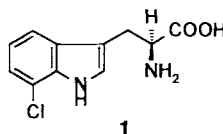
Not 15, but 16 sulfur atoms are found in $[\text{NH}_4]_3[\text{Ir}(\text{S}_4)(\text{S}_6)_2]$, which was first reported as “ $[\text{NH}_4]_3[\text{IrS}_{15}]$ ” in 1904. This was determined by comparing the results of the crystal structure analysis (structure shown on the right) with the optical goniometric data reported in the original work. $[\text{NH}_4]_3[\text{Ir}(\text{S}_4)(\text{S}_6)_2]$ spontaneously resolves upon crystallization. Therefore, these enantiomeric crystals were available a decade before Werner first separated optically active inorganic complexes.



T. E. Albrecht-Schmitt,
J. A. Ibers* 2010–2011

$[\text{NH}_4]_3[\text{Ir}(\text{S}_4)(\text{S}_6)_2]$: A Reevaluation of Hofmann and Höchtlen's Report of $[\text{NH}_4]_3[\text{Ir}(\text{S}_5)_3]$ from 1904

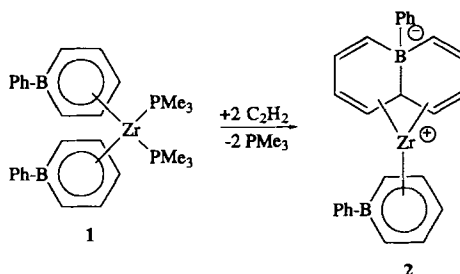
NADH instead of hydrogen peroxide is required by two newly identified, substrate-specific and regio-selective halogenases. Both were isolated from a pyrrolnitrin-producing *Pseudomonas fluorescens* strain. One enzyme catalyzes the chlorination of L-tryptophan to 7-chloro-L-tryptophan (**1**).



K. Hohaus, A. Altmann, W. Burd,
I. Fischer, P. E. Hammer, D. S. Hill,
J. M. Ligon, K.-H. van Pée* ... 2012–2013

NADH-Dependent Halogenases Are More Likely To Be Involved in Halometabolite Biosynthesis Than Haloperoxidases

The folding of the boratanaphthalene ring over the metal in **2** ensures that all ten non-hydrogen atoms are within bonding distance to Zr. This complex with the novel boratanaphthalene ligand was furnished in an unprecedented ring annulation reaction of ethyne with the boratabenzene ligand **1**.



A. J. Ashe III,* S. Al-Ahmad, J. W. Kampf,
V. G. Young, Jr. 2014–2016

Boratabenzene Zirconium(II) Complexes: An Unusual Annulation with Ethynes

* Author to whom correspondence should be addressed

| | |
|---|---|
| Trace Analysis: A Structured Approach to Obtaining Reliable Results · E. Pritchard, G. MacKay, U. Points | <i>R. Niessner</i> 2017 |
| Introduction to Liquid Crystals. Chemistry and Physics · P. J. Collings, M. Hird | <i>C. Tschierske</i> 2017 |
| Preparation of Alkenes. A Practical Approach · J. M. J. Williams | <i>A. Kirschning</i> 2018 |
| Color Atlas of Biochemistry · J. Koolman, K.-H. Böhm | <i>P. Wentworth Jr., K. D. Janda</i> 2019 |
| Molecular Modeling. Basic Principles and Applications · H.-D. Höltje, G. Folkers | <i>D. Schomburg</i> 2020 |
| Molecular Modelling. Principles and Applications · A. R. Leach | |

German versions of all reviews, communications, and highlights in this issue appear in the second September issue of *Angewandte Chemie*. The appropriate page numbers can be found at the end of each article and are also included in the Author Index on p. 2023.

All the Tables of Contents from 1995 onwards may be found on the WWW under:
<http://www.wiley-vch.de/home/angewandte>

SERVICES

| | |
|----------------|------|
| ● Sources | A-79 |
| ● Events | 1950 |
| ● Keywords | 2022 |
| ● Author Index | 2023 |
| ● Preview | 2024 |

The following reviews will appear in future issues:

N-Heterocyclic Carbenes
 W. A. Herrmann, C. Köcher

Synthesis, Conformational Analysis, and Molecular Biology in the Search for New LHRH Antagonists
 B. Kutscher, M. Bernd, T. Beckers, E. E. Polymeropoulos, J. Engel

The Covalent Chemistry of Higher Chemistry Fullerenes: C₇₀ and Beyond
 F. Diederich, C. Thilgen, A. Herrmann

Enantioselective Synthesis with Lithium/(–)-Sparteine–Carbanion Pairs
 D. Hoppe, T. Hense

Homoleptic Cationic Carbonyl Complexes of Electron-Rich Metals: Generation in Superacidic Media and Structural and Spectroscopic Characterization
 H. Willner, F. Aubke

Phanes with Three- and Four-Membered Rings as Building Elements
 R. Gleiter, M. Merger

Understanding Reactivity Patterns in Radical Cation Chemistry
 M. Schmittle, A. Burghart

Charge Transfer through the DNA Base Stack
 J. K. Barton

Supramolecular Electrochemistry
 L. Echegoyen, P. L. Bolas, M. Gómez-Kaifer

Catabolic Pathways and Their Biocatalysts: Bacterial Degradation of Quinoline and Derivatives
 S. Fetzner, B. Tshisuaka, F. Lingens, R. Kappl, J. Hüttermann

Four- π -Electron, Four-Membered λ^5 -Phosphorus Heterocycles: Electronic Isomers of Heterocyclobutadienes
 G. Bertrand

A New Model for Aluminophosphate Formation: Transformation of a Linear Aluminophosphate to Chain, Layer, and Framework Structural Types
 G. A. Ozin

Aerogels—Airy Materials: Chemistry—Structure—Properties

U. Schubert, N. Hüsing

C₃ Symmetry in Asymmetric Catalysis and Chiral Recognition

C. Moberg

Commercial, Synthetic Non-Nutritive Sweeteners

D. J. Ager, D. P. Pantaleone

Lithistid Sponges: Star Performers or Hosts to the Stars

C. A. Bewley, D. J. Faulkner

Electroluminescent Conjugated Polymers—Seeing Polymers in A New Light

A. Kraft, A. C. Grimsdale, A. B. Holmes

Protein Folding: A Perspective from Theory & Experiment

C. M. Dobson, A. Šali, M. Karplus

Vicinal Diamines: Biological and Chemical Interest, Methods of Preparation

D. Lucet, T. Le Gall, C. Mioskowski

Cationic Liposomes for Gene Therapy

A. D. Miller

Ligand Design for Electrochemically Controlling Transition Metal Stoichiometric and Catalytic Reactivity

A. M. Allgeier, C. A. Mirkin

About the Parametrization of Substituents - Fluorine and Other Heteroatom Effects on OH-, NH-, and CH-Acidity

M. Schlosser

Lipases: Interfacial Enzymes with Attractive Applications

R. D. Schmid, R. Verger

Transition Metal Catalysis in the Baeyer–Villiger Oxidation of Ketones

G. Strukul

The Glycopeptide Story—How to Kill the Deadly “Superbugs”

D. H. Williams

Polyvalent Interactions in Biological Systems: Implications for Design and Use of Multivalent Ligands and Inhibitors

M. Mammen, S.-K. Choi, G. M. Whitesides

ANGEWANDTE CHEMIE

A Journal of the
Gesellschaft
Deutscher Chemiker

International Edition in English

1997
36/17

Pages 1775–1914

EDITORIAL

Brief and concise contributions should be written for *Angewandte Chemie*, and starting in 1998 we'll help out a bit. The Editorial Board of the journal has decided to drop the words "in English" from the name of the English edition, since this has long been general usage. Contributions published from 1998 onwards will simply be cited as *Angew. Chem. Int. Ed.*; however, those papers appearing before the end of this year should continue to be cited as *Angew. Chem. Int. Ed. Engl.* Librarians, and others for whom this information is important, should note that *Angewandte Chemie International Edition* will have a new International Series Serial Number (ISSN) in 1998: 1433-7851 (previously 0570-0833).

What else will be new in 1998 at *Angewandte Chemie*? After many positive changes in the past few years—increase in the number of issues in 1994, introduction of full-page illustrations before reviews and the communications section in 1996, and presentation of the Table of Contents, Keywords, and Hot Papers on the WWW in 1997—we will not be slacking off in 1998. Presentation of Supporting Information on the WWW as well as on-line publication of the complete journal are planned. Detailed information on when this service will appear and what the requirements are for its use will be provided in due course.

Chemistry—A European Journal, the youngest fledgling of "Angewandte", has quickly flown the nest and will be completely independent in 1998. The number of manuscripts submitted from around the world is rising steadily, and at least 2500 pages are planned for next year. The cost for institutions will be \$ 645 (the highly attractive low price for personal subscribers will not change). The high quality of the manuscripts submitted and the number of subscriptions have already secured a top place for "Chemistry" among the chemistry journals.

Freedom to grow in 1998 has been granted to *Angewandte Chemie* to deal with the ever increasing number of manuscripts to be published. Figure 1 shows an overview of the development

of trends in submissions of communications over the past years, Figure 2 the details on submissions from outside Germany, and Figure 3 the growth in the number of pages and the increase in the rejection rate. Today *Angewandte Chemie* is truly an international chemistry journal, and this achievement has not been hindered by the German name nor the often heard lament of the decline of scientific journals in Europe. The two new European journals starting in 1998, *European Journal of Inorganic Chemistry* (EJIC) and *European Journal of Organic Chemistry* (EJOC), which are formed by the combination of six journals

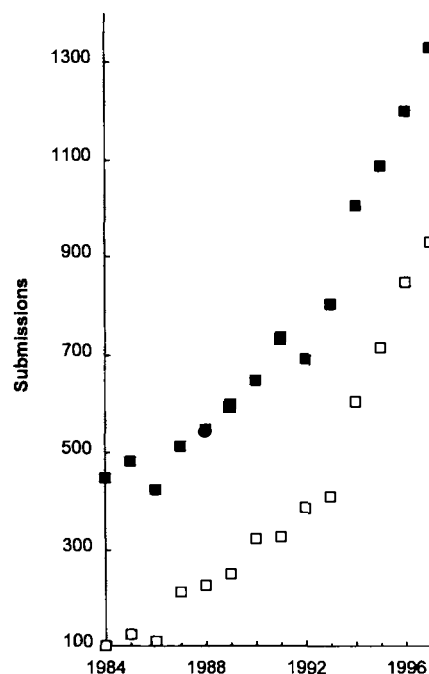


Figure 1. The development of trends in submissions of communications from 1984 to 1997: total number of submissions (■) and those from outside Germany (□).

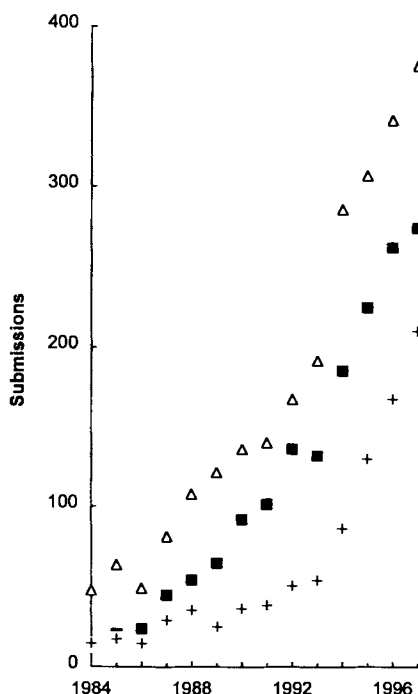


Figure 2. Trends in the number of submitted communications from western Europe (Δ , excluding Germany), the U.S. (\blacksquare), and East Asia ($+$). The internationalization of *Angewandte Chemie* started in the mid 1980s. Remarkable is the sharp increase in the number of manuscripts submitted from East Asia over the last years.

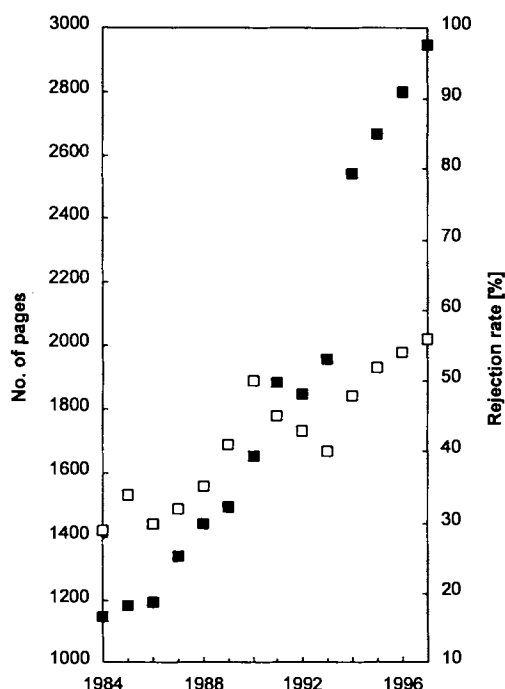


Figure 3. Trends in the number of pages published (\blacksquare) and the rejection rate (\square) from 1984 to 1997. Doubling the number of issues per year from 12 to 24 in 1994 allowed an over-proportional increase in the number of pages published.

(*Bulletin des Sociétés Chimiques Belges*, *Bulletin de la Société Chimique de France*, *Chemische Berichte*, *Gazzetta Chimica Italiana*, *Liebigs Annalen*, and *Receuil des Travaux Chimiques des Pays-Bas*), should face a similar development—this is already evident for “Chemistry”. These two journals will cover new advances in their respective fields, while *Chemistry—A European Journal* publishes from the whole range of chemistry and related areas.

Twenty percent more pages are planned for *Angewandte Chemie* in 1998. Nevertheless, the price for personal members of a national chemical society will remain at \$ 270 for full members and \$ 155 for students. With \$ 1740, institutional subscribers will pay no more in 1998 than they did this year for “Angewandte” and “Chemistry” (all prices valid for the U.S.). We are confident that the next—and also electronic—steps into the future will be on solid ground. The editorial preparations for 1999 and 2000 are already underway!

Quality first: Increasing the number of pages does not mean that we are forgetting this most important aspect of our work. Prof. W. Frühwald, President of the German Science Foundation (Deutsche Forschungsgemeinschaft), clearly stated in an interview with the weekly newspaper *Zeit* (July 11, 1997): “There is honestly enough garbage among all the publications that are poured into the market by the hundreds . . . Therefore, quality must be the most eminent criterion in the judgement of proposals and publications.” For *Angewandte Chemie* the quality of the information provided by a manuscript has always had highest priority for the decision on its acceptance or rejection. Even over-long communications are published if the reviewer, when specifically asked, confirms that the length is justified. However, when writing a manuscript for *Angewandte Chemie*, authors should not forget that the space there is valuable. A brief and concise manuscript saves time for the reader, the reviewer, and the editorial staff, and leaves space for more contributions.

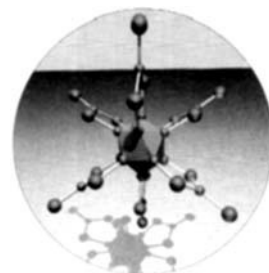
Optimal presentation is essential for a journal that publishes manuscripts from all areas of chemistry. This not only means clearer Figures and Schemes, but also thorough explanations of abbreviations and new terminology. Only in this way can the very large and heterogeneous readership make the best use of the offered information. Therefore, manuscripts that have been accepted for publication in *Angewandte Chemie* are also carefully edited. This is a rare exception for scientific journals nowadays; most often the manuscripts simply undergo copy editing or language polishing, that is, editing “lite”. From the many manuscripts that we receive—“garbage” is rarely among them—we sort out the most important ones for publication and polish them up. Therefore, our readers are assured of the quality demanded by W. Frühwald, and our authors find themselves in “good company” also in the 110th year of *Angewandte Chemie*!

Peter Göllitz

Peter Göllitz

COVER PICTURE

The cover picture shows the novel anion $[B_{12}(BSe_3)_6]^{8-}$, which was synthesized as the cesium salt by a solid-state reaction from the elements. The icosahedral species is the first example of a new class of polyhedral boron clusters that combines both the structural features of polyhedral boranes and boron chalcogenides. Each boron atom of the B_{12} icosahedron is coordinated by a selenium atom of one of the six trigonal-planar BSe_3 units (depicted as ball-and-stick models). The electron count of the molecular anion obeys Wade's rules. The bidentate binding mode of the BSe_3 groups to the B_{12} polyhedra results in a novel type of planar five-membered B_3Se_2 rings. The synthesis, structure, and bonding of this first boron icosahedron with complete chalcogen substitution are described by B. Krebs et al. on pages 1903 ff.



REVIEWS

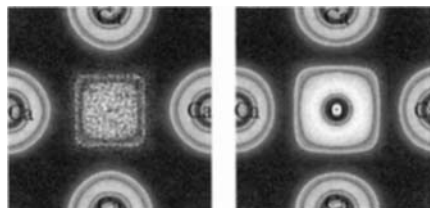
Contents

How is superconductivity explained from a chemist's point of view? This question is discussed in this review, starting from the bonding in carbides and carbide halides of the rare earth metals. A general view of the origin of superconductivity is developed, which is based on a tendency for (pairwise) localization of conduction electrons with formation of Cooper pairs $+k\uparrow -k\downarrow$.

A. Simon* 1788–1806

Superconductivity and Chemistry

Even missing atoms in solid-state structures can be localized by analyzing the electron density with the electron localization function (ELF). For instance, ELF analysis of the Ca_4Sb_2 structure revealed a high ELF value precisely at the position at which the originally overlooked oxygen atom was subsequently found.



The picture shows a section through the ELF of the Ca_6 octahedron without an interstitial O atom (left) and with this additional atom (right). The areas of application for ELF analysis range from ionic solids over intermetallic phases and covalent compounds to π systems of organic compounds.

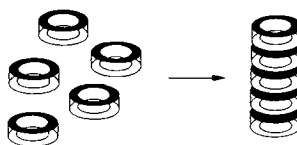
A. Savin,* R. Nesper,* S. Wengert,
T. F. Fässler 1808–1832

ELF: The Electron Localization Function

HIGHLIGHTS

Contents

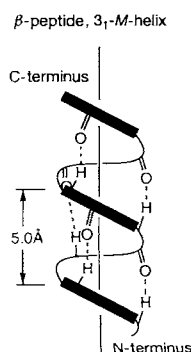
No magic triggers the stacking of macrocycles to nanotubes (see diagram). Instead, this is a consequence of complementarity and reciprocal molecular recognition of the subunits. The supramolecular structures then allow the transport of ions and molecules through membranes, just like their biological models.



B. König* 1833–1835

Well-Rounded Research:
Nanotubes through Self-Assembly

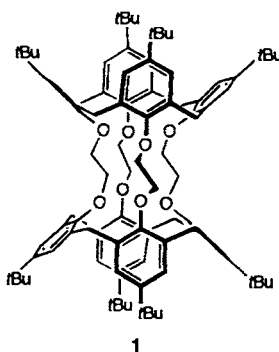
Why don't we live in a β -peptide world? This is a legitimate question in light of new findings by D. Seebach et al. and S. Gellman et al. on the secondary structures of β -peptides. Peptides composed of less than ten β -amino acid residues can form stable, secondary structure motifs like the 31-M-helix shown on the right. In one study a hepta- β -peptide, which had been thermally denatured, refolded within 200 ps!



U. Koert* 1836–1837

β -Peptides: Novel Secondary Structures
Take Shape

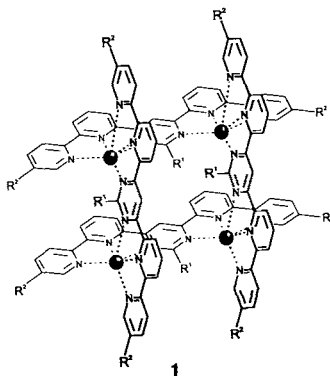
Even after three days the uptake of Li^+ , Na^+ , Cs^+ , and Rb^+ ions by the novel calix[4]tube receptor **1** is not significant (<7%), whereas K^+ ions are complexed within one hour. This remarkable selectivity for K^+ ions is reminiscent of that of potassium channel proteins.



P. Schmitt, P. D. Beer,* M. G. B. Drew,
P. D. Sheen 1840–1842

Calix[4]tube: A Tubular Receptor with
Remarkable Potassium Ion Selectivity

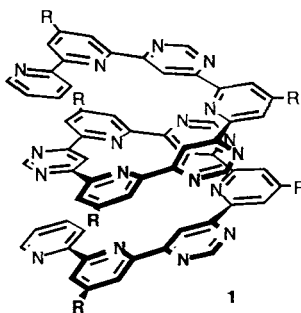
The use of two tridentate ligands is the secret of success for the self-assembly of structurally intriguing tetranuclear Co^{II} complexes. The cation $[\text{Co}_4(\text{L})_4]^{8+}$ (**1**) exists as a $[2 \times 2]$ -grid of octahedrally coordinated metal ions located at the corners of a square. The complex displays multiple redox processes and is of potential interest for the development of electrochemically addressable inorganic arrays (R^1 , $\text{R}^2 = \text{H}$, Me; $\bullet = \text{Co}^{\text{II}}$).



G. S. Hanan, D. Volkmer,
U. S. Schubert, J.-M. Lehn,* G. Baum,
D. Fenske 1842–1844

Coordination Arrays: Tetranuclear
Cobalt(II) Complexes with $[2 \times 2]$ -Grid
Structure

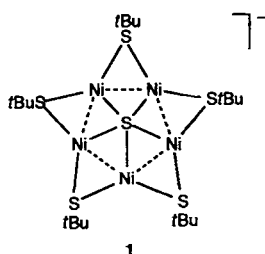
Both in solution and in the solid state the polyheterocyclic molecule **1** spontaneously adopts a helical structure with two turns. This convincingly demonstrates that the structural features encoded in the molecular strand can induce helicity, and points to the generality of this self-organization process.



D. M. Bassani, J.-M. Lehn,* G. Baum,
D. Fenske 1845–1847

Designed Self-Generation of an Extended
Helical Structure from an Achiral Poly-
heterocyclic Strand

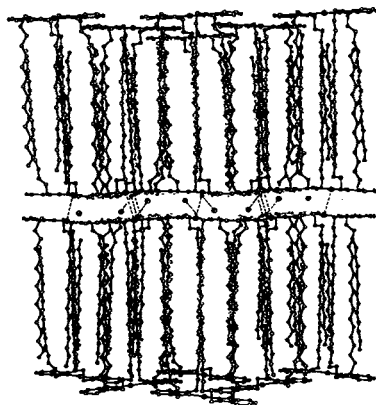
Contrary to the common belief that a simple description of the bonding in $\text{Ni-S}(\text{Se})$ clusters is not possible, the electronic structure of the cluster $[\text{Ni}_5\text{S}(\text{S}t\text{Bu})_5]^-$ (**1**) can be understood in terms of an idealized molecular orbital interaction diagram. The more complicated cluster $[\text{Ni}_{20}\text{Se}_{12}(\text{SeMe})_{10}]^{2-}$ can also be analyzed in this manner.



F.-W. Cheung, Z. Lin* 1847–1849

Analysis of the Bonding in
 $[\text{Ni}_5(\mu_5\text{-S})(\mu_2\text{-SR})_5]^-$, an Unprecedented
Pentanuclear Sulfide Cluster

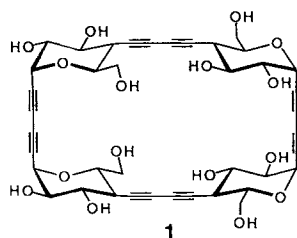
A highly ordered lamellar mesophase is exhibited by the thermally stable liquid-crystalline gold(I) dicarbene compounds presented here. The crystal structure of one of these compounds is depicted on the right.



K. M. Lee, C. K. Lee,
I. J. B. Lin* 1850–1852

A Facile Synthesis of Unusual Liquid-Crys-
talline Gold(I) Dicarbene Compounds

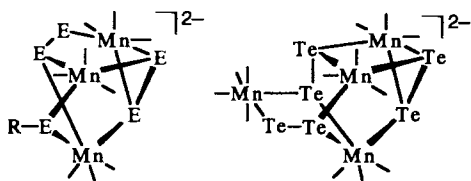
An antiparallel arrangement of water-containing tubes characterizes the crystal structure of the cyclotetramer **1**. The tetramer **1**, which binds to D- and L-adenosine in aqueous solution, was prepared in four steps in a yield of 50% from a 1,4-dialkynylated glucose derivative; the corresponding cyclohexamer and cyclooctamer were isolated as by-products.



R. Bürli, A. Vasella* 1852–1853

Cyclic “Acetylenosaccharides”—Novel Cyclodextrin Analogues

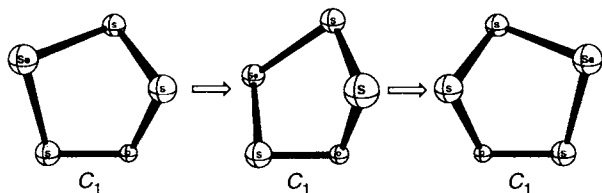
Different but so alike are the structures of the clusters $(\text{Ph}_4\text{P})_2[\text{Mn}_3(\text{CO})_9(\text{S}_2)_2(\text{SH})]$ and $(\text{Ph}_4\text{P})_2[\text{Mn}_4(\text{CO})_{13}(\text{Te}_2)_3]$ ($\text{E} = \text{S}$ or Te ; structures of the anions depicted below), which form in the reaction of $[\text{Mn}_2(\text{CO})_{10}]$, Na_2E_2 , Ph_4PBr , and ethanol in a sealed tube at 85°C . The fundamental difference lies in the substitution of a hydrochalcogen by a dichalcogen in the Te compound and the concomitant extension of the cluster framework by a $\text{Mn}(\text{CO})_4$ fragment.



S. D. Huang,* C. P. Lai,
C. L. Barnes 1854–1856

Organometallic Chemistry under
Hydro(solvo)thermal conditions:
Synthesis and X-ray structure of
 $(\text{Ph}_4\text{P})_2[\text{Mn}_3(\text{CO})_9(\text{S}_2)_2(\text{SH})]$,
 $(\text{Ph}_4\text{P})[\text{Mn}_2(\text{CO})_6(\text{SH})_3]$, and
 $(\text{Ph}_4\text{P})_2[\text{Mn}_4(\text{CO})_{13}(\text{Te}_2)_3]$

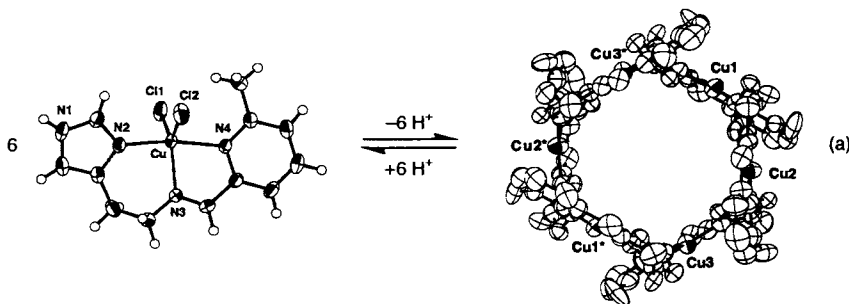
Synthetic chemists are challenged to find a five-atom molecule that, like cyclo-SeSSOS, can enantiomerize in a single step without passing through any achiral conformation. The barrier for the pseudorotation of *cyclo*-SeSSOS shown below is computed to be quite low: $6.2 \text{ kcal mol}^{-1}$.



M. Mauksch,
P. von R. Schleyer* 1856–1860

A Five-Atom Molecule That Enantiomerizes
in a Single Step via Chiral Transition
States

The reversible reaction of a monomeric Cu^{II} complex to a cyclic hexamer (crystal structures shown below) is the first example of the interconversion of a potential guest complex and a complex that cannot function as a guest [Eq. (a)]. It is—like in living organisms—controlled by a very common external signal, namely proton supply or abstraction.



N. Matsumoto,* Y. Mizuguchi, G. Mago,
S. Eguchi, H. Miyasaka, T. Nakashima,
J.-P. Tuchagues* 1860–1862

Proton-Dependent Monomer–Oligomer
Interconversion of Metal Complexes

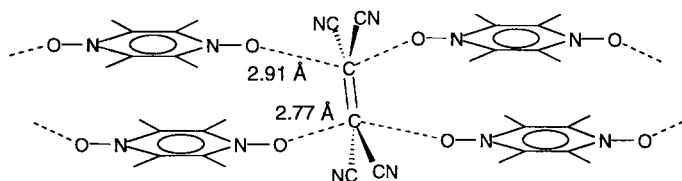
C_2S_2 can be detected in a matrix, whereas C_2O_2 cannot. What about C_2OS ? This question has now been answered with the generation of C_2OS in an Ar matrix [Eq. (a)] and the characterization with matrix-isolation spectroscopy. Under matrix conditions C_2OS is a stable molecule, which most likely exists in the triplet ground state.



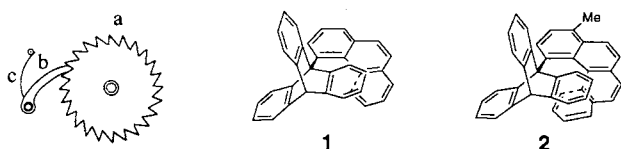
G. Maier,* H. P. Reisenauer,
R. Ruppel 1862–1864

2-Thioxoethen-1-one ($\text{O}=\text{C}=\text{C}=\text{S}$)

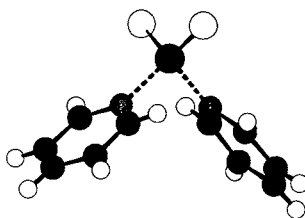
Ladder and web polymorphic forms of cocrystals of tetramethylpyrazinedioxide (TMPDO) and tetracyanoethylene (TCNE) are obtained by rapid or slow crystallization, respectively. In the thermodynamically less stable, purple (TMPDO)₂-TCNE crystals the donor and acceptor building blocks are linked through N⁺O⁻...C(alkene) interactions to form one-dimensional ladders (see picture below).



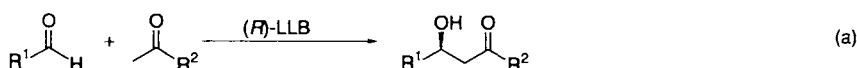
Triptycylhelicenes 1 and 2 were examined as molecular ratchets (see picture) in which the triptycene serves as the ratchet wheel (a) and the helicenes as pawl (b) and spring (c). The ease of rotation of the triptycene wheel depends on the helicene springs and pawls, but do these have any influence on the direction of rotation?



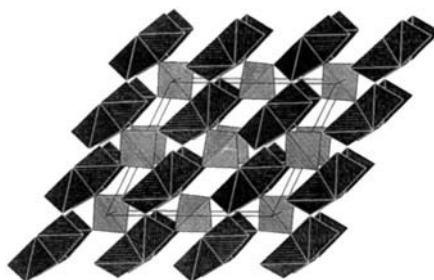
With pyridine as a neutral electron-donor ligand, the [S=P=S]⁺ ion can be isolated as a salt [(C₅H₅N)₂PS₂]⁺X⁻ (X = Br, I) that is stabilized both in the solid state and in solution. The structures of these salts were characterized by NMR spectroscopy and X-ray crystal structure analysis (structure depicted on the right). The position of the equilibrium that exists between [(C₅H₅N)₂PS₂]X and (C₅H₅N)PS₂X in acetonitrile is dependent on the basicity of the halogen.



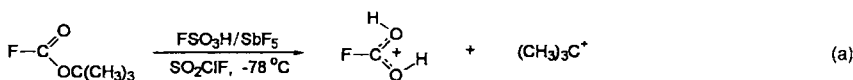
Up to 94% ee can be achieved in the title reaction [Eq. (a)], which was previously only possible with enzymes. In this reaction LaLi₃tris(binaphthoxide) (LLB) imitates the function of enzymes by displaying both Lewis acidity and Brønsted basicity.



A varied chemistry of ternary and higher phosphorus(v) nitrides has developed during the last few years. However, the crystal structure of the binary nitride P₃N₅ has proved elusive until now. The network structure built up by PN₄ tetrahedra (depicted on the right) resembles that of SiO₂ and Si₃N₄. Surprisingly, in α-P₃N₅ the PN₄ tetrahedra are also connected through edge-sharing.



Protolysis of *tert*-butyl fluoroformate [Eq. (a)] in a solution of FSO₃H/SbF₅-SO₂ClF at -78 °C yields the stable protonated form of the elusive fluoroformic acid [FC(OH)₂]⁺. It was characterized by ¹H, ¹³C, and ¹⁹F NMR spectroscopy. Evidence was also obtained for the formation of fluorocarbonyl cation [FCO]⁺, but not for diprotonated fluoroformic acid [FC(OH₂)OH₂]⁺.



M. L. Greer, B. J. McGee, R. D. Rogers, S. C. Blackstock * 1864–1866

Pyrazinedioxide–Tetracyanoethylene Arrays in the Solid State—New Donor–Acceptor Interactions for Crystal Engineering

T. R. Kelly,* I. Tellitu, J. Pérez-Sestelo 1866–1868

In Search of Molecular Ratchets

M. Meisel,* P. Lönnecke, A.-R. Grimmer, D. Wulff-Molder 1869–1870

The Donor-Stabilized [PS₂]⁺ Ion

Y. M. A. Yamada, N. Yoshikawa, H. Sasai, M. Shibasaki * 1871–1873

Direct Catalytic Asymmetric Aldol Reactions of Aldehydes with Unmodified Ketones

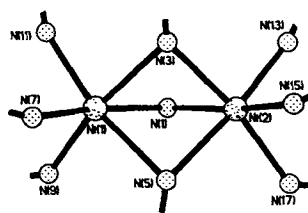
S. Horstmann, E. Irran, W. Schnick * 1873–1875

Synthesis and Crystal Structure of Phosphorus(v) Nitride α-P₃N₅

G. A. Olah,* A. Burrichter, T. Mathew, Y. D. Vankar, G. Rasul, G. K. S. Prakash* 1875–1877

Preparation, NMR, and Ab Initio/IGLO/GIAO-MP2 Study of the Elusive Protonated Fluoroformic Acid and Fluorocarbonyl Cation

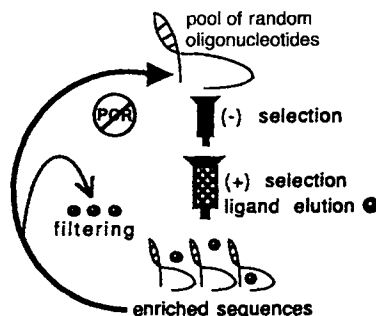
The nickel atoms are triply bridged in $[\text{Ni}_2\text{L}_9]^{4+}$ ($\text{L} = \text{N}\equiv\text{SF}_2\text{NMe}_2$), in which for the first time a nitrogen atom of a $\text{N}\equiv\text{S}$ bond acts as a bridging ligand. The structure of the Ni_2 unit with all the coordinating N atoms is shown on the right.



U. Behrens, J. Petersen, E. Lork,
P. G. Watson, R. Mews* 1878–1879

$[\text{L}_3\text{Ni}(\mu\text{-L})_3\text{NiL}_3](\text{AsF}_6)_4$,
($\text{L} = \text{N}\equiv\text{SF}_2\text{NMe}_2$), a Dinuclear Nickel
Complex with Bridging Thiazyl(dimethyl-
amide)difluoride Ligands

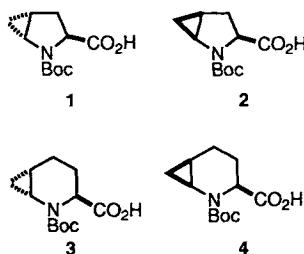
Iterative screenings without enzymatic amplification were successfully performed for DNA aptamers to ATP, thus demonstrating that in vitro selection of oligonucleotide libraries is possible without a polymerase step. The approach is shown schematically on the right.



J. Smith, E. V. Anslyn* 1879–1881

In Vitro Selection without Intervening
Amplification

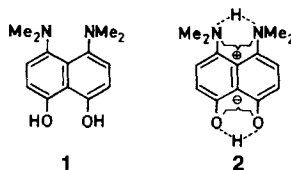
Conformationally constrained prolines (1, 2) and pipercolic acids (3, 4) can be synthesized stereoselectively by a novel cyclopropanation reaction. Considerable flattening of the ring can take place in the proline series. Such compounds are interesting, for instance, as precursors for the preparation of peptidomimetics of therapeutic interest. Boc = *tert*-butoxycarbonyl.



S. Hanessian,* U. Reinhold,
G. Gentile 1881–1884

The Synthesis of Enantiopure ω -
Methanoprolines and ω -Methanopipercolic
Acids by a Novel Cyclopropanation
Reaction: The “Flattening” of Proline

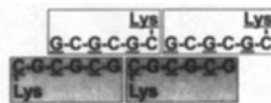
Not the expected structure 1, but the zwitterionic isomer 2 is found in crystals and solutions of the title compound. Molecules of 2 in the crystal form a type of belt, in which the positive part of the zwitterion faces the negative part of its neighbor. This belt is coordinated to a corresponding second belt, in which the zwitterions are oriented in the opposite direction. This very interesting crystal packing prompts further studies of anisotropic crystal properties.



H. A. Staab,* C. Krieger, G. Hieber,
K. Oberdorf 1884–1886

1,8-Bis(dimethylamino)-4,5-dihydroxy-
naphthalene, a Neutral, Intramolecularly
Protonated “Proton Sponge” with
Zwitterionic Structure

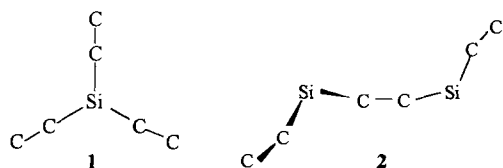
Remarkably stable, G–C pairing in alanyl peptide nucleic acids (PNAs) occurs in three possible pairing modes depending on the conditions. G/C alternating alanyl PNA oligomers can form linear, bandlike, higher order structures when the sequences overlap (see schematic representation on the right).



U. Diederichsen* 1886–1889

Alanyl PNA: Evidence for Linear Band
Structures Based on Guanine–Cytosine
Base Pairs

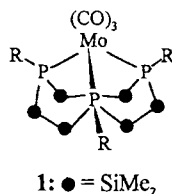
Structural characteristics significantly different to those of neutral Si–C clusters are exhibited by isolated dianionic Si–C clusters. The theoretical investigation of small, stable dianionic Si–C clusters indicates that the free dianions SiC_6^{2-} (1) and $\text{Si}_2\text{C}_6^{2-}$ (2) are capable of existence. These molecules are predicted to be sufficiently long-lived that they should be observable in a mass spectrometer.



A. Dreuw, T. Sommerfeld,
L. S. Cederbaum* 1889–1891

Stable Free Dianionic Silicon–Carbon
Clusters

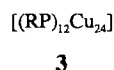
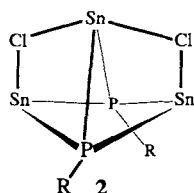
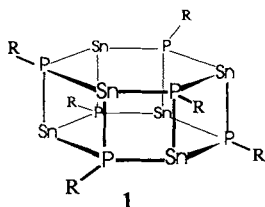
The right template makes it possible: a one-pot cyclocondensation starting from $fac\text{-}[\text{Mo}(\text{CO})_3(\text{PH}_2\text{R})_3]$ ($\text{R} = \text{cyclohexyl}$), $n\text{BuLi}$, and 1,2-dichlorotetra-methylsilane gives complex **1** in 48 % yield. This is the first complex with a nine-membered tridentate phosphorus ligand. The surprising "fusion" of two 1,3,5-triphospha-2,4,6-trisilacyclohexanes in the presence of Cu^{I} and Ag^{I} triflates leads to binuclear complexes with an unprecedented hexadentate phosphorus ligand.



M. Driess,* M. Faulhaber,
H. Pritzkow 1892–1894

Multidentate, Cyclic Phosphorus Ligands with a Silicon–Phosphorus Backbone: Template Synthesis of a 1,4,7-Triphospha-2,3,5,6,8,9-hexasilacyclononane and a 1,3,5,7,9,11-Hexaphospha-2,4,6,8,10,12-hexasilacyclododecane

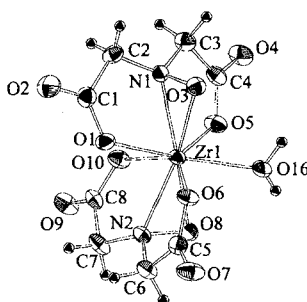
New structural motifs for main group or transition metal phosphanediyl clusters are obtained for the title compounds **1**, **2**, and **3**. They are synthesized by complex Brønsted acid–base reactions of the corresponding primary silylphosphanes and inert stannanediyl derivatives or $[\{\text{CuOtBu}\}_4]$. None of the three compounds needs terminal donor ligands on the metal centers to aid stability. $\text{R} = \text{triorganosilyl}$.



M. Driess,* S. Martin, K. Merz,
V. Pintchouk, H. Pritzkow,
H. Grützmacher, M. Kaupp .. 1894–1896

$[\text{Sn}_6(\text{PR})_6]$, $[\text{Sn}_3(\text{PR})_2\text{Cl}_2]$, and
 $[\text{Cu}_{24}(\text{PR})_{12}]$ ($\text{R} = \text{Triorganosilyl}$):
New Tin and Copper Phosphanediyl
Clusters

N-hydroxyiminodiacetic acid (H_3hida) reacts with $[\text{TiO}(\text{acac})_2]$ or $[\text{Zr}(\text{acac})_4]$ to form $[\text{Ti}(\text{hida})_2]^{2-}$ or $[\text{Zr}(\text{hida})_2(\text{H}_2\text{O})]^{2-}$. These complexes crystallize from water with Ca^{2+} counterions in the form of extended networks. The metal center in the Ti^{IV} complex is eight-coordinate, whereas the larger Zr^{IV} center is nine-coordinate with ligation of an additional H_2O molecule (see picture on the right).



S. M. Harben, P. D. Smith,
R. L. Beddoes, D. Collison,
C. D. Garner* 1897–1898

Eight-Coordinate $[\text{Bis}(\text{oxyiminodiacetate})\text{-titanium(IV)}]^{2-}$ and Nine-Coordinate $[\text{Bis}(\text{oxyiminodiacetate})\text{aquazirconium(IV)}]^{2-}$; Variation in Coordination Mode in Amavadin-Like Complexes

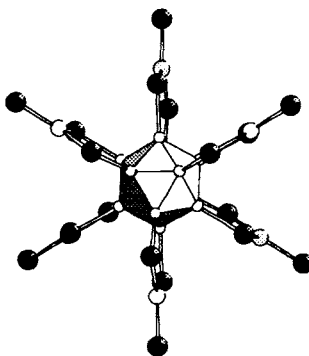
A cavity closed on one side is evident in the solid-state structure of α -cycloaltrin (see picture on the right). This novel non-glucose cyclooligosaccharide is constructed of alternating $^1\text{C}_4$ and $^4\text{C}_1$ chair conformations of the altropyranoid rings. In aqueous solution an equilibrium between the $^1\text{C}_4$ and $^0\text{S}_2$ (skew) forms is established. α -Cycloaltrin is prepared from α -cyclodextrin in a straightforward four-step protocol in which the 2,3-anhydro- α -cyclomannin is the key intermediate.



Y. Nogami, K. Nasu, T. Koga,
K. Ohta, K. Fujita,* S. Immel,
H. J. Lindner, G. E. Schmitt,
F. W. Lichtenhaler* 1899–1902

Synthesis, Structure, and Conformational Features of α -Cycloaltrin: A Cyclooligosaccharide with Alternating $^4\text{C}_1/^1\text{C}_4$ Pyranoid Chairs

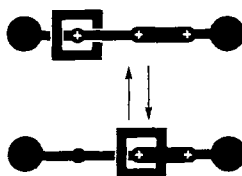
closo-Borate and selenoborate substructures are simultaneously present in the novel cesium hexa-selenoborato-closo-dodecaborate $\text{Cs}_8[\text{B}_{12}(\text{BSe}_3)_6]$ (structure of the anion depicted on the right). In this compound, which is accessible through solid-state syntheses, boron clusters and boron–chalcogen compounds are linked together for the first time. The B_{12} icosahedron in this borate is completely substituted with chalcogen atoms.



J. Küper, O. Conrad,
B. Krebs* 1903–1904

Selenoborato-borates $[\text{B}_{12}(\text{BSe}_3)_6]^{8-}$:
A New Class of Chalcogen-Substituted
Icosahedral Boron Clusters

A secondary dialkylammonium center and a bipyridinium unit form the two binding sites within the dumbbell-shaped component of a switchable [2]rotaxane. The shuttling of the dibenzo[24]crown-8 ring along the dumbbell so that it interacts either with the ammonium center or with the bipyridinium unit can be controlled by the pH and is reversible (depicted schematically on the right). Deprotonation of the NH_2^+ center is achieved with diisopropylethylamine, and reprotonation with trifluoroacetic acid.



M.-V. Martínez-Díaz, N. Spencer,
J. F. Stoddart* 1904–1907

The Self-Assembly of a Switchable
[2] Rotaxane

* Author to whom correspondence should be addressed

BOOKS

Chemistry and Technology of Isocyanates • H. Ulrich

H. Eckert 1909

Dictionary of Renewable Resources • H. Zobebelein

S. Kubik, G. Wulff 1909

Exercises in Synthetic Organic Chemistry • C. Ghiron, R. J. Thomas

J.-A. Gewert 1910

Grundlagen der Elektrochemie • W. Schmickler

B. Speiser 1910

German versions of all reviews, communications, and highlights in this issue appear in the first September issue of *Angewandte Chemie*. The appropriate page numbers can be found at the end of each article and are also included in the Author Index on p. 1913.

All the Tables of Contents from 1995 onwards may be
found on the WWW under:
<http://www.wiley-vch.de/home/angewandte>

SERVICES

| | |
|----------------|------|
| • Keywords | 1912 |
| • Author Index | 1913 |
| • Preview | 1914 |

ANGEWANDTE

CHEMIE

A Journal of the
Gesellschaft
Deutscher Chemiker

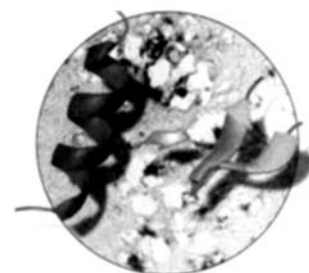
International Edition in English

1997
36/16

Pages 1663–1774

COVER PICTURE

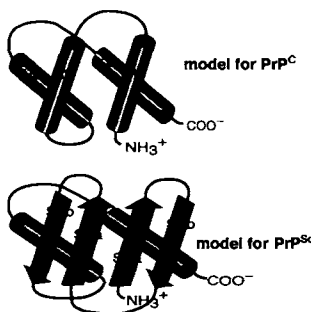
The cover picture shows a thin section of a brain from a patient who died of Creutzfeldt–Jakob disease. The severe perforation of the cortex is clearly seen. A class of neurodegenerative diseases, the transmissible spongiform encephalopathies, was named after these spongelike alterations in the tissue. Among them are also scrapie in sheep and bovine spongiform encephalopathy (BSE, the “Mad Cow Disease”). The biochemical mechanism discussed as the cause of this kind of disorder is shown in the foreground: the conversion of α -helices of the prion protein into β -sheet domains. The β -sheet-rich pathogenic form of the prion protein aggregates in the brain of the affected organisms and triggers the pathological changes. The pathogenic form of the prion protein seems to be intrinsically infectious—it might therefore represent a novel class of pathogens that replicate in the absence of a nucleic acid. The latest results on this topic are reported by E.-L. Winnacker, M. Famulok et al. on pp. 1674 ff.



REVIEW

Contents

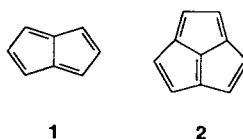
Replication without the information contained in nucleic acids seems to be possible for the pathogen of the transmissible spongiform encephalopathies. According to present-day knowledge, the pathogenic prion protein differs from the cellular form merely in its spatial structure (shown schematically on the right), and not in its amino acid sequence.



F. Edenhofer, S. Weiss, E.-L. Winnacker,*
M. Famulok* 1674–1694

Chemistry and Molecular Biology of Transmissible Spongiform Encephalopathies

A **totally new mode of complexation** is exhibited by the pentalene dianion (1^{2-}): All eight carbon atoms are coordinated to only one metal atom, and the pentalene ligand is folded along the central C–C bond. Like the complex-bound 1^{2-} , the acepentalene dianion (2^{2-}) is not planar, but has a shell-like structure, and is therefore also expected to be able to function as a ligand in transition metal complexes.



H. Butenschön* 1695–1697

Pentalene as a Complex Ligand: New Developments in the Chemistry of Non-alternant, Highly Unsaturated Hydrocarbons

A **third pathway** other than the known outer-sphere and inner-sphere processes needs to be considered, according to quantum mechanical studies of electron-transfer (ET) processes. This new outer-sphere reaction type, which proceeds via “bound” transition states, shows clear stereochemical preferences as well as significant intermolecular orbital overlap in the transition state. In contrast to inner-sphere ET processes, no bond formation occurs during the reaction.

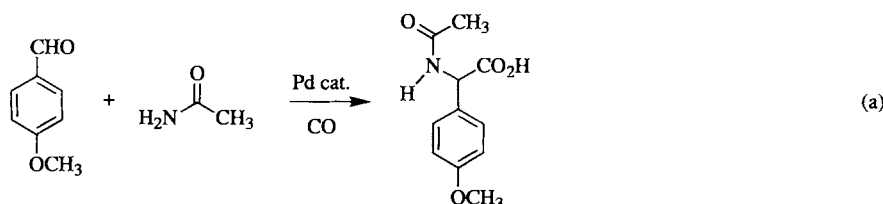
H. Zipse* 1697–1700

Electron-Transfer Transition States: Bound or Unbound—That is the Question!

The **ideal synthesis** uses simple, inexpensive starting materials that can be converted in a single step and in excellent yield into the final product. Multicomponent reactions such as the palladium-catalyzed amidocarbonylation (a) described by Beller et al. are aimed at approaching this ideal situation.

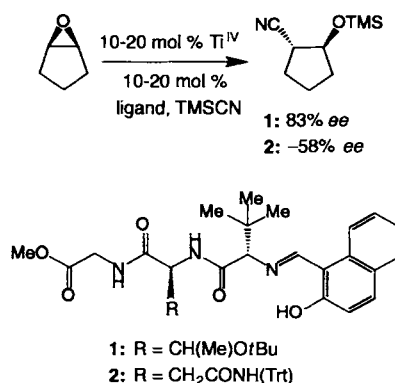
G. Dyker* 1700–1702

Amino Acid Derivatives by Multicomponent Reactions



COMMUNICATIONS

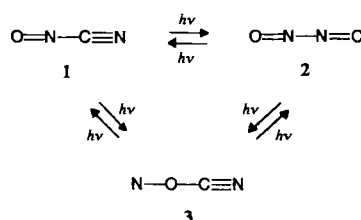
An **efficient strategy** in the search for chiral catalysts is ligand optimization on solid support. This diversity approach provides unique opportunities for the identification of substrate-specific catalysts and leads to the discovery of ligands with unusual properties that might have otherwise escaped detection. Thus, addition of TMSCN to cyclopentene oxide with ligands **1** or **2**, which are very similar, results in opposite enantioselectivities (see reaction on the right; TMS = trimethylsilyl).



K. D. Shimizu, B. M. Cole, C. A. Krueger, K. W. Kuntz, M. L. Snapper,*
A. H. Hoveyda* 1704–1707

Search for Chiral Catalysts Through Ligand Diversity: Substrate-Specific Catalysts and Ligand Screening on Solid Phase

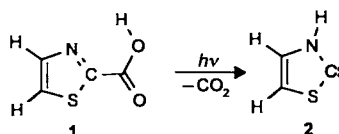
Do **isomers of nitrosyl cyanide (1) exist?** The answer is undoubtedly yes! Not only can matrix-isolated **1** be photochemically converted into nitrosyl isocyanide (**2**) by a reversible reaction, but also into isonitrosyl cyanide (**3**).



G. Maier,* H. P. Reisenauer, J. Eckwert, M. Naumann, M. De Marco 1707–1709

Isomers of the Elemental Composition CN_2O

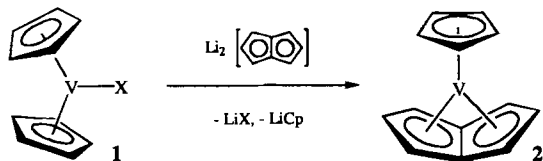
Nucleophilic carbenes are not only accessible as sterically hindered derivatives. Matrix-isolation techniques allow facile trapping of the unsubstituted parent compounds. An example is the formation of the title compound **2** from thiazole carboxylic acid (**1**).



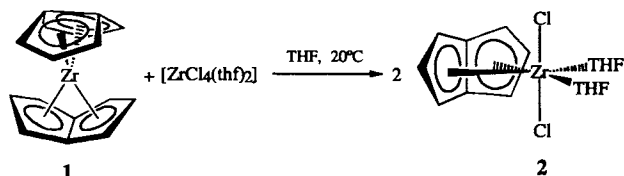
G. Maier,* J. Endres, H. P. Reisenauer 1709–1712

2,3-Dihydrothiazol-2-ylidene

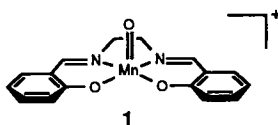
The pronounced folding of the η^8 -coordinated pentalene ligand along the bond between the two bridgehead carbon atoms is the most prominent structural feature of the vanadium complex **2**. This compound and further 18e complexes of this type are readily prepared by the reaction of vanadocene monohalides **1** or their derivatives with dilithium pentalenediide. Although these mononuclear complexes are air-sensitive, they are thermally so stable that they can be sublimed in high vacuum at 80–100 °C without decomposition.



Not only mononuclear complexes having a single pentalene or methylpentalene ligand but also homoleptic complexes with two η^8 -C₈H₆ or η^8 -C₈H₅CH₃ ligands can be formed by titanium, zirconium, and hafnium. The syntheses, which start from the corresponding metallocene dihalides, are particularly simple. The homoleptic pentalene complex **1** reacts with [ZrCl₄(thf)₂] to form the dichloro complex **2**, the first mononuclear “half-sandwich” complex having a pentalene ligand.



Electrospray mass spectrometry has finally provided proof for the formation of oxomanganese(v) complexes such as **1** under the conditions of the Kochi-Jacobson-Katsuki epoxidation. Collision of **1** with olefins or sulfides in the gas phase regenerates the initial (salen)Mn^{III} complex by transfer of the oxygen atom.



K. Jonas,* B. Gabor, R. Mynott, K. Angermund, O. Heinemann, C. Krüger 1712–1714

Novel Mononuclear Vanadium Complexes Having Pentalene Ligands η^8 -Bonded to a Single Metal Atom—A New Type of Coordination in Organometallic Chemistry

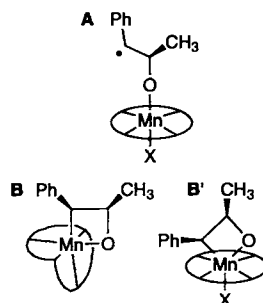
K. Jonas,* P. Kolb, G. Kollbach, B. Gabor, R. Mynott, K. Angermund, O. Heinemann, C. Krüger 1714–1718

Mononuclear Pentalene and Methylpentalene Complexes of Titanium, Zirconium, and Hafnium

D. Feichtinger, D. A. Plattner* 1718–1719

Direct Proof for O=Mn^V(salen) Complexes

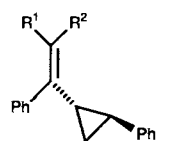
A mechanism that is simpler than that recently advanced is followed for the (salen)Mn-catalyzed asymmetric epoxidation of olefins. Oxametallacycles such as **B** or **B'** are not viable intermediates; radical species such as **A**, which are directly formed by attack of the olefin on the oxomanganese catalyst are more likely candidates; salen = *N,N'*-bis(salicylidene)ethylenediamine dianion.



N. S. Finney, P. J. Pospisil, S. Chang, M. Palucki, R. G. Konsler, K. B. Hansen, E. N. Jacobsen* 1720–1723

On the Viability of Oxametallacyclic Intermediates in the (salen)Mn-Catalyzed Asymmetric Epoxidation

For the direct epoxidation of alkenes radical intermediates play no role. Instead investigations with the radical traps **1a–c** indicate that manganoxetane intermediates are present. Radicals can form from the latter, particularly in the case of sterically crowded oxetanes, by homolytic cleavage of the Mn–C bond.

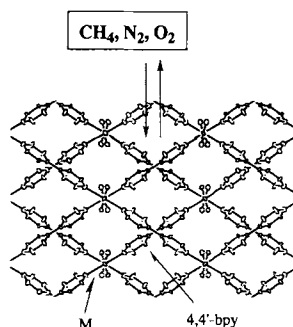


1a: R¹ = R² = H
1b: R¹ = H, R² = Me
1c: R¹ = Me, R² = H

C. Linde, M. Arnold, P.-O. Norrby,* B. Åkermark* 1723–1725

Is There a Radical Intermediate in the (salen)Mn-Catalyzed Epoxidation of Alkenes?

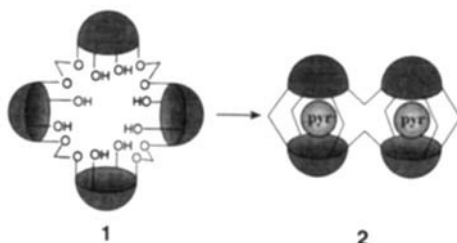
Reversible adsorption of gases distinguishes the coordination polymers $\{[M_2(4,4'\text{-bpy})_3(\text{NO}_3)_4](\text{H}_2\text{O})_x\}_n$ ($M = \text{Co}$, $x = 4$; $M = \text{Ni}$, $x = 4$; $M = \text{Zn}$, $x = 2$), which are formed from $M(\text{NO}_3)_2$ and 4,4'-bipyridine in acetone/ethanol. The channeling cavities in the crystal frameworks (shown schematically on the right) have dimensions of about $3 \times 6 \text{ \AA}$ along the a axis and about $3 \times 3 \text{ \AA}$ along the b axis, and reversibly adsorb CH_4 , N_2 , and O_2 in the pressure range of 1–36 atm without deformation of the crystal framework.



M. Kondo, T. Yoshitomi,
K. Seki, H. Matsuzaka,
S. Kitagawa* 1725–1727

Three-Dimensional Framework with
Channeling Cavities for Small Molecules:
 $\{[M_2(4,4'\text{-bpy})_3(\text{NO}_3)_4] \cdot x\text{H}_2\text{O}\}_n$ ($M = \text{Co}$,
 Ni , Zn)

Yields of 74% were obtained for the preparation of **2** from the tetrameric cavitand **1** in the presence of pyrazine. This first bis(carceplex) may provide a unique opportunity for studying guest–guest communication by virtue of the close proximity of the two covalently attached capsules, which, according to MM2 calculations, are rotated by 90° with respect to each other.



N. Chopra, J. C. Sherman* ... 1727–1729

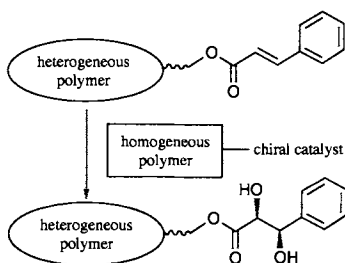
A Bis(carceplex) from a Cyclic Tetramer of
Cavitands

A combination of high-resolution spectroscopy and time-of-flight mass spectrometry was used for the first time to study the fundamental properties of supersonically expanded van der Waals complexes between (*R*)-(+)-1-phenyl-1-propanol (P_R) and the enantiomers of 2-butanol (B_R or B_S) at the microscopic level. Chiral discrimination is based on the different fragmentation patterns of P_RB_R and P_RB_S or on the different bathochromic shift of their electronic band origin relative to that of pure P_R .

S. Piccirillo, C. Bosman, D. Toja,
A. Giardini-Guidoni, M. Pierini,
A. Troiani, M. Speranza* 1729–1731

Gas-Phase Enantiodifferentiation of Chiral
Molecules: Chiral Recognition of 1-Phenyl-
1-propanol/2-Butanol Clusters by Reso-
nance Enhanced Multiphoton Ionization
Spectroscopy

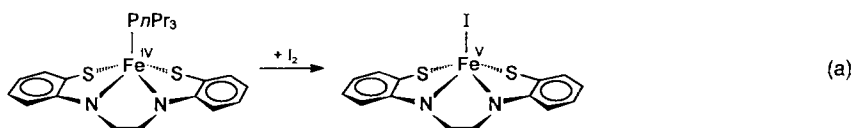
The correct combination of soluble and insoluble polymers allows a multipolymer reaction in which the substrate *trans*-cinnamate and the chiral ligand are bound to different polymer supports. The reactions (shown schematically on the right) proceed with 98% conversion and 98% *ee*.



H. Han, K. D. Janda* 1731–1733

Multipolymer-Supported Substrate and
Ligand Approach to the Sharpless Asym-
metric Dihydroxylation

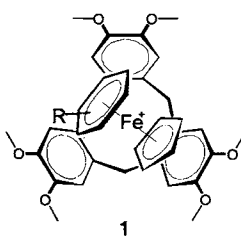
The first stable molecular Fe^V complex, $[\text{Fe}^V(\text{I})(\text{N}_2\text{S}_2)]$, forms in the metal-centered oxidation of the readily accessible Fe^{IV} complex $[\text{Fe}^{IV}(\text{PnPr}_3)(\text{N}_2\text{S}_2)]$ with elemental iodine according to Equation (a). The high-valent character of the iron center is proved by structural, spectroscopic, and electrochemical data.



D. Sellmann,* S. Emig,
F. W. Heinemann 1734–1736

Stabilization of Iron Centers in High Ox-
idation State in the Mononuclear Complex
 $[\text{Fe}^V(\text{I})(\text{N}_2\text{S}_2)]$

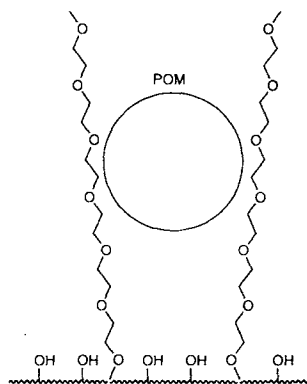
Polar one- and two-dimensional structural motifs feature in the crystal structures of the inclusion complexes **1** between $[\text{CpFe}^{II}(\text{arene})]^+$ and the cryptophane cyclotrimeratylene. These structures result from π -stacking interactions between the electron-rich host and the electron-deficient guest.



K. T. Holman, J. W. Steed,
J. L. Atwood* 1736–1738

Intra-Cavity Inclusion of $[\text{CpFe}^{II}(\text{arene})]^+$
Guests by Cyclotrimeratylene

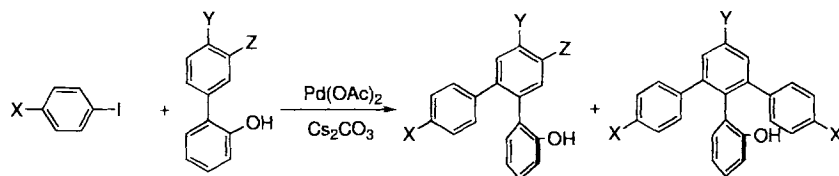
A new immobilization technique for homogeneous catalysts is represented by the title process. Polyethers that are covalently attached to silica surfaces (shown schematically on the right) act as solvent and/or ligands for the catalysts, in this case polyoxometalates (POM). Such systems allow, for example, the quantitative oxidation of cyclooctene to cyclooctene oxide. The catalyst can be recycled without loss of activity.



R. Neumann,* M. Cohen 1738–1740

Solvent-Anchored Supported Liquid Phase Catalysis: Polyoxometalate-Catalyzed Oxidations

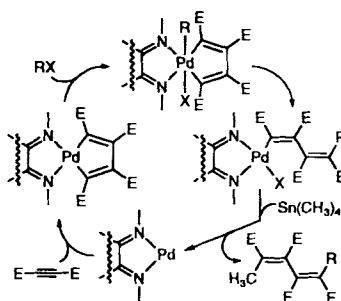
Not only monoarylation but also diarylation of 2-phenylphenols with aryl iodides proceeds effectively and regioselectively when a palladium catalyst and an appropriate base are employed. The products are 1,2-diphenyl- and 1,2,3-triphenylbenzene derivatives, respectively (see below). Also discussed is the arylation of 1- and 2-naphthols. X = H, OMe; Y = H, Me; Z = H, OMe, NO₂.



T. Satoh, Y. Kawamura, M. Miura,*
M. Nomura 1740–1742

Palladium-Catalyzed Regioselective Mono- and Diarylation Reactions of 2-Phenylphenols and Naphthols with Aryl Halides

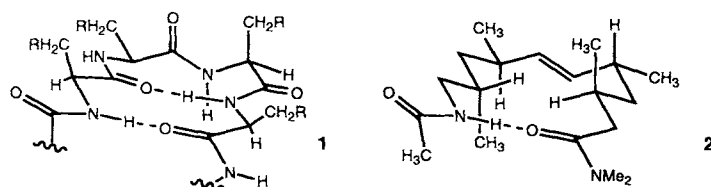
Direct, efficient, selective, and catalytic all describe the synthesis of conjugated dienes from two molecules of alkyne, an organic halide, and tetramethyltin with 1 mol% of a (1,2-diimine)palladium complex in DMF (see the catalytic cycle involving Pd⁰, Pd^{II}, and Pd^{IV} species on the right). Palladium–phosphane complexes do not catalyze this reaction. Furthermore, 1,4-dihalo-1,3-dienes were synthesized stoichiometrically from alkynes and molecular halogen.



R. van Belzen, H. Hoffmann,
C. J. Elsevier* 1743–1745

Catalytic Three-Component Synthesis of Conjugated Dienes from Alkynes via Pd⁰, Pd^{II}, and Pd^{IV} Intermediates Containing 1,2-Diimine

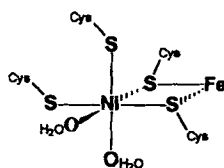
Almost congruent with the natural prototype **1**, β II-hairpin mimetic **2** was obtained through rational conformation design. The hydrocarbon backbone of **2** provides optimal preorganization of the hydrogen bond, which is decisive for inducing a β -sheet conformation.



U. Schopfer, M. Stahl, T. Brandl,
R. W. Hoffmann* 1745–1747

Conformation Design of a Fully Flexible β II-Hairpin Analogue

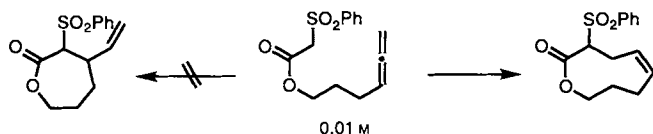
A heterobinuclear Ni-Fe-S center similar to that in the hydrogenase from *Desulfovibrio gigas* is also present in the considerably more complex soluble hydrogenase from the bacterium *Alcaligenes eutrophus*, as shown by high-resolution X-ray absorption spectroscopy. Reductive activation of this enzyme with NADH leads to a substantial change in the coordination of the nickel, which is probably due to specific substrate properties. A model for the active site after NADH reduction is shown on the right.



A. Müller, A. Erkens, K. Schneider,
A. Müller, H.-F. Nolting, V. A. Solé,
G. Henkel* 1747–1750

NADH-Induced Changes of the Nickel Coordination within the Active Site of the Soluble Hydrogenase from *Alcaligenes eutrophus*: XAFS Investigations on Three States Distinguishable by EPR Spectroscopy

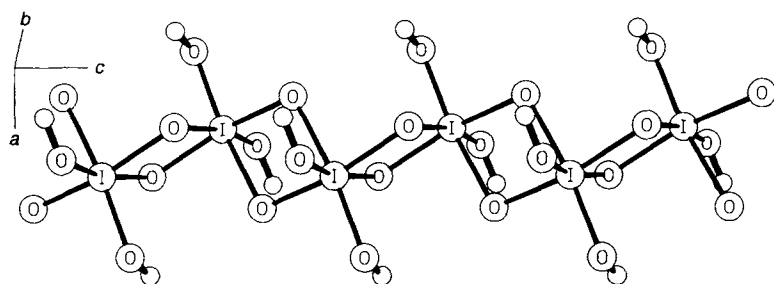
The use of allenes as proelectrophiles in Pd-catalyzed reactions provides a facile entry to macrocarbocycles, macrolactones, and macrolactams. Remarkably, medium-sized rings, notoriously the most difficult to generate, are produced in excellent yields, even in preference to the more easily formed ring sizes when both are feasible (see example below).



B. M. Trost,* P.-Y. Michellys,
V. J. Gerusz 1750–1753

A Facile Cycloisomerization for the Formation of Medium and Large Rings via Allenes

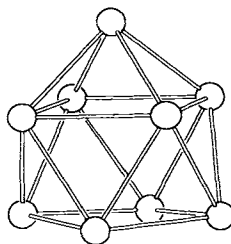
Neither HIO_4 molecules nor *trans*-edge-sharing IO_6 octahedra make up metaperiodic acid. Instead, chains of *cis*-edge-sharing IO_6 octahedra form the I–O skeleton, as shown in the picture of the structure below.



T. Kraft, M. Jansen* 1753–1754

Crystal Structure Determination of Metaperiodic Acid, HIO_4 , with Combined X-Ray and Neutron Diffraction

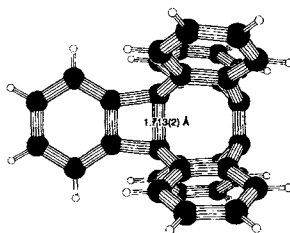
Direct fusion of the appropriate elements readily produces the A_4Ge_9 compounds ($\text{A} = \text{Rb}, \text{Cs}$), which contain discrete Ge_9^{4-} clusters with the shape of monocapped square antiprisms (structure shown on the right). The clusters are the first deltahedral Zintl ions that can be made from solution as well as by a solid-state reaction.



V. Queneau, S. C. Sevov* 1754–1756

Ge_9^{4-} : A Deltahedral Zintl Ion Now Made in the Solid State

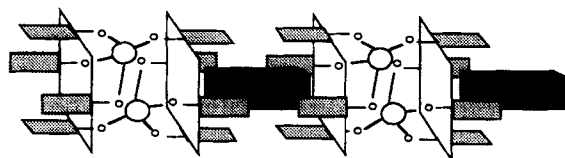
An extremely long C–C single bond of 1.713 Å is found in the [2+2] cycloadduct of *ortho*-didehydrobenzene and tetradehydroanthracene. The force constant of this central bond is reduced to only 30 % of that of the C–C bond in ethane. The corresponding C–C stretching vibration (687 cm^{-1}) in the Raman spectrum is red-shifted 300 cm^{-1} relative to the bands of “normal” hydrocarbons.



S. Kammermeier, P. G. Jones,
R. Herges* 1757–1760

[2+2]Cycloaddition Products of Tetradehydroanthracene: Experimental and Theoretical Proof of Extraordinary Long C–C Single Bonds

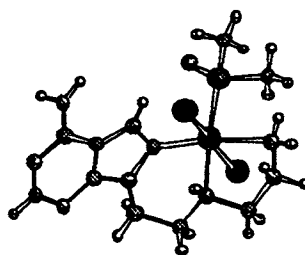
A biconcave molecular module (koiland) was fashioned by the double fusion of two *p*-allylcalix[4]arenes through two silicon atoms. Koilands and linear molecular connectors self-assemble to form an α -network (koilate) in the solid state (see the schematic representation below).



F. Hajek, M. W. Hosseini,* E. Graf,
A. De Cian, J. Fischer 1760–1762

Self-Assembly of Convex and Concave Molecular Tectons to Form a Linear Molecular Array in the Solid State

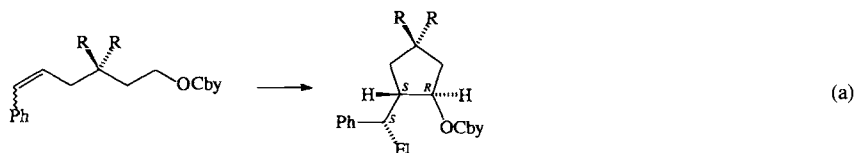
The nucleobase–ligand conjugate from ethylenediamine and 9-ethyladenine can function as a bidentate or tridentate ligand to Ru^{II} . Both modes of coordination involve the ethylenediamine group, while the latter additionally relies on carbon–metal bond formation through C^8 of the nucleobase (structure depicted on the right).



C. Price, M. R. J. Elsegood, W. Clegg,
N. H. Rees, A. Houlton* 1762–1764

Evidence for Directed Metalation: A Structural Intermediate in the Formation of a Novel C-bound Adenine Complex of Ruthenium

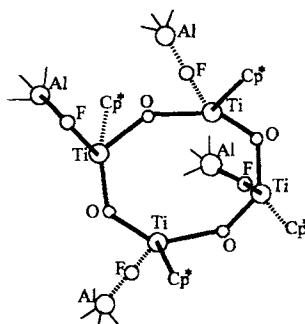
Three vicinal stereocenters are formed in the (–)-sparteine-induced cyclocarbolithiation of 6-phenyl-5-hexenyl carbamates. The anionic cyclization products can be trapped with various electrophiles (El) to provide enantiomerically pure cyclopentanol derivatives [Eq. (a); Cby = 2,2,4,4-tetramethyl-1,3-oxazolidin-3-carboxylate].



M. J. Woltering, R. Fröhlich,
D. Hoppe* 1764–1766

Synthesis of Enantiomerically and Diastereomerically Pure Cyclopentanol by Asymmetric Cyclocarbolithiation of 5-Alkenyl Carbamates

Hitherto only discussed, now isolated and characterized: The adducts of titanium fluoride oxide with trimethylaluminum contain activated Ti–F bonds (an example is depicted on the right). They are formed as intermediates in the methylation of compounds with sterically crowded titanium centers. $\text{Cp}^* = \text{C}_5\text{Me}_5$.



P. Yu, H. W. Roesky,* A. Demsar,
T. Albers, H.-G. Schmidt,
M. Noltemeyer 1766–1767

Activation of Ti–F Bonds in $[\{(\text{C}_5\text{Me}_5)\text{TiOF}\}_4]$ and $[\{(\text{C}_5\text{Me}_4\text{Et})\text{TiOF}\}_4]$ with AlMe_3

* Author to whom correspondence should be addressed

BOOKS

Organotin Chemistry • A. G. Davies

M. Weidenbruch 1769

Hypervalent Iodine in Organic Synthesis • A. Vargolis

A. Kirschning 1769

Macrocyclic Synthesis. A Practical Approach • D. Parker

H. Sonnenschein 1770

Stable Carbocation Chemistry • G. K. S. Prakash, P. von R. Schleyer

W. Kirmse 1771

German versions of all reviews, communications, and highlights in this issue appear in the second August issue of *Angewandte Chemie*. The appropriate page numbers can be found at the end of each article and are also included in the Author Index on p. 1773.

All the Tables of Contents from 1995 onwards may be found on the WWW under:
<http://www.wiley-vch.de/home/angewandte>

SERVICES

| | |
|----------------|------|
| • Keywords | 1772 |
| • Author Index | 1773 |
| • Preview | 1774 |

ANGEWANDTE

CHEMIE

A Journal of the
Gesellschaft
Deutscher Chemiker

International Edition in English

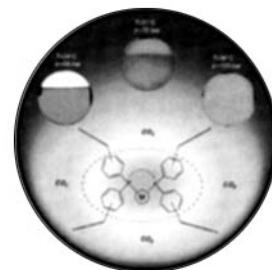
1997
36/15

Pages 1555–1662

COVER PICTURE

The cover picture shows the bright orange-colored solution of a catalyst containing the depicted phosphane–rhodium fragment ($M = Rh$) in pure compressed CO_2 . At $24^\circ C$, that is below the critical temperature, liquid and gaseous CO_2 are in a phase equilibrium, and the catalyst dissolves in the liquid phase. At the critical point ($T = 31^\circ C$) the difference between gaseous and liquid phase disappears, and the catalyst becomes distributed in the compressed medium. Above the critical point, at $36^\circ C$, a homogeneous, supercritical phase ($scCO_2$) exists. The high solubility of the catalysts in supercritical CO_2 is attributed to the $F(CF_2)_n(CH_2)_2$ side chains (shown as waved lines). Provided that a suitable substitution pattern is maintained at the aromatic ring, these chains do not change the chemical and catalytic behavior of the active center (dashed oval) in comparison to those of the unsubstituted fragment. Thus, for the first time the well-known potential of arylphosphorus compounds as ligands for homogeneous catalysis is available for applications in $scCO_2$. More about these findings is reported by W. Leitner et al. on pages 1628 ff.

Similar rhodium and iridium complexes, which can be applied in fluorous biphasic catalysis with $CF_3C_6F_{11}$ as solvent, are described by I. T. Horváth, J. A. Gladysz et al. on pages 1610 ff. and 1612 ff.



REVIEWS

Contents

Although counterintuitive, the conjecture that high-symmetry, low-entropy truncated icosahedron C_{60} spontaneously forms out of the chaos of condensing carbon vapor proved to be true. The observation that the cluster of 60 carbon atoms is singularly chemically unreactive, as exemplified by its flagpole prominence in mass spectra, could be explained only by this hypothesis. This resulted in more conjectures, some of which proved correct, whereas others relating C_{60} to diffuse interstellar bands and soot formation remain speculative. Even if of questionable validity, these speculations have played a useful role in driving chemists to think about the formation of fullerenes and other carbon morphologies.

R. F. Curl * 1566–1576

Dawn of the Fullerenes: Conjecture and Experiment (Nobel Lecture)

Basic research must continue to be supported! This is one of the conclusions clearly evident from the story behind the discovery of the fullerenes. The questions to which answers were originally sought would not have been posed within the current confines of programs aimed increasingly at applied research. This and the fascination associated with C_{60} and other members of the fullerene family are the central messages in this Nobel lecture.

H. Kroto 1578–1593

Symmetry, Space, Stars, and C_{60} (Nobel Lecture)

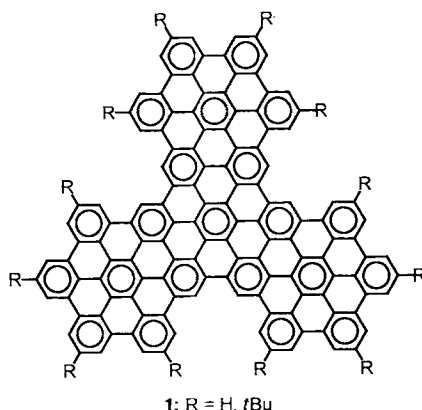
Bucky gets the prize—eleven years after the discovery of C_{60} in 1985, the realization that carbon makes this truncated icosahedral molecule, and larger geodesic cages, all by itself is honored with the Nobel Prize. Only with the development of laser-vaporization cluster beam methods did the particular significance of C_{60} become apparent. Indeed the discovery process with respect to fullerenes and the properties of carbon is far from being complete.

R. E. Smalley 1594–1601

Discovering the Fullerenes (Nobel Lecture)

COMMUNICATIONS

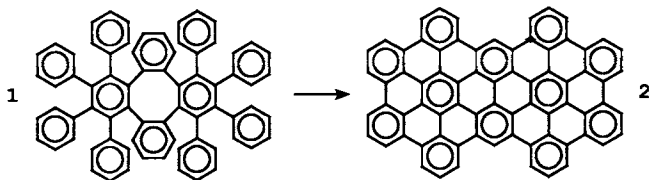
Very large, planar, polycyclic aromatic hydrocarbons such as “supernaphthalene” and “supertriphenylene” (1) are easily constructed by a Diels–Alder reaction and subsequent cyclodehydrogenation.



V. S. Iyer, M. Wehmeier,
J. D. Brand, M. A. Keegstra,
K. Müllen* 1604–1607

From Hexa-*peri*-hexabenzocoronene to
“Superacenes”

Quantitative skeletal rearrangements in the intramolecular cyclodehydrogenation of oligophenylenes such as 1 lead to planar polycyclic aromatic compounds such as 2.



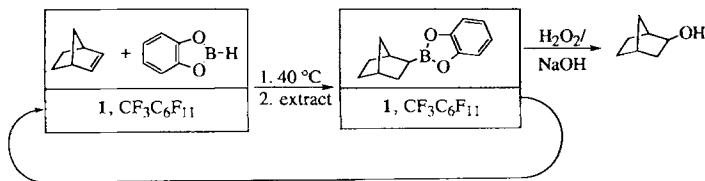
M. Müller, V. S. Iyer, C. Kübel,
V. Enkelmann, K. Müllen* ... 1607–1610

Polycyclic Aromatic Hydrocarbons by
Cyclodehydrogenation and Skeletal Re-
arrangement of Oligophenylenes

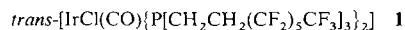
The “Teflon greaseball” $[RhCl\{P[CH_2CH_2(CF_2)_5CF_3]_3\}]$ (1) is highly soluble in $CF_3C_6F_{11}$ and catalyzes a variety of organic transformations. The products can be extracted with organic solvents, and the solution of 1 reused. This environmentally friendly protocol is showcased for hydroboration, in which the customary oxidative workup destroys the metal catalyst. Catalyst loadings of only 0.01–0.25 mol % are effective under mild conditions (25–40 °C, 1–40 h) and give turnover numbers as high as 8500.

J. J. Juliette, I. T. Horváth,*
J. A. Gladysz* 1610–1612

Transition Metal Catalysis in Fluorous
Media: Practical Application of a New
Immobilization Principle to Rhodium-
Catalyzed Hydroboration



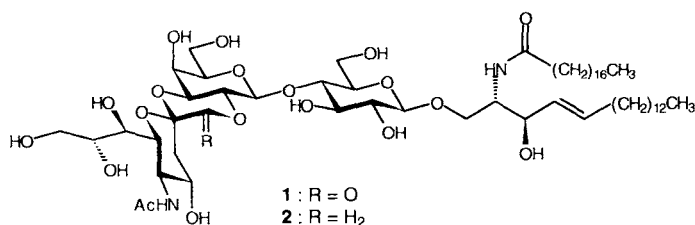
The most highly fluorinated aliphatic species crystallized to date is **1** an exceptionally interesting molecule with regard to its structure and from a mechanistic standpoint. Four of the fluoroalkyl groups form raftlike domains, which pack back-to-back in a motif that maximizes parallel chains (depicted on the right). Complex **1** and CH_3I react by a free radical chain mechanism in $\text{CF}_3\text{C}_6\text{F}_{11}$, as opposed to the polar pathway for Vaska's complex in organic solvents. Although O_2 is highly soluble in $\text{CF}_3\text{C}_6\text{F}_{11}$, its addition to **1** is slower than in common organic solvents.



M.-A. Guillevic, A. M. Arif, I. T. Horváth,*
J. A. Gladysz* 1612–1615

Synthesis, Structure, and Oxidative Additions of a Fluorous Analog of Vaska's Complex, *trans*-[IrCl(CO){P[CH₂CH₂-(CF₂)₅CF₃]₃}₂]-Altered Reactivity in Fluorocarbons and Implications for Catalysis

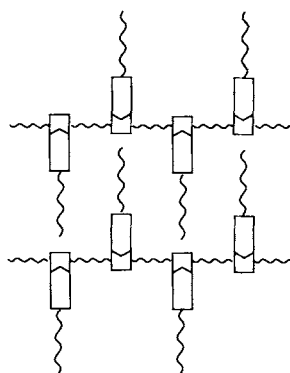
Chemotherapy of malignant tumors is extremely problematic because of the low selectivity of the available cytostatic agents. The now synthetically available ether **2**—the first stable analogue of lactone **1**, which was identified as the tumor-associated antigen—presents the possibility for an active immunization against cancer.



L. F. Tietze,* H. Keim 1615–1617

Synthesis of a Novel Stable GM₃-Lactone Analogue as Hapten for a Possible Immunization against Cancer

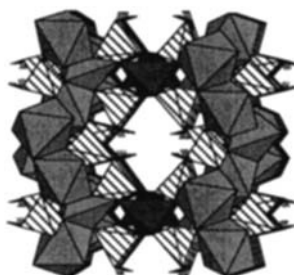
Thermal stability (up to 350 °C) is one of the characteristics of the supramolecular mesogenic polyamide formed by self-assembly during the complexation between a phenylbenzoic acid and a nylon containing pyridyl units in its backbone. The probable structure of the hydrogen-bonded complex is shown schematically on the right.



T. Kato,* Y. Kubota, T. Uryu,
S. Ujiie 1617–1618

Self-Assembly of a Mesogenic Polyamide: Induction and Significant Stabilization of a Liquid-Crystalline Phase through Complexation of a Phenylbenzoic Acid with a Polymer Backbone Derived from 2,6-Bis(amino)pyridine Units

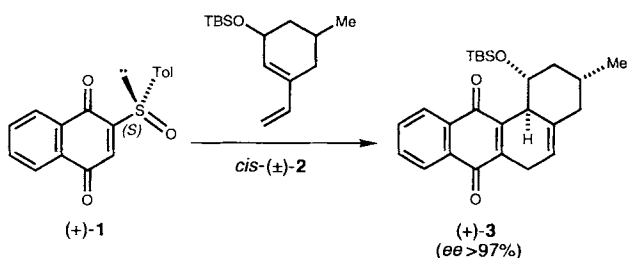
Rectangular channels lined with methylene groups characterize the structure of the title compound. The framework is constructed from CoO₆ octahedra and CoO₄ tetrahedra that are linked through O–P–O bonds (structure depicted on the right). The hydrophobic channels appear suitable for the uptake of flat guest molecules.



D. L. Lohse, S. C. Sevov* 1619–1621

Co₂(O₃P–CH₂–PO₃) · H₂O: A Novel Microporous Diphosphonate with an Inorganic Framework and Hydrocarbon-Lined Hydrophobic Channels

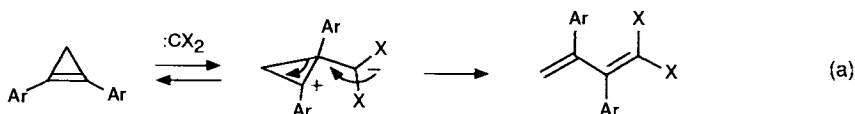
Generation of three stereogenic centers in the angular tetracyclic framework of **3** is possible starting from enantiomerically pure naphthoquinone **1** and the substituted racemic vinylcyclohexene **2**. The product **3** is formed in a one-pot domino reaction comprising Diels–Alder cycloaddition and pyrolytic elimination of the sulfoxide. The key step is the kinetic resolution of the racemic diene.



M. C. Carreño,* A. Urbano,
J. Fischer 1621–1623

Enantioselective Diels–Alder Approach to Angucyclinones from (*S*)-2-(*p*-Tolylsulfinyl)-1,4-naphthoquinone and Substituted Racemic Vinylcyclohexenes

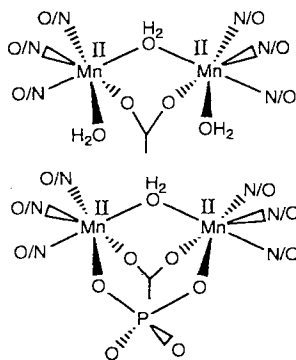
Zwitterionic species are most likely the intermediates for the formation of 1,1-dihalo-2,3-diarylbutadienes by addition of dihalocarbenes to 1,2-diarylcyclopropanes [Eq. (a)]. Bicyclobutanes can be ruled out as intermediates for the formation of butadienes.



J. Weber, U. H. Brinker* 1623–1626

Evidence for a Stepwise Addition of Carbenes to Strained Double Bonds: Reactions of Dihalocarbenes with Cyclopropanes

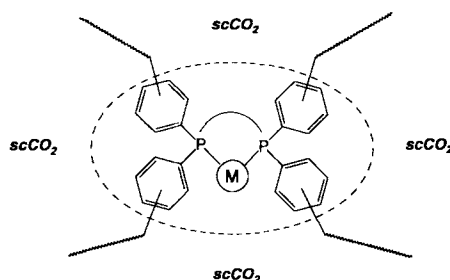
The presence of an aqua bridge in the active and phosphate-bound reduced form of manganese-containing catalases is the key finding from magnetization studies on these compounds. In addition several observations indicate that the phosphate group may form a second bridge, which suggests that two *syn* coordination sites of the active dimanganese center are occupied by easily exchangeable ligands, namely water molecules. The proposed structures are depicted on the right.



L. Jacquamet, I. Michaud-Soret,
N. Debaecker-Petit, V. V. Barynin,
J.-L. Zimmermann,
J.-M. Latour* 1626–1628

Magnetization Studies of the Reduced Active Form of the Catalase from *Thermus thermophilus*

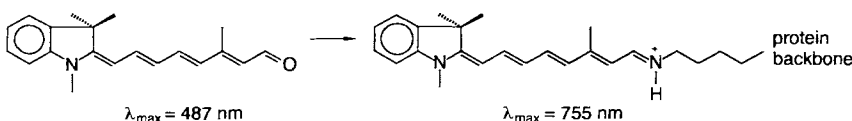
The solubility of complexes is one decisive factor for their use as homogeneous catalysts in supercritical carbon dioxide ($scCO_2$). Complexes with perfluoroalkyl-substituted arylphosphane ligands (shown schematically on the right), which can be prepared by a straightforward and variable synthetic methodology, exhibit high solubility in $scCO_2$ in contrast to unsubstituted parent compounds.



S. Kainz, D. Koch, W. Baumann,
W. Leitner* 1628–1630

Perfluoroalkyl-Substituted Arylphosphanes as Ligands for Homogeneous Catalysis in Supercritical Carbon Dioxide

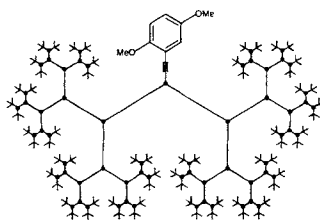
Extremely bathochromically absorbing derivatives of the halobacterial membrane protein bacteriorhodopsin ($\lambda_{\max} = 570$ nm) form upon incorporation of merocyanine dyes of the type shown below into the protein binding site. Upon covalent attachment to the protein (through formation of a protonated Schiff base), these compounds convert into hemicyanines in which the positive charge is distributed over the entire π system of the chromophore.



D. Hoischen, S. Steinmüller,
W. Gärtner,* V. Buss,*
H.-D. Martin* 1630–1633

Merocyanines as Extremely Bathochromically Absorbing Chromophores in the Halobacterial Membrane Protein Bacteriorhodopsin

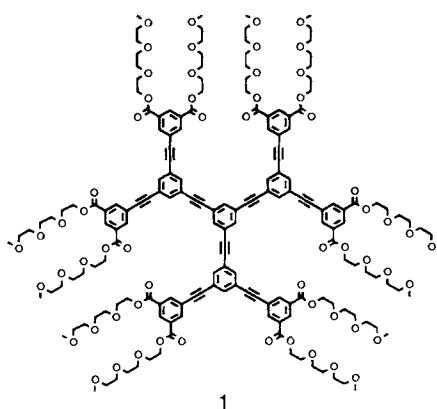
The size and shape of the molecules of the aliphatic hydrocarbon solvent have a strong influence on the magnitude of the anomalous spectral shift in the fluorescence maximum of the charge transfer (CT) state of a high-generation dendrimer (shown schematically on the right). Its molecules no longer exist in an open extended form but exhibit a compact, globular structure, and the dipole moment of the CT state in pentane is larger than in cyclohexane.



C. Devadoss, P. Bharathi,
J. S. Moore* 1633–1635

Anomalous Shift in the Fluorescence Spectra of a High-Generation Dendrimer in Nonpolar Solvents

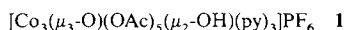
The molecular geometry is mirrored in the macroscopically ordered patterns found in a series of stiff, phenyl-acetylene dendrimers **1**. These compounds form hexagonal columnar liquid crystalline phases with snowflake-like morphologies.



D. J. Pesak, J. S. Moore* 1636–1639

Columnar Liquid Crystals from Shape-Persistent Dendritic Molecules

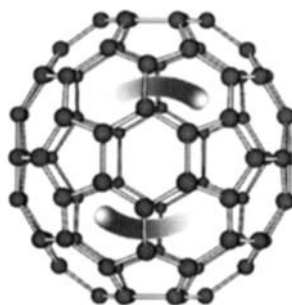
By immobilizing the cobalt complex 1 on the glycine-functionalized inner walls of mesoporous silica (MCM-41), an efficient heterogeneous catalyst for the selective oxidation of cyclohexane to cyclohexanone with *tert*-butyl hydroperoxide is produced. The detailed atomic structure of the active site during catalysis was determined by in-situ X-ray absorption spectroscopy. The findings are important for the design of new efficient oxidation catalysts.



T. Maschmeyer,* R. D. Oldroyd,
G. Sankar, J. M. Thomas,*
I. J. Shannon, J. A. Klepetko,
A. F. Masters, J. K. Beattie,
C. R. A. Catlow 1639–1642

Designing a Solid Catalyst for the Selective Low-Temperature Oxidation of Cyclohexane to Cyclohexanone

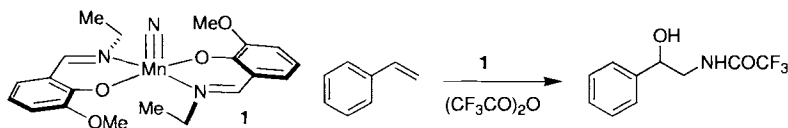
Clear confirmation of recent theoretical studies concerning the structure of the endohedral complexes formed by La and C_{80} is provided by the NMR spectroscopic investigations presented here. Complex $\text{La}_2@C_{80}$ is present, and its structure is based on the unstable “empty” I_h isomer of C_{80} . The two La atoms circulate inside this round cage even at room temperature (shown schematically on the right).



T. Akasaka,* S. Nagase,* K. Kobayashi,
M. Wälchli, K. Yamamoto,
H. Funasaka, M. Kako, T. Hoshino,
T. Erata 1643–1645

^{13}C and ^{139}La NMR Studies of $\text{La}_2@C_{80}$: First Evidence for Circular Motion of Metal Atoms in Endohedral Dimetallofullerenes

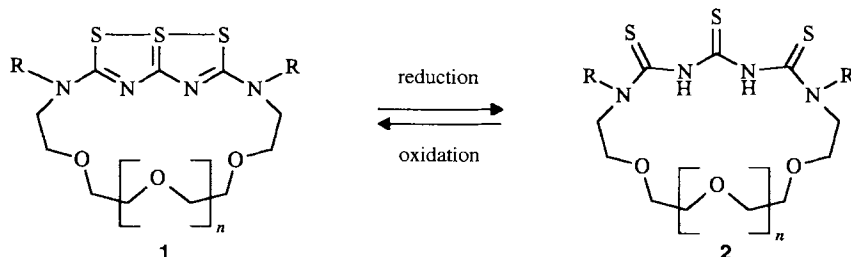
Novel reagents for olefin amination—A new class of manganese(v) nitrides containing Schiff bases as ligands was prepared from the corresponding Mn^{III} complexes following a new mild oxidative procedure. Structures of examples of both the Mn^{III} starting material and the Mn^{V} product have been confirmed by X-ray crystallography. These $\text{Mn}\equiv\text{N}$ complexes such as **1** are potentially effective reagents for nitrogen-atom transfer, as could be demonstrated by the reaction with styrene.



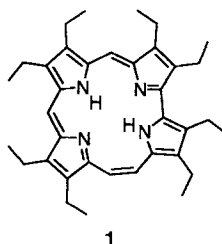
J. Du Bois, C. S. Tomooka, J. Hong,
E. M. Carreira,* M. W. Day .. 1645–1647

Synthesis and Structure of Novel Mn^{III} and Mn^{V} Complexes: Development of a New, Mild Method for Forming $\text{Mn}\equiv\text{N}$ Bonds

The differentiated recognition of Ag^+ and Hg^{2+} can be achieved with the pentaleno crown ethers **1** both by variation of the cavity size and through the reversible trithiadiazapentalene–trithiotriuret redox system (**1** \rightleftharpoons **2**). These compounds were obtained in a one-pot reaction of trithiadiazapentalenes with diamino polyethers of different chain lengths. $n = 1-3$, $\text{R} = \text{CH}_3$, $\text{CH}_2\text{C}_6\text{H}_5$.



Promising as a chelating agent and as a photosensitizer, hemiporphycene is the third porphyrin isomer after porphycene and corphycene with a central N_4 coordination sphere. The stable octaethyl derivative of hemiporphycene **1** was obtained by the combination of a McMurry reaction and a reductive CC cleavage from a bis(tetrapyrroledialdehyde). Like its congeners, **1** possesses a planar ring skeleton.



H. Graubaum,* F. Tittelbach, G. Lutze,
K. Gloe,* M. Mackrodt, T. Krüger,
N. Krauss, A. Deege,
H. Hinrichs 1648–1650

Novel Crown Ethers with a Trithiadiazapentalene–Trithiotriuret Redox System

E. Vogel,* M. Bröring, S. J. Weghorn,
P. Scholz, R. Deponte, J. Lex,
H. Schmickler, K. Schaffner,*
S. E. Braslavsky, M. Müller, S. Pörting,
C. J. Fowler, J. L. Sessler* 1651–1654

Octaethylhemiporphycene: Synthesis,
Molecular Structure, and Photophysics

* Author to whom correspondence should be addressed

BOOKS

Linus Pauling: A Life in Science and Politics • T. Goertzel, B. Goertzel
Force of Nature: The Life of Linus Pauling • T. Hager
Linus Pauling in His Own Words: Selections from His Writings, Speeches,
and Interviews • B. Marinacci

G. B. Kauffman, L. M. Kauffman .. 1655

Edward Frankland: Chemistry, Controversy and Conspiracy
in Victorian England • C. A. Russell

G. B. Kauffman, L. M. Kauffman .. 1657

Laser Techniques in Chemistry • A. B. Meyer, T. R. Rizzo

H. Baumgärtel 1658

German versions of all reviews, communications, and highlights in this issue appear in the second July issue of *Angewandte Chemie*. The appropriate page numbers can be found at the end of each article and are also included in the Author Index on p. 1661.

All the Tables of Contents from 1995 onwards may be
found on the WWW under:
<http://www.wiley-vch.de/home/angewandte>

SERVICES

| | |
|----------------|------|
| • Keywords | 1660 |
| • Author Index | 1661 |
| • Preview | 1662 |

ANGEWANDTE

CHEMIE

A Journal of the
Gesellschaft
Deutscher Chemiker

International Edition in English

1997/36
13/14

Pages 1359–1554

COVER PICTURE

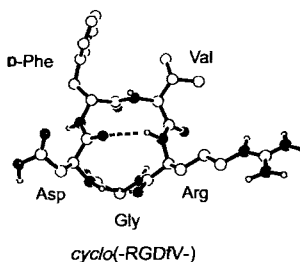
The cover picture shows the complex of the Melle11 (yellow) variant of the immuno-suppressive drug cyclosporin A (CsA, orange) bound to the protein cyclophilin (CyP, represented as a gray ribbon except for three protein residues in pink that make close contacts with Melle11 (Phe113, Phe60, Met61)). The structure including the water molecules comes from Monte Carlo simulations by A. C. Pierce and W. L. Jorgensen, which have been used to study the energetic and structural effects of introducing “bumps” and “holes” into the complex. The left inset shows a surface rendering of the Melle11 in contact with the three pink residues of CyP. The right inset shows that mutation of Phe113 to Ala opens a hole to accommodate the Melle11 side chain better; two water molecules also enter the cavity. More about these studies is reported on pages 1466ff. The picture was generated by Dr. E. M. Duffy with the Sybyl (Tripos Associates, Inc.) and ChemEdit (D. Lim, Yale University) programs.



REVIEWS

Contents

Preventing the formation of tumor metastases by inhibiting tumor-induced angiogenesis is made possible by the development of specific, high-affinity inhibitors of the integrin $\alpha_v\beta_3$ (vitronectin receptor), for example *cyclo(-RGDfV-)*, which is shown on the right. The required optimization of the spatial structure of the bioactive RGD motif with respect to activity and specificity is achieved by libraries of cyclic penta- and hexapeptides as well as peptidomimetics.



R. Haubner, D. Finsinger,
H. Kessler* 1374–1389

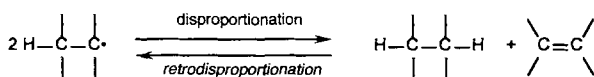
Stereoisomeric Peptide Libraries and
Peptidomimetics for Designing Selective
Inhibitors of the $\alpha_v\beta_3$ Integrin for a New
Cancer Therapy

Small, semiconductor aggregates (clusters) which are free of ligands and typically consist of 10 to 10^3 atoms (and thus cannot yet be formed in a narrow size range by the techniques of colloid chemistry) can be generated and studied by molecular beam experiments. These experiments are described with reference to the measurement of polarizabilities of ligand-free Si_N and Ga_NAs_M clusters, and simple physical chemistry models are discussed, which allow the interpretation of the polarizability in terms of the chemical bonds in the semiconductor clusters.

J. A. Becker* 1390–1404

Molecular Beam Studies on Semiconductor
Clusters: Polarizabilities and Chemical
Bonding

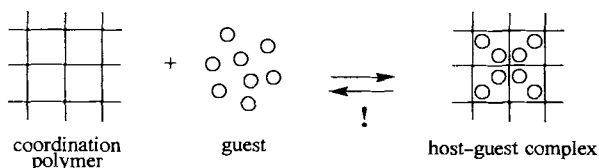
Retrodisproportionation—H-atom transfer onto unsaturated systems such as aryl-substituted alkenes, azo, nitro, and nitroso compounds as well as quinones—represents an important, though previously disregarded H-trapping reaction. The mechanism of the retrodisproportionation, the structures of the transition states, and the first examples of transfer hydrogenation are discussed.



HIGHLIGHTS

Contents

New host–guest chemistry: Porous organic frameworks that enable reversible guest inclusion within their stable host framework (shown schematically below) are called organic zeolite analogues. They promise a new range of applications, for example as molecular sieves.



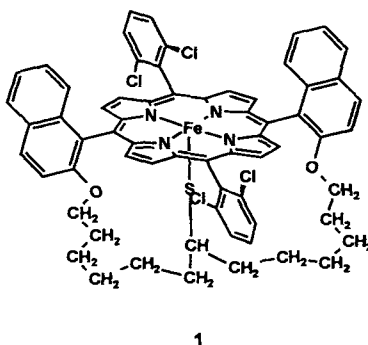
Jencks's principle is fulfilled in these examples of double proton transfer reactions in a variety of media. The reactions proceed in a concerted manner when a high-energy intermediate needs to be avoided and a stepwise manner when this is not necessary. This is the result of detailed studies by the research groups of Ahlberg (mutarotation of tetramethylglucose), Limbach (tautomerization of porphyrins), Petrich (tautomerization of 7-azaindole), and Zewail (tautomerization of 7-azaindole dimers in the gas phase), which are discussed here.

COMMUNICATIONS

Remarkable ability for self-recognition is displayed when a mixture of three different bis(catecholamide) ligands is allowed to react at room temperature with $[\text{Ga}(\text{acac})_3]$ and KOH in methanol (schematic representation below). These rigid, rodlike ligands differing only in the distance between the two coordination sites form M_2L_3 triple helical complexes containing only one type of ligand with the trivalent metal ions M.



Protection by shielding—the porphyrinophane complex **1**, a functionally active model compound of the cytochrome P-450 isozyme, was prepared in an 18-step convergent synthesis. Porphyrin complex **1** catalyzes the epoxidation of *cis*-stilbene with iodosylbenzene. The thiolate ligand is shielded from oxidative attack by the chloro substituents and the phane chain, while on the other side of the molecule the naphthalene groups and the chloro substituents hinder the formation of μ -oxo and μ -peroxo complexes.



C. Rüchardt,* M. Gerst,
J. Ebenhoch 1406–1430

Uncatalyzed Transfer Hydrogenation and
Transfer Hydrogenolysis: Two Novel Types
of Hydrogen-Transfer Reactions

C. Janiak* 1431–1434

Functional Organic Analogues of Zeolites
Based on Metal–Organic Coordination
Frameworks

R. L. Schowen* 1434–1438

Harmony and Dissonance in the Concert of
Proton Motions

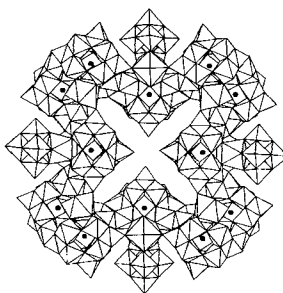
D. L. Caulder,
K. N. Raymond* 1440–1442

Supramolecular Self-Recognition and Self-
Assembly in Gallium(III) Catecholamide
Triple Helices

H. Volz,* M. Holzbecher 1442–1445

A Bridged Porphyrinato(thiolato)iron(III)
Complex as a Model of the Active Center of
the Cytochrome P-450 Isozyme

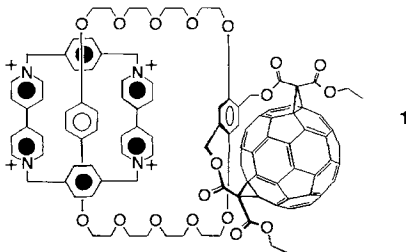
A relative molar mass of 40 000 and diameter of 4 nm are the remarkable dimensions of the title anion, which is, together with its La^{III} analogues, the most massive inorganic water-soluble cluster so far observed (see picture on the right). These polyanions with 164 metal atoms are easily synthesized in fair yield. The folded cyclic structure incorporates twelve $\text{AsW}_9\text{O}_{33}$ and four W_5O_{18} anionic subunits.



K. Wassermann, M. H. Dickman,
M. T. Pope* 1445–1448

Self-Assembly of Supramolecular Polyoxometalates: The Compact, Water-Soluble Heteropolytungstate Anion $[\text{As}_{12}^{\text{III}}\text{Ce}_{16}^{\text{III}}(\text{H}_2\text{O})_{36}\text{W}_{148}\text{O}_{524}]^{76-}$

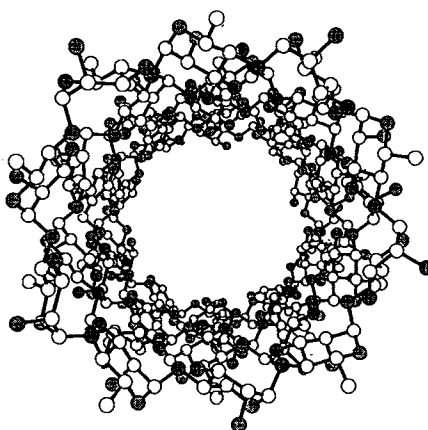
An aromatic crown ether tethered to C_{60} is a template for the formation of the [2]catenane shown on the right, in which cyclobis(paraquat-*p*-phenylene) cyclophane becomes mechanically interlocked with the fullerene-appended macrocyclic polyether. Since the hydroquinone ring connecting the bis(*p*-phenylene)-[34]crown-10 to C_{60} behaves as a π -electron-rich *exo* donor and undergoes additional interactions with the electron-accepting C_{60} moiety, this first fullerene catenane boasts an unprecedented intramolecular acceptor–donor–acceptor–donor–acceptor stack.



P. R. Ashton, F. Diederich,*
M. Gómez-López, J. F. Nierengarten,
J. A. Preece, F. M. Raymo,
J. F. Stoddart* 1448–1451

Self-Assembly of the First Fullerene-Containing [2]Catenane

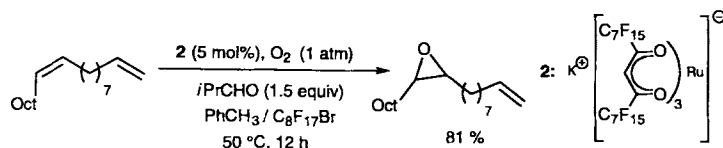
Assembly of units in an alternating disrotatory fashion is a feature of the solid-state structure of an achiral, synthetic cyclic decasaccharide composed of ten α -(1→4)-linked, alternating D- and L-rhamnopyranose residues. The unit cell contains two crystallographically independent, C_i -symmetrical, cylindrical molecules. This gives rise to parallel nanotubular arrays with internal diameters of about 13 nm as depicted on the right.



G. Gattuso, S. Menzer,
S. A. Nepogodiev, J. F. Stoddart,*
D. J. Williams* 1451–1454

Carbohydrate Nanotubes

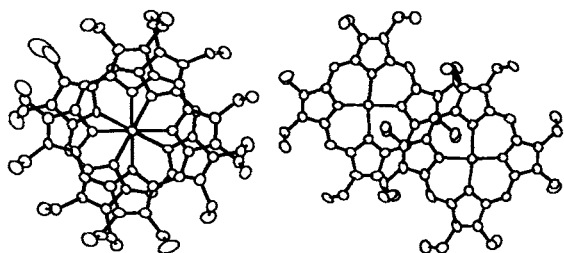
Success per fluorine! Metal complexes with perfluorinated ligands serve as catalysts for oxidations in perfluorinated solvents. By using a perfluorinated Ni catalyst aldehydes can be converted into carboxylic acids and sulfides into sulfoxides or sulfones. With a Ru catalyst a selective epoxidation of disubstituted olefins in the presence of a terminal double bond is possible (see example below).



I. Klement, H. Lütjens,
P. Knochel* 1454–1456

Transition Metal Catalyzed Oxidations in Perfluorinated Solvents

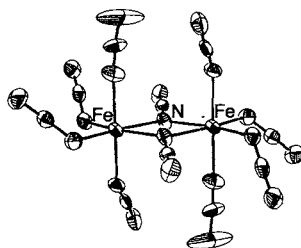
π - π Stacking interactions stabilize the dimer (structure shown below on the left) that is formed from $[\text{Mg}(\text{oep})]^{+}$ upon crystallization from $\text{CH}_2\text{Cl}_2/\text{CHCl}_3$ (5/1). In contrast, crystallization from toluene/ CH_2Cl_2 (4/1) gives a dimer whose porphyrin rings barely overlap (bottom right). The structural differences are attributed to the effect of solvent polarity. The solvent-dependence of the spectra is consistent with this interpretation. oep = octaethylporphyrin.



K. E. Brancato-Buentello,
W. R. Scheidt* 1456–1459

Inter-Ring Interactions in Dimers of
Magnesium π -Cation Radicals: Control by
Solvent Polarity

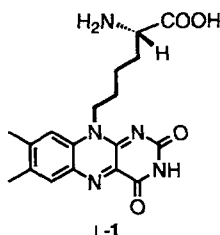
An energetically low-lying spin state with $S = 5$ is observed in the title compound, in which low-spin iron(II) $[\text{Fe}(\text{bpym})_3]^{2+}$ and high-spin iron(III) $[\text{Fe}_2(\text{N}_3)_{10}]^{4-}$ ions coexist. The magnitude of the ferromagnetic coupling in the dimer ($J = +4.8 \text{ cm}^{-1}$) is twice that reported for a high-spin Mn^{II} complex with the same bridging ligands. The structure of the anion is shown on the right.



G. DeMunno,* T. Poerio, G. Viau,
M. Julve,* F. Lloret 1459–1461

Ferromagnetic Coupling in the Bis(μ -
end-on-azido)iron(III) Dinuclear Complex
Anion of $[\text{Fe}^{\text{II}}(\text{bpym})_3]_2[\text{Fe}_2^{\text{III}}(\text{N}_3)_{10}] \cdot 2\text{H}_2\text{O}$

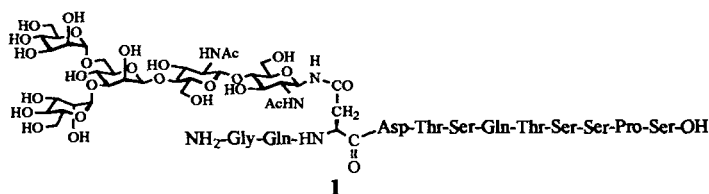
Mimicking DNA photolyases: Model proteins containing the flavin amino acid L-1 within the DNA-binding domain of a transcription factor are capable of completely repairing damage from the formation of pyrimidine dimers in single-stranded oligonucleotides. Cyclobutane pyrimidine dimers are thus photochemically reactivated.



T. Carell,* J. Butenandt 1461–1464

Towards Artificial DNA-Repair Enzymes:
Incorporation of a Flavin Amino Acid into
DNA-Binding Oligopeptides

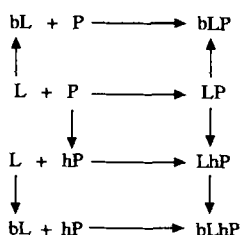
Yields of 98 and 94% are achieved for the coupling of the first part of the peptide chain (Asn^3 - Ser^{12}) of **1** with the pentasaccharide core and the elongation of the peptide chain to its desired length, respectively, in the solid-phase synthesis described here. This method should therefore smooth the way to the synthesis of more complex glycopeptides.



Z.-W. Guo, Y. Nakahara, Y. Nakahara,*
T. Ogawa* 1464–1466

Solid-Phase Synthesis of the CD52 Gly-
copeptide Carrying an N-Linked Core
Pentasaccharide Structure

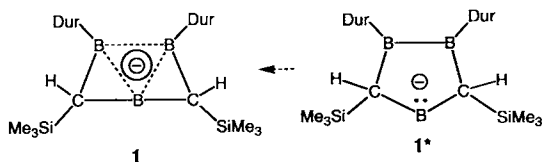
A valuable tool for the design of ligands for bioreceptors is provided by the presented combination of Monte Carlo simulations and free energy perturbation calculations. Application of this methodology to an orthogonal receptor–ligand pair based on cyclosporin A and human cyclophilin reproduced the experimentally observed differences in binding affinities and gave detailed insights into the origin of binding preferences with the thermodynamic cycles given on the right. L: reference ligand; P: original protein; bL: bumped ligand; hP: holed protein.



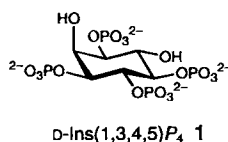
A. C. Pierce,
W. L. Jorgensen* 1466–1469

Computational Binding Studies of Orthog-
onal Cyclosporin-Cyclophilin Pairs

Delocalization in doubly aromatic compounds: Bishomotriboriranide **1** is the first carbene analogue of boron (a borenate ion) characterized in solution (NMR) and in the solid state (X-ray). With the 3c–2e π bond and 3c–2e σ bond that involves the borenate center of **1*** and the neighboring B–B unit, **1** belongs to the class of doubly aromatic compounds. The (hypothetical) classical borenate **1*** without these delocalizations is estimated to be about 90 kcal mol^{–1} higher in energy than **1** (Dur = 2,3,5,6-tetramethylphenyl).



As controversial as ever is the role of *D*-*myo*-inositol-1,3,4,5-tetrakisphosphate (**1**) in intracellular signaling. A new synthetic strategy that makes minimal use of protecting groups allows rapid, direct access not only to pure **1** in the amounts required for cocrystallographic and NMR studies with its recently identified macromolecular targets, but also to the little-known *L* enantiomer, which is invaluable as a control in radioligand binding and functional studies.



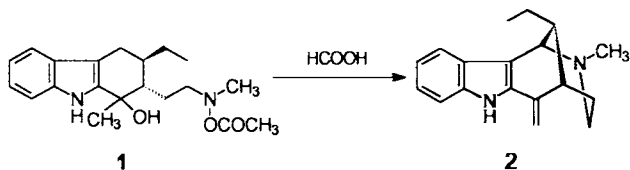
M. Unverzagt, G. Subramanian, M. Hofmann, P. von R. Schleyer, S. Berger, K. Harms, W. Massa, A. Berndt* 1469–1472

Carbene Analogues of Boron Stabilized by Neighboring B–B Moieties: Doubly Aromatic Bishomotriboriranides

A. M. Riley, M. F. Mahon, B. V. L. Potter* 1472–1474

Rapid Synthesis of the Enantiomers of *myo*-Inositol-1,3,4,5-tetrakisphosphate by Direct Chiral Desymmetrization of *myo*-Inositol Orthoformate

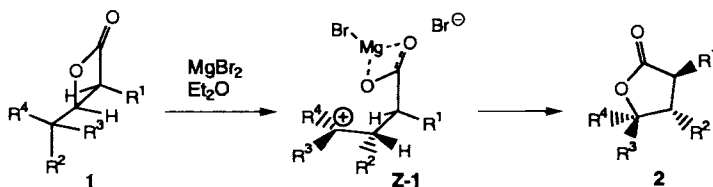
An amazing sequence of reactions is triggered when **1** is treated with formic acid. The formation of a benzyl cation sets off a domino reaction that ends with (\pm)-uleine (**2**), which thus allows a simple and stereoselective synthesis of this and possibly also other natural products from the group of strychnos alkaloids.



M. H. Schmitt, S. Blechert* .. 1474–1476

A New Cationic Domino Process to (\pm)-Uleine

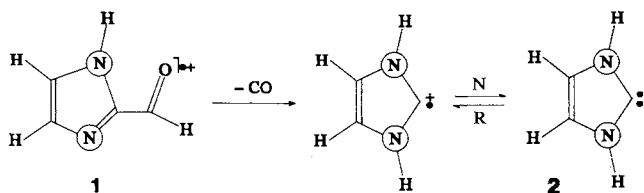
Not concerted, but stepwise: Dyotropic ring enlargement of β -lactones **1** to γ -lactones **2** proceeds via the zwitterionic intermediate **Z-1** (σ - and π -donor substituents). The relative migratory aptitude of the substituents is π -donor > n -donor > σ -donor.



J. Mulzer,* K. Hoyer, A. Müller-Fahrnow 1476–1478

Relative Migratory Aptitude of Substituents and Stereochemistry of Dyotropic Ring Enlargements of β -Lactones

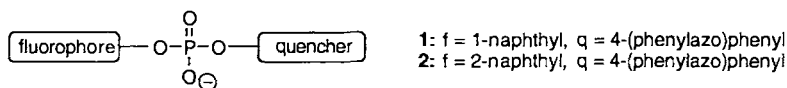
Though not yet available off-the-shelf, the generation the title molecule **2** from aldehyde **1** and its detection in the gas phase confirms quantum chemical predictions that it should be stable, in particular towards its 1,2-hydrogen shift isomer imidazole. Thus, substituents larger than hydrogen on the nitrogen atoms are not a feature essential to the inherent stability of imidazolylidene carbenes, although such groups may still play a role in hindering bimolecular processes (N = neutralization, R = reionization).



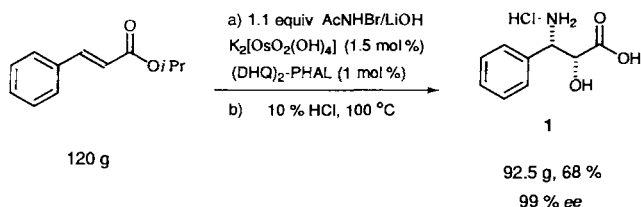
G. A. McGibbon, C. Heinemann, D. J. Lavorato, H. Schwarz* .. 1478–1481

Imidazol-2-ylidene: Generation of a Missing Carbene and Its Dication by Neutralization–Reionization and Charge-Stripping Mass Spectrometry

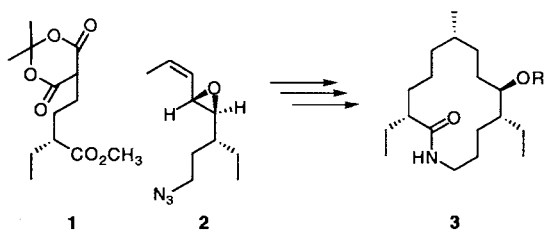
A sensitive indicator of nuclease activity is the fluorescence behavior of phosphodiesteres **1** and **2**. Although **1** and **2** do not fluoresce due to intramolecular quenching, the strongly fluorescent naphthyl phosphates and naphthols are liberated upon hydrolysis. This gives rise to an extremely strong increase in fluorescence intensity. Combined application of **1** and **2** allows detection of phosphatase in addition to phosphodiesterase activity. f = fluorophore, q = quencher.



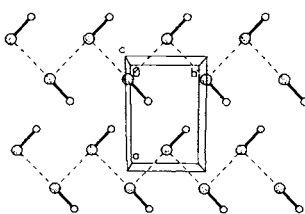
The efficient large-scale synthesis (see below) of an enantiomerically pure Taxol side chain precursor—3-phenylisoserine (**1**)—highlights the potential of the third modification of the asymmetric aminohydroxylation (AA). The use of *N*-bromoacetamide as the nitrogen source is the latest advance in the osmium-catalyzed AA of olefins.



Chirality transfer takes place during the Pd-catalyzed reaction of pronucleophiles with vinyl epoxides bearing an alkyl group at the vinyl terminus. The reaction is ideal to establish remote stereogenic centers. A synthesis of fluviricin B1 aglycone **3** from **1** and **2** illustrates the application of this new strategy for macrolactamization.



Infinite ribbons with only very short intermolecular Cl...Cl contacts, and not dipole-dipole interactions, characterize the crystal packing of ClF (depicted on the right). The explanation for this surprising finding is that chlorine in ClF may act simultaneously as an electron donor and acceptor, as shown by the experimental Laplacian charge density maps and ab initio calculations for the ClF dimer.



The novel heterocyclic ligand system in **2** is formed by thermal decomposition of 2*H*-azaphosphirene tungsten complexes in the presence of dimethylacetylenedicarboxylate (DMAD). The formation of the 2*H*-1,2-azaphosphole tungsten complexes **2** is interpreted as the reaction of the novel ylidic intermediates **1** with DMAD. The latter are very promising in view of the potential of known nitrile ylides in heterocycle syntheses. Ar = *p*-MeOC₆H₄, Ph, *p*-F₃CC₆H₄.



A. Berkessel,* R. Riedl 1481–1483

Fluorescence Reporters for Phosphodiesterase Activity

M. Bruncko, G. Schlingloff,
K. B. Sharpless* 1483–1486

N-Bromoacetamide—A New Nitrogen Source for the Catalytic Asymmetric Aminohydroxylation of Olefins

B. M. Trost,* M. A. Ceschi,
B. König 1486–1489

Palladium-Catalyzed Additions of Alkenyl Epoxides to Pronucleophiles: A Synthesis of the Macrolactam Aglycone of Fluviricin B1

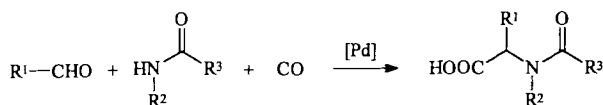
R. Boese,* A. D. Boese, D. Bläser,
M. Yu. Antipin, A. Ellern,
K. Seppelt 1489–1492

The Surprising Crystal Packing of Chlorinefluoride

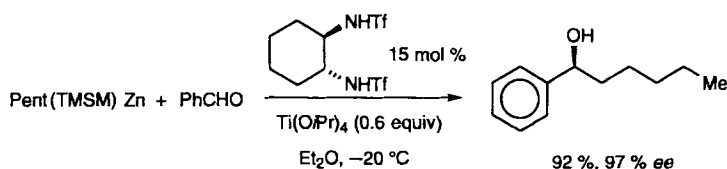
R. Streubel,* H. Wilkens, A. Ostrowski,
C. Neumann, F. Ruthe,
P. G. Jones 1492–1494

Formation of 2*H*-1,2-Azaphosphole Tungsten Complexes by Trapping Reactions of Nitrilium Phosphane Ylide Complexes

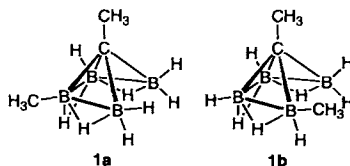
For the first time palladium catalysts have been used successfully for the amidocarbonylation reaction. The activity of the cobalt catalysts that were used exclusively beforehand has now been exceeded by an order of magnitude, and the reaction can be performed under far milder conditions. Palladium-catalyzed amidocarbonylation reactions can now be used for the synthesis of a much wider range of *N*-acyl amino acids.



Better synthetic efficiency is achieved in 1,4-additions in NMP:THF mixtures and in enantioselective additions to aldehydes (see below) when the diorganozinc compounds $\text{R}(\text{TMSM})\text{Zn}$ are used instead of R_2Zn (NMP = *N*-methylpyrrolidone, TMSM = Me_3SiCH_2 , R = alkyl, aryl). With these new reagents, which have been characterized by NMR spectroscopy, no group R is "wasted". The TMSM group behaves as a nontransferable ligand.



An interconverting mixture of isomers, *arachno*-1,3- (**1a**) and *arachno*-1,2- Me_2 -1- CB_4H_8 (**1b**), has been isolated from the quenched gas-phase reaction of B_4H_{10} with allene and characterized by the ab initio/IGLO/NMR method. The mechanisms of interchange between **1a** and **1b**, as well as the degenerate isomerizations in the parent compound 1- CB_4H_{10} and the isoelectronic B_3H_{10} , were clarified computationally.



M. Beller,* M. Eckert, F. Vollmüller, S. Bogdanovic, H. Geissler ... 1494–1496

Palladium-Catalyzed Amidocarbonylation—A New, Efficient Synthesis of *N*-Acyl Amino Acids

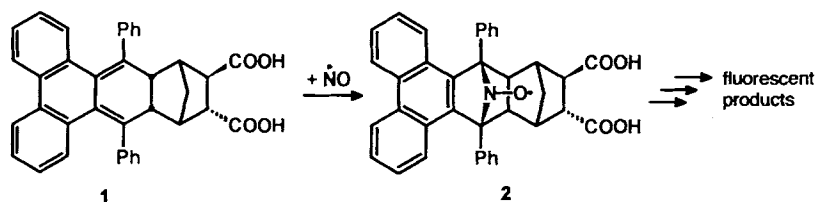
S. Berger, F. Langer, C. Lutz, P. Knochel,* T. A. Mobley, C. K. Reddy ... 1496–1498

β -Silyl Diorganozinc Compounds—A New Class of Useful Zinc Reagents

M. A. Fox, R. Greatrex,* M. Hofmann, P. von R. Schleyer,* R. E. Williams ... 1498–1501

Gas-Phase Reaction of Tetraborane(10) with Allene: The Fluxional *arachno*-1-Carbapentaborane(10) Isomeric System and Derivatives 1,2- and 1,3- Me_2 -1- CB_4H_8 ; Analogies in 1- CB_4H_{10} , $\text{MeB}_3\text{H}_{10}$, and $\text{B}_5\text{H}_{10}^-$

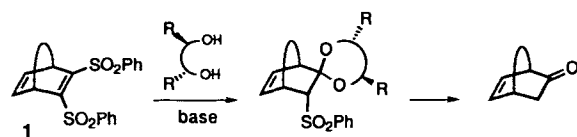
Selective reaction with NO provides fluorescent nitroxide radicals **2** from nonfluorescent *o*-quinodimethane derivatives of type **1** as a result of rearomatization. Intentional reduction of **2** to nonradical products with the intact fluorophore results in a strong increase in fluorescence intensity. The detection of low levels of nitric oxide, especially in biological systems, is thus possible.



M. Bätz, H.-G. Korth,* R. Sustmann* ... 1501–1503

A Novel Method for Detecting Nitric Oxide (NO) by Formation of Fluorescent Products Based on Chelotropic Spin Traps

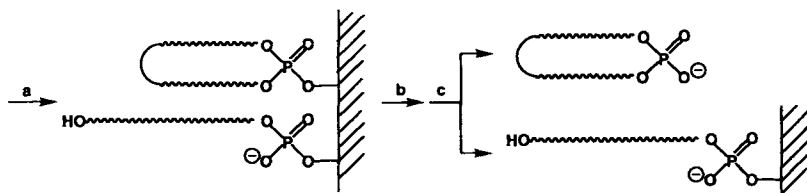
Desymmetrization of bis(phenylsulfonyl)alkenes **1** provides the desired enantiomer of polycyclic ketones rapidly, in high yields, and enantiopure (see below); **1** is also readily available in multigram quantities.



S. Cossu,* O. De Lucchi,* P. Pasetto ... 1504–1506

Total Enantiotopic Discrimination between Carbon Atoms of a Double Bond in the Reaction of Diolates with *meso*-Bis(phenylsulfonyl)alkenes—Synthesis of Enantiopure Ketones

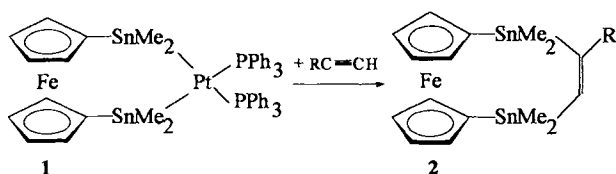
For possible use as antisense or antigene therapeutic agents, fairly pure crude cyclic oligonucleotides can easily be prepared by solid-phase synthesis (see below). After cyclization with formation of a phosphotriester (a) and cleavage (b), all noncyclized compounds, polymers, and other impurities are removed by filtration (c).



E. Alazzouzi, N. Escaja, A. Grandas,
E. Pedroso* 1506–1508

A Straightforward Solid-Phase Synthesis of
Cyclic Oligodeoxyribonucleotides

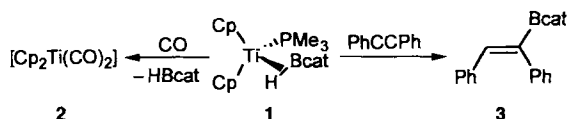
An intermediate in the metal-catalyzed distannylation of alkynes, the complex **1**, has been fully characterized for the first time by X-ray crystal structure analysis and multinuclear NMR spectroscopy. [4]Ferrocenophanes **2** are also directly obtained by addition of 1,2-bis(dimethylstanna)[2]ferrocenophane to alkynes in the presence of $[\text{Pt}(\text{PPh}_3)_2(\text{C}_2\text{H}_4)]$. R = H, Me, *n*Bu, Ph.



M. Herberhold,* U. Steffl, W. Milius,
B. Wrackmeyer 1508–1510

The First 1,3-Distanna-2-platina[3]ferro-
cenophane and the Pt^0 -Catalyzed Addition
of 1,1,2,2-Tetramethyl-1,2-distanna[2]ferro-
cenophane to $\text{C}\equiv\text{C}$ Bonds

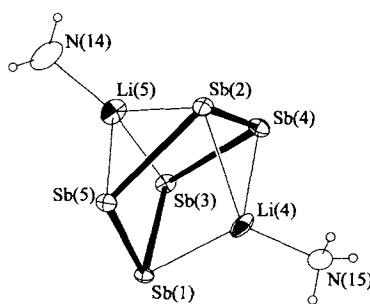
A significant B–H interaction is detected in the Ti^{II} compound **1**, the first monoborane σ complex. This complex undergoes ligand substitution with CO to form **2** and transfers catecholborane to diphenylacetylene to form **3**.



C. N. Muhoro,
J. F. Hartwig* 1510–1512

Synthesis, Structure, and Reactivity of
 $[\text{Cp}_2\text{Ti}(\text{HBCat})(\text{PMe}_3)]$: A Monoborane σ
Complex

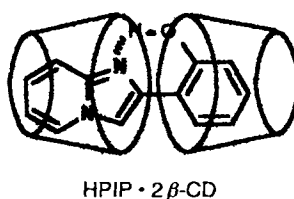
The direct reduction of main group metals with alkali metals in liquid ammonia almost seventy years ago got E. Zintl on the trail of the polyanions that were later named after him. The cyclo-Sb_5^{5-} ion in the title compound (structure of the $[\text{Li}_2(\text{NH}_3)_2\text{Sb}_5]^{3-}$ ion depicted on the right) demonstrates that the now feasible structure determination of the unstable ammoniates that are obtained from these solutions may still yield some surprises.



N. Korber,* F. Richter 1512–1514

cyclo-Sb_5^{5-} : A New, Highly Charged
Zintl Anion, Stabilized as an
Ion Complex in the Ammoniate
 $[\text{Li}(\text{NH}_3)_4]_3[\text{Li}_2(\text{NH}_3)_2\text{Sb}_5] \cdot 2\text{NH}_3$

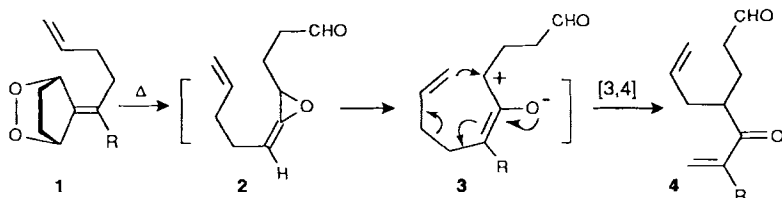
A spectral shift of up to 70 nm is observed for the dye HPIP depending on the size of the cyclodextrin cavity in which it is encapsulated. The fluorescence results from a phototautomerization in which proton transfer and twisting of the molecule are influenced by its surroundings. A model of a 1:2 complex of HPIP with a cyclodextrin is depicted on the right.



A. Douhal,* F. Amat-Guerri,
A. U. Acuña* 1514–1516

Probing Nanocavities with Proton-
Transfer Fluorescence

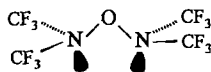
The 3-butenyl group makes it possible. The saturated endoperoxide **1** reacts at 60–80°C via the allene oxide **2** and its ring-opened product **3** by a [3,4]-sigmatropic shift to form the 5-oxo-6-heptenal derivatives **4**. The reaction might also be applicable to heteroatom analogues of **1**.



I. Erden,* F.-P. Xu,
W.-G. Cao 1516–1518

Sigmatropic Shifts in Allene Oxide Rearrangements: First General Route to [3,4]Shifts in Aliphatic Systems

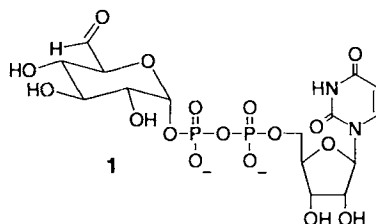
Synperiplanar orientation is observed for the electron lone pairs on the two nitrogen atoms in $(\text{CF}_3)_2\text{N}-\text{O}-\text{N}(\text{CF}_3)_2$ (**1**, depicted on the right). This is different from the theoretically predicted conformation for the model compound $\text{H}_2\text{N}-\text{O}-\text{NH}_2$. Compound **1** possesses an unusually small N-O-N bond angle of $105 \pm 3^\circ$.



S. Reinemann, R. Minkwitz,
H. Oberhammer* 1518–1519

Synthesis and Gas-Phase Structure of Perfluoro(2,4-dimethyl-3-oxa-2,4-diazapentane), $(\text{CF}_3)_2\text{N}-\text{O}-\text{N}(\text{CF}_3)_2$

The elusive aldehyde 1 has never been trapped nor detected during the enzymatic oxidation of UDP-glucose to UDP-glucuronic acid. Here the synthesis of **1** is reported; it proved to be kinetically competent to serve as an intermediate in the reaction catalyzed by UDP-glucose dehydrogenase.



R. E. Campbell,
M. E. Tanner* 1520–1522

Uridine Diphospho- α -D-glucosylaldehyde: Synthesis and Kinetic Competence in the Reaction Catalyzed by UDP-Glucose Dehydrogenase

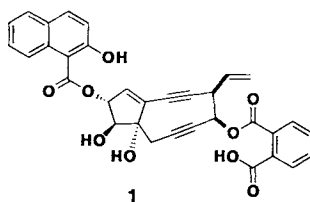
A possibly prebiotic RNA synthesis has been experimentally modeled with a 2',5'-linked RNA template. Mononucleoside 5'-phosphorimidazolides are incorporated after a primer, as directed by the unnaturally linked template (shown schematically on the right). The template linkage is not fully conserved in the product.



T. P. Prakash, C. Roberts,
C. Switzer* 1522–1523

Activity of 2',5'-Linked RNA in the Template-Directed Oligomerization of Mononucleotides

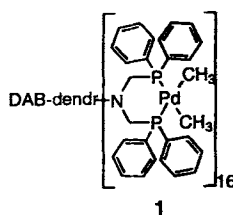
Ten times more active in cleaving DNA than other known enediynes, these effective hybrid compounds combine the nine-membered enediyne structure of the kedarcidin chromophore with the DNA intercalating group—a naphthoate group—of the neocarzinostatin chromophore. The precursor **1** of the active molecule is provided with a phthalate “trigger” and can generate linear DNA even in concentrations as low as 10–20 μM .



T. Takahashi,* H. Tanaka, H. Yamada,
T. Matsumoto, Y. Sugiura 1524–1526

Synthesis of Nine-Membered, Masked Enediyne Analogues with DNA Intercalators and Its DNA Cleaving Activities

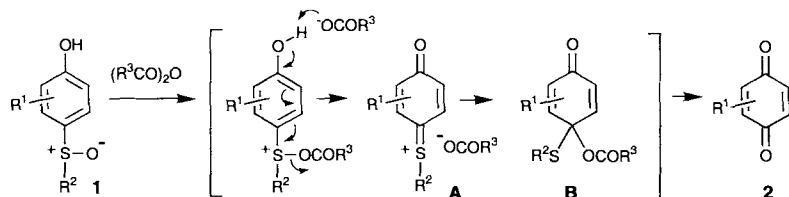
For Heck reactions and hydroformylations dendrimers loaded with palladium (for example **1**) or rhodium are suitable catalysts. A dendrimer with 16 outer bis(diphenylphosphinomethyl)amino end groups has been synthesized in one step by phosphinomethylation of a commercially available polyamino-dendrimer and converted into a catalyst by metalation.



M. T. Reetz,* G. Lohmer,
R. Schwickardi 1526–1529

Synthesis and Catalytic Activity of Dendritic Diphosphane Metal Complexes

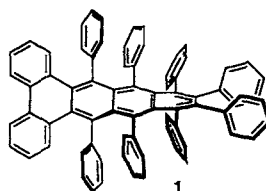
A versatile synthetic building block and evidence for the mechanism of the Pummerer-type rearrangement have been obtained in the form of the acetal intermediate **B**, isolated in the reaction of *p*-sulfinylphenols **1** to *p*-quinones **2** induced by acid anhydrides. Thus, a method is now also available for the efficient preparation of quinone monoacetals under nonoxidative conditions.



Y. Kita,* Y. Takeda, M. Matsugi,
K. Iio, K. Gotanda, K. Murata,
S. Akai 1529–1531

Isolation of the Quinone Mono *O,S*-Acetal
Intermediates of the Aromatic Pummerer-
Type Rearrangement of *p*-Sulfinylphenols
with 1-Ethoxyvinyl Esters

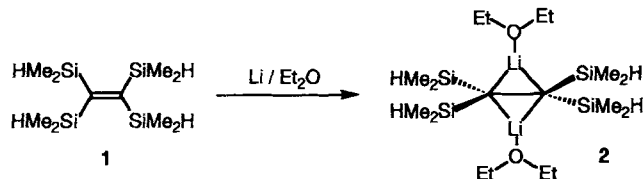
Overcrowding with phenyl groups forces the polycyclic, aromatic hydrocarbons out of planarity. The X-ray structure analysis of **1** shows that the molecule has a record end-to-end twist of 105°; yet it is very stable in the solid state and can be heated to 400 °C without decomposition.



X. Qiao, D. M. Ho,
R. A. Pascal, Jr.* 1531–1532

An Extraordinarily Twisted Polycyclic
Aromatic Hydrocarbon

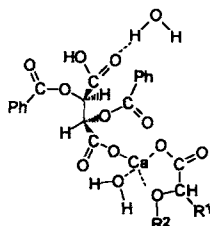
Structural and spectroscopic properties of the title compound **2** provide clear evidence for a SiH–Li agostic interaction. Compound **2** was prepared by the reaction of tetrakis(dimethylsilyl)ethene (**1**) with lithium metal in ether.



A. Sekiguchi,* M. Ichinohe,
M. Takahashi, C. Kabuto,
H. Sakurai* 1533–1534

1,1,2,2-Tetrakis(dimethylsilyl)-1,2-
ethanediylidilithium-bis(diethyl ether):
Observation of a SiH–Li Agostic
Interaction

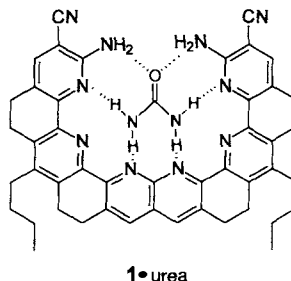
Chiral recognition in the coordination sphere of a calcium ion that is coordinated to a simple tartaric acid derivative offers new possibilities for the preparative-scale resolution of nonbasic compounds. An example of a mixed calcium salt formed upon resolution of racemic carboxylic acids is shown on the right.



A. Mravik,* Z. Böcskei, Z. Katona,
I. Markovits, E. Fogassy 1534–1536

Coordination-Mediated Optical Reso-
lution of Carboxylic Acids with
O,O'-Dibenzoyltartaric Acid

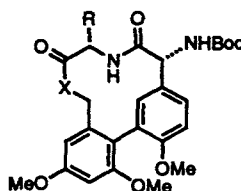
All the conceivable donor and acceptor sites of urea are involved in hydrogen bonds in the complex with the highly preorganized artificial receptor **1**. The resulting complex is so stable that it can be purified by thermal recrystallization from pure DMSO; a stability constant of $1.4 \times 10^4 \text{ M}^{-1}$ has been estimated from the urea-selective UV/Vis response of this receptor.



T. W. Bell,* Z. Hou 1536–1538

A Hydrogen-Bonding Receptor That Binds
Urea with High Affinity

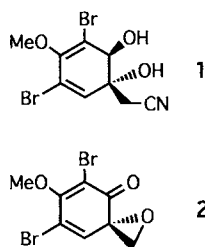
A mild, Ni⁰-promoted cyclization leads to the synthesis of rigid 12-membered peptide–biaryl ring systems (example on the right) of the type found in the glycopeptide antibiotic vancomycin. This synthetic method brings us a step closer to the total synthesis of vancomycin itself. Boc = *tert*-butoxycarbonyl; X, for example, O; R, for example, H.



K. C. Nicolaou,* X.-J. Chu,
J. M. Ramanjulu, S. Natarajan,
S. Bräse, F. Rübsam,
C. N. C. Boddy 1539–1540

New Technology for the Synthesis of
Vancomycin-Type Biaryl Ring Systems

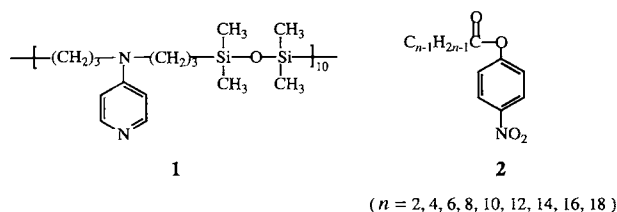
IC₅₀ values in the low micromolar range for the inhibition of receptor tyrosine kinases, which are critically involved in the transduction of mitogenic signals and thus in the regulation of cell growth and proliferation, are characteristic of synthetic analogues of marine natural product aeropylsinin **1** such as **2**. In addition, they show pronounced inhibitory activity in cultured cells in vivo.



H. Waldmann,* K. Hinterding,
P. Herrlich,* H. J. Rahmsdorf,
A. Knebel 1541–1542

Selective Inhibition of Receptor Tyrosine
Kinases by Synthetic Analogues of Aero-
pylsinin

Spheres, rods, or vesicles are formed by the polymer **1**, depending on the added salt (tris(hydroxymethyl)methylammonium chloride (TrisCl) or NaCl) and its concentration. Consequently, ion-induced substrate specificity occurs in the **1**-catalyzed solvolysis of *p*-nitrophenyl alkanoates **2** at pH 8.0 and 30 °C. With TrisCl, **2** (*n* = 6) is preferentially hydrolyzed and with NaCl, **2** (*n* = 14) or **2** (*n* = 12) depending on the concentration (*c* = 0–0.1 or 0.25–1.00 M, respectively).



G.-J. Wang, W. K. Fife* 1543–1545

Ion-Induced Specificity Change in Poly-
mer-Catalyzed Solvolyses of *p*-Nitrophenyl
Alkanoates

* Author to whom correspondence should be addressed

BOOKS

Applied Homogeneous Catalysis with Organometallic Compounds.
A Comprehensive Handbook • B. Cornils, A. Herrmann

I. Tkatchenko 1547

Comprehensive Organic Functional Group Transformations •
A. R. Katritzky, O. Meth-Cohn, C. W. Rees

H. Hopf, B. König, U. Jahn 1549

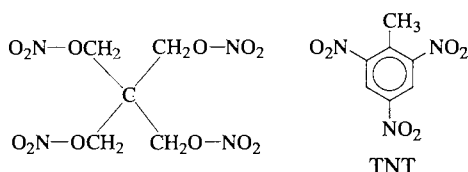
Arrhenius: From Ionic Theory to the Greenhouse Effect • E. Crawford

G. B. Kauffman 1550

CORRIGENDA

In the communication by **W. J. Evans et al.** in issue number 7, pp. 774–776, a starting material for reaction (d) has been incorrectly named: tetramethylfulvalene should read 1,2,3,4-tetramethylfulvene.

In the review by **P. Kolla** in issue number 8, pp. 800–811, the structural formulas of PETN and TNT in Scheme 1 are incorrect. The correct structures are given here:



The corrigendum in issue number 9, p. 951, for a communication by **T. F. Fässler et al.** unfortunately still depicts the original, incorrect picture. The axes *a* and *c* should be mirrored across the origin.

The date on the cover of the International Edition volume 36, no. 10, was incorrectly given as May 15, 1997. The correct date of publication is June 2, 1997.

SERVICES

| | |
|----------------|------|
| • Classified | A61 |
| • Keywords | 1552 |
| • Author Index | 1553 |
| • Preview | 1554 |

German versions of all reviews, communications, and highlights in this issue appear in the second June issue of *Angewandte Chemie*. The appropriate page numbers can be found at the end of each article and are also included in the Author Index on p. 1553.

All the Tables of Contents
from 1995 onwards may be
found on the WWW under:
[http://www.wiley-vch.de/
home/angewandte](http://www.wiley-vch.de/home/angewandte)

ANGEWANDTE CHEMIE

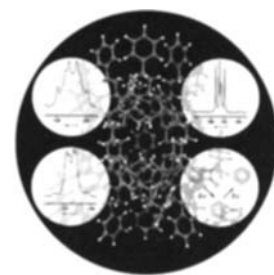
A Journal of the
Gesellschaft
Deutscher Chemiker

International Edition in English

1997
36/12
Pages 1225–1358

COVER PICTURE

The cover picture shows a ball-and-stick model of extremely strained, highly reactive *o*-benzyne (1,2-didehydrobenzene) (green) inside the protective inner phase of Cram's hemicarcerand (O atoms in red, C atoms in grey, and H atoms in white). The white, circular window in the lower right-hand corner represents the inner phase in which *o*-benzyne was photochemically generated from incarcerated benzocyclobutenedione in two steps via benzocyclopropenone and is stable for only a short time, even at -75°C . The other three windows highlight groups of signals in the ^{13}C NMR spectrum of the fully ^{13}C -labeled guest molecule. More about the NMR spectroscopic properties of this molecule is reported by R. Warmuth on page 1347 ff—one hundred years after the birth of Georg Wittig, who first postulated the existence of this “dehydrobenzene”. The graphic was generated by Jan Haller, University of California, Los Angeles, CA (USA) with the program POV-ray.

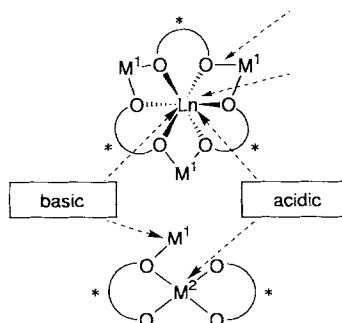


REVIEWS

Contents

Brønsted basic and Lewis acidic like many enzymes:

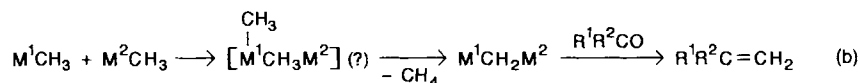
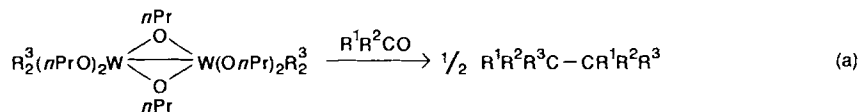
The multifunctional complexes shown on the right are made from a rare-earth metal (or a Group 13 element), an alkali metal, and an optically active (substituted) 2,2'-dihydroxy-1,1'-binaphthyl (BINOL) ligand. They are exceptionally suitable for asymmetric two-center catalysis of nitroaldol reactions, Michael reactions, Michael–aldol reactions, and hydrophosphonylations of imines and/or aldehydes. Ln = rare-earth metal, M^1 = alkali metal, M^2 = Al or Ga, $\text{HO}-\text{C}_6\text{H}_4-\text{OH}$ = BINOL.



M. Shibasaki,* H. Sasai,
T. Arai 1236–1256

Asymmetric Catalysis with Hetero-
bimetallic Compounds

High-valent molybdenum and tungsten atoms have long been important as components of catalysts and Schrock carbene complexes. As central atoms of CH_3 , alkyl, and $\mu\text{-CH}_2$ complexes, they permit new, preparatively interesting reactions according to Equations (a) and (b). $\text{M}^1 = \text{MoL}_n, \text{WL}_n$; $\text{M}^2 = \text{MoL}_n, \text{WL}_n, \text{AlL}_n$.



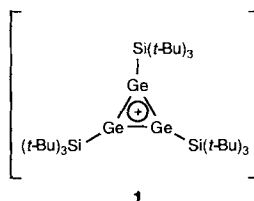
T. Kauffmann* 1258–1275

Novel Reactions of Organomolybdenum and Organotungsten Compounds: Additive–Reductive Carbonyl Dimerization, Spontaneous Transformation of Methyl Ligands into μ -Methylene Ligands, and Selective Carbonylmethylenation

HIGHLIGHTS

Contents

“The search for an isolable silyl cation must continue” was the title of a paper in this journal a few years ago. Recently, J. Lambert et al. reported the latest results of this continued search: the trimesitylsilyl cation is a practically free silyl cation in aromatic solvents. Kinetic and thermodynamic stabilization have now also allowed the isolation of the noncoordinated germirene cation **1** by A. Sekiguchi et al.



J. Belzner* 1277–1280

Free or Not, That Is the Question: Silyl and Germyl Cations in Condensed Phases

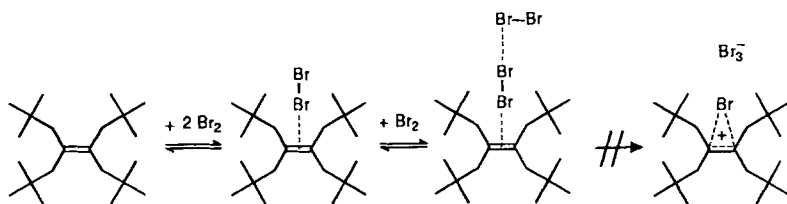
The first step has been made. The research groups of Hindsgaul, Boons, and Kahne have successfully synthesized libraries of di- and trisaccharides with combinatorial methods. The synthesis of this important class of oligosaccharides is thus more feasible and will have a great impact on the understanding of cell-surface interactions.

P. Arya,* R. N. Ben* 1280–1282

Combinatorial Chemistry for the Synthesis of Carbohydrate Libraries

COMMUNICATIONS

An L-shaped arrangement of bromine atoms is found in the 2:1 π complex formed by electrophilic bromination of tetraeneopentylethene (see below). The reaction stops at this stage, which for the first time allows detection and determination of the thermodynamic parameters by UV spectroscopy of a 2:1 bromine–olefin complex. Theoretical calculations predict an olefin· Br_2 · Br_2 rather than a Br_2 ·olefin· Br_2 structure.

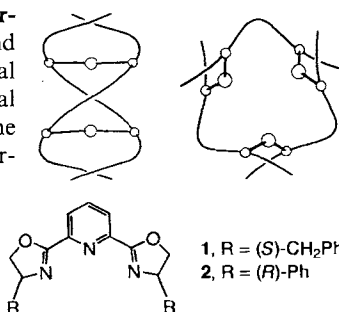


R. Bianchini,* C. Chiappe, D. Lenoir,* P. Lemmen, R. Herges,*

J. Grunenberg 1284–1287

Spectroscopic Detection and Theoretical Studies of a 2:1 Bromine–Olefin π Complex

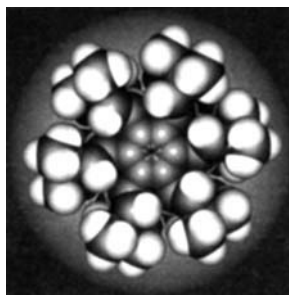
Despite having ligands with almost identical conformations, the structures of the Ag^I complexes of **1** and **2** differ significantly: ligand **1** forms a double-helical complex of *P* chirality, and **2** gives a triple-helical complex (depicted on the right). The reason for the difference appears to be the existence of strong interligand stacking in the latter case.



C. Provent, S. Hewage, G. Brand, G. Bernardinelli, L. J. Charbonnière, A. F. Williams* 1287–1289

Enantioselective Formation of Double and Triple Helicates of Silver(I): The Role of Stacking Interactions

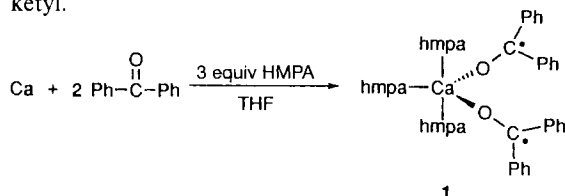
Bowl-shaped hexakis(3,3-dimethyl-1-butenyl)benzene (**1**, see space-filling model on the right) was obtained from the Pd-catalyzed coupling of hexabromobenzene with 2-(3,3-dimethyl-1-butenyl)-1,3,2-benzodioxaborole. All six alkenyl groups are directed to one side of the benzene ring. Catalytic hydrogenation of **1** provides the corresponding hexakisalkylbenzene, which crystallizes in regular stacks; here the alkyl groups are alternatingly above and below the ring.



P. Prinz, A. Lansky, T. Haumann,
R. Boese, M. Noltemeyer, B. Knieriem,
A. de Meijere* 1289–1292

Palladium-Catalyzed Sixfold Alkenylation
of Hexabromobenzene: An Interesting
Case of Self-Organization

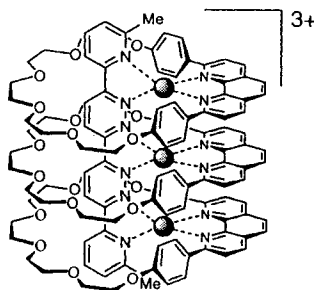
Highly reactive and yet isolable! The bis(benzophenone ketyl)calcium complex **1** was isolated as blue crystals from the reaction of calcium chips with benzophenone and hexamethylphosphoric acid triamide (HMPA) in THF (see below). Its X-ray crystal structure explains why benzophenone ketyl is much more reactive than fluorenone ketyl.



Z. Hou,* X. Jia, M. Hoshino,
Y. Wakatsuki 1292–1294

First Structural Characterization of a
Benzophenone Ketyl Complex

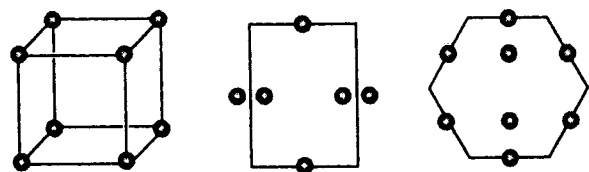
Like a molecular lance! A rigid-rack, pyridazine-containing ligand pierces through three macrocycles (see drawing on the right), and a trimetallic pseudorotaxane is formed by Cu^I-assisted self-assembly. Its structure was characterized by X-ray crystallography.



P. N. W. Baxter, H. Sleiman, J.-M. Lehn,*
K. Rissanen 1294–1296

Multicomponent Self-Assembly: Genera-
tion and Crystal Structure of a Trimetallic
[4]Pseudorotaxane

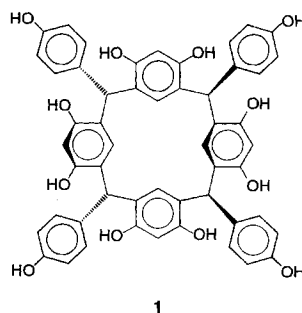
Depending on the configuration of the metal unit (*cis* or *trans*) and the sequence of coordination by six-membered heterocycles uracil, 1-methylcytosine, and 2-aminopyridine, complexes of different topologies—open box, rectangle, or hexagon—are obtained (see below). These complexes contain six or eight metal units (with Pt^{II}, Ni^{II}, Pd^{II}, Cu^{II}, or Ag^I; represented by spheres) in unusual relative arrangements.



H. Rauter, I. Mutikainen,* M. Blomberg,
C. J. L. Lock, P. Amo-Ochoa,
E. Freisinger, L. Randaccio,*
E. Zangrando, E. Chiarparin,
B. Lippert* 1296–1301

Cyclic Metal Complexes of Nucleobases
and Other Heterocycles: Molecular Boxes,
Rectangles, and Hexagons

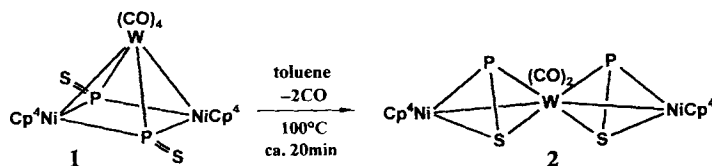
The maximum possible number of hydrogen bonds to the solvent are formed by the resorcarene **1** in crystals of 1:18 DMSO (DMSO = dimethyl sulfoxide). Whereas highly solvated, discrete molecules of **1** are found in 1:18 DMSO, hydrogen-bonded, infinite columns of **1** that are entirely wrapped by layers of pyridine molecules are present in crystals of the composition 1:14 pyridine.



A. Shivanyuk, E. F. Paulus, V. Böhmer,*
W. Vogt 1301–1303

Quasi-Complete Solvation of Organic
Molecules in the Crystalline State

A cluster with two chiral tetrahedrane fragments, which are linked through a common tungsten vertex (**2**), is formed on heating the tetragonal-pyramidal trinuclear complex **1** with two μ_3 -P=S ligands ($\text{Cp}^4 = \text{C}_5\text{H}_5\text{Pr}_4$). The terminally coordinated PS ligand in **1** is therefore converted into a doubly side-on bound $\mu\text{-}\eta^2\text{:}\eta^2\text{-PS}$ ligand.



O. J. Scherer,* C. Vondung,
G. Wolmershäuser 1303–1305

PS Ligands as Building Blocks of Chiral
Dimetallatetrahedranes with a Common
Vertex

The high thermodynamic barrier for ethane aromatization at lower temperatures (400–500 °C) over a H-GaAlMFI zeolite can be overcome. Both ethane conversion and the yield of arenes drastically increase (4–80 ×) by carrying out the aromatization in the presence of olefins or higher alkanes. The enhanced reactivity results from a change in the reaction mechanism, and a hydrogen-transfer reaction takes place between ethane and higher olefins.

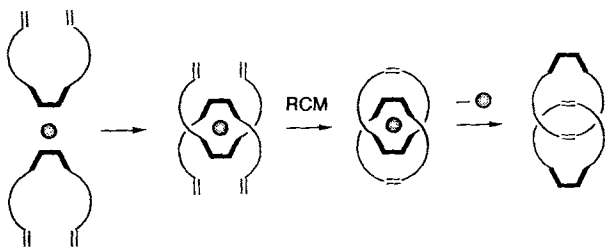
V. R. Choudhary,* A. K. Kinage,
T. V. Choudhary 1305–1308

Effective Low-Temperature Aromatization
of Ethane over H-GaAlMFI Zeolites in the Presence of Higher
Alkanes or Olefins

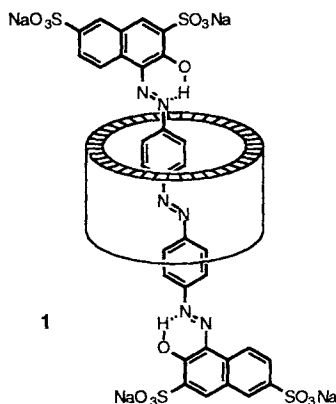
Almost quantitative formation of interlocking rings results upon cyclization of threaded or intertwined complexes. The synthesis concept is based on the combination of three-dimensional template effects and ruthenium benzylidene catalyzed ring-closing metathesis (RCM, see below)

B. Mohr, M. Weck, J.-P. Sauvage,*
R. H. Grubbs* 1308–1310

High-Yield Synthesis of [2]Catenanes by
Intramolecular Ring-Closing Metathesis



The hydrophobic effect was used to assemble encapsulated azo dyes such as **1** in water. The dumbbell-shaped dyes were synthesized inside α -cyclodextrin, β -cyclodextrin, or a cyclophane to yield stable rotaxanes.



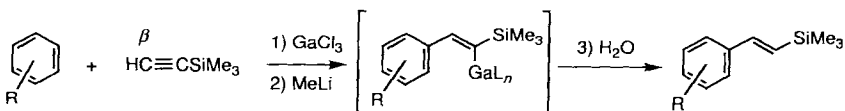
S. Anderson,* T. D. W. Claridge,
H. L. Anderson* 1310–1313

Azo-Dye Rotaxanes

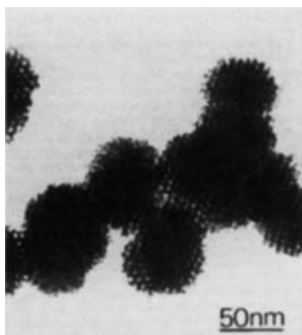
Novel vinylgallium intermediates occur in the β -silylvinylation of aromatic hydrocarbons with trimethylsilylacetylene in the presence of GaCl_3 at -78°C (see below). The interaction of silylacetylene and GaCl_3 initially generates a highly electrophilic cationic species, which is attacked by arenes at the β -carbon atom. $\text{L} = \text{Cl}, \text{Me}$.

M. Yamaguchi,* Y. Kido, A. Hayashi,
M. Hirama 1313–1315

Friedel–Crafts β -Silylvinylations



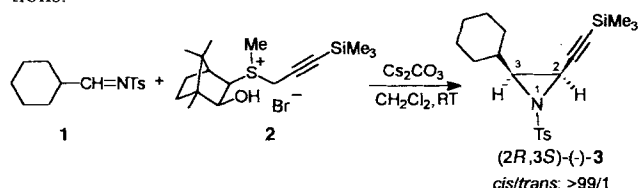
Hexagonally structured, mesoporous platinum (see picture on the right) is obtained by reduction of platinum salts in lyotropic liquid-crystalline phases. The template can be removed from the nanostructured metal colloid without affecting its structure.



G. S. Attard,* C. G. Göltner,*
J. M. Corker, S. Henke,
R. H. Templer 1315–1317

Liquid-Crystal Templates for Nanostructured Metals

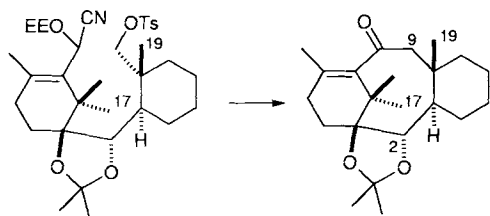
Phase-transfer conditions can be used to synthesize (–)- or (+)-*cis*-acetylenyl-*N*-sulfonylaziridines (for example **3**) by the reaction of *N*-sulfonylimines (**1**) with chiral sulfonium propargylides (**2**) derived from D-(+)-camphor. High *cis* selectivity and yields as well as moderate to good *ee* values are characteristic for these aziridinations.



A.-H. Li, Y.-G. Zhou, L.-X. Dai,*
X.-L. Hou, L.-J. Xia,
L. Lin 1317–1319

Asymmetric Aziridination over Ylides:
Highly Stereoselective Synthesis of
Acetylenyl-*N*-sulfonylaziridines

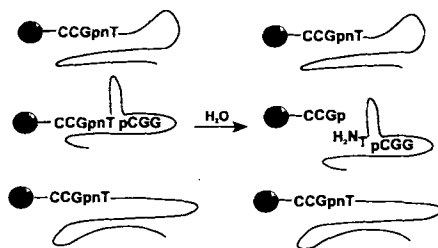
Cyanohydrin ethers are the structural elements required for intramolecular alkylation to give the eight-membered taxoid B ring. This was demonstrated both for aromatic as well as for nonaromatic C rings (see below). EE = ethoxyethyl.



T. Takahashi,* H. Iwamoto,
K. Nagashima, T. Okabe,
T. Doi 1319–1321

Synthesis of Taxoid Ring Systems:
AC → ABC Approach by Way of Intra-
molecular Alkylation

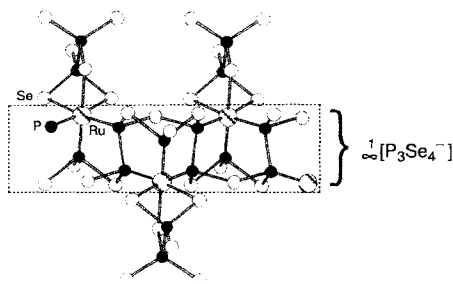
Catalytic activity in combinatorial DNA libraries is demonstrated for a cofactor-assisted self-cleavage reaction. In vitro selection allowed the isolation of one dominating sequence from a sequence library containing 72 randomized nucleotide positions. The selected sequence undergoes self-cleavage of an internal 3'–5' phosphoramidate bond by intramolecular catalysis in the presence of the trimer pCGG (see drawing on the right).



J. Burmeister, G. von Kiedrowski,*
A. D. Ellington 1321–1324

Cofactor-Assisted Self-Cleavage in DNA
Libraries with a 3'–5'-Phosphoramidate
Bond

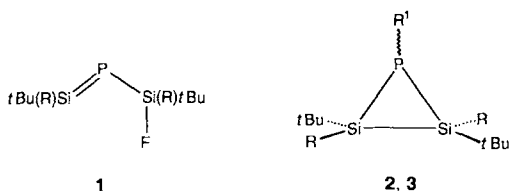
An infinite, one-dimensional chelating ligand $\infty[\text{P}_3\text{Se}_4^-]$ is present in $\text{K}_3\text{RuP}_5\text{Se}_{10}$ (depicted on the right), which was obtained by the reaction of ruthenium with a molten mixture of nominal stoichiometry $\text{K}_3\text{P}_6\text{Se}_{26.5}$ at 490 °C. $\text{K}_3\text{RuP}_5\text{Se}_{10}$ is the first structurally characterized ruthenium chalcophosphate, and features very short Ru–P bonds (2.288(2), 2.262(2) Å).



K. Chondroudis,
M. G. Kanatzidis* 1324–1326

$\infty[\text{P}_3\text{Se}_4^-]$: A Novel Polyanion in
 $\text{K}_3\text{RuP}_5\text{Se}_{10}$; Formation of Ru–P Bonds in
a Molten Polyselenophosphate Flux

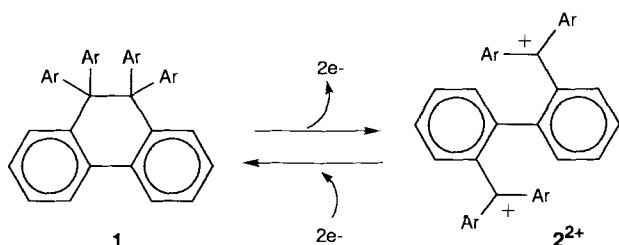
More electronically diverse than the behavior of allyl is that of the 2-phospha-1,3-disilaallyl fragment. This was confirmed by the [1,3]-sigmatropic shift of fluorine in the title compound **1**, which occurred rapidly at temperatures above 40 °C. Ab initio calculations show that the transition state of the migration does not have a symmetrically bridging F atom. The phosphadisilacyclopropanide **2** ($R^1 = \text{Li}(\text{thf})_x$)—obtained from **1** by addition of lithium to the Si=P bond, subsequent elimination of LiF, and rearrangement—readily reacts to give the PH compound **3** ($R^1 = \text{H}$). $R = 2,4,6$ -triisopropylphenyl.



M. Driess,* S. Rell, H. Pritzkow,
R. Janoschek * 1326–1329

$R_2\text{Si}=\text{P}-\text{SiR}_2\text{F}$: 1,3-Sigmatropic Migration of Fluorine in a 2-Phospha-1,3-disilaallyl Derivative Capable of Conjugation and Its Conversion to Phosphadisilacyclopropanes

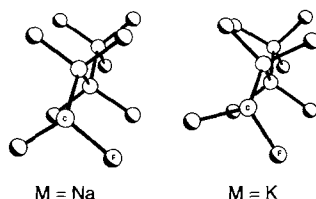
Reversible C–C bond breaking/making as well as drastic change in color are induced upon electron transfer in the novel redox couples of hexaarylethanes **1** and bis(triarylmethyl) dications **2**²⁺. Their hysteretic redox behaviors result from the quite different geometries of **1** and **2**²⁺. $\text{Ar} = p\text{-Me}_2\text{NC}_6\text{H}_4$, $p\text{-MeOC}_6\text{H}_4$.



T. Suzuki,* J.-i. Nishida,
T. Tsuji 1329–1331

Hexaphenylethane Derivatives Exhibiting Novel Electrochromic Behavior

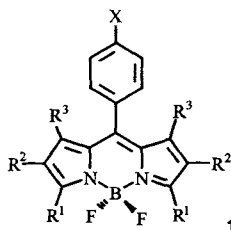
The type of counterion determines whether the perfluoroalkyl chains extending from the hydrophilic core of a layered structure in compounds of the type $\text{M}[\text{C}_n\text{F}_{2m+1}\text{SO}_2\text{NSO}_2\text{C}_n\text{F}_{2n+1}]$ ($n, m = 4, 6$) possess an all-staggered conformation ($\text{M} = \text{Na}$) or a more typical helical conformation ($\text{M} = \text{K}$; see picture on the right). In the sodium complex the perfluoroalkyl chains are too closely packed to assume a twisted conformation.



L. Xue, D. D. DesMarteau,*
W. T. Pennington * 1331–1333

Perfectly Staggered and Twisted Difluoromethylene Groups in Perfluoroalkyl Chains: Structure of $\text{M}[\text{C}_4\text{F}_9\text{SO}_2\text{NSO}_2\text{C}_4\text{F}_9]$ ($\text{M} = \text{Na}, \text{K}$)

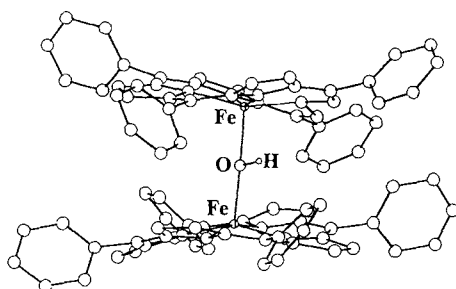
Suitable for light-emitting diodes or as pH sensors, the difluoroboradiazas-indacenes of type **1** luminesce after electrochemical excitation ($\text{X} = \text{H}$) or show on/off switching of fluorescence sensitivity depending on pH ($\text{X} = \text{NMe}_2$). $R^1 = \text{Me}, \text{H}, \text{CO}_2\text{Et}$; $R^2 = \text{Et}, \text{H}$; $R^3 = \text{Me}$.



M. Kollmannsberger, T. Gareis, S. Heinl,
J. Breu, J. Daub * 1333–1335

Electrogenerated Chemiluminescence and Proton-Dependent Switching of Fluorescence: Functionalized Difluoroboradiazas-indacenes

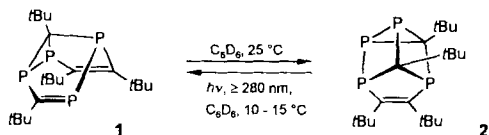
The linear Fe–O–Fe bridge in μ -oxo tetraphenylporphyrin iron(III) dimer can be protonated without structural rehybridization at the O atom (the structure of the μ -hydroxo-bridged complex is depicted on the right). Antiferromagnetic coupling between the iron centers is greatly attenuated, and proton self-exchange is slow.



D. R. Evans, R. S. Mathur, K. Heerwegh,
C. A. Reed,* Z. Xie 1335–1337

Protonation of a Linear Oxo-Bridged Diiron Unit without Rehybridization of the Bridging Oxygen: Structure of the (μ -Hydroxo)bis-(tetraphenylporphyrinato)-iron(III) Cation

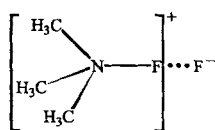
Stable only up to -25°C , the semibullvalene **1** does not possess a fluctuating structure in solution at room temperature, but rather isomerizes to give the "bis(homo)prismane" **2**. The latter valence isomer is accessible by numerous, widely varying routes, and the isomerization can be reversed photochemically (**2** \rightarrow **1**).



A. Mack, B. Breit, T. Wettling,
U. Bergsträsser, S. Leininger,
M. Regitz* 1337–1340

Tetraphosphasemibullvalene: First Valence
Isomerizations in the Phosphaalkyne
Cyclotetramer System

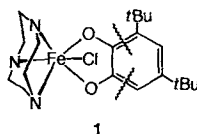
Abstraction of a F^+ ion from F_2 leading to formation of the ion pair $[(\text{CH}_3)_3\text{N}]^+\text{F}^- \cdots \text{F}^-$ occurs when trimethylamine and F_2 are mixed in the gas phase under conditions that preclude production of F atoms. The presence of this ion pair in $(\text{CH}_3)_3\text{N}/\text{F}_2$ mixtures emerging from a fast-mixing nozzle has been unambiguously established from several of its properties determined by rotational spectroscopy.



H. I. Bloemink, S. A. Cooke,
J. H. Holloway,
A. C. Legon* 1340–1342

Rotational Spectroscopy of Mixtures of
Trimethylamine and Fluorine: Identifica-
tion of the Ion Pair $[(\text{CH}_3)_3\text{N}]^+\text{F}^- \cdots \text{F}^-$ in
the Gas Phase

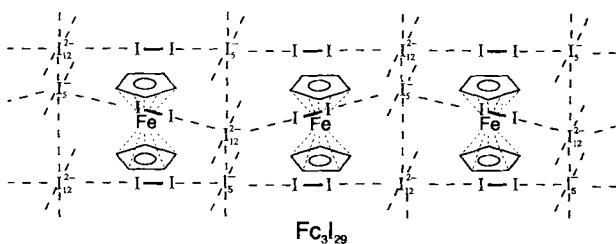
Quantitative extradiol cleavage of a catechol derivative is achieved by exposure of complex **1** to O_2 in the presence of AgBF_4 and an aromatic nitrogen base. These results provide insight into how the regiochemistry of oxidative cleavage may be controlled by the metal centers of the catechol dioxygenases.



M. Ito, L. Que, Jr.* 1342–1344

Biomimetic Extradiol Cleavage of Cate-
chols: Insights into the Enzyme Mechanism

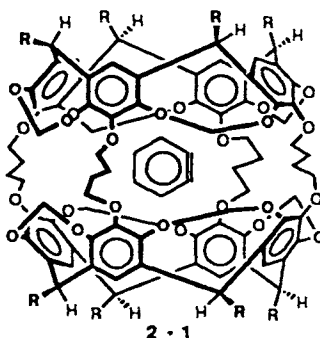
$\text{FcI}_{9.67}$ contains bands and chains as substructures, which are linked together by up to sixfold-coordinated iodine atoms to form a novel three-dimensional network (see below). The ferrocenium ions Fc^+ are intercalated in the cavities. These cations stabilize crystalline solids that contain not only known polyiodide ions but also $\text{FcI}_{9.67}$, which can be described as the triply charged nonacosaiodide Fc_3I_{29} and is the most iodine-rich polyiodide known to date.



K.-F. Tebbe,* R. Buchem 1345–1346

The Most Iodine-Rich Polyiodide Yet:
 Fc_3I_{29}

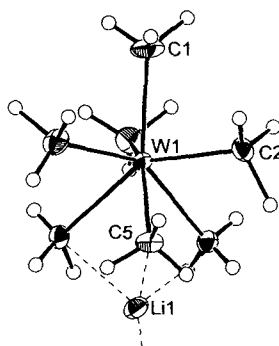
One hundred years after the birth of Georg Wittig the ^1H and ^{13}C NMR spectra of *o*-benzyne (**1**) were recorded in solution. Compound **1** was generated-photochemically in the inner cavity of hemicarcarand **2** from an incarcerated benzocyclobutenedione in two steps via a benzocyclopropenone hemicarcarplex.



R. Warmuth 1347–1350

o-Benzyne: Strained Alkyne or
Cumulene?—NMR Characterization in a
Molecular Container

Capped octahedral and square antiprismatic structures are seen for the homoleptic anions $[\text{W}(\text{CH}_3)_7]^-$ and $[\text{Re}(\text{CH}_3)_8]^{2-}$. Therefore these anions show no structural anomalies, in contrast to the neutral molecules $[\text{W}(\text{CH}_3)_6]$ and $[\text{Re}(\text{CH}_3)_6]$. The picture on the right shows the structure of $[\text{Li}(\text{OEt}_2)][\text{W}(\text{CH}_3)_7]$ without the diethyl ether molecule.



V. Pfennig, N. Robertson,
K. Seppelt* 1350–1352

The Anions $[\text{W}(\text{CH}_3)_7]^-$ and $[\text{Re}(\text{CH}_3)_8]^{2-}$

* Author to whom correspondence should be addressed

BOOKS

Crystal Structures. I: Patterns and Symmetry · M. O'Keeffe, B. G. Hyde

W. H. Baur 1353

Electronic Conference on Trends in Organic Chemistry, ECTOC 1 ·
H. S. Rzepa, C. Leach, J. M. Goodman

J. Grunenberg 1353

pH and Buffer Theory—A New Approach · H. Rilbe

B. Neumüller 1354

Introduction to Theoretical Organic Chemistry and Molecular Modeling · W. B. Smith

R. Herges 1355

German versions of all reviews, communications, and highlights in this issue appear in the second June issue of *Angewandte Chemie*. The appropriate page numbers can be found at the end of each article and are also included in the Author Index on p. 1357.

All the Tables of Contents from 1995 onwards may be
found on the WWW under:
<http://www.vchgroup.de/home/angewandte>

SERVICES

| | |
|----------------|------|
| • Keywords | 1356 |
| • Author Index | 1357 |
| • Preview | 1358 |

ANGEWANDTE CHEMIE

A Journal of the
Gesellschaft
Deutscher Chemiker

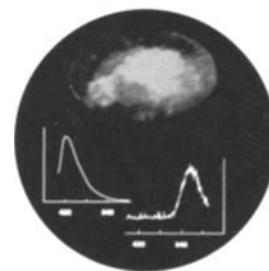
International Edition in English

1997
36/11

Pages 1133–1224

COVER PICTURE

The cover picture shows the intense yellow luminescence that is triggered when crystals of the trinuclear gold(I) complex $[\text{Au}_3(\text{CH}_3=\text{COCH}_3)_3]$ come in contact with a drop of solvent. The prerequisite for this solvent-stimulated luminescence is the prior irradiation with long-wavelength UV light. This luminescence was totally unexpected, and was first discovered during the isolation of the complex when the resulting crystals were filtered and subsequently washed. The two emission spectra clearly reveal that the yellow luminescence (lower right spectrum) cannot arise from the dissolved species (upper left spectrum). Investigations into the origins of this phenomenon are reported by A. L. Balch et al. on pages 1179 ff.



REVIEWS

Contents

Incorporation of redox metals into the framework of zeolites and related molecular sieves considerably extends their utility in organic synthesis. The structural diversity—including variation of the redox metal as well as size and polarity of the micropores—provides the possibility of designing tailor-made solid catalysts for liquid-phase oxidations under mild conditions with O_2 , H_2O_2 , and RO_2H as oxidants. Important considerations for designing or choosing a suitable catalyst based on molecular sieves can be derived from the numerous examples, some of which are even in industrial use, of oxidation of synthetically interesting compounds (alkenes, alcohols, aldehydes, amines, arenes) as well as the different methods for synthesizing redox molecular sieves (incorporation of redox metal by ion exchange by substitution of framework atoms or encapsulating a metal complex).

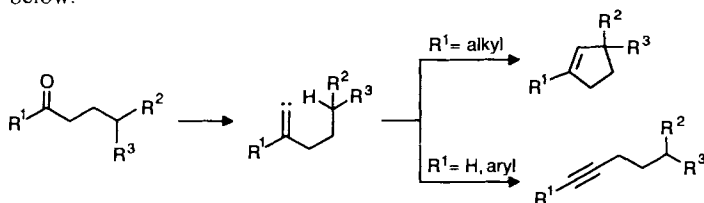
I. W. C. E. Arends, R. A. Sheldon,*
M. Wallau, U. Schuchardt* . . . 1144–1163

Oxidative Transformations of Organic
Compounds Mediated by Redox Molecular
Sieves

Diversity and efficiency is offered by the method of converting ketones into cyclopentenones by selective intramolecular insertion of alkenylidenes $\text{R}_2\text{C}=\text{C}:$ into C–H bonds. The chain extension that converts an aldehyde into an alkyne can also be achieved with these carbenes. These two possibilities are generalized in the equation below.

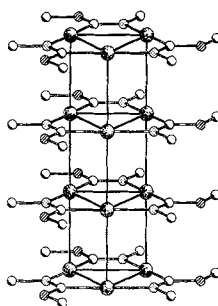
W. Kirmse* 1164–1170

Alkenylidenes in Organic Synthesis



HIGHLIGHTS

Photochemical switches, energy storage devices, or photochemical sensors are potential applications of luminescent gold complexes. The basis for this expectation is the spectacular discovery by Balch et al., who observed that a trinuclear gold complex (see picture) gave rise to an intense emission upon dissolution in an organic solvent after previous irradiation with near-UV light (*Angew. Chem. Int. Ed. Engl.* **1997**, *36*, 1179).



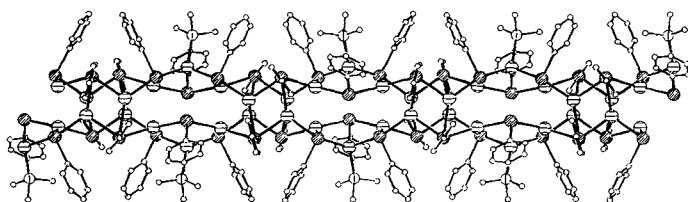
L. H. Gade* 1171–1173
 “Hyt was of Gold, and Shon so
 Bryghte...”: Luminescent Gold(I)
 Compounds

Some enzymes tolerate bases and transition metal catalysts at elevated temperatures—conditions which, for example, Williams et al. and Bäckvall et al. have shown are suitable for racemizing secondary alcohols by Meerwein–Ponndorf reduction/Oppenauer oxidation. Enzyme-catalyzed acylation under Meerwein–Ponndorf–Verley conditions facilitates dynamic kinetic resolutions of alcohols.

R. Stürmer* 1173–1174
 Enzymes and Transition Metal Complexes
 in Tandem—A New Concept for Dynamic
 Kinetic Resolution

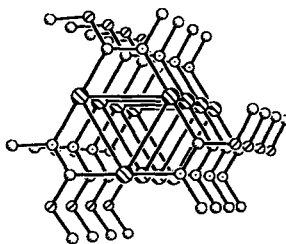
COMMUNICATIONS

In the presence of tertiary phosphanes, AgCl reacts readily with the reagent Te(Ph)SiMe₃ to yield silver–telluroate polynuclear complexes. In the case of PMe₃, the polymer [Ag₁₀(μ₃-TePh)₁₀(PMe₃)₂]_∞ (shown below) is formed, in which the TePh ligands serve as both inter- and intracuster bridges.



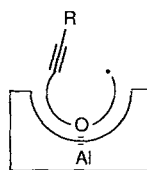
J. F. Corrigan, D. Fenske,*
 W. P. Power 1176–1179
 Silver–Telluroate Polynuclear Complexes:
 From Isolated Cluster Units to Extended
 Polymer Chains

Striking yellow luminescence is observed upon addition of a drop of solvent to colorless crystals of [Au₃(CH₃N=COCH₃)₃] that were previously irradiated with near-visible light. The trigonal prismatic stacking of individual molecules of the triangular cluster in the solid state (shown on the right) sheds light on the possible mechanisms for this luminescence.



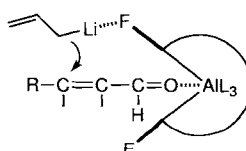
J. C. Vickery, M. M. Olmstead, E. Y. Fung,
 A. L. Balch* 1179–1181
 Solvent-Stimulated Luminescence from the
 Supramolecular Aggregation of a Tri-
 nuclear Gold(I) Complex that Displays
 Extensive Intermolecular Au···Au
 Interactions

The bowl-shaped reaction environment created by the Lewis acid aluminum tris(2,6-diphenylphenoxide) has been utilized as an efficient template in intramolecular radical cyclizations. The pathway and the stereoselectivity of the radical cyclization can be altered by using this template. A schematic representation of the transition state of the template-assisted reaction is shown on the right.



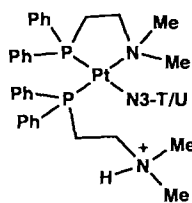
T. Ooi, Y. Hokke,
 K. Maruoka* 1181–1183
 Remarkable Template Effect of a Lewis
 Acidic Receptor in Intramolecular Radical
 Cyclizations

Success at last: The 1,4-allylation of α,β-unsaturated aldehydes with selectivities up to 95/5 and yields of 83% has been achieved thanks to the newly developed Lewis acidic receptor *p*-F-ATPH (L = 2,6-(*p*-FC₆H₄)₂C₆H₃O[−]). In addition to a coordination site for the aldehyde, this possesses an appropriate coordination site for a reactive nucleophile, as shown schematically on the right.



T. Ooi, Y. Kondo,
 K. Maruoka* 1183–1185
 Conjugate Allylation to α,β-Unsaturated
 Aldehydes with the New Chemzyme
p-F-ATPH

Novel chelate ring-opening occurs when cytotoxic bis(aminoethylphosphanyl)platinum(II) binds rapidly to the N3 atom of the DNA base thymine (T) and RNA base uracil (U) at pH 7 in the presence of chloride ions (depicted on the right). This is in contrast to cisplatin, which shows little binding to thymine or uracil under similar conditions, and thus opens the possibility for base-specific attack on DNA and RNA.

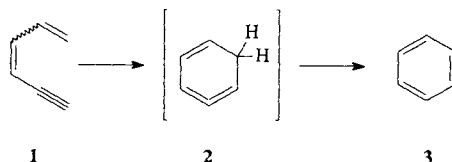


N. Margiotta, A. Habtemariam,
P. J. Sadler* 1185–1187

Strong, Rapid Binding of a Platinum Complex to Thymine and Uracil Under Physiological Conditions

Prototype of a new aromatization reaction:

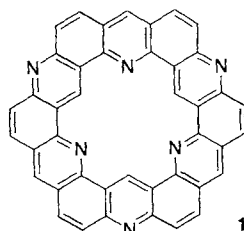
thermal rearrangement of 1,3-hexadiene-5-yne (**1**) to benzene (**3**) via isobenzene **2**, a highly reactive benzene isomer. Trapping experiments with styrene and the behavior of arenes containing **1** as a subunit indicate that this isomerization is also suitable for preparing condensed arenes and fullerene fragments.



H. Hopf,* H. Berger, G. Zimmermann,*
U. Nüchter, P. G. Jones,
I. Dix 1187–1190

Formation of Isobenzenes by Thermal Isomerization of 1,3-hexadiene-5-yne Derivatives

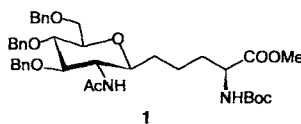
Blue fluorescence is exhibited by the hexaazakekulene **1**, the first fully aromatic heteroanalogue of kekulene. It was synthesized in four steps from formaldehyde and proflavine (3,6-diaminoacridine). Although **1** is insoluble in organic solvents, it is slightly soluble in strong acids such as methanesulfonic or trifluoroacetic acid—probably due to protonation.



A. Tatibouët, R. Hancock,
M. Demeunynck,*
J. Lhomme 1190–1191

Synthesis of 3,9,15,19,21,23-Hexaazakekulene

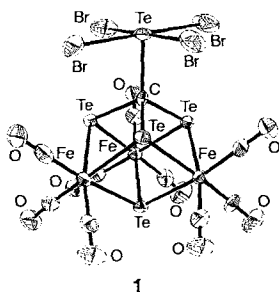
The orthogonally protected glycosylated amino acid building block 1 for the synthesis of peptidomimetics was prepared by the coupling of an amino acid aldehyde with a glycosyl dianion of glucosamine. This new C-glycosylated amino acid displays an improved metabolic stability and thus an improved bioavailability because of the single carbon chain between the sugar residue and the amino acid and because of the C–C linkage at the anomeric center.



F. Burkhart, M. Hoffmann,
H. Kessler* 1191–1192

Stereoselective Synthesis of a C-Glycosidic Analog of N-Glucoasparagine

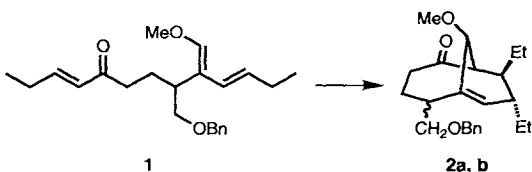
A carbide carbon atom as a vertex stabilized by coordination to the Lewis acid TeBr_4 is a feature of the cubane-like cluster **1** shown on the right. This complex, which is indefinitely stable in the solid state but dissolves only in DMSO—and then with rapid decomposition—is the ultimate product in the reaction between $[\text{Te}_2\text{Fe}_3(\text{CO})_9]$ and CBr_4 .



J. R. Eveland,
K. H. Whitmire* 1193–1194

Synthesis and Characterization of the Carbide Cubane Cluster $[\text{Fe}_3(\text{CO})_9\text{Te}_4(\mu_3\text{-CTeBr}_4)]$ with an Unusual Tetrahedral CTe_4 Unit

New lead compounds with promising biological activity are represented by CP-225,917 and CP-263,114. An approach based on an intramolecular Diels–Alder reaction for the total synthesis of these compounds is exemplified by the synthesis of racemic bicyclo[4.3.1]dec-1(9),4-dienes **2a, b** from triene **1**.

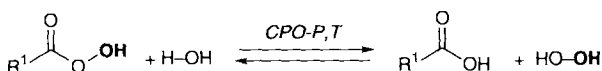
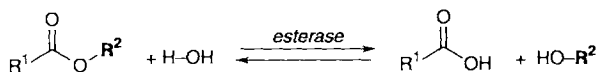


K. C. Nicolaou,* M. W. Härter,
L. Boulton, B. Jandeleit 1194–1196

Synthesis of the Bicyclic Core of CP-225,917 and CP-263,114 by an Intramolecular Diels–Alder Reaction

How does the catalytic set-up of a hydrolase activate H_2O_2 for enzymatic oxidations?

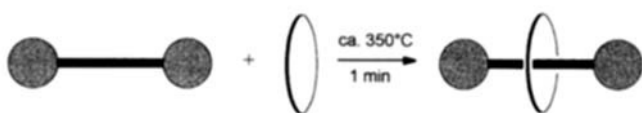
The oxidizing species is a peracid, as these studies with the metal-free haloperoxidases CPO-P and CPO-T clearly show. The analogy between the hydrolase and haloperoxidase reactions is elucidated in the reactions below.



M. Picard, J. Gross, E. Lübbert,
S. Tölzer, S. Krauss, K.-H. van Pée,
A. Berkessel* 1196–1199

Metal-Free Bacterial Haloperoxidases as
Unusual Hydrolases: Activation of H_2O_2
by the Formation of Peracetic Acid

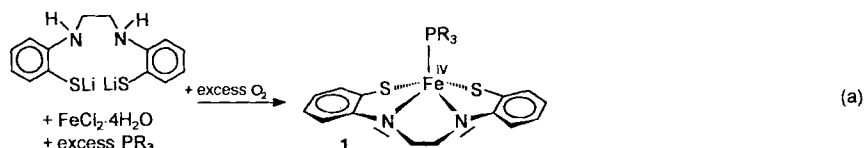
Fast and simple: Rotaxanes and pseudorotaxanes are synthesized by simply melting their wheel and axle components for one minute. The complementarity between the cavity of the wheel and the spatial demands of the stopper groups was designed to permit a temperature-controlled “slipping off” process in solution.



M. Händel, M. Plevoets, S. Gestermann,
F. Vögtle* 1199–1201

Synthesis of Rotaxanes by Brief Melting of
Wheel and Axle Components

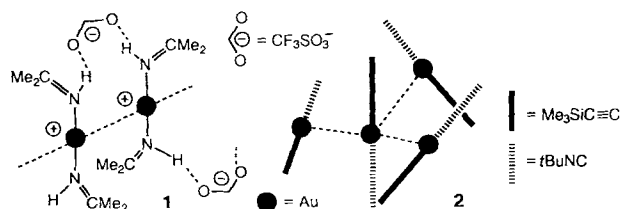
A simple one-pot reaction with readily accessible compounds [Eq. (a)] provides a route to high-valent molecular Fe^{IV} complexes with a N/S/P coordination sphere. The Fe^{IV} character of the metal center, which is stabilized by π -donor bonds from the lone pairs of electrons of the amide N and thiolate S donors, is confirmed by spectroscopic and structural data of **1** ($\text{R} = n\text{Pr}$). The L^4 ligand is “innocent”!



D. Sellmann,* S. Emig, F. W. Heinemann,
F. Knoch 1201–1203

A Convenient Way to Novel Fe^{IV} Com-
plexes with Mixed N/S/P Coordination
Spheres and “Innocent” Ligands

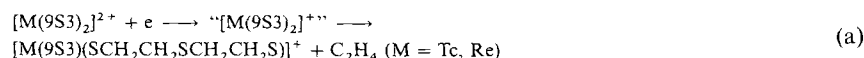
Two new types of gold–gold interactions are described. Crystals of **1** contain polymer-ic chains with short contacts between cationic gold centers, while in **2** one gold atom is coordinated nearly trigonally by three others.



J. Vicente,* M.-T. Chicote,*
M.-D. Abrisqueta, R. Guerrero,
P. G. Jones* 1203–1205

New Motifs in Aurophilic Self-Assembly:
Synthesis and Structures of
[Au(NH=CMe₂)₂]₂CF₃SO₃ and
[Au(C≡CSiMe₃)(CN*t*Bu)]

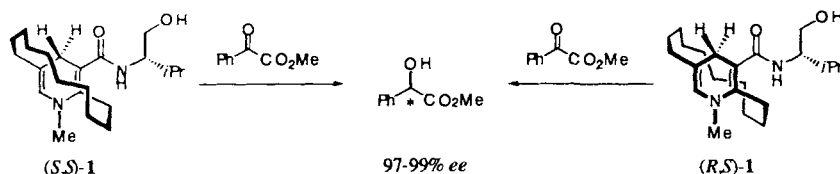
The trends in carbon–sulfur bond length for complexes of 1,4,7-trithiacyclononane (9S3) provide compelling evidence that C–S σ^* orbitals accept π -electron density from the metal. As the metal d-orbital energy and occupancy increase, this leads ultimately to cleavage of the C–S bonds with concomitant release of ethene in the Re and Tc complexes [Eq. (a)].



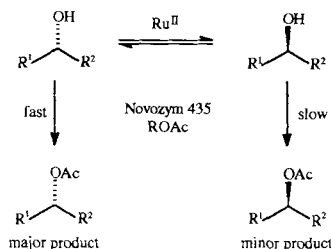
G. E. D. Mullen, M. J. Went,
S. Wocadlo, A. K. Powell,
P. J. Blower* 1205–1207

Electron Transfer Induced C–S Bond
Cleavage in Rhenium and Technetium
Thioether Complexes: Structural and
Chemical Evidence for π Back-Donation to
C–S σ^* Orbitals

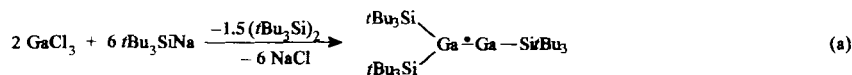
Biomimetic reduction of benzoylformate to mandelate with 97–99% *ee* was achieved with the diastereomeric, bridged NADH models (*S,S*)-**1** and (*R,S*)-**1**. The oligomethylene bridge acts as an “enzyme wall” and hinders the approach of the substrate from one side of the dihydropyridine ring. Isomers **1** were synthesized from the corresponding bridged nicotinate precursor, which was prepared by the reaction of formyl-substituted (vinylimino)phosphorane with methyl propiolate.



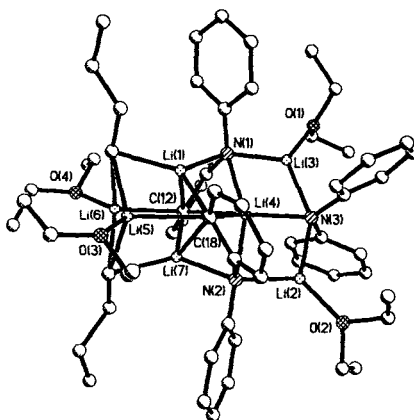
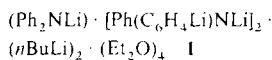
A specifically designed acyl donor, an efficient enzyme, and a stable and reliable ruthenium catalyst are fundamental for the resolution of the racemic alcohols described here (see scheme on the right). For $R^1 = \text{Ph}$ and $R^2 = \text{Me}$, 100% conversion into the corresponding acetate was achieved with greater than 99.5% *ee*.



Blue-black trisupersilyldigallanyl, a new metastable inorganic radical, forms in the reaction of GaCl_3 with $t\text{Bu}_3\text{SiNa}$ in pentane at room temperature according to Equation (a). The X-ray structure analysis reveals that it contains a planar $\text{Si}_2\text{Ga}^{\text{II}}\text{Ga}^{\text{I}}\text{Si}$ and a nearly linear $\text{Ga}^{\text{II}}\text{Ga}^{\text{I}}\text{Si}$ framework; according to the ESR spectrum the unpaired electron resides on both Ga atoms. Surprisingly, the analogous reaction of AlCl_3 and $t\text{Bu}_3\text{SiNa}$ (Al instead of Ga in Equation (a)) does not lead to trisupersilyldigallanyl, but to red tetrasupersilyldigallane ($t\text{Bu}_3\text{Si})_2\text{Al}-\text{Al}(\text{Si}t\text{Bu}_3)_2$.



What lithiates what? In a reaction between Ph_3NH and excess $n\text{BuLi}$ the aggregate **1** comprising $n\text{BuLi}$, monolithiated amine, and doubly lithiated amine units forms. The structure (see picture) raises interesting questions about lithiation reaction mechanisms.



N. Kanomata,* T. Nakata ... 1207–1211

Highly Enantioselective Reduction with Novel, Bridged NADH Models

A. L. E. Larsson, B. A. Persson, J.-E. Bäckvall* ... 1211–1212

Enzymatic Resolution of Alcohols Coupled with Ruthenium-Catalyzed Racemization of the Substrate Alcohol

N. Wiberg,* K. Amelunxen, H. Nöth, H. Schwenk, W. Kaim, A. Klein, T. Scheiring ... 1213–1215

Tris(*tert*-butylsilyl)digallanyl ($t\text{Bu}_3\text{Si})_3\text{Ga}_2$: A New Type of Compound for a Heavy Group 13 Element

R. P. Davies, P. R. Raithby, R. Snaith* ... 1215–1217

Lithiation of a Simple Amine with a Large Excess of *n*-Butyllithium: The Remarkable Product $(\text{Ph}_2\text{NLi}) \cdot [\text{Ph}(\text{C}_6\text{H}_4\text{Li})\text{NLi}]_2 \cdot (n\text{BuLi})_2 \cdot (\text{Et}_2\text{O})_4$

* Author to whom correspondence should be addressed

BOOKS

| | | |
|---|-----------------------------|------|
| Data Analysis for Chemists. Applications to QSAR and Chemical Products Design · D. Livingstone | <i>R. Fleischer</i> | 1219 |
| Photochemistry · C. E. Wayne, R. P. Wayne | <i>M. Oelgemöller</i> | 1219 |
| Electrochemical Phase Formation and Growth · E. Budevski, G. Staikov, W. J. Lorenz | <i>K. E. Heusler</i> | 1220 |
| The Chemistry of C-Glycosides · D. E. Levy, C. Tang | <i>G. Lemanski</i> | 1221 |

German versions of all reviews, communications, and highlights in this issue appear in the first June issue of *Angewandte Chemie*. The appropriate page numbers can be found at the end of each article and are also included in the Author Index on p. 1223.

All the Tables of Contents from 1995 onwards may be found on the WWW under:
<http://www.vchgroup.de/home/angewandte>

SERVICES

| | |
|------------------|------|
| • • Keywords | 1222 |
| • • Author Index | 1223 |
| • • Preview | 1224 |

ANGEWANDTE CHEMIE

A Journal of the
Gesellschaft
Deutscher Chemiker

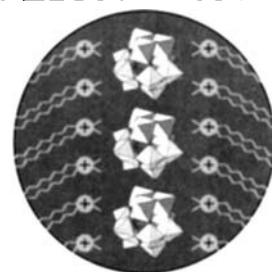
International Edition in English

1997
36/10

Pages 1021–1132

COVER PICTURE

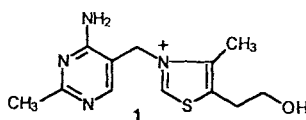
The cover picture shows a representation of organic–inorganic films containing well-organized layers of a polyoxometalate Keggin anion and a cationic surfactant. This new kind of supramolecular assembly has been obtained by using the Langmuir–Blodgett technique, and, considering the photochemical, electrochromic, magnetic, and catalytic properties associated with these metal-oxide clusters, it opens a wide range of new possibilities for applications. More about these organic–inorganic films is reported by E. Coronado and C. Mingotaud et al. on pages 1114ff.



REVIEWS

Contents

Even though more than half a century has elapsed since the isolation of Vitamin B₁ (thiamin, **1**), the determination of its structure, and the elucidation of its biochemical function, present day understanding of its biosynthesis is still incomplete. This review summarizes the current state of knowledge of thiamin biosynthesis, based on investigations with isotopic tracers and on genetic studies.



I. D. Spenser,* R. L. White ... 1032–1046

Biosynthesis of Vitamin B₁ (Thiamin):
An Instance of Biochemical Diversity

Less apodictic! That homogeneous and heterogeneous catalysis will be better integrated with one another in the future is certain when one peruses the developments of the past few years. Tailor-made homogeneous and surface-bound catalysts, multiple-component catalysts, and electroenzymatic processes are just a few of the advances that will bridge the gap between the “two cultures”. An approach to unification can be seen in research as well as industry. Catalysis is a central theme in chemical research.

W. A. Herrmann,*
B. Cornils* 1049–1067

Organometallic Homogeneous Catalysis—
Quo vadis?

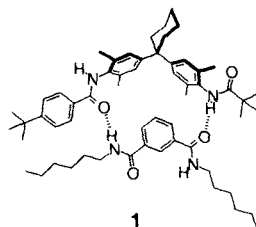
Orthogonal and native chemical ligation are two terms for a novel method for synthesizing proteins. It is particularly useful where molecular biology techniques fail, for example, for the synthesis of analogs of natural proteins from unnatural building blocks. Since this innovative method proceeds without carboxyl-group activation or side-chain protection, it is very easy to use and will find application by the average organic chemist.

M. A. Walker* 1069–1071

Protein Synthesis by Chemical Ligation of Unprotected Peptides in Aqueous Solution

CORRESPONDENCE

How can meaningful values be determined for the energies of weak interactions? That this is not a trivial question is revealed by the printed correspondence, which is concerned with the correct choice of model and method for the analysis of π - π interactions between aromatic rings with the help of complexes such as **1**.

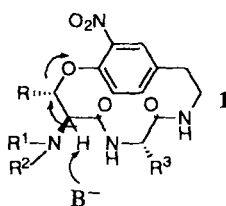


H.-J. Schneider* 1072–1073

C. Hunter* 1073

Requirements for Quantifications of Weak Intermolecular Interactions from Equilibrium Studies with Supramolecular Complexes

Fourteen-membered cyclopeptides are strained (J. Zhu) or only rigid (U. Schmidt) and therefore difficult to prepare. However, in the opinion of U. Schmidt the degree of novelty of the work by Zhu et al. is less than the latter claim, while Zhu regards their success in avoiding the ring opening of **1** by an attack of a base as a remarkable feature of their synthesis.



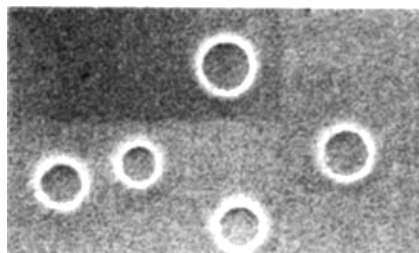
U. Schmidt* 1074

J. Zhu* 1074–1075

A Novel Strategy towards the Total Synthesis of Cyclopeptide Alkaloids

COMMUNICATIONS

Thousands of individual metal nanocrystals with a diameter of 2.5 nm form the five particle rings shown in the transmission electron microscope image on the right. Each ring has a diameter of about 1 μ m. The experimental and theoretical explanation for these rings are discussed.



P. C. Ohara, J. R. Heath,*

W. M. Gelbart* 1078–1080

Self-Assembly of Submicrometer Rings of Particles from Solutions of Nanoparticles

How can patterned thin films of nanocrystals be self-assembled? This contribution describes a general strategy that combines biochemical and lithographic techniques to restrict the assembly of nanocrystals to parts of a surface previously exposed to UV/Vis irradiation. The scanning electron microscope image on the right shows a pattern of gold nanoparticles assembled on a silicon substrate.

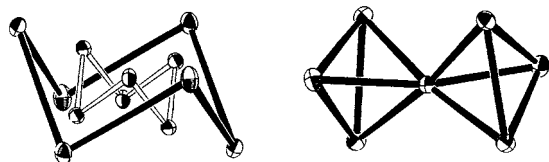


T. Vossmeier, E. DeIonno,

J. R. Heath* 1080–1083

Light-Directed Assembly of Nanoparticles

A chair-within-a-chair arrangement of the twelve copper atoms (bottom left) is characteristic of one of the complexes reported here; the other complex features two Cu tetrahedra sharing a common vertex (bottom right). Both were isolated from the reaction mixture $[\text{Cu}_2(\text{O}_2\text{CMe})_4(\text{H}_2\text{O})_2]/(\text{py})_2\text{CO}$ in MeCN. Magnetic susceptibility data show that the heptanuclear complex has an $S = 1/2$ ground state.

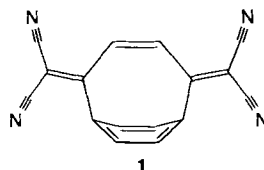


V. Tangoulis, C. P. Raptopoulou, S. Paschalidou, E. G. Bakalbassis,*

S. P. Perlepes,* A. Terzis* 1083–1085

The $[\text{Cu}_2(\text{O}_2\text{CMe})_4(\text{H}_2\text{O})_2]/(\text{py})_2\text{CO}$ System as the Source of an Unusual Heptanuclear Complex and a Novel Dodecanuclear "Flywheel" Cluster

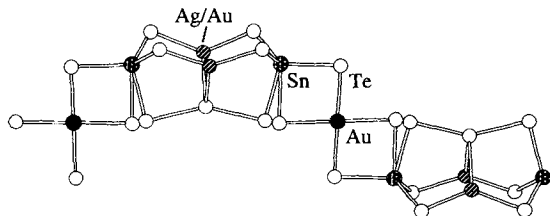
The benzene ring is nonplanar but sustains significant aromatic ring current in [4]paracyclophane **1**. The strained skeleton of this molecule was kinetically stabilized by substituents, which permitted the measurement of the ^1H NMR spectrum of a [4]paracyclophane for the first time.



M. Okuyama, T. Tsuji* 1085–1087

Kinetically Stabilized [4]Paracyclophane—The 1,4-Bis(dicyanomethylene)-2-ene Derivative: ^1H NMR Measurement and Assessment of its Diatropicity

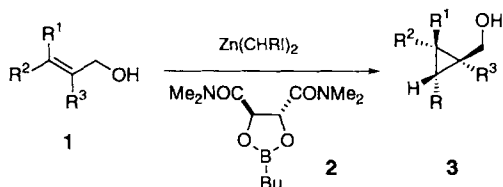
Metal atoms in isolated chains are the sole components of the first quaternary Zintl anion $[\text{Au}(\text{Ag}_{1-x}\text{Au}_x)_2\text{Sn}_2\text{Te}_9]^{4-}$ ($x = 0.32$; structure of depicted below) in the compound $(\text{Et}_4\text{N})_4[\text{Au}(\text{Ag}_{1-x}\text{Au}_x)_2\text{Sn}_2\text{Te}_9]$. Electronic structure calculations and the diamagnetic and semiconducting properties of this new compound show that the anion displays a Peierls distortion at room temperature.



S. S. Dhingra, D.-K. Seo, G. R. Kowach, R. K. Kremer, J. L. Shreeve-Keyer, R. C. Haushalter,*
M.-H. Whangbo* 1087–1090

One-Dimensional Semiconducting Chains of the Quaternary Zintl Anion in $(\text{Et}_4\text{N})_4[\text{Au}(\text{Ag}_{1-x}\text{Au}_x)_2\text{Sn}_2\text{Te}_9]$

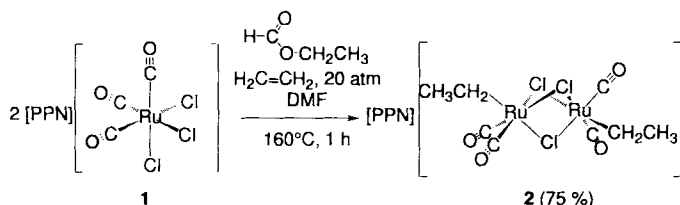
Substituted, functionalized iodoalkylzinc reagents in combination with the chiral dioxaborolane **2** give excellent diastereo- and enantiomeric selectivities in cyclopropanations when substituted allyl alcohols **1** ($\text{R}^1 = \text{H}, \text{Et}, \text{CH}_2\text{OBn}$; $\text{R}^2 = \text{H}, \text{Ph}, n\text{Pr}$; $\text{R}^3 = \text{H}, \text{Me}$) are used as starting materials and CH_2Cl_2 as solvent. This efficient preparation of chiral, nonracemic 1,2,3-trisubstituted cyclopropanes **3** might be useful in natural product synthesis.



A. B. Charette,* J. Lemay 1090–1092

Diastereo- and Enantioselective Synthesis of 1,2,3-Substituted Cyclopropanes with Zinc Carbenoids

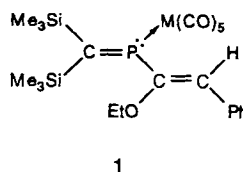
An unusual migration of the alkyl group away from the C–O bond of added formate leads to strictly stereospecific formation of the stable ethyl complex **2** when the catalytic addition of ethyl formate to ethylene (catalyst = **1**) is terminated by freezing. Both ethylene and the alkyl formate act as sources of the alkyl groups and can thus be used for C–C bond-forming reactions below ambient temperature. $\text{PPN}^+ = (\text{Ph}_3\text{P})_2\text{N}^+$.



S. Fabre, P. Kalck,*
G. Lavigne* 1092–1095

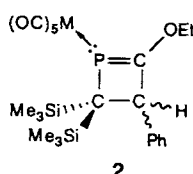
Generation of Alkyl(dicarbonyl)(chloro)-ruthenium Dimers in the Ruthenium-Catalyzed Addition of Alkyl Formates to Ethylene

Unexpected reactivity of in situ generated carbene complex anions is seen upon treatment with a *P*-chloro(methylene)phosphane. A stereoselective P–C coupling reaction provides the η^1 -2-phosphabutadiene complexes **1a,b**. Thermal isomerization of these compounds leads to the novel η^1 -2,3-dihydrophosphete complexes **2a,b**. **a**: $\text{M} = \text{Cr}$; **b**: $\text{M} = \text{W}$.

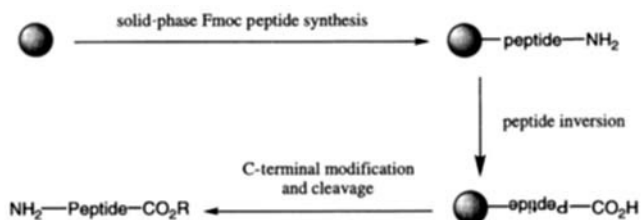


R. Streubel,* M. Hobbold, J. Jeske, P. G. Jones 1095–1097

Stereoselective Synthesis and Isomerization of η^1 -2-Phosphabutadiene Complexes to η^1 -2,3-Dihydrophosphete Complexes



Conventional solid-phase synthesis and a novel inversion step allows ready access to peptides modified at the C-terminus (the principle is outlined below). These compounds have important biological roles and a wide range of applications in research.

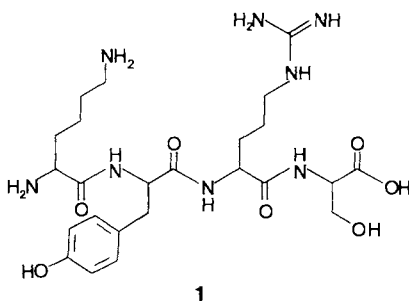


M. Davies, M. Bradley* 1097–1099

C-Terminally Modified Peptides and Peptide Libraries—Another End to Peptide Synthesis

Not possible with chemical methods:

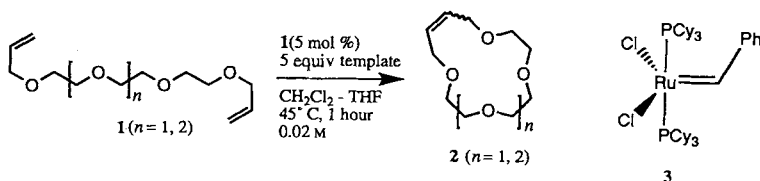
Protein synthesis from the N- to C-terminus using the reverse hydrolysis potential of proteases was accomplished for the model peptide **1**. The stereo- and regiospecificity of the enzymes used ensured integrity of the stereogenic center and allowed ecological reaction conditions without side-chain protection.



F. Bordusa, D. Ullmann, H.-D. Jakubke* 1099–1101

Protease-Catalyzed Peptide Synthesis from N- to C-Terminus: An Advantageous Strategy

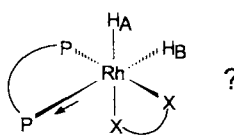
A highly efficient combination: template directing and olefin metathesis. The polyether dienes **1** react in good yields to give crown ethers **2** in the presence of LiClO_4 and the Ru catalyst **3** (Cy = cyclohexyl). Ring-opening metathesis polymerization (ROMP) of the cyclic olefins **2** results in polymers that are capable of regenerating **2** by template-directed methathesis depolymerization.



M. J. Marsella, H. D. Maynard, R. H. Grubbs* 1101–1103

Template-Directed Ring-Closing Metathesis: Synthesis and Polymerization of Unsaturated Crown Ether Analogs

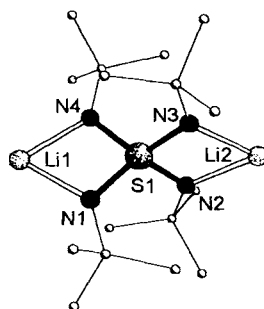
The PHIP-NMR method (PHIP = parahydrogen-induced polarization) can be used to detect dihydride catalyst–substrate complexes of the general formula $[\text{Rh}(\text{P}-\text{P})(\text{X}-\text{X})(\text{H})_2]\text{BF}_4$ (shown on the right, X–X = dimethyl itaconate as substrate), which are formed in situ under hydrogenation conditions with chiral bis(phosphinite)rhodium(I) catalysts. Remarkable is the absence of typical $(\text{H}, \text{P})_{\text{trans}}$ coupling ($^2J(\text{H}, \text{P})_{\text{trans}}$); the Rh–P bond *trans* to H_B is therefore lengthened, and the octahedral geometry distorted.



A. Harthun, R. Kadyrov, R. Selke,* J. Bargon* 1103–1105

Proof of Chiral Dihydride Complexes Including Catalyst and Substrate during the Bis(phosphinite)rhodium(I)-Catalyzed Hydrogenation of Dimethyl Itaconate

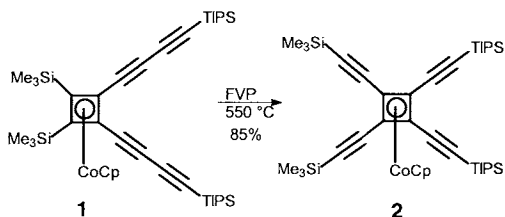
The nitrogen analogue of the sulfate ion, tetraimidosulfate $\text{S}(\text{NR})_4^{2-}$ is easily accessible from $\text{S}(\text{NR})_3$ and $\text{LiN}(\text{H})\text{R}$. $\text{S}(\text{NR})_3$ can be prepared from $\text{S}(\text{NR})_2$ and $\text{LiN}(\text{H})\text{R}$ by oxidation of the resulting $[\text{Li}_2(\text{NR})_3\text{S}]_2$ with bromine or iodine. In an addition reaction organolithium compounds and $\text{S}(\text{NR})_3$ yield the related triimidosulfonate $\text{RS}(\text{NR})_3^-$. Both anions form molecular contact ion pairs with lithium cations (structure of $\text{S}(\text{NR})_4^{2-}$ shown on the right, the thf ligands on Li1 and Li2 have been omitted), which makes them promising ligands in coordination chemistry.



R. Fleischer, A. Rothenberger, D. Stalke* 1105–1107

$\text{S}(\text{N}^t\text{Bu})_4^{2-}$: A Dianion Isoelectronic to SO_4^{2-} and the Related $\text{MeS}(\text{N}^t\text{Bu})_3^-$

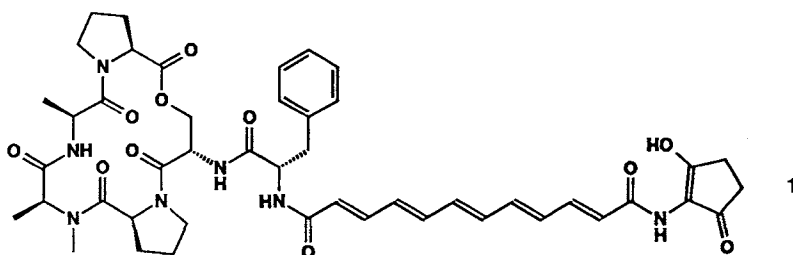
Conditions of flash vacuum pyrolysis (FVP) result in the conversion of bisdiyne **1** into the complexed, tetraethynylated cyclobutadiene **2**, which is isolated as the sole product in high yield. Complex **2** can be deprotected, and both the partially as well as the fully deprotected, complexed, tetraethynylated cyclobutadienes are stable under ambient conditions. TIPS = triisopropylsilyl.



M. Altmann, G. Roidl, V. Enkelmann,
U. H. F. Bunz* 1107–1109

A Restitutive Bergman Rearrangement:
Synthesis of a CpCo-Complexed, Tetra-
ethynylated Cyclobutadiene

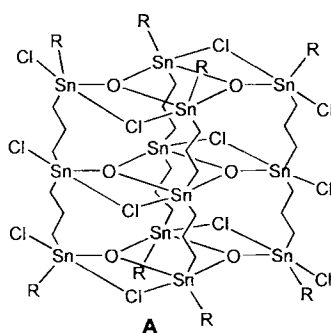
A cyclopeptolide, a polyene, and an aminoreductone—species with completely different biogenetic origins—are the components of the antibiotically active natural product enopeptin B (**1**, see schematic representation below), which is particularly active against *Staphylococcus aureus*. The first total synthesis of this compound, which belongs to a new class of substances, was achieved by the clever use of the arsenal of methods available to modern peptide chemistry. The three basic units were coupled by two different routes.



U. Schmidt,* K. Neumann,
A. Schumacher,
S. Weinbrenner 1110–1112

Synthesis of Enopeptin B from *Strepto-*
myces sp RK-1051

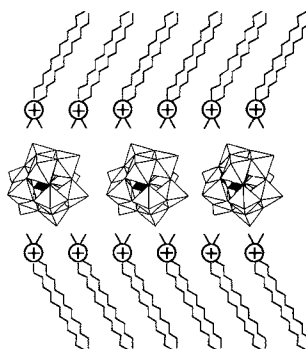
Pillar-shaped organostannoxanes with the first triple-ladder structure of type **A** are obtained in almost quantitative yield by reaction of the tritin compound $[RCl_2Sn(CH_2)_3]_2SnCl_2$ with $(tBu_2SnO)_3$. In contrast, treating $[RCl_2Sn(CH_2)_3SnCl_2(CH_2)_2SiMe_3]$ with $(tBu_2SnO)_3$ affords an organostannoxane with a folded double-ladder structure. $R = CH_2SiMe_3$.



M. Mehring, M. Schürmann,
H. Reuter, D. Dakternieks,
K. Jurkschat* 1112–1114

Trimethylene-Bridged Tri- and Tetra-
tin Compounds as Building Blocks for
Unusual Double and Triple Ladders

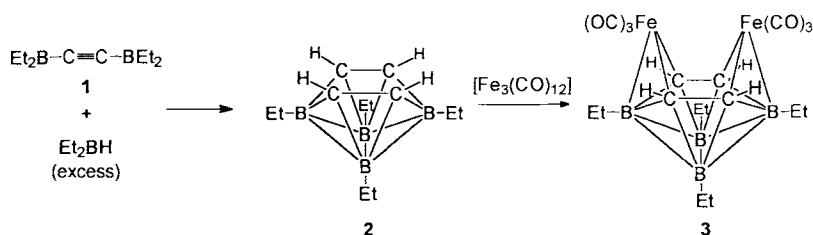
A new method for the synthesis of inorganic–organic composites with promising properties is the incorporation of polyoxometalates into well-ordered organic films by the Langmuir–Blodgett (LB) method. The structure of such an LB film is depicted schematically on the right.



M. Clemente-León, C. Mingotaud,*
B. Agricole, C. J. Gómez-García,
E. Coronado,* P. Delhaès 1114–1116

Application of the Langmuir–Blodgett
Technique to Polyoxometalates: Towards
New Magnetic Films

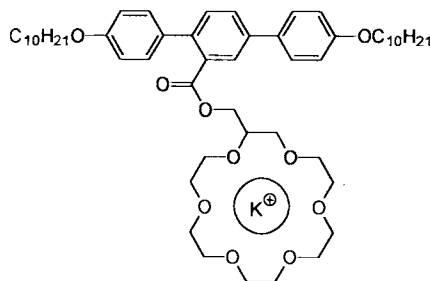
The first polyborane with six heteroatoms (3) is formed when the new tetracarba-*nido*-octaborane(8) (2), readily available by the reaction of **1** with Et_2BH , reacts with $[\text{Fe}_3(\text{CO})_{12}]$.



B. Wrackmeyer,* H.-J. Schanz,
W. Milius 1117–1119

A New Route to Tetracarba-*nido*-octaboranes(8); Molecular Structure of a 6,9-Diferra-5,7,8,10-tetracarba-*nido*-decaborane(10) Derivative

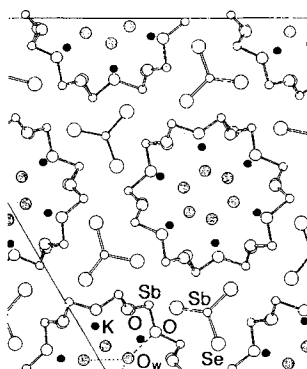
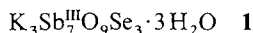
Rodlike 4,4''-didecyloxy-*p*-terphenyl derivatives with a laterally attached [18]crown-6 moiety form columnar, liquid-crystalline phases in the presence of aqueous potassium salt solutions. The building block is shown on the right.



J. A. Schröter, C. Tschierske,*
M. Wittenberg,
J. H. Wendorff 1119–1121

Liquid-Crystalline Crown Ether: Forming Columnar Mesophases by Molecular Recognition

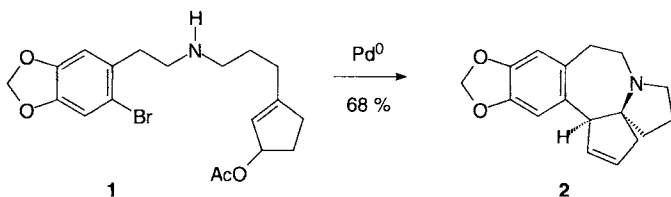
The natural mineral cetineite was prototype for the synthesis of the compound **1**. Its nanoporous, template-free host structure is an ideal object for numerous investigations. Electronic excitation and transport processes, for example, can be studied on this nanostructured semiconducting material. A part of the crystal structure is shown on the right.



U. Simon,* F. Schüth, S. Schunk,
X. Wang, F. Liebau 1121–1124

$\text{K}_3\text{Sb}_7^{\text{III}}\text{O}_9\text{Se}_3 \cdot 3\text{H}_2\text{O}$: The First Crystalline Nanoporous Material with a Photo-Semiconducting Host Structure

Interesting for cancer therapy: The unique pentacyclic alkaloid cephalotaxine is the parent compound of the strongly cytotoxic harringtonines, which are isolable from the south-east Asian yewtree. Now the cephalotaxine precursor **2** has been synthesized highly efficiently and selectively in two steps from the readily accessible amine **1** through an intramolecular Pd-catalyzed allylic amination to form the spirocycle (85% yield) and subsequent Heck reaction to construct the seven-membered ring (80% yield).



L. F. Tietze,* H. Schirok 1124–1125

Highly Efficient Synthesis of Cephalotaxine by Two Palladium-Catalyzed Cyclizations

* Author to whom correspondence should be addressed

BOOKS

| | |
|---|--------------------------------|
| Surface Analysis with STM and AFM · S. N. Magonow, M.-H. Whangbo | <i>W. Weiss</i> 1127 |
| X-ray Powder Diffractometry. An Introduction · R. Jenkins, R. L. Snyder | <i>R. J. Cernik</i> 1128 |
| Concise Chemical Thermodynamics · J. R. W. Warn, A. P. H. Peters | <i>J. A. Becker</i> 1129 |

German versions of all reviews, communications, and highlights in this issue appear in the first May issue of *Angewandte Chemie*. The appropriate page numbers can be found at the end of each article and are also included in the Author Index on p. 1131.

All the Tables of Contents from 1995 onwards may be found on the WWW under:
<http://www.vchgroup.de/home/angewandte>

SERVICES

| | |
|----------------|------|
| ● Sources | A-37 |
| ● Events | 1031 |
| ● Keywords | 1130 |
| ● Author Index | 1131 |
| ● Preview | 1132 |

ANGEWANDTE CHEMIE

A Journal of the
Gesellschaft
Deutscher Chemiker

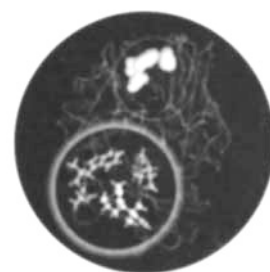
International Edition in English

1997
36/9

Pages 897–1020

COVER PICTURE

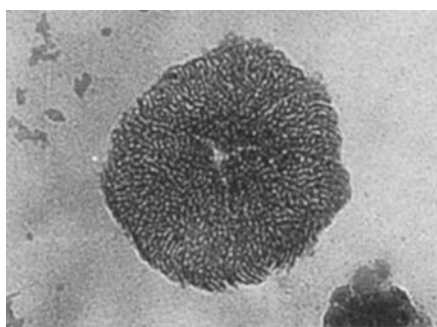
The cover picture shows a model of the binding of a protonated cyclopropane in a cation-binding site of an antibody. The larger circle gives an enlarged view of the actual binding of the organic intermediate. The aromatic and carboxylate groups are yellow, the organic intermediate silver, and the carbon atoms of the protonated cyclopropane red. The image was created with the programs Persistence of Vision and RasMol as well as proprietary software by Dr. Nicholas C. DeMello. More on the stabilization of cyclopropane intermediates is reported by J. K. Lee and K. N. Houk on pages 1003ff.



REVIEWS

Contents

Suitable handling of a delicate balance of van der Waals, hydrogen bonding, and electrostatic interaction allows the preorganization of matter on the nanometer scale and hence the controlled synthesis of functional colloids. This approach opens access to materials with unique properties or combinations of properties, and sometimes of great beauty. The picture shows

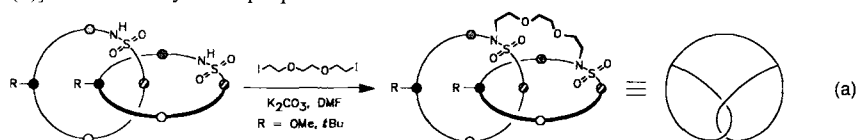


calcium carbonate "chrysanthemum particles" with a diameter of about 210 nm, which are grown in the presence of structure-regulating functional polymers.

M. Antonietti,* C. Göltner 910–928

Superstructures of Functional Colloids:
Chemistry on the Nanometer Scale

Prepared from simple diacid dichlorides and diamines, catenanes and rotaxanes, once thought exotic, can be synthesized in up to 40% yield, sometimes in one-step syntheses. The process of threading a stringlike molecule through a neutral template discovered in 1992 is supported by hydrogen bonding and π - π interactions. The quantities of these mechanically bonded molecules are sufficient for further preparative conversions; even complicated topologies like a "molecular pretzel" [Equation (a)] have already been prepared.

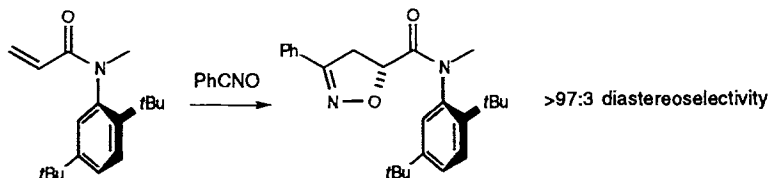


R. Jäger, F. Vögtle* 930–944

A New Synthetic Strategy towards
Molecules with Mechanical Bonds: Non-
ionic Template Synthesis of Amide-Linked
Catenanes and Rotaxanes

Noncrystalline organic photorefractive materials appear to be on the verge of widespread applications such as holographic storage and real-time holographic processing. The performance levels of these materials, which are attracting increasing interest, are close to, and in some respects even beyond those of their long-known inorganic counterparts.

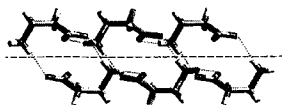
Commonly observed, but rarely exploited, is the restricted rotation about C—C single bonds inherent in certain non-biaryl compounds. Recent examples of stereoselective reactions directed by atropisomeric amides (such as that shown below) point the way to a future for these compounds as tools for asymmetric synthesis.



COMMUNICATIONS

The pitch of the columnar cholesteric mesophase formed by the dinucleoside phosphate d(GpG) and water becomes shorter after exposure to γ radiation. This effect can be measured directly with an optical microscope from the distance between the fingerprint lines. The inverse pitch is linearly correlated to the dose absorbed between 0 and 20 kGy.

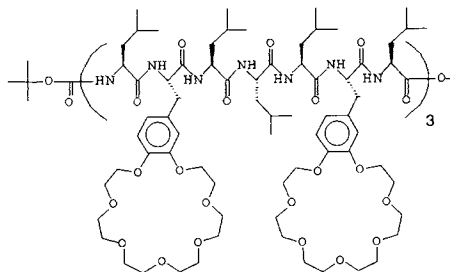
Cyclic, hydrogen-bonded dimers are shown to be the building blocks of α -glycine and of β -alanine crystals by atomic force microscopy and surface X-ray diffraction experiments on their growth and dissolution (one such unit of β -alanine is shown on the right). Both processes take place in steps of hydrogen-bonded bilayers.



An ordered layer of (S)-methionine is attached to the (0 $\bar{1}$ 0) face of α -glycine when the crystals are brought into contact with a saturated solution of glycine containing (S)-methionine as additive. The direct evidence was obtained by grazing incidence X-ray scattering experiments, which also indicated different behavior for the (010) and (0 $\bar{1}$ 0) faces. The concentration of the surface-bound methionine molecules was determined to be 4:1.

The ability of sense peptides (coded for by sense DNA) and corresponding antisense peptides (coded for by corresponding antisense DNA) to interact specifically was used to design antisense peptide inhibitors of interleukin-1 isoforms IL-1 β and IL-1 α . These inhibitors appear to act as "mini receptors", binding to both isoforms and thereby sterically blocking the normal interaction between interleukin-1 and its receptors.

An artificial ion channel active in planar lipid membranes: the 21 amino acid peptide **1** mimics the K⁺ ion transport ability of natural ion-channel proteins. Peptide **1** assumes an α -helical conformation in the membrane, and its crown ether units are aligned to form a polar passageway for ions across the lipid bilayer.



K. Meerholz* 945–948

Amorphous Plastics Pave the Way to Widespread Holographic Applications

J. Clayden* 949–951

Non-Biaryl Atropisomers: New Classes of Chiral Reagents, Auxiliaries, and Ligands?

F. M. H. de Groot, G. Gottarelli,*
S. Masiero, G. Proni, G. P. Spada,
N. Dolci 954–955

Towards Radiation-Sensitive Quasi-Biological Display

D. Gidalevitz, R. Feidenhansl,* S. Matlis,
D. M. Smilgies, M. J. Christensen,
L. Leiserowitz* 955–959

Monitoring In Situ Growth and Dissolution of Molecular Crystals: Towards Determination of the Growth Units

D. Gidalevitz, R. Feidenhansl,
L. Leiserowitz* 959–962

Surface X-ray Scattering Study of Stereospecific Adsorption of Additives onto the Surface of a Molecular Crystal Grown from Solution

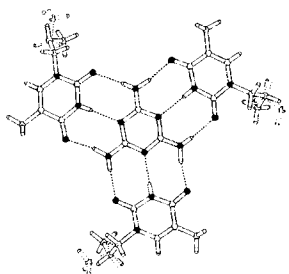
J. W. Davids, A. El-Bakri, J. Heal,
G. Christie, G. W. Roberts, J. G. Raynes,
A. D. Miller* 962–967

Design of Antisense (Complementary) Peptides as Selective Inhibitors of Cytokine Interleukin-1

J.-C. Meillon, N. Voyer* 967–969

A Synthetic Transmembrane Channel Active in Lipid Bilayers

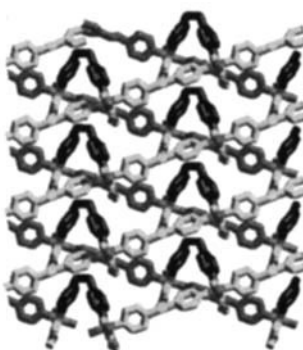
A defined melamine–imide ratio in cocrystals can be selected by changing the steric hindrance around the hydrogen-bond acceptor sites of the imides. Crystalline 1:1, 1:2, and 1:3 complexes of melamine may thus be obtained with succinimide, glutarimide, and 1-*N*-propylthymine (see picture), respectively.



R. F. M. Lange, F. H. Beijer,
R. P. Sijbesma, R. W. W. Hoofst,
H. Kooijman, A. L. Spek, J. Kroon,
E. W. Meijer* 969–971

Crystal Engineering of Melamine–Imide
Complexes; Tuning the Stoichiometry by
Steric Hindrance of the Imide Carbonyl
Groups

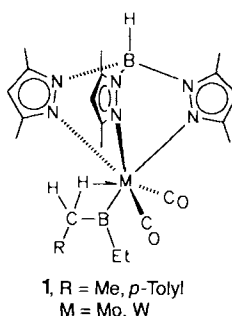
Bilayers or open-framework ladder structure? Which supramolecular isomer is formed from $\text{Co}(\text{NO}_3)_2$ and the nonrigid spacer 1,2-bis(2-pyridyl)ethane depends on the crystallization conditions. The open-framework coordination polymer contains large, square cavities of $10 \times 10 \text{ \AA}$. A section of the bilayer motif is shown on the right.



T. L. Hennigar, D. C. MacQuarrie,
P. Losier, R. D. Rogers,
M. J. Zaworotko* 972–973

Supramolecular Isomerism in Coordination
Polymers: Conformational Freedom
of Ligands in $[\text{Co}(\text{NO}_3)_2(1,2\text{-bis}(4\text{-pyridyl})\text{-ethane})_{1.5}]_n$

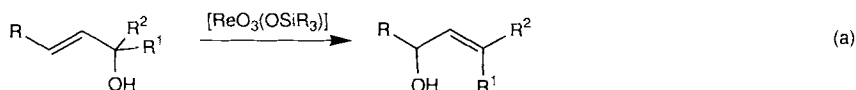
At first glance, the products **1** obtained from the hydroboration of some Fischer carbyne complexes are rather unexpected. They are of interest, not only because of the agostic interaction, but also because X-ray crystallographic and spectroscopic findings point to considerable multiple-bond character of the $\text{M}–\text{B}$ bonds.



H. Wadehoff,* U. Arnold,
H. Pritzkow 974–976

Synthesis of Boryl Metal Complexes with
Additional Agostic Stabilization by Hydro-
boration of Fischer Carbyne Complexes

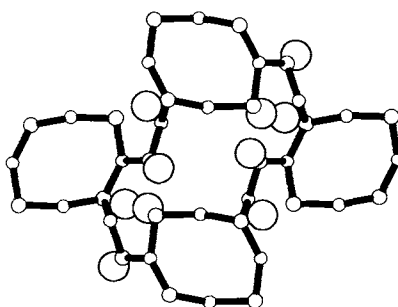
The catalytic isomerization of allyl alcohols by a 1,3-OH shift can be carried out very rapidly in the presence of $[\text{ReO}_3\text{OSiR}_3]$ catalysts at 25°C or below [Eq. (a)]. Kinetic studies suggest that the rearrangement takes place via a cyclic transition state involving a $\text{Re}=\text{O}$ group. R = Me, Ph.



S. Bellemin-Lapponnaz, H. Gisie,
J. Pierre Le Ny, J. A. Osborn* ... 976–978

Mechanistic Insights into the Very Efficient
 $[\text{ReO}_3\text{OSiR}_3]$ -Catalyzed Isomerization of
Allyl Alcohols

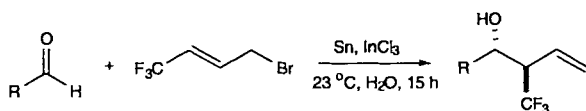
Colorless *en*- SnPO-1 , the title compound, crystallizes in the space group *Pnaa* and forms a network of alternating pyramidal SnO_3 and tetrahedral PO_4 moieties in which all the vertices are shared. The structure-directing agent, diprotonated ethylenediamine, is located in an eight-ring channel system. The Sn^{II} lone pairs protrude into a second channel system comprising squashed twenty-rings (see picture).



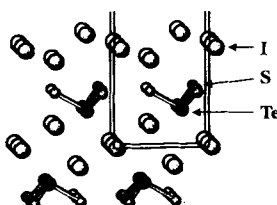
S. Natarajan, M. P. Attfield,
A. K. Cheetham* 978–980

$[\text{H}_3\text{N}(\text{CH}_2)_2\text{NH}_3]^{2+}[\text{Sn}_4\text{P}_3\text{O}_{12}]^-$:
An Open-Framework Tin(II) Phosphate

A tin-mediated, indium trichloride promoted allylation reaction provided β -trifluoromethylated homoallylic alcohols, the building blocks of biologically active substances, in high yields and excellent stereoselectivity (see below; R = H, Cy, Ar, COOH). Since the syntheses can be carried out in water, the reactive OH groups do not need to be protected, and even compounds that are insoluble in organic solvents can be used.



A description as a composite of Cu_2TeS_3 and CuI is possible for $(\text{CuI})_3\text{Cu}_2\text{TeS}_3$, the first representative of a series of compounds formed by complex chalcogenometalate ions and copper(I) halides. The $(\text{TeS}_3)^{2-}$ groups are oriented in parallel columns between layers of iodide ions (section of the crystal structure depicted on the right).



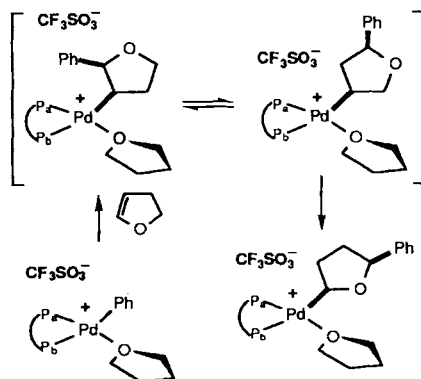
T.-P. Loh,* X.-R. Li 980–982

A Highly Stereoselective Synthesis of β -Tri-fluoromethylated Homoallylic Alcohols in Water

A. Pfitzner,* S. Zimmerer 982–984

$(\text{CuI})_3\text{Cu}_2\text{TeS}_3$: Layers of Cu_2TeS_3 in Copper(I) Iodide

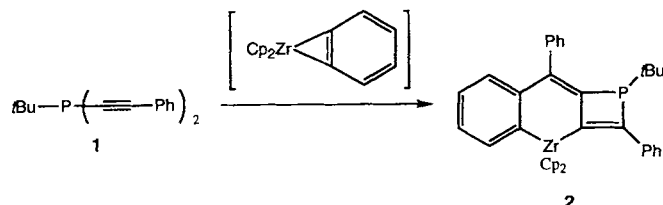
Double isomerization results in a Pd-alkyl compound with unexpected structure, which is stable until -40° , from the reaction of the Pd complex shown on the right with 2,3-dihydrofuran. The course of the asymmetric Heck reaction was followed by NMR spectroscopy. $\text{P}_a\text{P}_b = (S)$ -BINAP.



K. K. Hii, T. D. W. Claridge, J. M. Brown* 984–987

Intermediates in the Intermolecular, Asymmetric Heck Arylation of Dihydrofurans

The tricyclic zirconium complex 2 is formed when transient zirconocene-benzynes are allowed to react with bis(alkynyl)phosphane 1. Further reactions with 2 lead to mono- and tricyclic 1,2-dihydrophosphates.



L. Dupuis, N. Pirio, P. Meunier,* A. Igau, B. Donnadieu, J.-P. Majoral* 987–989

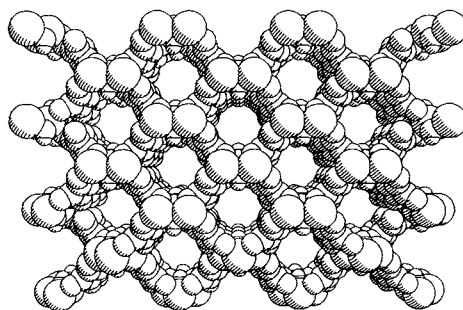
Zirconocene-Benzynes-Mediated Intramolecular Coupling of Bis(alkynyl)phosphane: A Way to Mono- and Tricyclic 1,2-Dihydrophosphates

Little or no Brønsted acidity is exhibited by the large-pore molecular sieve cloverite according to quantitative IR spectroscopic investigations. Only 3.5% of the expected 192 hydroxyl groups per unit cell suggested by the X-ray structure are detected.

F. Thibault-Starzyk, A. Janin, J.-C. Lavalley* 989–991

IR Spectroscopic Evidence for the Absence of Structural Hydroxyl Groups in Cloverite

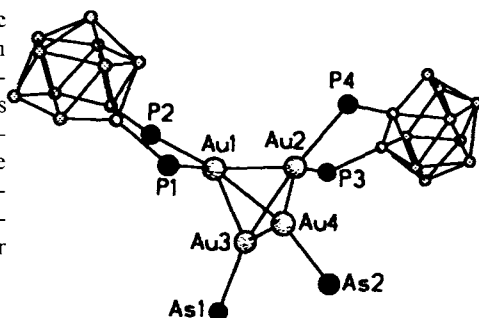
A cobalt hydroxide backbone with a structure reminiscent of that found in cobalt(II) hydroxide forms the basis of the framework of the title compound. The squarate ligands of this coordination solid link the metal hydroxide strips together and form the walls of channels with a diameter of approximately 7 Å.



S. O. H. Gutschke, M. Molinier, A. K. Powell, P. T. Wood* 991–992

Hydrothermal Synthesis of Microporous Transition Metal Squarates: Preparation and Structure of $[\text{Co}_3(\mu_3\text{-OH})_2(\text{C}_4\text{O}_4)_2] \cdot 3\text{H}_2\text{O}$

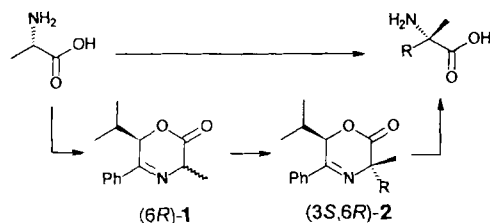
Depending on the stoichiometric ratio of the reactants, the reaction of $[\text{AuCl}(\text{AsPh}_3)]$ with $(\text{PPh}_2)_2\text{-C}_2\text{B}_{10}\text{H}_{10}$ in ethanol at reflux gives two very different compounds containing partially degraded carborane moieties: the four-coordinate complex $[\text{Au}\{(\text{PPh}_2)_2\text{C}_2\text{B}_9\text{H}_{10}\}\{(\text{PPh}_2)_2\text{-C}_2\text{B}_{10}\text{H}_{10}\}]$ or the novel gold cluster $[\text{Au}_4\{(\text{PPh}_2)_2\text{C}_2\text{B}_9\text{H}_{10}\}_2(\text{AsPh}_3)_2]$ (depicted on the right).



O. Crespo, M. C. Gimeno,
P. G. Jones, A. Laguna,*
M. D. Villacampa 993–995

Small Gold Clusters with Carborane Ligands: Synthesis and Structural Characterization of the Novel Compound $[\text{Au}_4\{(\text{PPh}_2)_2\text{C}_2\text{B}_9\text{H}_{10}\}_2(\text{AsPh}_3)_2]$

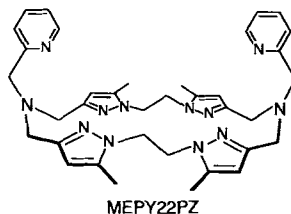
At room temperature already highly diastereoselective alkylation of the new, cyclic, chiral alanine ester derivatives (**6R**)-**1** can be achieved with either K_2CO_3 as base under solid–liquid phase-transfer catalysis or Pd catalysis under neutral conditions. The products (**3S,6R**)-**2** can be easily hydrolyzed to form (*S*)- α -methyl α -amino acids.



R. Chinchilla, L. R. Falvello,
N. Galindo, C. Nájera* 995–997

Asymmetric Synthesis of α -Methyl α -Amino Acids by Diastereoselective Alkylation of Optically Active 6-Isopropyl-3-methyl-2,3-dihydro-6*H*-1,4-oxazin-2-ones

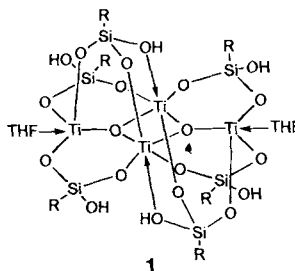
The protective pocket of hemocyanin is mimicked by the novel macrocyclic ligand MEPY22PZ (see schematic drawing on the right), which was used to make a $\text{Cu}_2\text{-O}_2$ adduct. Proper design of a ligand with azole donors connected by ethylene spacers illustrates how metal– O_2 adducts can be stabilized at ambient temperatures and in protic solvents. The purple *trans*- μ -1,2- $\text{Cu}^{\text{II}}\text{-O}_2\text{-Cu}^{\text{II}}$ species was obtained by oxygenation of the parent Cu^{I} compound and by addition of H_2O_2 and base to the dinuclear Cu^{II} complex.



J. E. Bol, W. L. Driessen,*
R. Y. N. Ho, B. Maase, L. Que, Jr.,*
J. Reedijk 998–1000

Dioxygen Binding at Ambient Temperature: Formation of a Novel Peroxodicopper(II) Complex with an Azole Macrocyclic Ligand

Titanosilicates with structural characteristics similar to those of many Ti-containing zeolites were synthesized from the reactions of (arylamino)silanetriol $[\text{RSi}(\text{OH})_3]$ with organometallic titanium precursors $[\text{Cp}^*\text{TiCl}_3]$, $\text{TiCl}_4 \cdot 2\text{THF}$, and $[\text{Cp}^*\text{TiMe}(\mu\text{-O})]_3$. The product of the reaction with $[\text{Cp}^*\text{TiCl}_3]$, **1**, is a soluble molecular silicate in which formal TiO_2 fragments are trapped inside. $\text{Cp}^* = \text{C}_5\text{Me}_5$; $\text{R} = (2,6\text{-iPr}_2\text{C}_6\text{H}_3)\text{NSiMe}_3$.



A. Voigt, R. Murugavel,
M. L. Montero, H. Wessel, F.-Q. Liu,
H. W. Roesky,* I. Usón, T. Albers,
E. Parisini 1001–1003

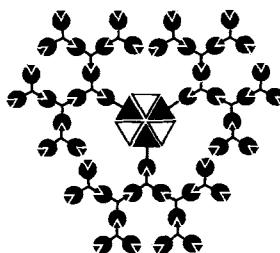
Soluble Molecular Titanosilicates

A nonclassical, protonated cyclopropane is the intermediate formed in an antibody-catalyzed cyclization reaction. The selectivity in favor of the cyclopropane product is increased upon binding of the catalytic antibody, which amplifies the inherent preference for one reaction pathway.

J. K. Lee, K. N. Houk* 1003–1005

Cation-Cyclization Selectivity: Variable Structures of Protonated Cyclopropanes and Selectivity Control by Catalytic Antibodies

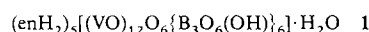
Rosettes that are held together by hydrogen bonds (see sketch on the right) were synthesized from metallodendrimers constructed by coordination chemistry. Two orthogonal, noncovalent interactions (metal–ligand and hydrogen bonding) were employed to build these nanosized dendrimers ($M \approx 7\text{--}28\text{ kDa}$).



W. T. S. Huck, R. Hulst, P. Timmerman,
F. C. J. M. van Veggel,*
D. N. Reinhoudt* 1006–1008

Noncovalent Synthesis of Nanostructures: Combining Coordination Chemistry and Hydrogen Bonding

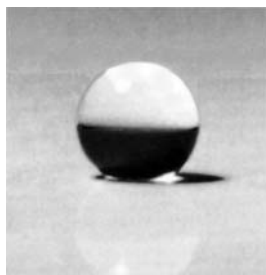
Unprecedented structural and compositional features are exhibited by these large vanadium borate clusters (for example 1, see picture on the right). Facile solubilization and crystallization of transition metal oxides by these large, multidentate polyborate ligands portends a rich and diverse chemistry for transition element/polyborate clusters. en = ethylenediamine.



J. T. Rijssenbeek, D. J. Rose,
R. C. Haushalter,*
J. Zubieta * 1008–1010

Novel Clusters of Transition Metals
and Main Group Oxides in the
Alkylamine/Oxovanadium/Borate System

Without sticking to the surface rapeseed oil droplets roll around on a surface prepared in two steps: An aluminum plate is first anodically oxidized and then treated with fluorinated monoalkylphosphates. The contact angles for some polar oils on such surfaces are greater than 150°.



K. Tsujii,* T. Yamamoto, T. Onda,
S. Shibuichi 1011–1012

Super Oil-Repellent Surfaces

Together with the M^I ions, the tetrahedral ribbons of the title compounds form double helices, the central channels of which are filled with water helices (see picture). Coordination octahedra M^{II}O₄(H₂O)₂ link the spiral ribbons, which run parallel to one another. Partial dehydration of the title compounds leads to microporous phases with channeled structure and is reversible in the sense of a topochemical reaction.



R. Kniep,* H. G. Will, I. Boy,
C. Röhr 1013–1014

6₁ Helices from Tetrahedral Ribbons
[BP₂O₈³⁻]: Isostructural Borophosphates
M^IM^{II}(H₂O)₂[BP₂O₈]·H₂O and Their
Dehydration to Microporous Phases
M^IM^{II}(H₂O)[BP₂O₈] (M^I = Na, K; M^{II} =
Mg, Mn, Fe, Co, Ni, Zn)

* Author to whom correspondence should be addressed

BOOKS

Catalytic RNA · F. Eckstein, D. M. J. Lilley

A. Jäschke 1015

Crop Protection Agents from Nature. Natural Products and Analogues ·
L. G. Copping

K. Naumann 1015

Golf Balls, Boomerangs and Asteroids—The Impact of Missiles on Society ·
B. H. Kaye

S. J. Zilker 1017

German versions of all reviews, communications, and highlights in this issue appear in the first May issue of *Angewandte Chemie*. The appropriate page numbers can be found at the end of each article and are also included in the Author Index on p. 1019.

SERVICES

| | |
|----------------|------|
| • Events | 907 |
| • Corrigendum | 951 |
| • Keywords | 1018 |
| • Author Index | 1019 |
| • Preview | 1020 |

All the Tables of Contents from 1995 onwards may be found on the WWW under <http://www.vchgroup.de/home/angewandte>

ANGEWANDTE CHEMIE

A Journal of the
Gesellschaft
Deutscher Chemiker

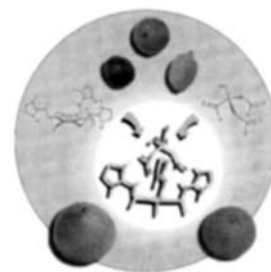
International Edition in English

1997
36/8

Pages 789–896

COVER PICTURE

The cover picture shows the structural formulas in red of citrate and a synthetic receptor that is selective for binding citrate in aqueous media. The center picture is the structure of the host–guest complex, derived by molecular mechanics, that was patterned after the crystal structure of the receptor and tricarballate. The receptor is preorganized for citrate recognition because of the alternation of steric interactions around the benzene ring. Selectivity for citrate was demonstrated in competition experiments. Further, the receptor can be used to bind citrate in juices, as is highlighted by the pictures of fruit. More on the recognition properties and synthesis of this receptor is reported by E. V. Anslyn et al. on pp. 862. (Graphics developed with assistance from B. Iverson at the University of Texas at Austin.)



REVIEWS

Contents

Chemistry for criminologists: How do analysts track down hidden explosives? When is a radio not a radio—and how can this be exposed? Why do some explosives slip through the net in spite of all the refinements of modern trace analysis? These questions highlight some of the challenges to instrumental analysis from forensic science that are of particular significance especially in the context of public safety.

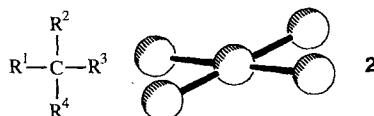
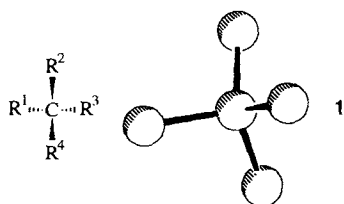
P. Kolla* 800–811

The Application of Analytical Methods to the Detection of Hidden Explosives and Explosive Devices

Though no longer mere curiosities, compounds containing planar-tetracoordinate carbon atoms (**2**) are not at all common. Some of the successes from the combined endeavors of different branches of chemistry in the synthesis and understanding of this “unnatural” structural unit (with respect to the usual tetrahedral **1**) are presented here. Coordination to metal atoms plays a key role in this stabilization.

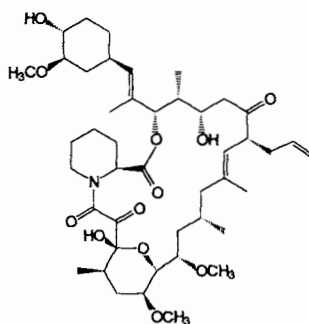
D. Rüttger, G. Erker* 812–827

Compounds Containing Planar-Tetracoordinate Carbon



HIGHLIGHTS

Combinatorial chemistry and rational design were elegantly combined in the "SAR (structure–activity relationship) by NMR" procedure, in which even ligands that are weakly bound to proteins could be quickly identified, optimized, and linked by rational design. The procedure is demonstrated by searching for ligands for FK binding proteins (see sketch of FK506 on the right).

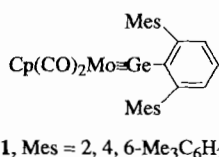


FK506

H. Kessler* 829–831

Structure–Activity Relationships by NMR:
A New Procedure for Drug Discovery by a
Combinatorial–Rational Approach

"Triple bonds" is now the motto: Exceptions to the classic double bond rule were sought over many years, and these efforts were so successful that compounds with doubly bonded silicon or germanium are no longer regarded as unusual. Attention has now switched to compounds with triple bonds between the elements of higher periods. After the preparation of complexes with W–P and Mo–P triple bonds in 1995, in 1996 a compound with a Mo–Ge triple bond was synthesized; this germanetriyl complex **1** also contains the first example of a heavier homologue of a terminal alkylidyne ligand.

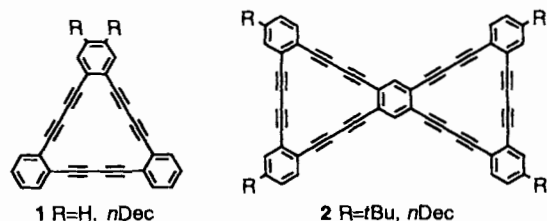


U. Siemeling* 831–833

The First Triple Bond between Germanium
and a Transition Metal

COMMUNICATIONS

Nearly 22 Å in diameter, bismacrocycle **2** is the largest known substructure of any network. This molecule and macrocycle **1** represent the first examples of subunits of graphdiyne, the most stable diacetylenic carbon allotrope comprising *sp* and *sp*² hybridized carbons. Spectroscopic evidence suggests that the dehydro[18]annulene core of **1** and **2** retains its diatropic character.

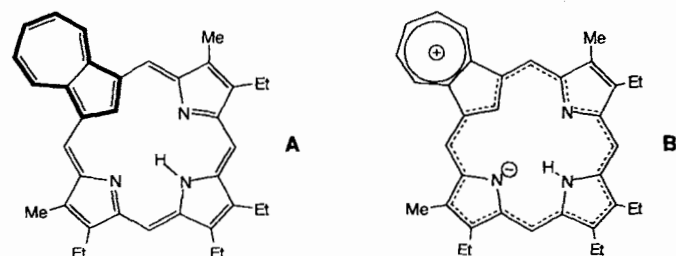


M. M. Haley,* S. C. Brand,

J. J. Pak 836–838

Carbon Networks Based on Dehydro-
benzoannulenes: Synthesis of Graphdiyne
Substructures

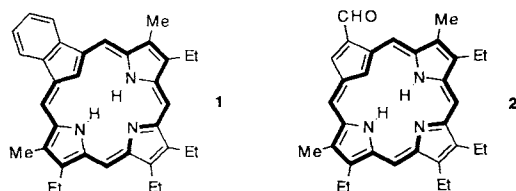
Through "electronic separation" of the seven-membered ring the formally cross-conjugated, azulene-containing macrocycle (limiting structure **A**) becomes a porphyrin-like species with a weak, diamagnetic ring current (limiting structure **B**). This aromatic character is further accentuated upon twofold protonation.



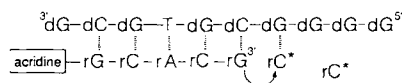
T. D. Lash,* S. T. Chaney 839–840

Azuliporphyrin: A Case of Borderline
Porphyrinoid Aromaticity

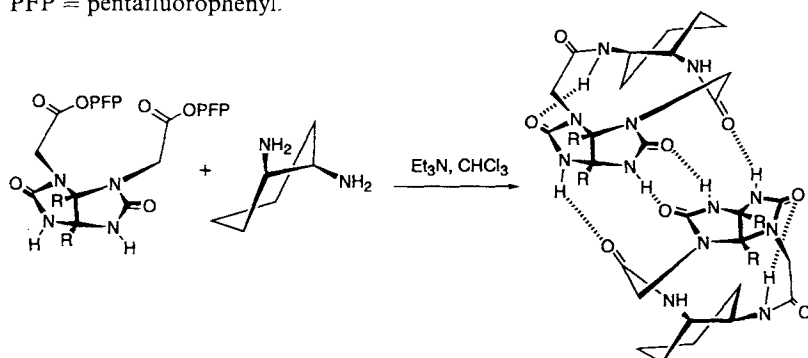
Excellent yields of the carbaporphyrin **1** are obtained by application of the "3 + 1" methodology for the reaction of 1,3-indenedicarboxaldehyde with a tripyrrane in the presence of 5% CF₃CO₂H in CH₂Cl₂. The related formylcarbaporphyrin **2** was prepared similarly. In contrast to earlier claims, no unusual tautomers or conformers are observed in solution.



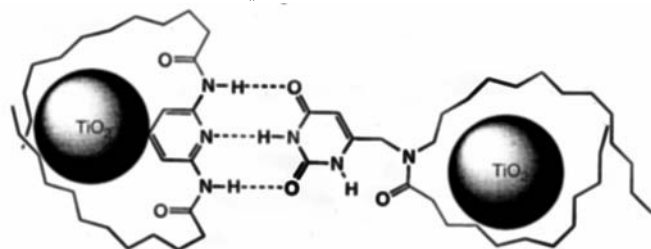
Acridine-labeled primers have been shown to be a very valuable tool for the study of the template-directed oligomerization of RNA (shown schematically below). Conditions for the efficient incorporation of cytidine have been established by using such compounds. The aggregation of guanosine-rich templates, which has long been considered a major obstacle for nonenzymatic replication of RNA, can thus be reduced to a minimum.



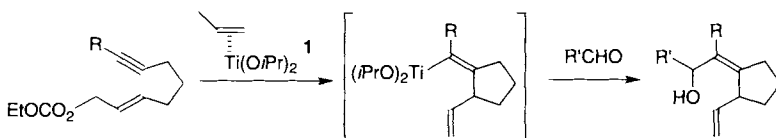
Self-help: A reaction product recognizes a stable intermediate and channels its reactivity to the formation of an eleven-membered ring (see below). A template effect is proposed, which involves molecular recognition through hydrogen bonding. PFP = pentafluorophenyl.



Modified TiO₂ nanocrystallites can recognize and selectively bind to each other by complementary hydrogen bonding. Subsequent self-organization yields an ordered array or semiconductor superlattice.



An ideal supplement to Li-, Mg-, and Zn-ene reactions is provided by the cyclization of 2,7- and 2,8-dienes, -enynes, and -diynes having a leaving group at the C1 position with the Ti^{IV} equivalent **1** (see below; R = R' = alkyl, aryl). In this reaction, the alkenyltitanium intermediate is presumably formed via a bicyclic titanium compound and not via an open-chain alkenyltitanium compound.



T. D. Lash,* M. J. Hayes 840–842

Carbaporphyrins

M. Kurz, K. Göbel, C. Hartel,
M. W. Göbel* 842–845

Nonenzymatic Oligomerization of Ribonucleotides on Guanosine-Rich Templates: Suppression of the Self-Pairing of Guanosine

D. M. Rudkevich,
J. Rebek, Jr.* 846–848

Chemical Selection and Self-Assembly in a Cyclization Reaction

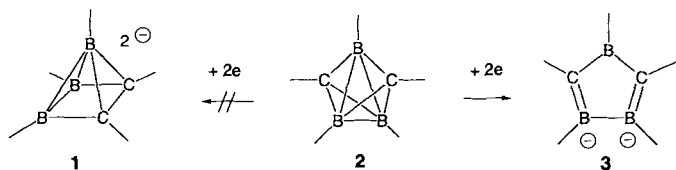
L. Cusack, R. Rizza, A. Gorelov,
D. Fitzmaurice* 848–851

Self-Assembly and Subsequent Self-Organization of a Semiconductor Nanocrystallite Superlattice

Y. Takayama, Y. Gao,
F. Sato* 851–853

Titanium(II)-Mediated Intramolecular Cyclizations of 2,7- and 2,8-Bis-Unsaturated Carbonates and Acetates: A New and Efficient Synthesis of Cycloalkanes

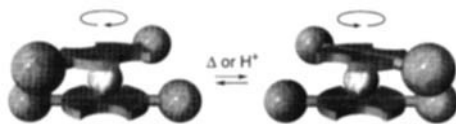
Instead of tetragonal pyramids like 1, the antiaromatic 1,2-diborata-4-boracyclopentadiene five-membered rings **3** are formed on two-electron reduction of dicarbapentaboranes(5) **2**.



M. Unverzagt, H.-J. Winkler, M. Brock,
M. Hofmann, P. von R. Schleyer,
W. Massa, A. Berndt* 853–855

Reduction of Dicarbpentaboranes(5)
to 1,2-Diborata-4-boracyclopentadienes:
Antiaromatic Compounds with
4 π -Electron Systems

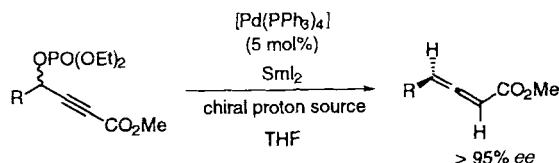
The porphyrin–porphyrin distance and the spatial requirements of the porphyrin substituents are parameters that influence the rotatability of the ligands in metal bis(porphyrinate)s (shown on the right): the chiral cerium complexes were much easier to racemize than the zirconium complexes. The porphyrin ligands in the latter rotate in response to H^+ .



K. Tashiro, K. Konishi,
T. Aida* 856–858

Enantiomeric Resolution of Chiral Metal-
lobis(porphyrin)s: Studies on Rotatability
of Electronically Coupled Porphyrin
Ligands

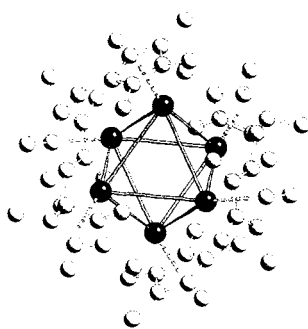
The selective protonation of one enantiomer in a racemic mixture of allenylmetal compounds is possible with Pd^0/SmI_2 and a chiral alcohol (see reaction scheme below). The products, enantiomerically pure allenic esters, are an important class of natural products and synthetic intermediates. This type of dynamic kinetic resolution by asymmetric protonation is an effective method for the asymmetric synthesis of allenes from racemic allenyl-/propargylmetal compounds.



K. Mikami,* A. Yoshida 858–860

Dynamic Kinetic Protonation of Racemic
Allenylmetal Species for the Asymmetric
Synthesis of Allenic Esters

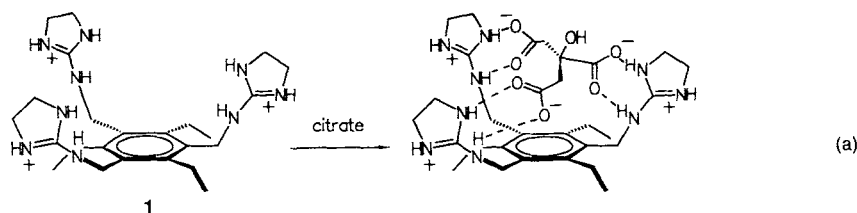
A hexameric cluster with only weak metal–metal bonding is found in crystalline (pentamethylcyclopentadienyl)gallium(I). A shell of $\eta^5-C_5Me_5$ ligands encloses a near-octahedral Ga_6 array with unusually long $Ga \cdots Ga$ distances (407.3 and 417.2 pm, see picture on the right).



D. Loos, E. Baum, A. Ecker,
H. Schnöckel,* A. J. Downs 860–862

Hexameric Aggregates in Crystalline
(Pentamethylcyclopentadienyl)gallium(I) at
200 K

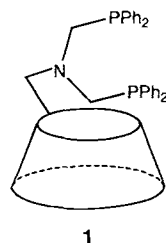
Applied molecular recognition—strong and selective binding of citrate in highly competitive media such as water and orange juice is reported. Five steps are enough to synthesize receptor **1** that is complementary in charge and shape to citrate. Electrostatic interactions and a network of hydrogen bonds, preorganized by steric effects, are the design principles responsible for the binding of receptor and citrate [Eq. (a)].



A. Metzger, V. M. Lynch,
E. V. Anslyn* 862–865

A Synthetic Receptor Selective for Citrate

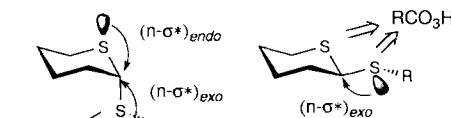
Hydrogenation and hydroformylation occur highly selectively with rhodium complexes of β -cyclodextrin-modified phosphanes (such as **1**) as catalysts. These are of interest particularly for industrial applications, in which transition-metal catalysis and phase-transfer catalysis are combined in one and the same catalyst.



M. T. Reetz,* S. R. Waldvogel ... 865–867

β -Cyclodextrin-Modified Diphosphanes as Ligands for Supramolecular Rhodium Catalysts

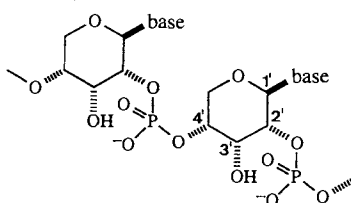
First experimental evidence for a relationship between structure and the relative nucleophilicities of the sulfur atoms in dithioacetals was obtained from a systematic investigation of the electrophilic oxidation of aryl 5-thioglucopyranosides. The diminished nucleophilicity of the ring heteroatoms thus recognized in the α -anomer is rationalized by the $n-\sigma^*$ theory of the anomeric effect (shown schematically), but by none of the other theories.



H. Yuasa, Y. Kamata,
H. Hashimoto* ... 868–870

Relative Nucleophilicity of the Two Sulfur Atoms in 1,5-Dithioglucoopyranoside

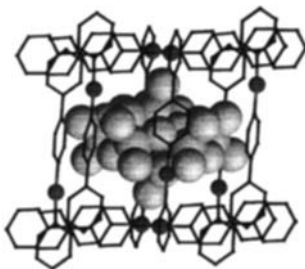
A minimum of three nucleotides in the loop are necessary for p-RNA oligomers to assume a hairpin rather than a duplex structure. Such hairpin structures form with comparable ease, as they do in RNA, in spite of the (conjectured) higher rigidity of the p-RNA backbone. Base stacking in p-RNA duplexes is interstrand rather than intrastrand; therefore, dangling bases enhance duplex stability when they are at the 2'-end (and not at the 4'-end).



R. Micura, M. Bolli, N. Windhab,
A. Eschenmoser* ... 870–873

Pyranosyl-RNA Also Forms Hairpin Structures

Soft chemical methods were used for preparing the new class of composite materials presented here. One example is $[\{\text{Cu}(4,4'\text{-bpy})\}_4\text{Mo}_8\text{O}_{26}]$ (4,4'-bpy = 4,4'-bipyridine), whose unique structure (shown on the right) consists of $[\text{Mo}_8\text{O}_{26}]^{4-}$ clusters embedded in a web of $\{\text{Cu}(4,4'\text{-bpy})\}_n^{n+}$ one-dimensional chains.



D. Hagrman, C. Zubieta, D. J. Rose,
J. Zubieta,* R. C. Haushalter* ... 873–876

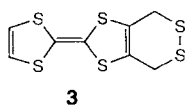
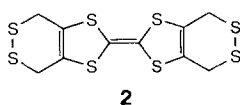
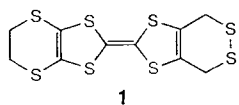
Composite Solids Constructed From One-Dimensional Coordination Polymer Matrices and Molybdenum Oxide Subunits: Polyoxomolybdate Clusters within $[\{\text{Cu}(4,4'\text{-bpy})\}_4\text{Mo}_8\text{O}_{26}]$ and $[\{\text{Ni}(\text{H}_2\text{O})_2(4,4'\text{-bpy})_2\}_2\text{Mo}_8\text{O}_{26}]$ and One-Dimensional Oxide Chains in $[\{\text{Cu}(4,4'\text{-bpy})\}_4\text{Mo}_{15}\text{O}_{47}] \cdot 8\text{H}_2\text{O}$

The organic template within molecular sieves may readily be studied by FT-Raman spectroscopy with virtually no interference from bands due to framework vibrations. FT-Raman spectra show that morpholine and cyclohexylamine are in the protonated form within AlPO_4 -based materials with the chabazite structure, while splittings of certain bands indicate specific interactions between the organic template and the framework.

S. Ashtekar, P. J. Barrie,* M. Hargreaves,
L. F. Gladden* ... 876–878

An FT-Raman Study of the Template-Framework Interaction in AlPO_4 -Based Molecular Sieves

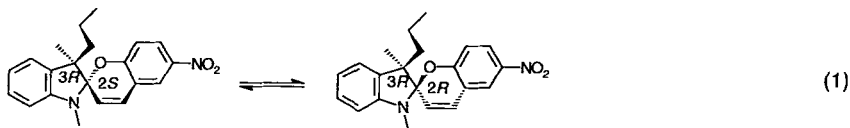
Worthwhile goals for the synthesis of conducting materials are compounds **1–3**, which contain the tetrathiafulvalene (TTF) framework. Compound **1** and a bis(methylsulfanyl) analogue have now been synthesized. Their oxidation behavior resembles that of the title compound, whose cation-radical salts are superconductors. The TTF core of these systems is essentially planar, and the outer sulfur atoms play a role in the crystallographic network.



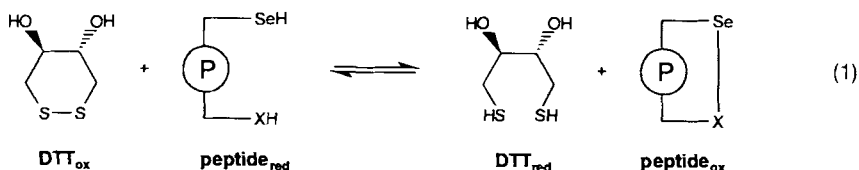
P. Hudhomme,* P. Blanchard,* M. Sallé,
S. Le Moustarder, A. Riou, M. Jubault,
A. Gorgues, G. Duguay ... 878–881

Studies of the First S-Position Isomer of Bis(ethylenedithio)tetrathiafulvalene

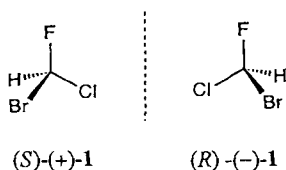
Photochemical switching between the diastereomeric spiropyrans [equilibrium (1)] surprisingly does not lead to a decay of the optical activity. This behavior can be attributed to the asymmetric induction by the stereogenic center C3. If the room-temperature equilibrium concentrations of the diastereomers are frozen below -40°C , irradiation with UV light displaces the equilibrium, thus causing information to be stored. The chiroptical properties enable subsequent reading of the data.



A much lower redox potential than that of the mixed Sec,Cys-peptide and particularly of the related Cys,Cys-peptide is a feature of the cyclic selenocystine-peptide (Sec,Sec-peptide). These findings that were obtained with appropriately modified glutaredoxin-octa-peptides at pH 7 [Eq. (1); X = S, Se; DTT = dithiothreitol], open interesting new approaches for the design of productive intermediates in the oxidative folding of synthetic peptides and recombinant proteins. Moreover, such seleno derivatives may represent useful heavy metal analogs for X-ray structure analysis.



After more than 100 years, the absolute configurations of the dextro- and levorotatory enantiomers of bromochlorofluoromethane **1**, one of the simplest chiral molecules, have now been determined. Comparison of the measured Raman optical activity spectrum (in the range of vibrational modes) of an enantiomerically enriched sample of **1** with the calculated spectra allow the assignments (*S*)-(+) and *R*-(-) to be made.



L. Eggers, V. Buss* 881–883

A Spiroindolinopyran with Switchable Optical Activity

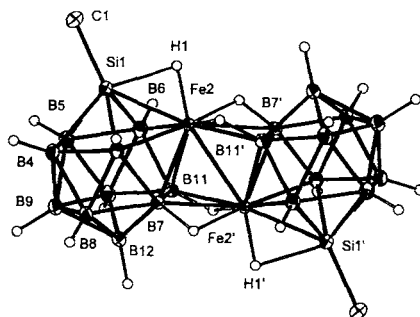
D. Besse, F. Siedler, T. Diercks, H. Kessler, L. Moroder* 883–885

The Redox Potential of Selenocystine in Unconstrained Cyclic Peptides

J. Costante, L. Hecht, P. L. Polavarapu,* A. Collet,* L. D. Barron* 885–887

Absolute Configuration of Bromochlorofluoromethane from Experimental and Ab Initio Theoretical Vibrational Raman Optical Activity

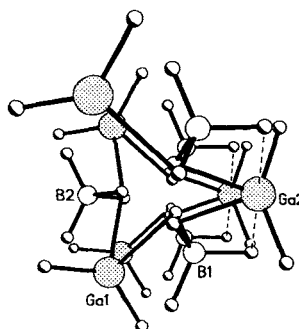
An unprecedented structural motif for metallaboranes is exhibited by the anion $[\{\text{HFe}(\text{MeSiB}_{10}\text{H}_{10})\}_2]^{2-}$ (see picture), which was isolated as the $[\text{nBu}_4\text{N}]_2$ salt in 63% yield from the reaction of deprotonated sila-*nido*-undecaborate and FeBr_2 .



L. Wesemann,* Y. Ramjoie, B. Ganter, B. Wrackmeyer 888–890

The First Transition Metal Complex of a Silaborane

Distorted tetrahedral GaH_4 and tetrahedral BH_4 moieties are the building blocks of the helical, polymeric chains formed by gallaborane at 110 K (schematically shown on the right). There are two distinct types of BH_4 groups: one is involved in $\text{Ga}(\mu\text{-H})_2\text{B}$ coordination and the other in unusual monohydrogen bridging of two adjacent GaH_2 units. The structure invites comparison with those of other main group hydrides.



A. J. Downs,* S. Parsons, C. R. Pulham, P. F. Souter 890–891

Helical, Polymeric Chains in Crystalline Gallaborane $[\text{GaBH}_6]_n$ at 110 K**

* Author to whom correspondence should be addressed

German versions of all reviews, communications, and highlights in this issue appear in the second April issue of *Angewandte Chemie*. The appropriate page numbers can be found at the end of each article and are also included in the Author Index on p. 895.

All the Tables of Contents from 1995 onwards may be found on the WWW under:
<http://www.vchgroup.de/home/angewandte>

SERVICES

| | |
|----------------|-----|
| • Keywords | 894 |
| • Author Index | 895 |
| • Preview | 896 |

WILEY-VCH ist eine Tochter der internationalen Verlagsgruppe John Wiley and Sons. In der Redaktion der *Angewandten Chemie* ist ehestmöglich eine

Redakteurs-Traineeestelle

zu besetzen. Die Ausbildung zum Redakteur dauert ein Jahr, eine anschließende Übernahme in ein festes Anstellungsverhältnis ist möglich. Sie erhalten eine betriebsspezifische zielorientierte Ausbildung, in der Sie insbesondere die Redaktion durch „training on the job“, daneben aber auch Herstellung, Zeitschriftenmarketing und andere Verlagsbereiche kennenlernen.

Sie sollten eine breit angelegte Chemieausbildung mit der Promotion abgeschlossen haben. Wir erwarten von Ihnen ferner Gewandtheit im Umgang mit der deutschen Sprache, sehr gute Englischkenntnisse, intensive Erfahrung mit gängigen PC-Programmen sowie ein überdurchschnittliches Engagement; ein längerer Aufenthalt im englischsprachigen Ausland während oder nach dem Studium ist erwünscht.

Wenn wir Ihr Interesse geweckt haben, senden Sie Ihre vollständigen Bewerbungsunterlagen an:

VCH Verlagsgesellschaft mbH
 Personalabteilung
 Postfach 10 11 61
 69469 Weinheim



WILEY-VCH

ANGEWANDTE CHEMIE

A Journal of the
Gesellschaft
Deutscher Chemiker

International Edition in English

1997
36/7

Pages 661–788

EDITORIAL

Electronic Keyword Searches

Not without reason does the phrase “to the best of our knowledge” appear in many scientific papers. No scientist may neglect a search of the literature on a new field or the perusal of the current literature. Chemical Abstracts and other secondary sources play an extremely important role in retrospective searches, but subject indexes based on keywords are often used to uncover the papers from the previous year.

Since keywords are a *subjective* selection of concepts intended to guide a reader to information relevant to the topic they wish to research, no one entirely trusts finding all the articles of interest. If synonyms or spelling variants exist, each must be searched. Even then, articles on basically the same theme can be allotted a totally different set of keywords, especially if the choice is left entirely to the author. Some journals have done away with subject indexes, which forces researchers to rely on full-text searches (if available), author indexes, and citations in relevant articles to find to the recent literature they seek. This places a heavy emphasis on a complete literature study...the circle is complete!

The electronic age should speed up literature surveys. An electronic search is undeniably faster than a manual one, but if spelling variants, plurals, or different parts of speech (tumor, tumour; catalysis, catalyses, catalytic) complicate the search, the human eye will probably pick up more of the targeted papers. A fair amount of skill is required to select keywords general enough to ensure finding most relevant articles, but specific enough to limit the hit list to the most likely targets. This is also the snag with full-text searches: the hit list is generally long, because articles in which the selected topic is mentioned, for instance, only in the introduction are given as much prominence as those devoted entirely to the subject. It can be time-consuming and frustrating to find the truly important papers by consulting each original article.

Since January 1997 four VCH journals have joined forces to minimize the problem of synonyms and to increase the probability of finding the articles on the same theme. *Angewandte Chemie* is one of the four initial journals, together with

Chemische Berichte/Recueil, *Liebigs Annalen/Recueil*, and *Chemistry—A European Journal*, that have created a common keyword thesaurus that is available on the Internet at:

<http://www.vchgroup.de/home/angewandte>

Authors are requested to choose at least two of the five keywords for their articles from the thesaurus. In this way they help direct others to their work, because researchers will use the same list to design their searches for these four journals. Nevertheless, the author is free to complete the keyword list for each paper with topics not in the thesaurus.

The thesaurus has another function: it allows fast electronic browsing of new issues. Thesaurus terms are highlighted in color as hyperlinks in the electronic Tables of Contents, so that with a click of the mouse you can jump to a list of the articles from the four journals that have a particular keyword. Even from the short list, you can generate another search through a different hyperlink. Moreover, a researcher is also not limited to the core keywords in his electronic searches. VCH's Article Finder on the WWW compiles a hit list in order of publication for any search term, not only from the complete keyword list for each article but also from titles (truncations are allowed to find, for instance, “catalyst”, “catalyzed”, “catalysis” and “catalytic”) and authors. An explanation on how to incorporate logical OR and AND functions is provided immediately below the search box.

The thesaurus is intended to be a living reflection of the most important topics researched today. As its usefulness can only be improved by a honing of the selection, comments are welcomed. Already the first suggestions from readers have led to changes in the list, which was also published in *Angewandte Chemie* at the beginning of 1997. For a current list it is therefore essential to refer to our Home Page.

The more intensely authors work with this keyword system, the more useful it can become. We invite you, both readers and authors, to start browsing electronically and then help us to tailor the system to suit your needs. It cannot be easier to contact us—*Angewandte Chemie*'s e-mail address can be accessed from our home page by a click of the mouse.

Karen Hindson
Angewandte Chemie

COVER PICTURE

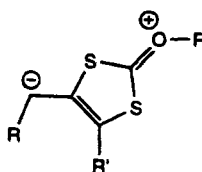
The cover picture shows the crystal structure of $[U(C_5Me_5)_3]$, the first 5f-element compound of this type. Previously, formation of tris(pentamethylcyclopentadienyl) complexes was limited to samarium since the only available syntheses required the special chemistry of samarium(II) precursors. Now it is possible to make these molecules from trivalent metal hydrides and tetramethylfulvalene. This new synthetic method should open up the area of $[M(C_5Me_5)_3]$ chemistry so that the unusual reactivity of these sterically crowded molecules can be explored. The structural diagram (generated by Michael Greci with the program Spartan 4.1.1 from Wavefunction) is superimposed on a picture of a crystal of the samarium compound $[Sm(C_5Me_5)_3]$, which was taken inside a specially modified Vacuum/Atmospheres glovebox by using a Panasonic videomicroscope, a McBain fiber-optic light pipe, and a Minolta Snappy video capture device. More details on the chemistry of $[U(C_5Me_5)_3]$ are reported by W. J. Evans et al. on pages 774ff.



REVIEWS

Contents

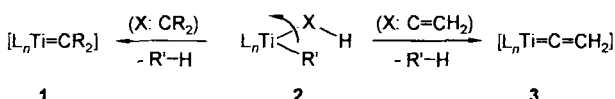
Known for nearly two centuries, yet hardly researched! The rich chemistry of xanthates leaves much to be discovered. Xanthates are cheap precursors to a great variety of radicals that can be efficiently captured in reactions free of heavy metals. *S*-propargyl xanthates also undergo thermal conversion into betaines of a novel type that are at the center of a host of nonradical transformations as diverse as diene formation and inversion of the configuration of secondary alcohols.



S. Z. Zard* 672–685

On the Trail of Xanthates: Some New Chemistry from an Old Functional Group

Rotatable or not rotatable? The rotation of the XH group about the M–C σ -bond makes a considerable contribution to the activation energy of the conversions of **2** into carbene complexes of electron-deficient transition metals such as **1** and into the highly reactive titanallenes **3**. The multitude of reactions that **3** can undergo has increased knowledge of the chemistry of these electron-deficient transition metal complexes, which in turn has led to new discoveries about the reactivity of the alkyl and alkenyl derivatives **2** as well as of various metallacycles of titanium group metals.



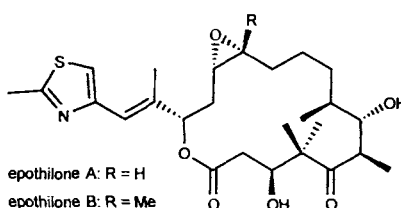
R. Beckhaus* 686–713

Carbenoid Complexes of Electron-Deficient Transition Metals—Syntheses of and with Short-Lived Building Blocks

HIGHLIGHTS

Contents

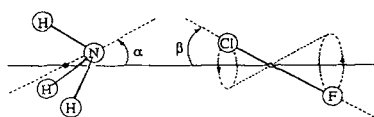
Antitumor agents possibly better than taxol might be derived from the epothilones (depicted on the right), which likewise bind to microtubules. The epothilones, which were discovered by Höfle et al. and Reichenbach et al., are easier to synthesize and more soluble in polar solvents than taxol. The results of *in vivo* activity studies are now eagerly awaited. The exceptional importance of these new tubulin stabilizers is reflected in the race for synthetic approaches to these compounds that has already led to the first total syntheses and several partial solutions.



L. Wessjohann* 715–718

Epothilones: Promising Natural Products with Taxol-Like Activity

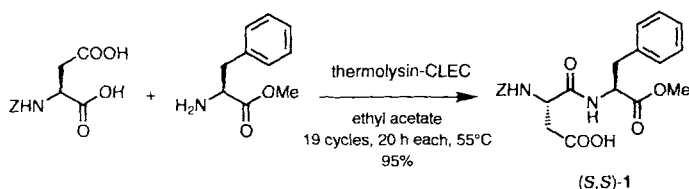
Molecular beams with the carrier gas argon contain prereactive complexes of halogens and interhalogens with NH_3 , H_2O , and H_2S , as detected by Fourier-transform microwave spectroscopy; the structures have been elucidated. The partial structures of NH_3 , H_2O , and H_2S as well as F_2 , ClF (cf. picture), Cl_2 , $BrCl$, and Br_2 are almost the same for the complexes as for the free molecules. The weak complex bonds result from electrostatic forces.



H. Bürger* 718–721

Gas-Phase Complexes: Possible Prereactive Gateways for Reactions of Halogens with NH_3 , H_2O , and H_2S

Enzyme preparations that are stable in organic solvents and in aqueous media can be obtained by covalently cross-linking enzyme crystals. The resulting exceptionally stable biocatalysts, the “cross-linked enzyme crystals” (CLECs), efficiently catalyze enzymatic peptide syntheses (see example below), esterifications, hydrolyses, C–C bond-forming reactions, and reductions. Z = benzyloxycarbonyl.

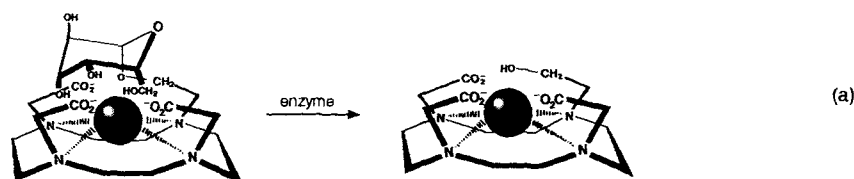


T. Zelinski, H. Waldmann* 722–724

Cross-Linked Enzyme Crystals (CLECs): Efficient and Stable Biocatalysts for Preparative Organic Chemistry

COMMUNICATIONS

A noninvasive means to map biological structure is offered by magnetic resonance imaging (MRI). A new class of MRI contrast agents is described where the relaxivity of the complex is modified by the activity of a specific enzyme (β -galactosidase, [Eq. (a)]). This type of agent offers the promise of direct three-dimensional visualization of gene expression in the form of an acquired MR image.

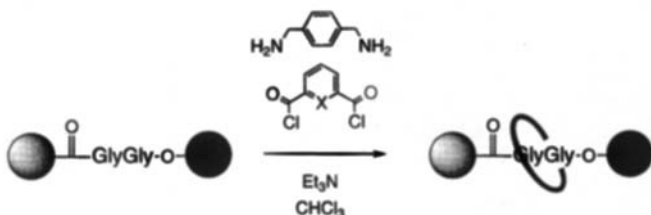


R. A. Moats, S. E. Fraser,

T. J. Meade* 726–728

A “Smart” Magnetic Resonance Imaging Agent That Reports on Specific Enzymatic Activity

Ring a peptide (not-so-dumb)bell: the amide groups in the glycyglycine derivative shown below provide the information required to template the formation of benzylic amide macrocycles to yield peptide [2]rotaxanes. The four key hydrogen bonds responsible for cyclization remain intact in the rotaxane in nonpolar solvents, in the solid state, and (when X = N) even in polar solvents such as $[D_6]DMSO$ and $[D_6]DMSO/D_2O$ mixtures. X = CH, N; shaded sphere = Ph_2CH , black sphere = Ph_2CHCH_2 .



D. A. Leigh,* A. Murphy, J. P. Smart,

A. M. Z. Slawin 728–732

Glycyglycine Rotaxanes—The Hydrogen Bond Directed Assembly of Synthetic Peptide Rotaxanes

Thirty-six peripheral glucopyranosidic units are placed in the higher generation dendrimer prepared by a convergent growth strategy from dendrimer wedges and an acid core (see schematic drawing on right). These compounds permit a novel entry into hitherto unknown neoglycoconjugate systems, which can be used for studying carbohydrate–protein interactions.



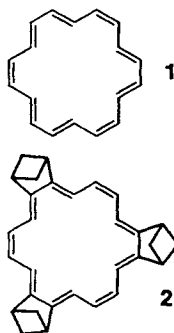
P. R. Ashton, S. E. Boyd,

C. L. Brown, N. Jayaraman,

J. F. Stoddart* 732–735

A Convergent Synthesis of a Carbohydrate-Containing Dendrimer

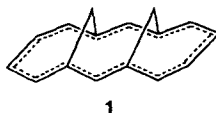
Threshold levels for the correct theoretical description of the delocalized [18]annulene (**1**) have been established with hybrid ab initio density functional computations. Analogous calculations on the bicycloannulated derivative **2** predict a clearly bond-localized structure and earmark this molecule as a new synthetic target for the study of aromaticity.



K. K. Baldridge, J. S. Siegel* 745–748

Ab Initio Density Functional vs Hartree Fock Predictions for the Structure of [18]Annulene: Evidence for Bond Localization and Diminished Ring Currents in Bicycloannulated [18]Annulenes

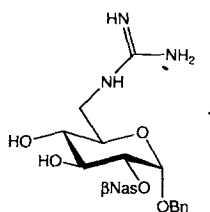
An energy increase of only 6 kcal mol⁻¹ is associated with the double-bond localization of the aromatic *syn*-bismethano[14]annulene (**1**). The correct prediction of aromaticity is surprisingly difficult, as shown by comparison of several theoretical predictions to experimental results.



M. Nendel, K. N. Houk,* L. M. Tolbert, E. Vogel, H. Jiao, P. von R. Schleyer* 748–750

The Bond Localization Energies in the Aromatic Bismethano[14]annulenes

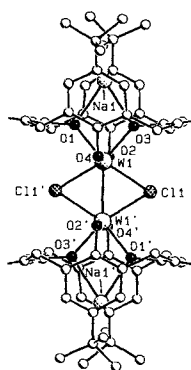
The position of the carbohydrate derivative 1 in the recognition pocket of thrombin has been determined by X-ray structure analysis of the inhibitor/thrombin complex. This confirms the structural mimicking of a peptide substrate by **1**. The concept behind the synthesis of this peptidomimetic is based on attachment of the characteristic functional group of an amino acid to a carbohydrate backbone. Nas = naphthylsulfonyl.



H. P. Wessel,* D. Banner, K. Gubernator, K. Hilpert, K. Müller, T. Tschopp 751–752

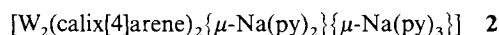
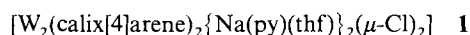
6-Guanidinopyranoses: Novel Carbohydrate-Based Peptidomimetics

Tungsten–tungsten double and triple bonds are found in the dimers **1** (structure depicted on the right; calixarene substituents partly omitted) and **2**, respectively, formed by the reductive coupling of the corresponding dichlorotungsten compounds. In **1** the two Na⁺ ions are located in the calixarene cavity; in **2** they bridge the two calixarene units. py = pyridine.

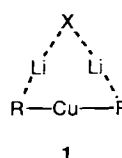


L. Giannini, E. Solari, A. Zanotti-Gerosa, C. Floriani,* A. Chiesi-Villa, C. Rizzoli 753–754

Metal–Metal Multiple Bonds Formed Across Two Tungsten-Calix[4]arenes by a Reductive Coupling Reaction



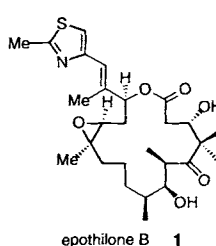
Organocuprates are mostly monomeric in solution! This is the result of the investigation of the aggregation behavior of reagents with the stoichiometry $[R_2Cu(X)Li_2]$, carried out for the first time by cryoscopy in tetrahydrofuran. Thus, Gilman cuprates ($X = I$) and cyanocuprates ($X = CN$) may belong to the same structural type **1**.



A. Gerold, J. T. B. H. Jastrzebski, C. M. P. Kronenburg, N. Krause,* G. van Koten* 755–757

Determination of the Degree of Aggregation of Organocopper Compounds by Cryoscopy in Tetrahydrofuran

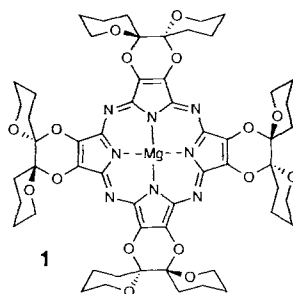
The highest biological activities displayed by epothilone-related compounds have been found for epothilone B (**1**) and a derivative that was prepared en route to the natural product. Key steps in the total synthesis were a Suzuki coupling providing a trisubstituted double bond in the macrocycle and its subsequent stereoselective epoxidation with dimethyldioxirane.



D.-S. Su, D. Meng, P. Bertinato, A. Balog, E. J. Sorensen, S. J. Danishefsky,* Y.-H. Zheng, T.-C. Chou, L. He, S. B. Horwitz 757–759

Total Synthesis of (–)-Epothilone B: An Extension of the Suzuki Coupling Method and Insights into Structure–Activity Relationships of the Epothilones

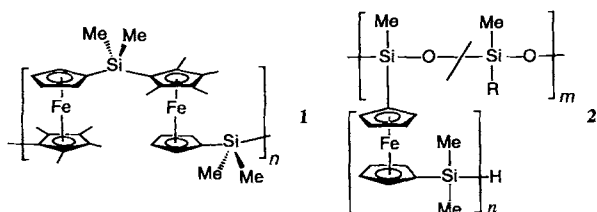
Macrocyclization of 2,3-dicyano-1,4-diox-2-ene with magnesium propoxide in propanol provided the enantiomerically pure C_4 -symmetric (porphyrinato)magnesium(II) complex **1**. The structure of the macrocycle was confirmed by an X-ray crystallographic study on the demetalated porphyrine.



A. S. Cook, D. B. G. Williams,
A. J. P. White, D. J. Williams,
S. J. Lange, A. G. M. Barrett,*
B. M. Hoffman* 760–761

Enantiomerically Pure “Winged” Spirane
Porphyrinoctaoles

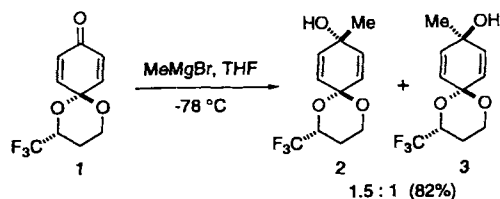
Regioregular poly(ferrocenylsilane)s **1**, end-group-functionalized polymers of controlled molecular weight, and novel graft copolymers **2** are accessible by transition-metal-catalyzed ring-opening polymerization of strained ferrocenophanes at ambient temperature.



P. Gómez-Elipe, P. M. Macdonald,
I. Manners* 762–764

Architectural Control in the Transition-
Metal-Catalyzed Ring-Opening Polymer-
ization of Silicon-Bridged [1]Ferroceno-
phanes

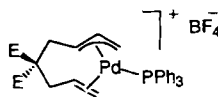
Trifluoromethylacetal groups as chiral auxiliaries enhance diastereoselectivity in nucleophilic additions to benzo- and naphthoquinone derivatives. In the methylation of **1** to give **2** and **3** facial selectivity is induced not by steric effects but by long-range electrostatic effects. This principle may be used in the design of a new class of chiral auxiliaries.



P. Wipf,* J.-K. Jung 764–767

Long-Range Electrostatic Effects in Syn-
thesis: Dipole-Controlled Nucleophilic Ad-
dition to a Naphthoquinone Acetal in
Model Studies toward Diepoxin σ

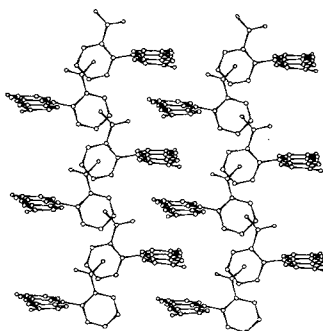
The palladium-catalyzed carbocyclization of allyl carboxylates with alkenes developed by Oppolzer proceeds smoothly via cationic complexes (depicted schematically on the right). In contrast, complexes with two donor phosphane ligands or a bidentate ligand are not productive intermediates in the cyclization process.



E. Gómez-Bengoa, J. M. Cuerva,
A. M. Echavarren,*
G. Martorell 767–769

Cationic Intermediates in the Intramolecu-
lar Insertion of Alkenes into (η^3 -Allyl)-
palladium(II) Complexes

The lack of suitable crystals has meant that it has not been possible to carry out a conventional single-crystal X-ray structure analysis to determine the structure of red fluorescein. Instead, the application of a Monte Carlo method has allowed the crystal structure to be determined directly from powder X-ray diffraction data. Importantly, fluorescein was treated as a nonrigid fragment in the structure solution calculation, illustrating the generalized application of the Monte Carlo method. The molecules form layers in the crystal (with extensive $C=O \cdots H-O$ hydrogen bonding), and within each layer the molecules are stacked in columns (as shown on the right).



M. Tremayne, B. M. Kariuki,
K. D. M. Harris* 770–772

Structure Determination of a Complex Or-
ganic Solid from X-Ray Powder Diffrac-
tion Data by a Generalized Monte Carlo
Method: The Crystal Structure of Red
Fluorescein

VIth European Conference on Solid State Chemistry

First Circular,
Second Announcement
and Call for Papers

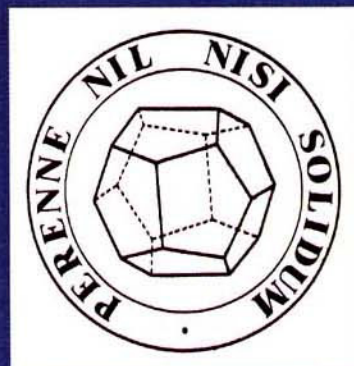
September 17 - 20, 1997



Switzerland



New Swiss
Chemical
Society



Information from:

Mrs. E. Fahrnbühl

ECSSC '97

Laboratory of Inorganic Chemistry

Universitätstr. 6

CH 8092 Zürich

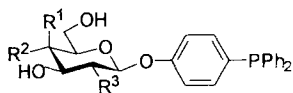
phone: (41-1)-632-9101

fax: (41-1)-632-1149



Current information can be found on the World Wide Web at:
<http://www.inorg.chem.ethz.ch/ecssc/ecssc.html>
Registration and abstracts information may also be ordered by email from:
ECSSC@inorg.chem.ethz.ch
(indicating ECSSC/registration and ECSSC/abstract)

Two-phase catalysts with sugar-substituted ligands, such as glycoside-triarylphosphanes **1a–c**, reveal advantages over catalysts with the classical TPPTS ligands in Heck and Suzuki reactions. A simple and generally applicable synthesis has been developed for this new class of neutral, hydrophilic ligands. On account of thermoreversible solvation, the concentration of the two-phase catalyst in the nonpolar medium increases with increasing temperature, as shown by the Nernst distribution coefficient determined for one of the new ligands at different temperatures.

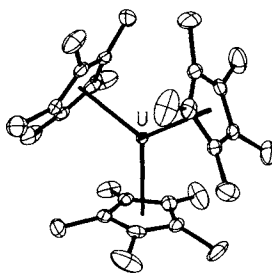


- 1a** $R^1 = \text{H}$, $R^2 = \text{OH}$, $R^3 = \text{NHAc}$
1b $R^1 = \text{OH}$, $R^2 = \text{H}$, $R^3 = \text{OH}$
1c $R^1 = \text{H}$, $R^2 = \text{OH}$, $R^3 = \text{OH}$

M. Beller,* J. G. E. Krauter,
A. Zapf 772–774

Carbohydrate-Substituted Triarylphosphanes—A New Class of Ligands for Two-Phase Catalysis

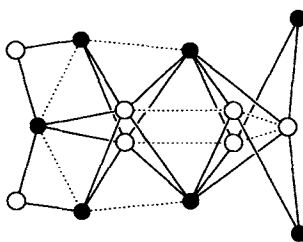
Polymerization of ethylene is initiated by $[\text{Sm}(\text{C}_5\text{Me}_5)_3]$, an observation that led to a new synthetic route to this Sm^{III} compound. Tetramethylfulvalene proved to be the crucial reagent and was also used in the synthesis of $[\text{U}(\text{C}_5\text{Me}_5)_3]$, the first tris(pentamethylcyclopentadienyl) complex of an actinide metal (see structure on right).



W. J. Evans,* K. J. Forrestal,
J. W. Ziller 774–776

Activity of $[\text{Sm}(\text{C}_5\text{Me}_5)_3]$ in Ethylene Polymerization and Synthesis of $[\text{U}(\text{C}_5\text{Me}_5)_3]$, the First Tris(pentamethylcyclopentadienyl) 5f-Element Complex

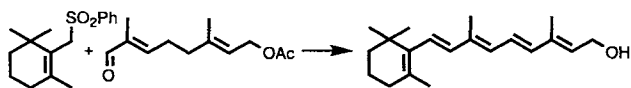
Calcium ions and organic ligands—in this case deprotonated erythritol—together are capable of reducing aggregation of oxoiron(III) species to such an extent that well-defined oxoclusters can be isolated. In the title cluster, an Fe_8O_{32} rutile core is extended by further iron centers to yield a hematite-type microtwin ($\text{Fe}_{14}\text{O}_{48}$; arrangement of iron centers depicted on the right), which may be related to metastable oxoiron(III) phases in terms of structure and magnetism.



J. Burger, P. Klüfers* 776–779

Stabilization of Iron Clusters by Polyolato Ligands and Calcium Ions: An Fe_{14} Oxo-cluster from Aqueous Alkaline Solution

Optimizing reactions for one set of conditions, although they normally proceed under different conditions, is a promising method for the directed development of one-pot reaction sequences. The validity of such “integrated” chemical processes has been shown by an extremely concise synthesis of vitamin A, which involves coupling of two C_{10} building blocks [Eq. (a)].



(a)

A. Orita, Y. Yamashita, A. Toh,
J. Otera* 779–780

Integrated Chemical Process: An Extremely Concise Synthesis of Vitamin A

A new strategy for solid-phase combinatorial synthesis: Application of laser optical synthesis chips (shown schematically on the right; other end groups include OH, COOH, and Cl) and directed sorting allows formation and reliable characterization of libraries of small organic molecules, peptides, and oligonucleotides.



X.-y. Xiao,* C. Zhao, H. Potash,
M. P. Nova 780–782

Combinatorial Chemistry with Laser Optical Encoding

* Author to whom correspondence should be addressed

BOOKS

Green Chemistry. Designing Chemistry for the Environment ·
P. T. Anastas, T. C. Williamson

J. O. Metzger 783

Multiply Bonded Main Group Metals and Metalloids · R. West, F. G. A. Stone

M. Weidenbruch 784

The Chemistry of Heterocycles · T. Eicher, S. Hauptmann

T. D. Lash 785

German versions of all reviews, communications, and highlights in this issue appear in the first April issue of *Angewandte Chemie*. The appropriate page numbers can be found at the end of each article and are also included in the Author Index on p. 787.


All the Tables of Contents from 1995 onwards may be found on the WWW under:
<http://www.vchgroup.de/home/angewandte>

SERVICES

| | |
|----------------|----------|
| • Events | 669, 714 |
| • Keywords | 786 |
| • Author Index | 787 |
| • Preview | 788 |

CLASSIFIED

Chemistry Know-how




direct

FIZ CHEMIE Structures & Reactions
always informed about the newest syntheses
- prepared by experts

FIZ CHEMIE Engineering Data
for planning, construction, process control,
processes and processing


FIZ CHEMIE Service & Consulting
literature searches - training - consulting

FIZ CHEMIE Input Service
setting up customized
information systems



For more information please contact: • internet: <http://www.fiz-chemie.de>
• email: info@fiz-chemie.de • Infoline: fon +49 30 399 77 - 111, fax -134
• P. O. Box 12 60 50, D-10593 Berlin, Germany

FIZ CHEMIE BERLIN



Fachinformationszentrum Chemie GmbH

Your Partner for CAS-Databases on STN



University of Geneva
The Faculty of Sciences invites
applications for a position of:

Professor of Organic Chemistry

in the Department of Organic Chemistry at the level of
Full Professor (succession Prof. W. Oppolzer).

The successful candidate will be expected to carry out
active and innovative research in the area of organic
synthesis. Academic duties include participation in
teaching at all University levels.

Candidates must have previous experience in directing
research and in teaching. Applications including a cur-
riculum vitae and publication list should be sent to:

**Secrétariat de la Faculté des Sciences - 30, quai
Ernest Ansermet - CH-1211 Genève 4 (Switzerland).
Closing date for applications: May 15.** Further in-
formation is available from the Dean's office (Fax
+41 22 702 66 98).

Applications from women scientists are especially
invited.

Visit our stand at

ACHEMA 09/06-14/06/97 Frankfurt/M., Stand 1.2 C 12

ANGEWANDTE CHEMIE

A Journal of the
Gesellschaft
Deutscher Chemiker

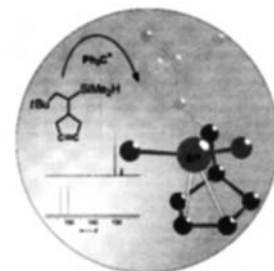
International Edition in English

1997
36/6

Pages 539–660

COVER PICTURE

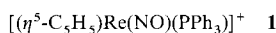
The cover picture shows the calculated structure of a 2-silanorbornyl cation and its synthesis by a hydride transfer reaction, both of which show similarities to the structure and synthesis of the carbon analog, the 2-norbornyl cation. The depicted structure emphasizes the intramolecular π complexation of the “siliconium ion”. Electron transfer from the double bond to the positively charged silicon is corroborated by the characteristic, low-field shift of the vinylic ^{13}C signals of the cation (red) relative to those of the starting silane (blue). Efficient intramolecular stabilization of the siliconium ion reduces the tendency to form complexes with solvent molecules or counterions. More details on the synthesis and properties of this novel silyl cation are reported by N. Auner and P. von R. Schleyer et al. on pages 626ff.



REVIEW

Contents

A general model for chiral recognition in the complexation of alkenes, aldehydes, and ketones—the most frequently used starting materials in enantioselective organic synthesis—has been formulated. A wealth of supporting data was obtained from studies with the Lewis acidic 16e rhenium complex cation **1**. The picture on the right shows the superposition of two alkene complexes of **1**.

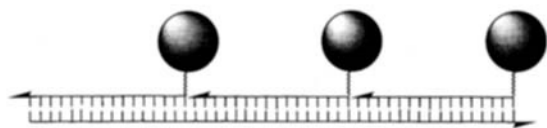


J. A. Gladysz,* B. J. Boone 551–583

Chiral Recognition in π Complexes of Alkenes, Aldehydes, and Ketones with Transition Metal Lewis Acids; Development of a General Model for Enantioface Binding Selectivities

HIGHLIGHTS

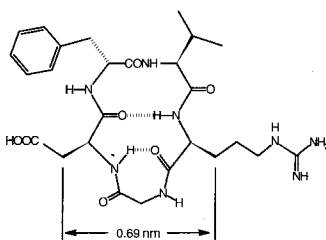
Nanostructured systems and functionalized supramolecular aggregates are accessible by DNA hybridization. The nanocrystalline molecule (see schematic representation below) is constructed from gold clusters (shaded spheres) and oligonucleotides (ladderlike framework) by self-assembly. Complex DNA networks could serve as high-resolution matrices for the production of microchips. DNA technology is thus in the process of expanding to include applications in microelectronics.



C. M. Niemeyer* 585–587

DNA as a Material for Nanotechnology

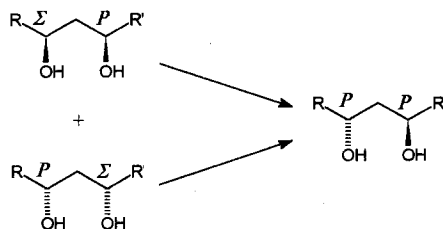
Arthritis, rheumatism, and diabetic retinopathy, conditions accompanied by excessive angiogenesis, may be amenable to treatment with the same drugs proposed for cancer therapy. A promising new concept in tumor treatment is the application of integrin antagonists such as **1** and other low molecular weight compounds with antiangiogenic activity. A number of drugs are currently in preclinical and clinical trials.



A. Giannis,* F. Rübsam 588–590

Integrin Antagonists and Other Low Molecular Weight Compounds as Inhibitors of Angiogenesis: New Drugs in Cancer Therapy

From a 1:1 mixture of enantiomers to an enantiomerically pure product—the method of “enantiodifferentiating inversion” can be used to convert a complex mixture of diol isomers into a single product, containing a sequence of four asymmetric centers found in several important natural products. In this approach a 1,3-diol with a *P* and a Σ center reacts to give a diol with two *P* centers (see reaction on the right).

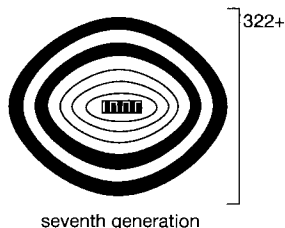


A. P. Davis* 591–594

Deracemization by Enantiodifferentiating Inversion in 1,3-Diols

COMMUNICATIONS

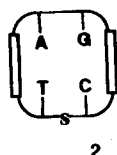
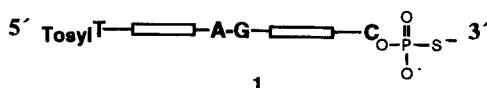
At the core, at the core and at the surface, within the cascade structure, or within the cascade structure and at the surface are different ways in which the dendrimers described here can be selectively alkylated. These phosphorus-containing dendrimers have generations of different constitution (example depicted on the right, □ and ■ are neutral and cationic generations, respectively). Remarkably, even the core of a sixth generation dendrimer is shown to be accessible.



C. Larré, A.-M. Caminade,*
J.-P. Majoral* 596–599

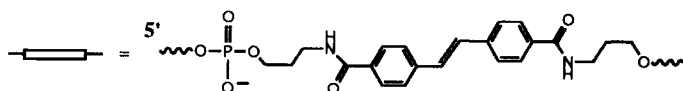
Chemoselective Polyalkylations of Phosphorus-Containing Dendrimers

A remarkably stable base-stacked structure is shown by the 70-membered ring **2**, which possesses only four nucleotide bases and is formed by efficient cyclization of the oligonucleotide conjugate **1**. In the presence of alkali, **2** twists to bring the stilbene groups into close proximity, as indicated by an excimer emission upon irradiation.

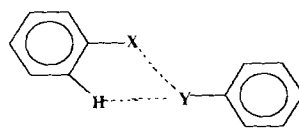


M. K. Herrlein,
R. L. Letsinger* 599–601

Stability and Conformational Switching in a Mini-Cyclic Oligonucleotide Conjugate



A recurring motif in a variety of crystal structures is represented by the atomic arrangement **I**. The participating molecules are stabilized by two intermolecular interactions (dashed lines) into a nonminimal energy conformation. This motif is useful for molecular recognition and the generation of crystal structures.

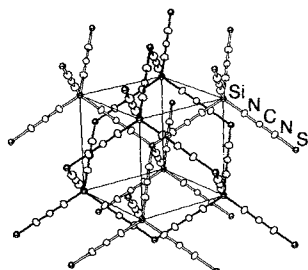


I, X, Y = Cl, Br

O. Navon, J. Bernstein,*
V. Khodorkovsky 601–603

Chains, Ladders, and Two-Dimensional Sheets with Halogen···Halogen and Halogen···Hydrogen Interactions

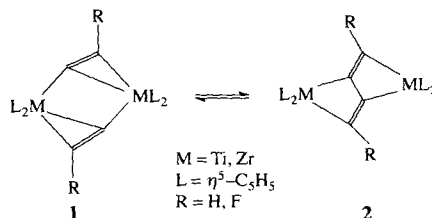
The reaction of SiCl_4 with bis(trimethylsilyl)carbodiimide in a 1:2 molar ratio followed by annealing at temperatures above 400 or 900 °C provides the first crystalline ternary Si-C-N solids, namely silicon dicarbodiimide (SiC_2N_4) and silicon (carbodiimide)nitride (Si_2CN_4), in near quantitative yields. The anti-cuprite type structure of SiC_2N_4 is shown on the right.



R. Riedel,* A. Greiner, G. Mieke,
W. Dressler, H. Fuess, J. Bill,
F. Aldinger 603–606

The First Crystalline Solids in the Ternary Si-C-N System

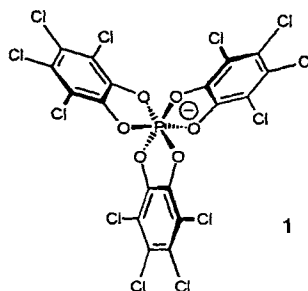
Substituents on the ethynyl group influence the fate of the title complexes: unusual C–C coupling and formation of complex type **2** is observed in dimeric bis(η^5 -cyclopentadienyl)-phenylethynyltitanium ($\text{R} = \text{Ph}$), but not in the zirconium analogue. Theoretical studies of **1** and **2** at the ab initio MO and DFT levels demonstrate that the electron-withdrawing substituent $\text{R} = \text{F}$ drives the equilibrium towards **2** for $\text{M} = \text{Zr}$.



E. D. Jemmis,* K. T. Giju 606–608

To Couple or Not To Couple: The Dilemma of Acetylide Carbons in $[(\eta^5\text{-C}_5\text{H}_5)_2\text{M}(\mu\text{-CCR})_2\text{M}(\eta^5\text{-C}_5\text{H}_5)_2]$ complexes ($\text{M} = \text{Ti, Zr}$)—A Theoretical Study for $\text{R} = \text{H, F}$

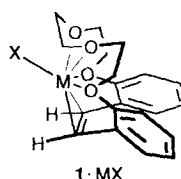
Easily accessible and configurationally stable are words that describe the enantiopure tris(tetrachlorobenzenediolato)phosphate(v) ion (**1**). These qualities predetermine **1** for use in enantiomeric resolution and asymmetric synthesis. X-ray structure analysis of the cinchonidinium salt of **1** confirmed the octahedral geometry and provided the absolute configuration of the anion.



J. Lacour,* C. Ginglinger, C. Grivet,
G. Bernardinelli 608–610

Synthesis and Resolution of the Configurationally Stable Tris(tetrachlorobenzenediolato)phosphate(v) Ion

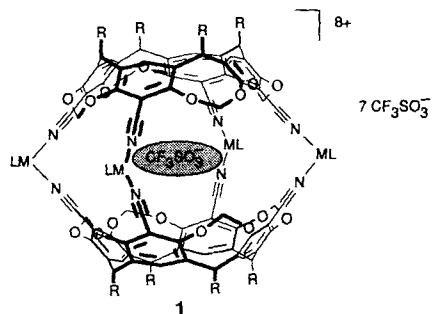
Four oxygen atoms and a double bond coordinate to the Ag^+ ion in the complex with the stilbene crown ether **1**. Surprisingly, the Na^+ ion is also complexed by **1** in a similar geometry. The coordinative bond between a Na^+ ion and a π bond, which is detected here for the first time, is probably induced and supported by the oligo(ethylenoxy)oxy bridge. $\text{M}^+\text{X}^- = \text{AgNO}_3, \text{NaClO}_4$.



T. Futterer, A. Merz,*
J. Lex* 611–613

Oligo(ethylenoxy)oxy-Bridged Stilbenes as Ligands for σ - and π -Coordinated Ag^+ and Na^+ Ions

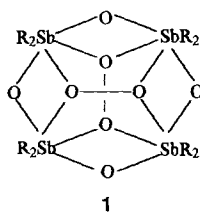
Opening and closing of the stable, molecular-sized cages **1** ($\text{M} = \text{Pd, Pt}$; $\text{L} = 1,3\text{-bis(diphenylphosphino)propane}$) can be efficiently controlled by ligand exchange. Simply mixing the preorganized cavitand with the appropriate metal complex precursor provides **1** quantitatively in one step. One triflate ion is encapsulated in the self-assembly process.



P. Jacopozi, E. Dalcanele* 613–615

Metal-Induced Self-Assembly of Cavitand-Based Cage Molecules

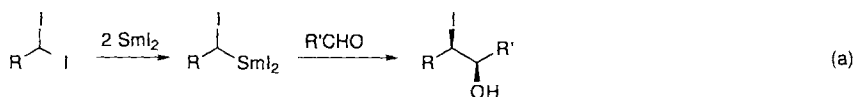
A cage structure with two quadruply bridging peroxo groups forms the center of the organoantimony peroxide **1** ($R = o$ -tolyl), which is readily accessible by oxidation of the corresponding tetraaryldistibane with atmospheric oxygen and H_2O_2 . The protecting periphery of o -tolyl groups is responsible for the good solubility of the antimony–oxygen cage.



H. J. Breunig,* T. Krüger,
E. Lork 615–617

A μ_4 -Peroxo Complex of Antimony: Synthesis and Structure of $(o\text{-Tol}_2\text{SbO})_4(\text{O}_2)_2$

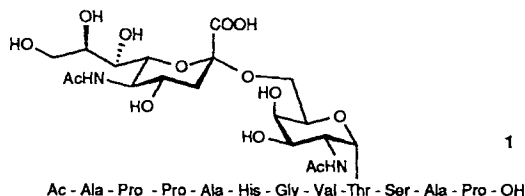
High syn-selectivity and an extremely convenient procedure characterize the novel SmI_2 -mediated addition of α -iodoalkyl building blocks to aldehydes [Eq. (a); $R, R' = \text{alkyl}$]. The chiral 1,2-iodohydrins formed are attractive synthetic intermediates for further conversions.



S. Matsubara, M. Yoshioka,
K. Utimoto* 617–618

A Samarium-Mediated, Highly Stereoselective Reaction of 1,1-Dihaloalkanes with Aldehydes: Generation of a Chiral α -Iodoethyl Building Block from Achiral 1,1-Diiodoethane

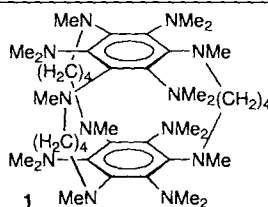
An allylic anchor was used for the solid-phase synthesis of glycopeptide **1** from the tandem repeat of the tumor-associated mucin MUC-1 with a sialyl- T_N antigen side chain. The sialyl- T_N antigen is one of the most promising of the tumor-associated antigens for the development of vaccines against epithelial tumors. Subsequent hydrolysis of the sialic acid methyl ester proceeds without epimerization in the peptide or β -elimination of the carbohydrate side chain.



B. Liebe, H. Kunz* 618–621

Solid-Phase Synthesis of a Tumor-Associated Sialyl- T_N Antigen Glycopeptide with a Partial Sequence of the “Tandem Repeat” of the MUC-1 Mucin

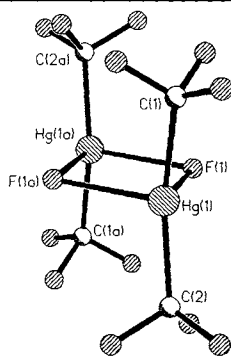
Increasing the reorganization energy slows intramolecular electron transfer (ET) in **1**, a compound thus well-suited for studying the kinetics of ET processes. A surprisingly smooth, threefold nucleophilic aromatic substitution reaction is the key step in the synthesis of **1**.



J. J. Wolff,* A. Zietsch, H. Irngartinger,
T. Oeser 621–623

Synthesis and Structure of a Dimeric Peralkylated Hexaaminobenzene: Hexakis(dimethylamino)hexamethylhexaaza[6,3]-(1,3,5)cyclophane

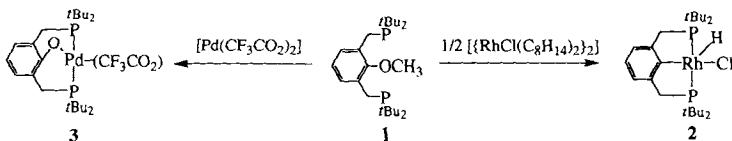
The first anionic fluoromercury complex $[(\text{CF}_3)_2\text{Hg}(\mu\text{-F})_2\text{Hg}(\text{CF}_3)_2]^{2-}$ was prepared from $\text{Hg}(\text{CF}_3)_2$ and TAS fluoride $(\text{Me}_2\text{N})_3\text{S}^+(\text{Me}_3\text{Si})\text{F}_2^-$, and characterized by X-ray crystal structure analysis (structure depicted on the right). In contrast to the neutral compound, the anions can be used as nucleophilic CF_3 -transfer reagents.



D. Viets, E. Lork, P. G. Watson,
R. Mews* 623–624

$[(\text{CF}_3)_2\text{Hg}(\mu\text{-F})_2\text{Hg}(\text{CF}_3)_2]^{2-}$: Synthesis, Structure, and Reactivity

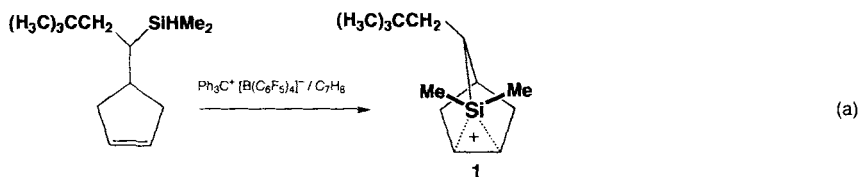
An unprecedented metal insertion into the strong sp^2 – sp^3 aryl–O bond to form **2** is observed for the reaction of $[\{\text{RhCl}(\text{C}_8\text{H}_{14})_2\}_2]$ (C_8H_{14} = cyclooctene) with two equivalents of the aryl ether phosphane **1**. This reaction proceeds directly, even at room temperature, with no rhodium insertion into the adjacent weaker $\text{ArO}-\text{CH}_3$ bond. However, the alkyl–O bond is activated by the reaction of **1** with $[\text{Pd}(\text{CF}_3\text{CO}_2)_2]$ to give **3**. Selectivity of C–O activation can therefore be directed by choice of metal complex.



M. E. van der Boom, S.-Y. Liou,
Y. Ben-David, A. Vigalok,
D. Milstein* 625–626

Selective Activation of Alkyl- and Aryl-Oxygen Single Bonds in Solution with Transition Metal Complexes

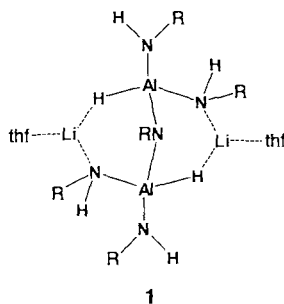
The Si analog of the norbornyl cation is a free but internally π -stabilized silyl cation (**1**) prepared by a hydride transfer reaction [Eq. (a)]. Ab initio calculations confirm the experimental observation that there is no coordination to solvent or counterions.



H.-U. Steinberger, T. Müller,
N. Auner,* C. Maerker,
P. von R. Schleyer* 626–628

The 2-Silanorbornyl Cation: An Internally
Stabilized Silyl Cation

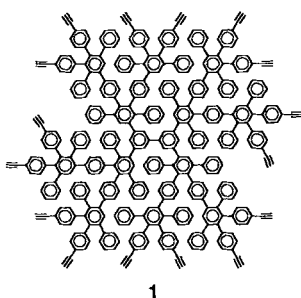
Cyclic and bicyclic intermediates such as the THF-adduct **1** can be isolated from the reaction of a primary amine with LiAlH_4 . It is assumed that these compounds are generally formed in the reduction of organic nitrogen-containing compounds with LiAlH_4 . The reaction of $\text{Na}(\text{AlHR}_3)$ with secondary amines also affords crystalline intermediates, but with polymeric structure.



M. L. Montero, H. Wessel, H. W. Roesky,*
M. Teichert, I. Usón 629–631

The Reaction of Primary and Secondary
Amines with LiAlH_4 and $\text{Na}(\text{AlHEt}_3)$

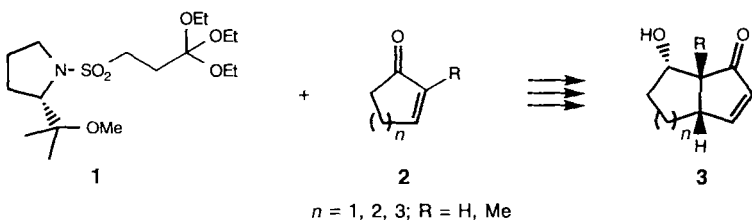
An elegant route to aromatic hydrocarbon dendrimers, such as **1** with pentaphenylbenzene units, and to extremely large polybenzenoid hydrocarbons is based on Diels–Alder cycloadditions of 3,4-bis-[4-(triisopropylsilyl)ethynyl]phenyl]-2,5-diphenylcyclopenta-2,4-dienone and aromatic oligoethynyl compounds such as 3,3',5,5'-tetraethynylbiphenyl. The type of linkage and the high packing density of the benzene rings facilitate the cyclodehydrogenation of appropriate dendrimeric subunits to yield planar disks.



F. Morgenroth, E. Reuther,
K. Müllen* 631–634

Polyphenylene Dendrimers: From Three-
Dimensional to Two-Dimensional Structures

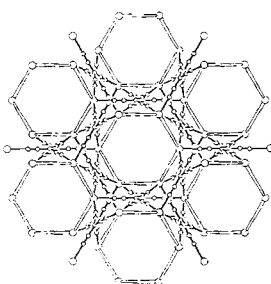
A highly selective *cis*-fusion is observed for the reaction of the chiral 1,3-dipole equivalent **1** with cyclic enone **2** to form the bicyclic cyclopentenone **3**. This multistep method, which does not require isolation of intermediates, is conceptually analogous to the Robinson annulation and should find wide applicability.



C. Huart, L. Ghosez* 634–636

Asymmetric Cyclopentannulation of Cyclic
Enones with a Chiral 1,3-Dipole Equivalent

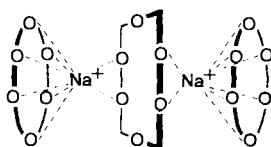
Sixfold helices of the borate-bridged cadmium ion are the outstanding structural feature of this chiral, channel-containing coordination polymer (shown schematically on the right), which was formed by solvolysis of $[\text{BPh}_4]^-$ in methanol in the presence of Cd^{2+} and $[\text{C}(\text{CN})_3]^-$.



S. R. Batten, B. F. Hoskins,
R. Robson* 636–637

Solvolysis of $[\text{B}(\text{C}_6\text{H}_5)_4]^-$ in Methanol To
Give the Chiral Coordination Polymer
 $\text{Cd}(\text{tcm})[\text{B}(\text{OMe})_4] \cdot x \text{MeOH}$, $x \approx 1.6$

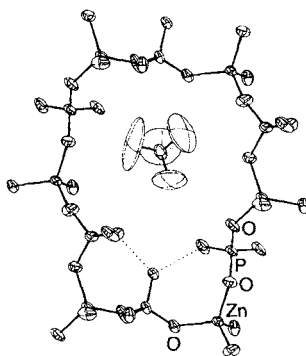
Three [18]crown-6 ligands and two sodium ions surprisingly form a triple-decker sandwich dication, pictured schematically on the right. Due to sixfold O-coordination of each sodium ion to the outer crown ethers, but only two $\text{Na}^+ \cdots \text{O}$ contacts each to the central ligand, the outer macrocyclic rings are distorted to a hemispherical conformation, whereas the central ring adopts a rectangular shape.



H. Bock,* T. Hauck, C. Näther,
Z. Havlas 638–639

News from an Old Ligand: The Triple-Decker Ion Triple, $\text{Tris}([\text{18}]\text{Crown-6})\text{disodium Bis}(\text{tetraphenylcyclopentadienide})$

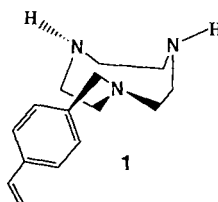
An open framework structure built up from tetrahedral building blocks characterizes the zincophosphate $\text{N}(\text{CH}_3)_4 \cdot \text{ZnH}_3(\text{PO}_4)_2$. Its topology is based on 12-rings (depicted on the right) that form a pear-shaped cavity occupied by tetramethylammonium ions. $\text{N}(\text{CH}_3)_4 \cdot \text{ZnH}_3(\text{PO}_4)_2$ has the lowest framework density yet observed in microporous materials built up from tetrahedral building blocks.



W. T. A. Harrison,*
L. Hannooman 640–641

$\text{N}(\text{CH}_3)_4 \cdot \text{ZnH}_3(\text{PO}_4)_2$: A Large-Pore Zincophosphate Built Up from a 12-Ring Architecture with a Remarkably Low Tetrahedral-Framework-Atom Density

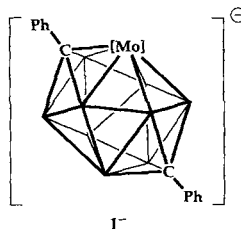
The spatial arrangement of ligands 1 oriented by the complexed template ion during polymerization explains the unexpectedly high $\text{Cu}^{2+}:\text{Fe}^{3+}$ selectivity of the polymer formed from $[\text{Zn}(\text{1})]^{2+}$ with a cross-linking agent, divinylbenzene. The ionic radius of the Cu^{2+} ion is similar to that of the Zn^{2+} template. The distinct loss of Zn^{2+} on polymerization strongly suggests that a sandwich arrangement results; that is, the $[\text{Zn}(\text{1})_2]^{2+}$ complex forms from $[\text{Zn}(\text{1})]^{2+}$.



H. Chen, M. M. Olmstead, R. L. Albright,
J. Devenyi, R. H. Fish* 642–645

Metal-Ion-Templated Polymers: Synthesis and Structure of *N*-(4-Vinylbenzyl)-1,4,7-Triazacyclononanezinc(II) Complexes, their Copolymerization with Divinylbenzene, and Metal-Ion Selectivity Studies of the Demetallated Resins—Evidence for a Sandwich Complex in the Polymer Matrix

After more than 30 years of speculation on the mechanism of the isomerization of icosahedral carboranes and their analogues, isolation of I^- provides the first clue. This intermediate has an unprecedented, closed, nonicosahedral structure. $[\text{Mo}] = [\text{Mo}(\eta^3\text{-C}_3\text{H}_5)(\text{CO})_2]$.



S. Dunn, G. M. Rosair, Rh. Ll. Thomas,
A. S. Weller, A. J. Welch* 645–647

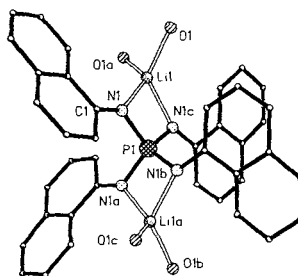
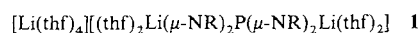
Isolation of a Nonicosahedral Intermediate in the Isomerization of an Icosahedral Metallocarborane

Penicillin G acylase from *E. coli* was used to cleave the phenylacetyl group—the first enzyme-labile protecting group for the amino function of nucleobases. Now protected oligonucleotides can be unmasked both in solution and on solid supports with this versatile enzyme under mild conditions (pH 7, room temperature). These results may lead to the development of new enzymatic reactions in oligonucleotide and solid-phase chemistry as well as in combinatorial chemistry.

H. Waldmann,* A. Reidel 647–649

The Phenylacetyl Group—The First Amino Protecting Group That Can Be Removed Enzymatically from Oligonucleotides in Solution and on a Solid Support

The product of 1-aminonaphthalene and P_2I_4 reacts with $n\text{BuLi}$ to form complex **1**, whose anion (structure on the right; only oxygen atoms of thf ligands are shown) is isoelectronic with orthophosphate. $\text{R} = \text{naphthyl}$.



P. R. Raithby, C. A. Russell,*
A. Steiner, D. S. Wright 649–650

A Tetrakis(imido) Phosphate Anion Isoelectronic with PO_4^{3-}

* Author to whom correspondence should be addressed

BOOKS

| | |
|---|---|
| Lise Meitner: A Life in Physics · R. L. Sime | <i>G. B. Kauffman, L. M. Kauffman</i> 661 |
| Deciphering the Chemical Code · N. D. Epitotis | <i>W. Koch</i> 662 |
| Physical Inorganic Chemistry. A Coordination Chemistry Approach · S. F. A. Kettle | <i>R. van Eldik</i> 663 |
| Introduction to Molecular Dynamics and Chemical Kinetics · G. D. Billing, K. V. Mikkelsen | <i>N. P. Ernsting, N. Heineking</i> 664 |
| Directory of Solvents · B. P. Whim, P. G. Johnson | <i>C. Reichardt</i> 665 |
| Chemistry of the Environment · T. C. Spiro, W. M. Stigliani | <i>Y. Zuo, Y. Deng</i> 666 |
| Electrochemical Processes for Clean Technology · K. Scott | <i>F. Beck</i> 667 |

German versions of all reviews, communications, and highlights in this issue appear in the second March issue of *Angewandte Chemie*. The appropriate page numbers can be found at the end of each article and are also included in the Author Index on p. 659.

All the Tables of Contents from 1995 onwards may be
found on the WWW under:
<http://www.vchgroup.de/home/angewandte>

SERVICES

| | |
|----------------|-----|
| ● Keywords | 658 |
| ● Author Index | 659 |
| ● Preview | 660 |

ANGEWANDTE CHEMIE

A Journal of the
Gesellschaft
Deutscher Chemiker

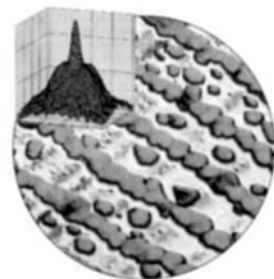
International Edition in English

1997
36/5

Pages 421–538

COVER PICTURE

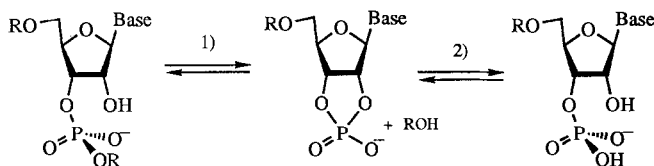
The cover picture shows, at the top left, a two-dimensional intensity profile of a (0,0) reflection that was obtained by low-energy electron diffraction. In this case the sample was a thin, well-ordered aluminum oxide film, which was prepared on a NiAl(110) crystal by oxidation in an ultrahigh vacuum apparatus, and subsequently coated with rhodium by vapor deposition at room temperature. At this temperature rhodium grows in the form of small particles that develop preferably on defects of the oxide film. It is clear from the scanning tunneling micrograph (cover background) that the particles form parallel rows. These lines can be identified as borders between antiphase domains of the oxide film. The anisotropic diffuse shoulder around the reflection is the result of an anisotropic correlation of the positions of the islands resulting from the network of the domain borders. More about the structural characterization of small metal particles on oxide surfaces, their electronic structure, and their adsorption behavior is reported in the review by H.-J. Freund on pages 452ff.



REVIEWS

Contents

Among the points of contention in discussions on the mechanism of RNA hydrolysis are the roles of acids and bases, the timing of proton transfers, and the reactivity of the phosphorane intermediate (see below; 1) transesterification–cleavage, 2) hydrolysis). Detailed and careful analysis of the available experimental and theoretical data have led to the formulation of two mechanisms, which differ primarily in the protonation state of the phosphorane intermediate.



D. M. Perreault,
E. V. Anslyn* 432–450

Unifying the Current Data on the Mechanism of Cleavage–Transesterification of RNA

Major advances have been made in surface chemistry and physics over the last 30 years. These have a significant role for the understanding of elementary steps in heterogeneous catalytic processes. Initially the main focus of this research was on metal surfaces, but nowadays the techniques have developed to such an extent that better models for real catalyst surfaces can also be studied. This review describes, for instance, how model systems for dispersed transition-metal/support catalysts can be characterized in terms of their morphology and electronic structure as well as their adsorption and reaction capabilities.

H.-J. Freund* 452–475

Adsorption of Gases on Complex Solid Surfaces

HIGHLIGHTS

Contents

The more than two hundred papers that have appeared in 1996 in a relatively narrow field clearly show that something is happening in the area of titanosilicates, which are used as heterogeneous oxidation catalysts. Particularly important are those titanosilicate compounds which have a zeolite-type structure and those molecular precursors that serve as model substances.

R. Murugavel, H. W. Roesky* ... 477–479

Titanosilicates: Recent Developments in Synthesis and Use as Oxidation Catalysts

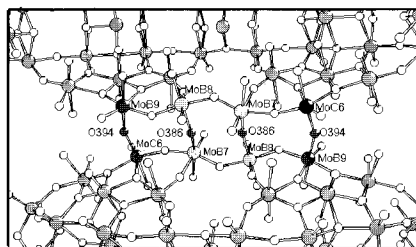
Mystery solved! The structural principles behind RNA's receptor properties have been probed by solution NMR studies of substrate/RNA aptamer complexes. Differences with the interactions in protein–DNA complexes are apparent. Small organic molecules recognize not merely nucleotide sequences but also certain three-dimensional structural motifs of the receptor.

M. Egli* 480–482

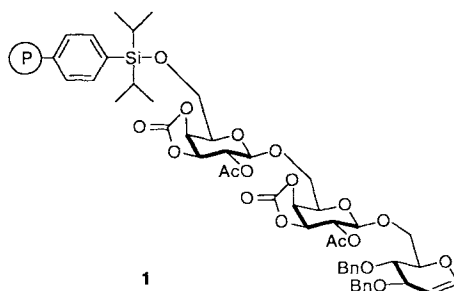
In Vitro Selected Receptors Rationalized: The First 3D Structures of RNA Aptamer/Substrate Complexes

COMMUNICATIONS

Rings containing 144 Mo atoms are linked by Mo–O–Mo bridges (depicted on the right) to form chains in the polyoxometalate presented here. The blue mixed-valent compound is formed by the reduction with iron powder of an acidified solution of polymolybdate in the presence of Na^+ ions.



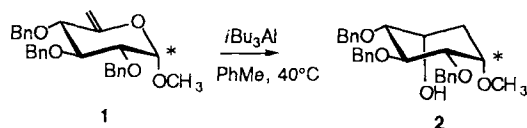
Four hours is all one needs to analyze trisaccharide **1**, the product of a multistep solid-phase synthesis, with high-resolution magic-angle-spinning NMR spectroscopy. This efficient method allows the investigation of the intermediates of a solid-phase synthesis as well as the determination of selectivity of independent coupling steps.



P. H. Seeberger,* X. Beebe,
G. D. Sukenick, S. Pochapsky,
S. J. Danishefsky* 491–493

Monitoring the Progress of Solid-Phase Oligosaccharide Synthesis by High-Resolution Magic Angle Spinning NMR: Observations of Enhanced Selectivity for β -Glycoside Formation from α -1,2-Anhydro-sugar Donors in Solid-Phase Couplings

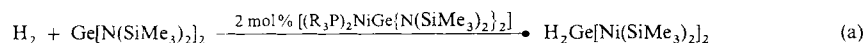
Retention of configuration at the anomeric carbon atom is observed for a novel rearrangement of carbohydrates. The readily accessible vinyl acetal **1** undergoes a triisobutylaluminum-assisted, stereoselective transposition of an oxygen atom on the ring with an exocyclic carbon atom. This reaction provides a new entry to the highly functionalized cyclohexane **2**.



S. K. Das, J.-M. Mallet,
P. Sinaÿ* 493–496

Novel Carbocyclic Ring Closure of Hex-5-enopyranosides

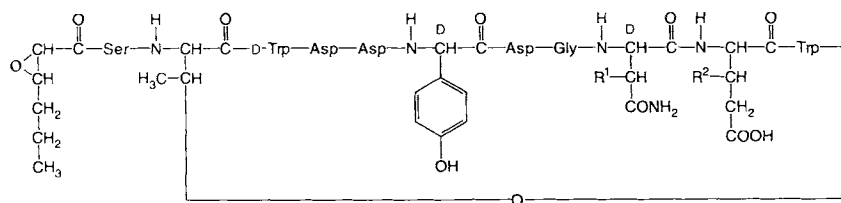
Mild conditions avoid the common problem of Ge–N bond scission in the stoichiometric and catalytic synthesis of a rare example of a stable bis(amino)germane from Group 10 metal–germylene complexes [Eq. (a), R = Et, Ph]. The reaction generates an interesting GeH₂ building block..



K. E. Litz, J. E. Bender IV, J. W. Kampf,
M. M. Banaszak Holl* 496–498

Transition Metal Germylene Complexes as Hydrogenation Catalysts: The Synthesis of a Rare Bis(amino)germane

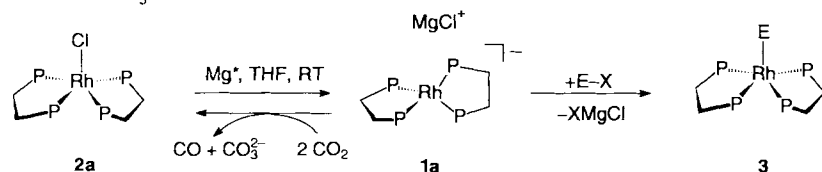
Only in the presence of Ca²⁺ are ions channels formed by peptides of the group of calcium-dependent antibiotics (CDA). O-Phosphorylated D-3-hydroxyasparagine is one of the unusual residues in the microheterogeneous CDA undecapeptide lactone isolated from *Streptomyces coelicolor* A3(2) (see below). By combination of modern analytical methods, such as the coupling of a gas-phase sequencer to a mass spectrometer, a total of four structures could be elucidated from only a few milligrams of product.



C. Kempter, D. Kaiser, S. Haag,
G. Nicholson, V. Gnau, T. Walk,
K. H. Gierling, H. Decker, H. Zähler,
G. Jung, J. W. Metzger* 498–501

CDA: Calcium-Dependent Peptide Antibiotics from *Streptomyces coelicolor* A3(2) Containing Unusual Residues

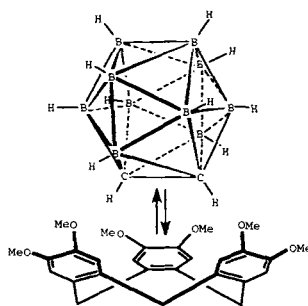
Interesting stoichiometric and catalytic reactions are possible with the rhodium phosphane complexes [$\{\text{Ph}_2\text{P}(\text{CH}_2)_n\text{PPh}_2\}_2\text{Rh}\}[\text{MgCl}]$ (**1**: **a**, $n = 2$; **b**, $n = 3$), which are readily accessible by reaction of the chloride complexes **2** with active magnesium. The “Grignard-analogous” compounds **1** react to form **3** ($E = \text{H}, \text{Me}, \text{SiMe}_3$) by protolysis, alkylation, and silylation. The interconversion of complexes **2a** and **1a** can be used for catalytic transfer of two electrons from magnesium to CO₂ to yield CO and CO₃²⁻.



B. Bogdanović,* W. Leitner,* C. Six,
U. Wilczok, K. Wittmann 502–504

“Grignard-Analogous” Rhodium Phosphane Complexes

An inclusion complex is formed between $o\text{-C}_2\text{B}_{10}\text{H}_{12}$ and cyclotrimeratrylene (CTV) in solution and in the solid state. The vector of approach of the carborane to the CTV cavity optimizes nonclassical hydrogen bonding between the C–H groups and the aromatic ring centroids (shown schematically, right). The energy of each interaction is calculated to be $2.72\text{ kcal mol}^{-1}$.



R. J. Blanch,* M. Williams, G. D. Fallon,
M. G. Gardiner, R. Kaddour,
C. L. Raston* 504–506

Supramolecular Complexation of 1,2-Dicarbadodecaborane(12)

Conjugated and nonconjugated diynes can be readily converted to poly(phenylene)-ethynylene derivatives and polyalkynynes by acyclic diyne metathesis. The catalyst for these condensation reactions is $[(t\text{BuO})_3\text{W}\equiv\text{CtBu}]$, and they proceed with cleavage of volatile alkynes such as 2-butyne and 3-hexyne. The chain lengths of the polymers are controlled by reaction temperature and pressure.

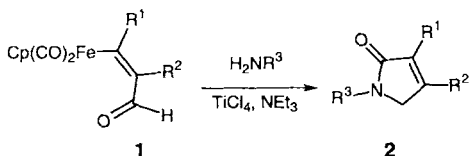
K. Weiss,* A. Michel, E.-M. Auth,
U. H. F. Bunz, T. Mangel,
K. Müllen 506–509

Acyclic Diyne Metathesis (ADIMET), an Efficient Route to Poly(phenylene)-ethynylenes (PPEs) and Nonconjugated Polyalkynynes of High Molecular Weight

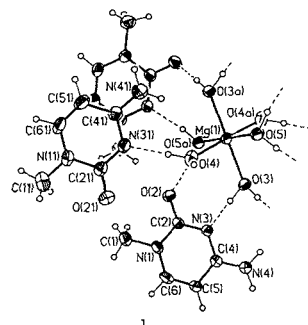
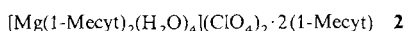
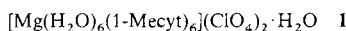
Domino processes to achieve C–C bond formation and carbonylation in the coordination sphere of the transition metal are possible for (Z)-configured, vinylogous iron formyl complexes **1**. Thus, γ -lactams **2** are formed by the TiCl_4 -mediated reaction of **1** with donor-substituted primary amines in the presence of NEt_3 .

K. Rück-Braun* 509–511

α,β -Unsaturated γ -Lactams from TiCl_4 -Mediated Transformations of Vinylogous Iron Formyl Complexes



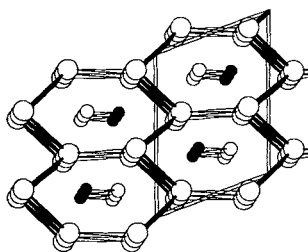
A hydrogen bonding network stabilizes the supramolecular assembly **1**, which comprises $[\text{Mg}(\text{H}_2\text{O})_6]^{2+}$ units and six methylcytosine (1-Mecyt) molecules (structure depicted on the right, three 1-Mecyt molecules omitted). Complex **1** is transformed with time into complex **2**, which contains two 1-Mecyt molecules directly linked through O(2) atoms to magnesium(II) ions.



M. A. Geday, G. De Munno,*
M. Medaglia, J. Anastassopoulou,
T. Theophanides 511–513

Supramolecular Assemblies Containing Nucleic Bases and Magnesium(II) Hexahydrate Ions

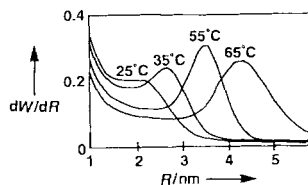
Planned synthesis in solid-state chemistry: Formal substitution of every other Ni atom in HfNi by P led, as predicted, to the synthesis of Hf_2NiP , which crystallizes in a monoclinic superstructure of the CrB structure type (structure depicted on the right; $\bullet = \text{Ni}$, $\circ = \text{P}$, $\bigcirc = \text{Hf}$). The resulting structural and physical differences between the phases HfNi and Hf_2NiP are discussed.



H. Kleinke, H. F. Franzen* 513–516

Hf_2NiP : The Planned Modification of an Intermetallic Phase by (Formal) Substitution of Nickel by Phosphorus

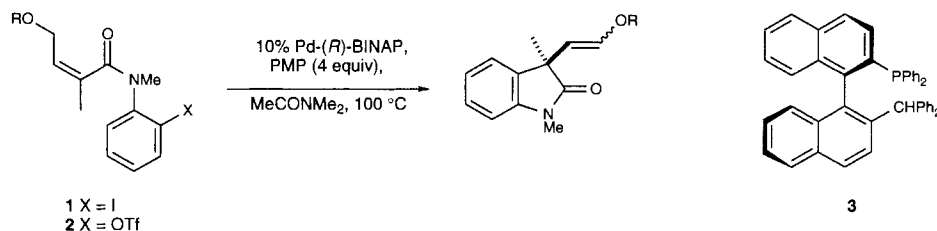
Nonionic polyethylene oxide surfactants are versatile structure-directing agents for the assembly of mesoporous molecular sieves, but their greatest benefit may lie in their ability to control the pore size of the mesostructure by the assembly temperature (see dependence of pore diameter R on temperature shown on the right). For mesostructured silicas with wormhole motifs, the average pore diameter can be altered by as much as 2.4 nm by varying the assembly temperature over a relatively narrow range below the cloud point temperature of the surfactant.



E. Prouzet, T. J. Pinnavaia* 516–518

Assembly of Mesoporous Molecular Sieves Containing Wormhole Motifs by a Non-ionic Surfactant Pathway: Control of Pore Size by Synthesis Temperature

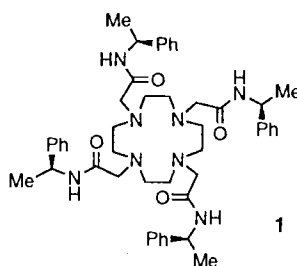
Both phosphorus atoms of the bis(phosphane) BINAP and the iodide ion are bound to Pd during the enantioselective step of the asymmetric Heck cyclization of iodide **1**. This is the conclusion of an investigation of the halide effect on Pd-(*R*)-BINAP-catalyzed cyclization of triflate **2** and the cyclization of iodide **1** with Pd-(*R*)-**3**, a model for a monocoordinated Pd-BINAP catalyst. BINAP-catalyzed reaction with **1**—or **2** in the presence of Cl[−], Br[−], or I[−]—proceeds to give **4** with an *ee* value of greater than 90%. PMP = 1,2,2,6,6-pentamethylpiperidine.



L. E. Overman,* D. J. Poon 518–521

Asymmetric Heck Reactions via Neutral Intermediates: Enhanced Enantioselectivity with Halide Additives Gives Mechanistic Insights

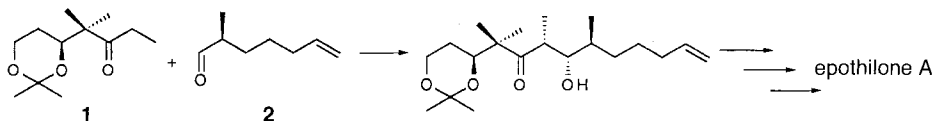
The enantiopure europium and terbium complexes of the macrocyclic ligand **1** are conformationally rigid in solution. The cationic terbium complex gives rise to an intense circularly polarized emission, which offers much promise for its use as a chiral probe.



R. S. Dickens, J. A. K. Howard, C. W. Lehmann, J. Moloney, D. Parker,* R. D. Peacock 521–523

Structural Rigidity and Luminescence of Chiral Lanthanide Tetraamide Complexes Based on 1,4,7,10-Tetraazacyclododecane

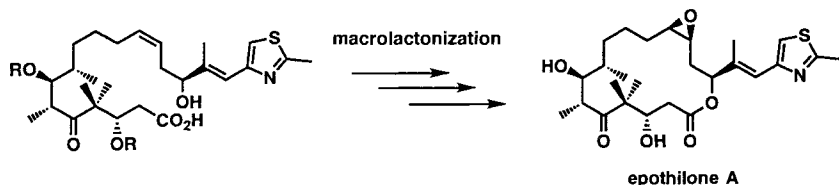
High diastereoselectivity is observed for the aldol reaction of the optically active building blocks **1** and **2**. Another key step in the total synthesis of epothilone A is a ring-closing metathesis. This highly convergent strategy offers many alternatives for the synthesis of biologically active analogs.



D. Schinzer,* A. Limberg, A. Bauer, O. M. Böhm, M. Cordes 523–524

Total Synthesis of (–)-Epothilone A

This highly convergent and practical total synthesis of the antitumor agent epothilone A uses a macrolactonization (see below) as the key step. The strategy may provide access to a variety of epothilones desirable for biological screening.



K. C. Nicolaou,* F. Sarabia, S. Ninkovic, Z. Yang 525–527

Total Synthesis of Epothilone A: The Macrolactonization Approach

* Author to whom correspondence should be addressed

BOOKS

| | |
|---|--|
| Science of Fullerenes and Carbon Nanotubes · J. S. Dresselhaus, G. Dresselhaus, P. C. Eklund | <i>L. Dunsch</i> 529 |
| Comprehensive Supramolecular Chemistry · J. L. Atwood, J. E. D. Davies, D. D. MacNicol, F. Vögtle, J.-M. Lehn | <i>B. König</i> 530 |
| The Crystal as a Supramolecular Entity · G. R. Desiraju | <i>J. S. Moore</i> 531 |
| Energetics of Organic Free Radicals · J. A. M. Simões, A. Greenberg, J. F. Liebman | <i>J. Hartung</i> 532 |
| The Chemistry of Free Radical Polymerization · G. Moad, D. H. Solomon | <i>O. Nuyken</i> 532 |
| Polypropylene Handbook. Polymerization, Characterization, Properties, Processing, Applications · E. P. Moore, Jr | <i>W. Spaleck</i> 534 |
| The Chemistry of Paper · J. C. Roberts | <i>R. Dyllick-Brenzinger</i> 534 |

German versions of all reviews, communications, and highlights in this issue appear in the first March issue of *Angewandte Chemie*. The appropriate page numbers can be found at the end of each article and are also included in the Author Index on p. 537.

SERVICES

| | |
|----------------|-----|
| • Classified | 430 |
| • Events | 431 |
| • Keywords | 536 |
| • Author Index | 537 |
| • Preview | 538 |

All the Tables of Contents from 1995 onwards may be found on the WWW under:
<http://www.vchgroup.de/home/angewandte>

ANGEWANDTE CHEMIE

A Journal of the
Gesellschaft
Deutscher Chemiker

International Edition in English

1997
36/4

Pages 303–420

COVER PICTURE

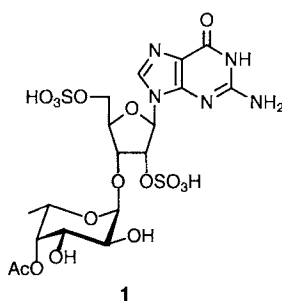
The cover picture shows a “wheel with a hydrocarbon tire”. This is how the authors F. H. Köhler et al. describe the molecule that they isolated from the reaction of FeCl_2 with tetrahydro-4,4,8,8-tetramethyl-4,8-disila-*s*-indacenediyl dilithium. In this hexane-soluble compound, seven ferrocene units are linked by seven pairs of Me_2Si groups to form an almost regular cycle. The compound can undergo three chemically reversible oxidations in which three, one, and again three electrons are transferred. More about this fascinating “super-ferrocene” is reported on pages 387 ff.



REVIEWS

Contents

Found previously nowhere else in nature, compounds with highly interesting functions were discovered amongst the low molecular weight components of spiders' silks and toxins. Examples are the long-chain, methyl-branched 1-methoxyalkanes, acyl-polyamines consisting of polyazaalkane chains linked to aromatic acids and amino acids, and the guanosine fucopyranoside derivative **1**. Isolation and identification of these compounds is difficult, because they are often available only in microgram quantities and in complex mixtures.



S. Schulz* 314–327

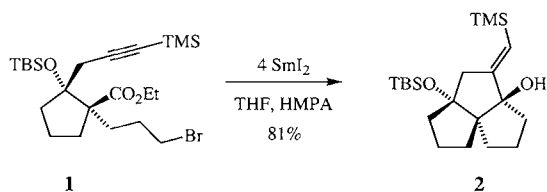
The Chemistry of Spider Toxins and Spider Silk

High thermal stabilities are a characteristic feature of ceramic Si/B/N/C materials, which consist of amorphous inorganic networks. For instance, SiBN_3C is not only the most stable nonoxide ceramic known to date with respect to oxidation but also under inert conditions it remains amorphous up to 1900°C . These properties are attributed to the presence of boron and carbon, which seem to occur in the ideal ratio. Additional advantages of this ceramic include its ready accessibility, its low thermal conductivity, and its high mechanical durability.

H.-P. Baldus, M. Jansen* 328–343

Novel High-Performance Ceramics—Amorphous Inorganic Networks from Molecular Precursors

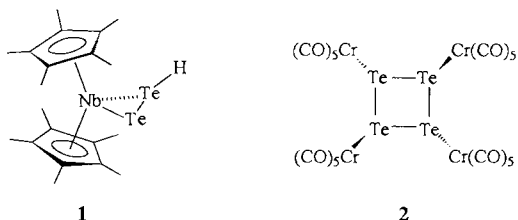
Complex polycyclic ring systems related to those of many natural products can be prepared from readily accessible starting materials by novel sequential reactions promoted by either SmI_2 or tetrathiafulvalene. Combinations of anionic and radical steps are possible, as in, for example, the SmI_2 -promoted transformation of **1** into **2** with twofold cyclization, which was described by Molander and Harris. TBS = $t\text{BuSiMe}_2$, TMS = Me_3Si , HMPA = $(\text{Me}_3\text{N})_2\text{PO}$.



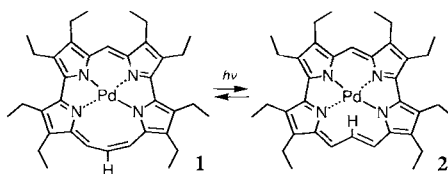
Coupling reactions in the coordination spheres of metal ions are the most important steps in the synthesis of very large inorganic ring complexes. The majority of such compounds can be categorized as coordination complexes. In addition, there are also examples from organometallic chemistry, such as the ferrocene scoop wheel presented by F. H. Köhler et al. in this issue. Before a planned synthesis of these compounds can be achieved, principles that govern the formation of these unusually large macrocycles must be determined. Insights into these principles are given herein.

COMMUNICATIONS

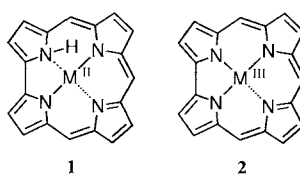
Elimination of tellurium from the niobocene complex 1, which contains the novel $\eta^2\text{-Te}_2\text{H}$ ligand, leads to the title compound **2** under the action of $[\text{Cr}(\text{CO})_5(\text{thf})]$. Characteristic for the structure of **2** is the folded four-membered ring in which all adjacent $\text{Cr}(\text{CO})_5$ fragments are in a *trans* arrangement.



Template-controlled syntheses open the way to stable metal complexes of the previously unknown, energy-rich porphyrin structural isomer isoporphycene. The rapid photochemical equilibrium between (*Z*)- and (*E*)-octaethylisoporphycene Pd complexes **1** and **2** confirms the prediction that (*Z*)- and (*E*)-isoporphycene have similar energies. The small Pd–H distance in **2**, a C–C–C bond angle of almost 150° in **1**, and parallels in ^1H NMR spectra to the all-*cis*- and the mono-*trans*-cyclononatetraenyl anion make **1** and **2** very interesting objects of study.



Until very recently the Ni and Cu corroles, already described in the sixties, were regarded as the M^{II} complexes **1** ($\text{M} = \text{Ni}, \text{Cu}$). Some doubt arose about this interpretation after the existence of Fe^{IV} corroles demonstrated that corroles can stabilize metals in unusual oxidation states. Thorough physical studies have now shown that the metal atoms in the Ni and Cu corroles do in fact have the formal oxidation state $+III$ (**2**).



T. Skrydstrup* 345–347

New Sequential Reactions with Single-Electron-Donating Agents

H. Plenio* 348–350

The Fascination of Large Rings: Cyclic Metal Complexes of Polydentate Ligands

O. Blacque, H. Brunner, M. M. Kubicki, B. Nuber, B. Stubenhofer, J. Wachter,* B. Wrackmeyer 352–353

Coordinative Stabilization of *cyclo*-Tetra-tellurium as $[\text{Te}_4\{\text{Cr}(\text{CO})_5\}_4]$: The First Organometallic Derivative of a Tellurium Allotrope

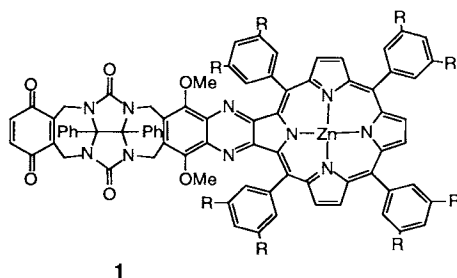
E. Vogel,* M. Bröring, C. Erben, R. Demuth, J. Lex, M. Nendel, K. N. Houk* 353–357

Palladium Complexes of the New Porphyrin Isomers (*Z*)- and (*E*)-Isoporphycene--Pd^{II}-Induced Cyclization of Tetrapyrrolealdehydes

S. Will, J. Lex, E. Vogel,* H. Schmickler, J.-P. Gisselbrecht, C. Hauptmann, M. Bernard, M. Gross* 357–361

Nickel and Copper Corroles: Well-Known Complexes in a New Light

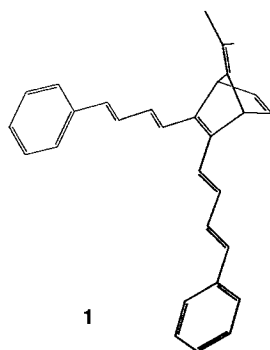
The photoinduced electron transfer between the zinc porphyrin and the quinone unit of the U-shaped host **1** ($R = t\text{Bu}$) is accelerated by an aromatic guest molecule complexed within its cavity. This rate enhancement is due to through-space electron transfer across the interspaced guest. This process mimics the proposed behavior of some aromatic protein residues in certain photosynthetic centers.



J. N. H. Reek, A. E. Rowan, R. de Gelder, P. T. Beurskens, M. J. Crossley, S. De Feyter, F. de Schryver, R. J. M. Nolte* 361–363

Novel Cleft-Containing Porphyrins as Models for Studying Electron Transfer Processes

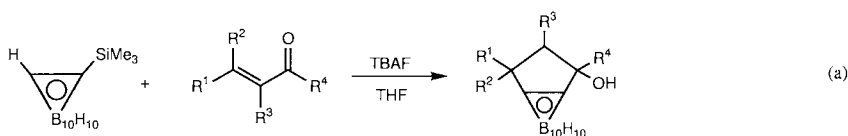
A new interpretation of the charge storage mechanism of conducting polymers is provided by the results of cyclic voltammetric studies of diphenylpolyenes like **1**. For the first time these investigations indicate the formation of σ bonds in the reversible dimerization of radical cations of these conjugated systems. Furthermore, these reactions also have general importance for the understanding of the chemistry of radical ions.



A. Smie, J. Heinze* 363–367

Reversible Dimerization of Diphenylpolyene Radical Cations: An Alternative to the Bipolaron Model

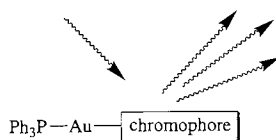
Carborane-annulated cyclopentanols were produced by the reaction between 1,2-carboranes as dianionic C_2 building blocks and α,β -unsaturated ketones or aldehydes as dicationic C_3 units [see, for example, Eq. (a)]. This is a conceptionally unusual route to five-membered carbocycles.



H. Nakamura, K. Aoyagi, B. Singaram, J. Cai, H. Nemoto, Y. Yamamoto* 367–369

A Novel [3+2] Annulation between *ortho*-Carboranyltrimethylsilane and Conjugated Carbonyl Compounds

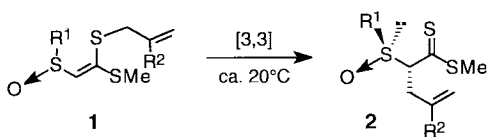
The largest cubic nonlinear optical activities thus far determined for monomeric organometallic complexes in solution (schematic representation on the right) have been found for alkynyl(triphenylphosphane)gold complexes. In structure–property studies the influence of structural changes in the chromophore on the nonlinear response was systematically investigated.



I. R. Whittall, M. G. Humphrey,* M. Samoc, B. Luther-Davies 370–371

Molecular Cubic Hyperpolarizabilities of Systematically Varied (Triphenylphosphane)gold- σ -Arylalkynyl Complexes

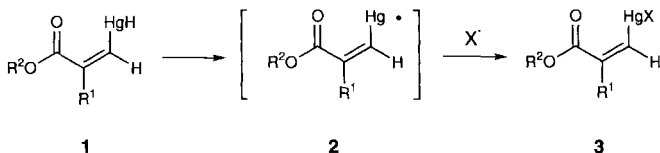
Diastereomeric excesses up to 98 % are a characteristic of the Claisen rearrangement of ketene dithioacetals **1**, which contain a chiral sulfinyl group, to afford γ -unsaturated α -sulfinyl dithioesters **2**. This reaction is the first example of a [3,3] rearrangement whose stereochemical course is controlled by a sulfinyl group. Owing to the mild thermal conditions (room temperature) undesired elimination of sulfenic acid was not observed.



C. Alayrac, C. Fromont, P. Metzner,* N. T. Anh 371–374

First Examples of a Claisen Rearrangement Stereocontrolled by a Sulfinyl Group: Synthesis of Novel α -Sulfinyl Dithioesters

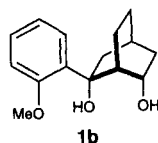
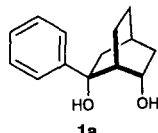
A remarkably long half-life of 74 h has been observed for the HgH-substituted *p*-nitrophenylacrylate **1** ($R^1 = \text{Et}$, $R^2 = p\text{-NO}_2\text{C}_6\text{H}_4$) at 75 °C in C_6D_6 . This unusual stability stems from the electron-withdrawing effects of the acrylic ester moiety, as revealed by quantum mechanical calculations. The corresponding organomercury radical **2** is also stable enough to be trapped intermolecularly (\rightarrow **3**; $\text{X} = \text{Cl}, \text{Br}$).



E. Nakamura,* Y. Yu, S. Mori,
S. Yamago 374–376

Unusually Stable Organomercury Hydrides
and Radicals

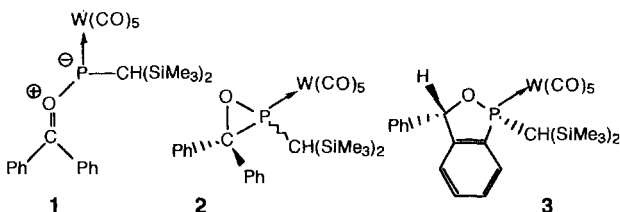
High to moderate enantiomeric excesses were achieved for the reduction of ketones with catecholborane in the presence of a titanium-based catalyst bearing the new optically active diols **1a** or **1b** as ligands. Of particular interest is the relatively high enantiomeric excess obtained in the reductions of linear nonaromatic methyl ketones.



F. Almqvist, L. Torstensson,
A. Gudmundsson, T. Frejd* 376–377

New Ligands for the Titanium(IV)-Induced
Asymmetric Reduction of Ketones with
Catecholborane

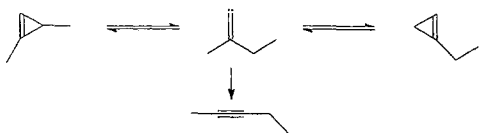
Thermolysis of a 2*H*-azaphosphirene tungsten complex in the presence of benzophenone generates the phosphacarbonyl ylide complex **1** as an intermediate, as confirmed by the formation of the complexes **2** and **3**. The use of acetophenone and (*E*)-*N*-methyl(benzylidene)amine as trapping reagents leads to an acyclic rearrangement product and an azaphosphiridine tungsten complex, respectively.



R. Streubel,* A. Ostrowski,
H. Wilkens, F. Ruthe, J. Jeske,
P. G. Jones 378–381

Unexpected Intramolecular Reactions of
Intermediate Phosphacarbonyl Ylide
Tungsten Complexes

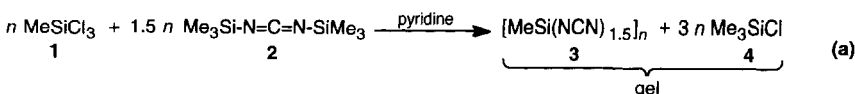
Cyclopropenes interconvert upon heating! This remarkable process takes place via vinylidene intermediates, namely unsaturated carbenes that are also involved in the ring opening of these highly strained hydrocarbons (see below).



H. Hopf,* W. Graf von der Schulenburg,
R. Walsh* 381–383

Direct Study of a Nondegenerate Cyclo-
propene-to-Cyclopropene Isomerization

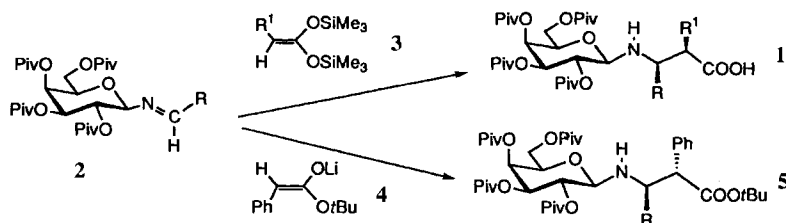
A crack-free, transparent monolithic gel composed of **3** and **4** is obtained from silane **1** and carbodiimide **2**. This is the first example of the application of the sol–gel process, which has frequently been used for the synthesis of oxidic glasses and ceramics, to nonoxidic systems for the preparation of oxygen-free Si–C–N ceramics.



A. O. Gabriel, R. Riedel* 384–386

Preparation of Non-Oxidic Silicon Ceram-
ics by an Anhydrous Sol–Gel Process

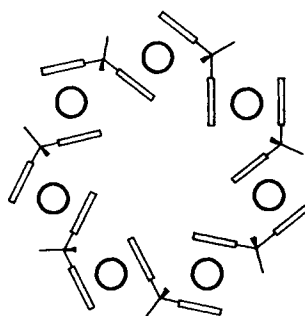
α -Branched β -amino acids 1 with *erythro* configuration can be made selectively and with high asymmetric induction by the reaction of O-pivaloyl-protected *N*-galactosylaldimines 2 with prochiral bis(silyl) ketene acetals 3. The corresponding reaction with the prochiral lithium ester enolate 4 exclusively leads to the *threo*-configured β -amino acid derivatives 5.



H. Kunz,* A. Burgard,
D. Schanzenbach 386–387

Asymmetric Mannich Synthesis of β -Amino Acids with Two New Stereogenic Centers at the α and β Positions

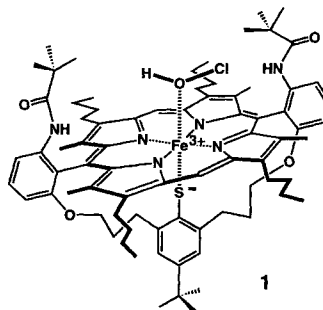
What looks like a scoop wheel on the right are seven ferrocene units, which are linked by four Me_2Si groups to the two nearest neighbors. The cycle, which is formed in a polygemination reaction (that is, the reaction of a transition metal halide with a biscyclopentadienyl dianion to give a polymer), has the rare C_{7h} symmetry (idealized). The compound is stable up to 360 °C and can be oxidized in three steps up to a heptacation.



B. Grossmann, J. Heinze, E. Herdtweck,
F. H. Köhler,* H. Nöth, H. Schwenk,
M. Spiegler, W. Wachter,
B. Weber 387–389

Seven Doubly Bridged Ferrocene Units in a Cycle

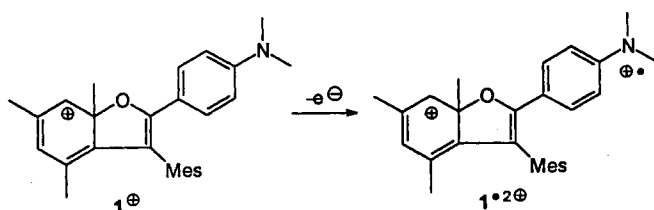
The iron(III) porphyrin 1 catalyzes the chlorination of activated C–H bonds. It is therefore a model compound for the as yet unidentified intermediate of the catalytic cycle of the heme–thiolate protein chloroperoxidase (CPO). Neither “free HOCl” nor Cl^\bullet are involved in the CPO-catalyzed chlorination, but rather an iron-bound HOCl is the source of Cl^+ .



H.-A. Wagenknecht,
W.-D. Woggon* 390–392

New Active-Site Analogues of Chloroperoxidase—Syntheses and Catalytic Reactions

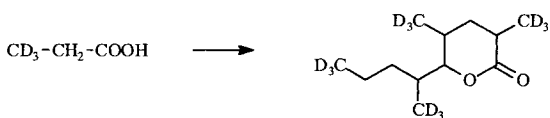
Almost completely unknown—the chemistry of radical dications. A reactive intermediate of this type ($1^{\bullet 2+}$) plays a key role in the oxidative rearrangement of the persistent cation **1**⁺.



M. Schmittl,* A. Langels 392–395

A Short-Lived Radical Dication as a Key Intermediate in the Rearrangement of a Persistent Cation: The Oxidative Cyclization of 2,2-Dimesityl-1-(4-*N,N*-dimethylaminophenyl)ethanol

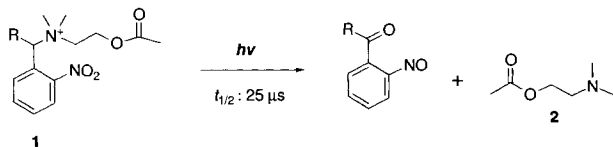
On the trail of ants! For the first time the biosynthesis of trail pheromones in ants of one subfamily could be traced. The odorous substances are formed by the lipid metabolism pathway by incorporation of acetate or propionate or both, as shown by feeding experiments with deuterated compounds (see below).



H. J. Bestmann,* E. Übler,
B. Hölldobler 395–397

First Biosynthetic Studies on Trail Pheromones in Ants

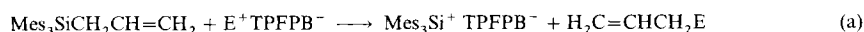
The rapid and efficient photochemical release of noracetylcholine **2**, an analogue of the neurotransmitter acetylcholine, from its precursor **1** makes this probe well-suited for a dynamic study of the mechanism of hydrolysis of acetylcholine by acetylcholinesterase. The nitrobenzyl derivative **1**, the most promising candidate for time-resolved crystallographic studies of this rapid enzyme, displays the required photo-fragmentation kinetics in the microsecond time-range and inhibitory properties of acetylcholinesterase.



L. Peng, J. Wirz,
M. Goeldner* 398–400

Synthesis and Characterization of Photo-
labile Compounds Releasing Noracetyl-
choline in the Microsecond Time Range

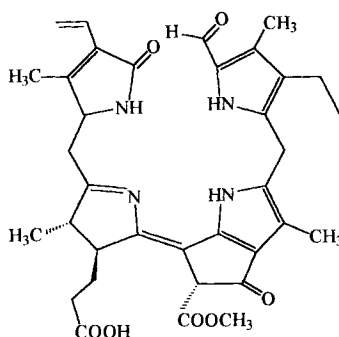
Clever choice of a leaving group produced the first free silylium ion, Mes_3Si^+ [Eq. (a)]. The low-field resonance at $\delta = 225.5$ is characteristic for the tricoordinated triarylsilylium ion. Constancy of this value in several aromatic solvents indicates that the silicon center is well protected by the *ortho* methyl groups. Mes = 2,4,6-trimethylphenyl, TPFPB^- = tetrakis(pentafluorophenyl)borate.



J. B. Lambert,* Y. Zhao 400–401

The Trimesitylsilylium Cation

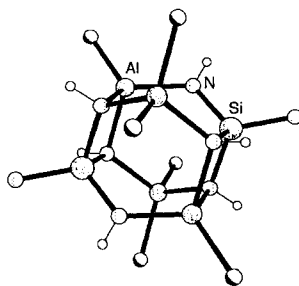
The biological enigma of the break-down of chlorophyll in plants only recently began to be understood. The structure elucidation of a “fluorescent” catabolite (depicted on the right) from senescent rape cotyledons provides further insight into this process. For this purpose, the catabolite was prepared from pheophorbide *a* with an enzyme extract from senescent chloroplasts.



W. Mühlecker, K.-H. Ongania,
B. Kräutler,* P. Matile,
S. Hörtensteiner 401–404

Tracking Down Chlorophyll Breakdown in
Plants: Elucidation of the Constitution of a
“Fluorescent” Chlorophyll Catabolite

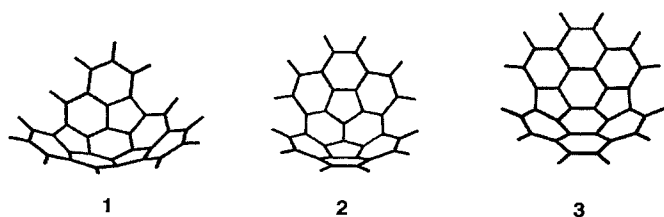
Access to iminoaluminosilicate chemistry has been achieved by the reaction of a soluble triaminosilane with Me_3Al . The resulting Si–Al–NH compound—the first of its kind—has a prismatic Si–Al–NH cage as the central structural unit (depicted on the right) and thus has a structure analogous to those of known siloxane cage compounds.



C. Rennekamp, A. Gouzyr, A. Klemp,
H. W. Roesky,* C. Brönneke, J. Kärcher,
R. Herbst-Irmer 404–406

Synthesis and Structure of the First
Si–Al–NH Cage Compound from a Stable
Triaminosilane and Trimethylaluminum

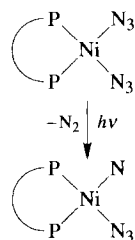
The missing links between the normal, planar polycyclic aromatic hydrocarbons and buckyballs are the bowl-shaped $\text{C}_{30}\text{H}_{12}$ buckybawls **1**, **2**, and **3**. All three were prepared by flash vacuum pyrolysis of suitable aromatic precursors. The best yields are obtained when radical centers are generated at defined positions by the homolysis of C–Br and C–C bonds to initiate the critical cyclizations.



S. Hagen, M. S. Bratcher,
M. S. Erickson, G. Zimmermann,
L. T. Scott* 406–408

Novel Syntheses of Three $\text{C}_{30}\text{H}_{12}$ Bowl-
Shaped Polycyclic Aromatic Hydrocarbons

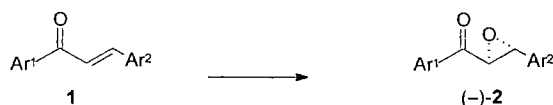
Insertions into C–H or C=C bonds and addition reactions with CO or CS₂ confirm the formation of nitrenenickel(II) complexes as intermediates in the photolysis of diazido(phosphane)nickel(II) complexes. Without reactive substrates the nitrene intermediates decay to coordinatively unsaturated phosphane–nickel(0) complexes, which may initiate the photocatalytic cyclization of alkynes to the corresponding benzene derivatives. \widehat{PP} = bis(phosphane) ligand or (PEt₃)₂.



H. Hennig,* K. Hofbauer, K. Handke,
R. Stich 408–410

Unusual Reaction Pathways in the Photolysis of Diazido(phosphane)nickel(II) Complexes: Nitrenes As Intermediates in the Formation of Nickel(0) Complexes

A new, efficient use for that most venerable chiral ligand, diethyl tartrate: Chalcone derivatives **1** can be converted, as shown below, into the corresponding epoxy ketones (–)-**2** with good to excellent enantiomeric excess by using *tert*-butyl hydroperoxide in the presence of catalytic amounts of dibutylmagnesium (10 mol%) and (+)-diethyl tartrate (11 mol%).



C. L. Elston, R. F. W. Jackson,*
S. J. F. MacDonald,
P. J. Murray 410–412

Asymmetric Epoxidation of Chalcones with Chirally Modified Lithium and Magnesium *tert*-Butyl Peroxides

* Author to whom correspondence should be addressed

BOOKS

Guidebook on Molecular Modeling in Drug Design • N. C. Cohen
Fundamental Principles of Molecular Modeling • W. Gans, A. Amann, J. C. A. Boeyens
Modelling Molecular Structures • A. Hinchliffe

D. Schomburg 413

Nonlinear Computer Modeling of Chemical and Biochemical Data •
J. F. Rusling, T. F. Kumosinski

J. Heinze 415

Understanding Medications. What the Label Doesn't Tell You • A. Burger

H. Waldmann 415

Ways to Successful Strategies in Drug Research and Development •
H. H. Sedlacek, A. M. Sapienza, V. Eid

K. Müller 416

Critical Success Factors in Biomedical Research and Pharmaceutical Innovations •
S. W. F. Omta

Combinatorial Peptide and Nonpeptide Libraries. A Handbook • G. Jung

J. T. M. Linders, H. C. J. Ottenheijm,
C. J. van Staveren 416

German versions of all reviews, communications, and highlights in this issue appear in the second February issue of *Angewandte Chemie*. The appropriate page numbers can be found at the end of each article and are also included in the Author Index on p. 419.

SERVICES

| | |
|----------------|-----|
| • Corrigendum | 412 |
| • Keywords | 418 |
| • Author Index | 419 |
| • Preview | 420 |
| • Sources | A11 |

All the Tables of Contents from 1995 onwards may be found on the WWW under <http://www.vchgroup.de/home/angewandte>

ANGEWANDTE

CHEMIE

A Journal of the
Gesellschaft
Deutscher Chemiker

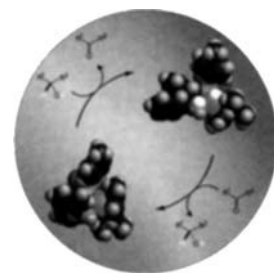
International Edition in English

1997
36/3

Pages 177–302

COVER PICTURE

The cover picture shows the molecular structures of two chiral ruthenium complexes that mediate the asymmetric hydrogen transfer between 2-propanol and ketones: on the violet background an amidoruthenium(II) and an amine(hydrido)ruthenium complex (yellow). The examination of the reactivities of the two complexes as well as the kinetics of the reaction showed that these two compounds are the only intermediates in this catalytic hydrogen transfer involving secondary alcohols and ketones. In principle this two-component catalytic cycle can continue indefinitely. The structural characteristics and the synthetic utility of these chiral complexes in asymmetric synthesis are discussed by R. Noyori et al. in two communications on pages 285 ff. and 288 ff.



REVIEWS

Contents

Organometallic reagents of unsurpassed versatility! Organocopper reagents are superbly suited for stereo- and regioselective syntheses, in particular those based on conjugate additions and S_N2' reactions. They have thus become indispensable in the synthesis of complex natural products and pharmaceuticals, chiral auxiliaries, and molecules with interesting structural features. One of the important new developments in this area is the extension of Michael additions to 1,6-, 1,8-, 1,10-, and 1,12-additions to acetylenic substrates.

N. Krause,* A. Gerold 186–204

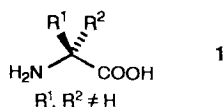
Regio- und Stereoselective Syntheses with
Organocopper Reagents

Superheated solvents such as water, methanol, and amines at temperatures in the range 110–220 °C provide expedient polar reaction media for the designed construction of chalcogenide-based open-sheet and framework materials. Such conditions greatly enhance solubility, diffusion, and crystallization, but are still mild enough to leave molecular units such as chains and rings intact to participate in the self-assembly of zeolite-like structures. Methanolothermal techniques are particularly suitable for the preparation of Se- and Te-based frameworks.

W. S. Sheldrick,*
M. Wachhold 206–224

Solventothermal Synthesis of Solid-State
Chalcogenidometalates

The repertoire for the synthesis of α -alkylated α -amino acids **1** is restricted, but constantly expanding. Since these amino acids are of interest for the construction of peptides with a fixed conformation, as ligands for enantioselective catalytic aldol reactions, and also from a pharmaceutical point of view, the development of simple methods to synthesize these important, nonproteinogenic amino acids is still a challenge for the synthetic chemist.



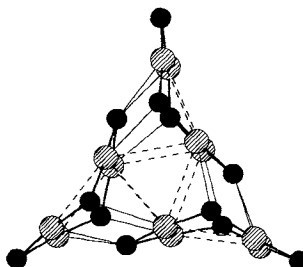
T. Wirth* 225–227
New Strategies to α -Alkylated α -Amino Acids

COMMUNICATIONS

Clusters containing 18, 45, and 50 silver atoms can be synthesized from the reaction of AgCl with PhP(SiMe₃)₂ in the presence of PnPr₃. The structures of the phosphinidene-bridged silver clusters formed depends upon the temperature and the stoichiometric ratio of the reactants. [Ag₅₀(PPh)₂₀Cl₇P(PnPr₃)₁₃] is the biggest known silver cluster and one of the largest structurally characterized cluster complexes to date.

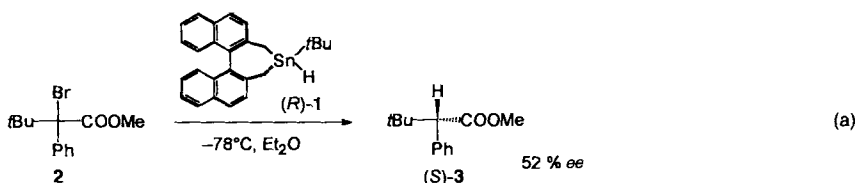
D. Fenske,* F. Simon 230–233
Phosphinidene-Bridged Silver Clusters

A phosphinidene-bridged multinuclear mercury complex is now accessible in high yield from the reaction of [Fe(CO)₄(HgOAc)₂] with *t*BuP(SiMe₃)₂. The crystal structure of the title compound is depicted on the right (Hg striped, P black). In order to describe the bonding in this trimer of (HgP) eight-membered rings, the structures of (HgPMe)_{*n*} clusters (*n* = 2–6, 8, 12) were calculated by using ab initio methods.



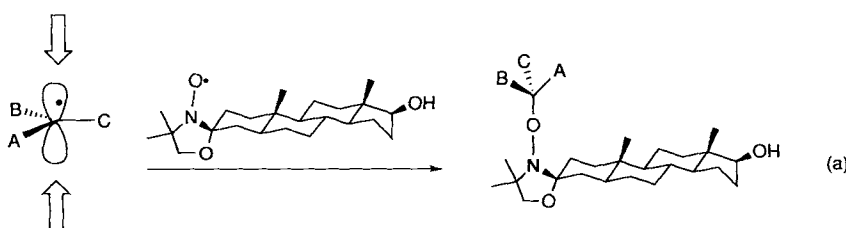
R. Ahlrichs,* M. von Arnim,
J. Eisenmann, D. Fenske* 233–235
[(HgPtBu)₄]₃—Synthesis, Structure, and Bonding

Synthetically useful enantiomeric excesses were obtained for the first time in radical reductions with optically active tin hydrides, as illustrated in the reaction of **2** with **1** [Eq. (a)]. Moreover, the reaction can also be performed catalytically by using the appropriate tin bromide and Na[B(CN)H₃] instead of **1**.



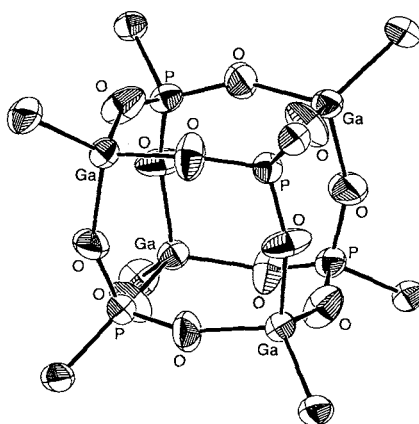
M. Blumenstein, K. Schwarzkopf,
J. O. Metzger* 235–236
Enantioselective Hydrogen Transfer from a Chiral Tin Hydride to a Prochiral Carbon-Centered Radical

Differentiation between the two enantiotopic faces of prochiral carbon radicals by optically active nitroxyl radicals is demonstrated in this novel approach to the control of stereochemistry. In the first experiments, the steroid nitroxyl radical shown in Equation (a) gave selectivities of up to 92:8.



R. Braslau,* L. C. Burrill II,
L. K. Mahal, T. Wedeking 237–238
A Totally Radical Approach to the Control of Stereochemistry: Coupling of Prochiral Radicals with Chiral Nitroxyl Radicals

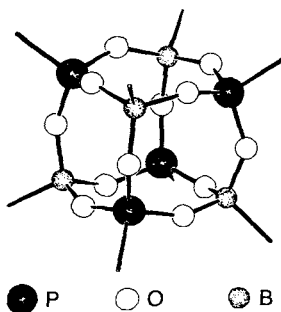
A potential precursor to new gallophosphate materials. The cubic $\text{Ga}_4\text{P}_4\text{O}_{12}$ unit common to several gallophosphate molecular sieves has now been prepared in a soluble, molecular form. On the right is shown the $\text{Ga}_4\text{P}_4\text{O}_{12}$ core of $[\text{tBuGa}(\mu_3\text{-O}_3\text{PPh})]_4$ as confirmed by X-ray crystallography.



M. R. Mason,* M. S. Mashuta,
J. F. Richardson 239–241

Cyclic and Cubic Organophosphonates of Gallium and Their Relationship to Structural Motifs in Gallophosphate Molecular Sieves

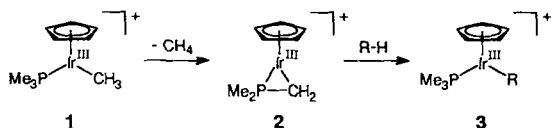
Molecules that behave like large atoms!—molecules of the mixed anhydride formed from the acids tBu-P(O)(OH)_2 and PhB(OH)_2 exhibit this characteristic since in the crystal lattice they occupy the corners and centers of weakly distorted cubooctahedra. The molecules reveal a cubane framework (depicted on the right), whose corners are occupied alternately by phosphorus and boron atoms and whose edges are bridged by oxygen atoms.



K. Diemert, U. Englert, W. Kuchen,*
F. Sandt 241–243

A Cage Molecule with a Cubanoid P_4B_4 Framework: $\text{tBu}_4\text{P}_4\text{Ph}_4\text{B}_4\text{O}_{12}$ —A Structural Analogue of the Isovalence Electronic Organosilasesquioxanes $\text{R}_8\text{Si}_8\text{O}_{12}$

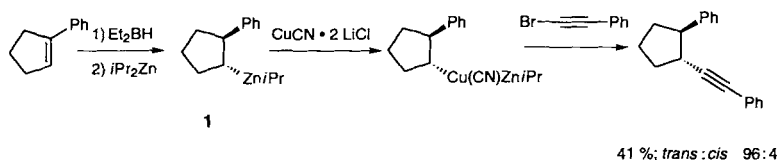
An unexpected dissociative mechanism was found for the alkane activation reaction by cation **1** in the gas phase. The reactivity of **1** was studied by electrospray ionization of dilute solutions of $[\text{I}(\text{N}\equiv\text{CCH}_3)]^+\text{ClO}_4^-$. The reaction proceeds via the reactive cyclic Ir^{III} complex **2**, which then adds to the C–H bonds of saturated and aromatic hydrocarbons to form **3**.



C. Hinderling, D. A. Plattner,*
P. Chen* 243–244

Direct Observation of a Dissociative Mechanism for C–H Activation by a Cationic Iridium(III) Complex

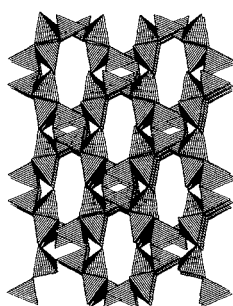
Configurationally well-defined cycloalkylzinc compounds (1) were prepared for the first time from olefins by hydroboration and subsequent boron–zinc exchange with iPr_2Zn . The resulting secondary alkylzinc reagents are configurationally stable and can be allylated or alkynylated stereoselectively in the presence of $\text{CuCN} \cdot 2\text{LiCl}$ with retention of configuration (see the example below).



L. Micouin, M. Oestreich,
P. Knochel* 245–246

Stereoselective Preparation and Reactions of Cycloalkylzinc Compounds

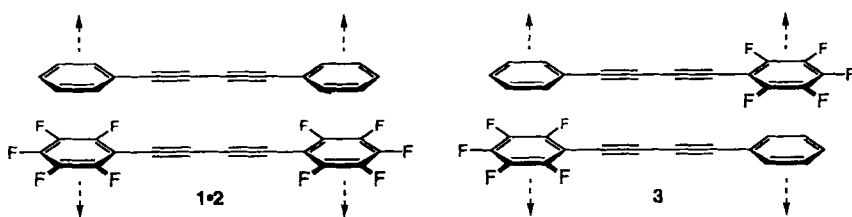
Coordination networks that mimic silicate mineral structures are formed by a new class of coordination polymers, which are accessible through the self-assembly of tetrahedral copper(I) cations and bent, bifunctional pyrimidine ligands. Thus, extended organometallic frameworks can be produced, which show optical activity (as quartz), or microporosity (as zeolites)...or both! The first example of such a framework is $[\text{Cu}(\text{pyrimidine})_2]\text{BF}_4$ (depicted on the right), which can be described as a “stuffed feldspar”, and contains channels that house both BF_4^- ions and disordered solvent molecules.



S. W. Keller* 247–248

An Acentric, Three-Dimensional Coordination Polymer: Synthesis and Structure of $[\text{Cu}(\text{pyrimidine})_2]\text{BF}_4$

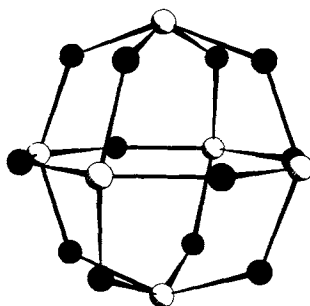
Photochemically induced polymerizations in the solid state of **1 · 2** and **3** depend on the intriguing interaction between phenyl and perfluorophenyl groups, which leads to an appropriate alignment of the molecules in the crystal. As with the 1:1 complex of benzene and hexafluorobenzene the diyne monomers are stacked alternately to form columns of arene groups.



G. W. Coates, A. R. Dunn,
L. M. Henling, D. A. Dougherty,*
R. H. Grubbs* 248–251

Phenyl–Perfluorophenyl Stacking Interactions: A New Strategy for Supramolecular Construction

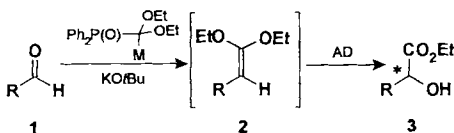
Strong electron-deficient bonds with four equivalent copper(I) centers as well as the carbon atom of the organic group are a feature of the thiolate sulfur atoms of the new cage $[(\text{CuCl})_{12}(\text{SR})_6]$ ($\text{R} = \text{CH}_2\text{CH}_2\text{NH}_3$; structure on the right, Cl and R omitted). This is part of the polymeric complex $[\text{Cu}_{13}\text{Cl}_{13}(\text{SR})_6]$, which is accessible from cysteamine hydrochloride and copper(I) chloride.



R. V. Parish,* Z. Salehi,
R. G. Pritchard 251–253

Five-Coordinate Sulfur in a Polymeric Copper(I) Thiolate Complex

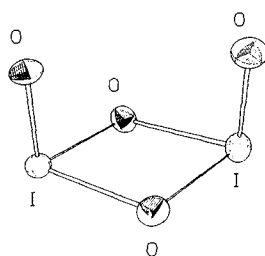
Efficient asymmetric formylation of aldehydes is possible by Horner–Wittig homologation of aldehydes and subsequent Sharpless asymmetric dihydroxylation of the intermediate prochiral ketene acetals **2**. As is demonstrated for compounds **1**, this novel sequence allows synthesis of α -hydroxy carboxylates **3** in high enantiomeric purity.



A. Kirschning,* G. Dräger,
A. Jung 253–255

A New Asymmetric Formylation of Aldehydes

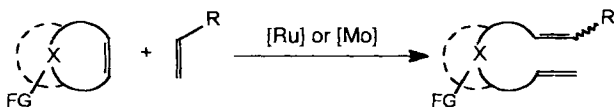
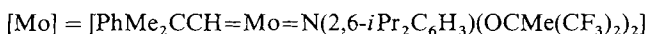
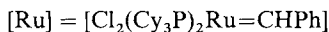
Unexpectedly a dimeric structure is found for the iodyl cation in $(\text{IO}_2)_2\text{S}_2\text{O}_7$. For the first time a representative of this type of complex cation could be characterized by X-ray crystal structure analysis (see picture). The description as an ionic crystal comprising $(\text{IO}_2)_2^{2+}$ and $\text{S}_2\text{O}_7^{2-}$ is an oversimplification because of the strong intermolecular bonds forming a polymeric network.



M. Jansen,* R. Müller 255–256

Constitution of the Iodyl Cation

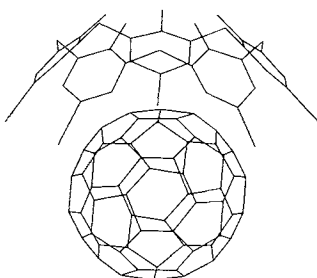
Not only high selectivity, but also atom economy are the attractive features of this synthetic strategy. Most crossed olefin metatheses between strained and monosubstituted olefins can be carried out with Grubbs's or Schrock's catalyst ($[\text{Ru}]$ and $[\text{Mo}]$, respectively, see below) even when the ratio of starting materials is 1:1! The high tolerance displayed towards many functional groups makes the prospect of subsequent reactions exciting.



M. F. Schneider, N. Lucas, J. Velder,
S. Blechert* 257–259

Selective Ring-Opening Olefin Metathesis of Functionalized Monosubstituted Olefins

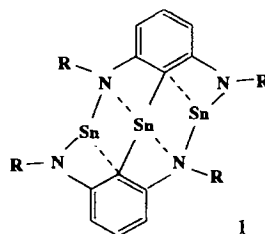
Usually the host, C_{60} is here the guest in a complex between C_{60} and calix[5]arenes (see picture) that was studied both in solution and in the solid state. In solution, as disclosed by the ring current method of analysis for ^{13}C NMR spectra based on the X-ray crystallographic analysis, van der Waals interactions between the host and guest play an important role in the complexation.



T. Haino, M. Yanase,
Y. Fukazawa* 259–260

New Supramolecular Complex of C_{60}
Based on Calix[5]arene—Its Structure in
the Crystal and in Solution

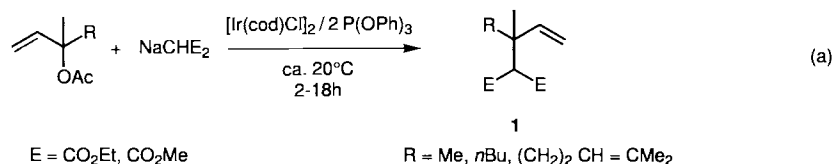
A nearly equilateral triangle is formed by the three Sn atoms in **1**. This complex is the product of a hitherto unknown 2-stannylation of a 1,3-diaminobenzene and is thus of general significance in the context of the metalation of arenes. $R = SiMe_3$.



H. Braunschweig, C. Drost,
P. B. Hitchcock, M. F. Lappert,*
L. J.-M. Pierrssens 261–263

A Dinuclear Tin(II) Amide, a *meta*-Stannyl-
aminocyclophane and Its Orthostannylated
Derivative, a Dimeric Trinuclear Tin(II)
Cluster

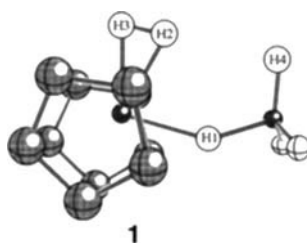
The selective construction of quaternary carbon centers, which are frequently found in natural products, is essential to many syntheses. A new method relying on the iridium complex $[Ir(cod)Cl]_2$ as the catalyst can be used for the allylic alkylation of acyclic compounds **1** [Eq (a)]. The products are obtained in yields between 70 and 85% and with a selectivity of 100%. cod = cyclooctadiene.



R. Takeuchi,* M. Kashio 263–265

Highly Selective Allylic Alkylation with a
Carbon Nucleophile at the More Substituted
Allylic Terminus Catalyzed by an Iridium
Complex: An Efficient Method for
Constructing Quaternary Carbon Centers

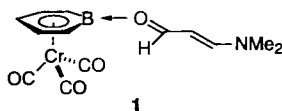
Theoretical evidence confirms the large influence that a Lewis acid (here BH_3) exerts on the type of H-coordination in metallocene trihydrides (here $[Cp_2NbH_3]$). The coordination of the Lewis acid facilitates both the formation of a dihydrogen structure (**1**) and the loss of a hydrogen molecule. This could be useful in the storage or elimination of molecular hydrogen using transition metal complexes.



S. Camanyes, F. Maseras, M. Moreno,
A. Lledós,* J. M. Lluch,*
J. Bertrán 265–266

Dihydrogen Formation in a Trihydride
Metallocene and Its Elimination, Both
Assisted by Lewis Acids:
The $[Cp_2NbH_3] + BH_3$ System

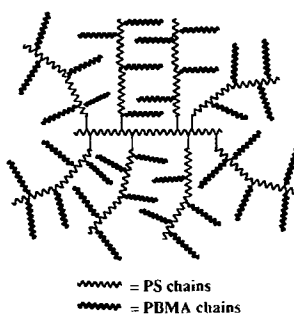
An additional π -symmetry interaction can define the conformation of a complex formed between a carbonyl compound and a Lewis acid. This was demonstrated in studies of the borabenzene adduct **1** in solution and in the solid state. Studies like this are relevant to the design of effective chiral Lewis acid catalysts.



M. C. Amendola, K. E. Stockman,
D. A. Hoic, W. M. Davis,
G. C. Fu* 267–269

Defining the Conformation of Lewis Acid/
Lewis Base Complexes: Crystallographic
Evidence for Simultaneous σ and π Donation
by a Carbonyl Group to a Divalent
Boron Lewis Acid

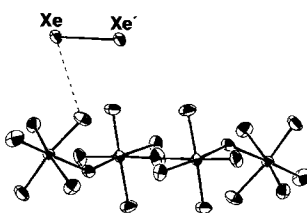
Owing to their inherent differences, consecutive “living” free radical polymerizations can yield graft and dendritic graft (dendrigrft) copolymers with multiple chain-end functionalities such as that shown schematically on the right (PS = polystyrene, PBMA = poly(*n*-butyl methacrylate)). The first polymerization leads to the linear backbone, and subsequent polymerizations introduce grafted chains.



R. B. Grubbs, C. J. Hawker,* J. Dao,
J. M. J. Fréchet* 270–272

A Tandem Approach to Graft and
Dendritic Graft Copolymers Based on
“Living” Free Radical Polymerizations

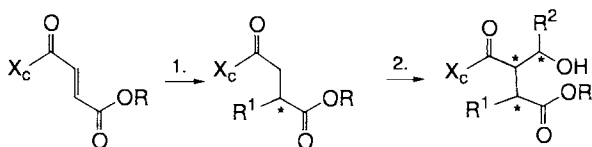
One of the longest element–element bonds is present in the Xe_2^+ ion, which had been predicted by theoretical calculations and detected by mass spectrometry as well as by ESR spectroscopy in solution. The cation occurs in $\text{Xe}_2^+\text{Sb}_4\text{F}_{21}^-$ (depicted on the right), which has been obtained as dark green crystals. The Xe–Xe bond length (308.7(1) pm) is significantly shorter than theoretically predicted (317–327 pm).



T. Drews, K. Seppelt* 273–274

The Xe_2^+ Ion—Preparation and Structure

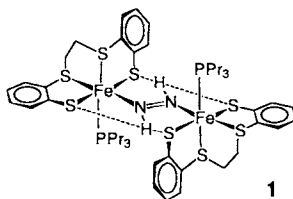
Multiple stereocenters can be introduced with high selectivity by lanthanide Lewis acid mediated conjugate radical addition to a desymmetrized fumarate derivative (step 1 in the reaction sequence below) followed by an aldol reaction (step 2). The regio- and stereoselectivities of the first step with $\text{Sm}(\text{OTf})_3$, $\text{Tm}(\text{OTf})_3$, and $\text{Er}(\text{OTf})_3$ are particularly impressive ($>100:1$ and $\leq 47:1$, respectively). This method was also applied in the synthesis of the trisubstituted butyrolactone natural products mentioned in the title. Tf = CF_3SO_2 , X_c = chiral auxiliary.



M. P. Sibi,* J. Ji 274–276

Regio- and Stereocontrolled Conjugate Radical Addition to a Desymmetrized Fumarate Derivative: An Efficient Synthesis of (–)-Nephrosteranic Acid and (–)-Roccellaric Acid

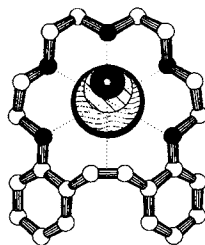
Diazene was trapped for the first time from solution by coordination to the complex $[\text{Fe}(\text{PPr}_3)_2(\text{SC}_6\text{H}_4\text{SCH}_2\text{CH}_2\text{SC}_6\text{H}_4\text{S})]$ (generated in situ) to form **1** in which it is in the *trans* configuration! This raises the question whether the *cis*-diazene structure postulated for N_2H_2 in solution is really indispensable to explain the stereoselective *cis* hydrogenations of multiple bonds by diazene.



D. Sellmann,* A. Hennige 276–278

Direct Proof of *trans*-Diazene in Solution by Trapping and Isolation of the Trapping Products

Though apparently a strange structural feature, the (Z)-stilbene unit is in fact a hinge that determines the shape of the title crown ether. Alkali metal ions from Li to Rb are accommodated in the conformation depicted on the right (spheres in the cavity illustrate the relative sizes of the ions); the crown compound shows high lithium selectivity.

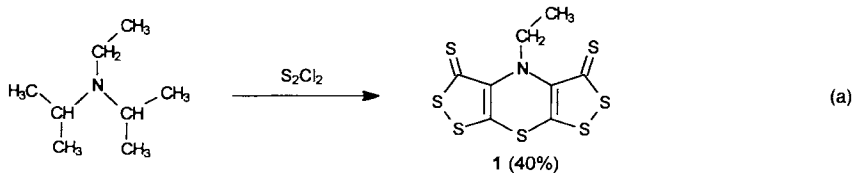


A. Merz,* T. Futterer, J. Lex,*

H. Inerowicz 278–280

Alkali Metal Complexes of *o,o'*-(Tetraethyleneglycoldiyl)-(Z)-stilbene: One Common Ligand Conformation for Li, Na, K, and Rb Ions

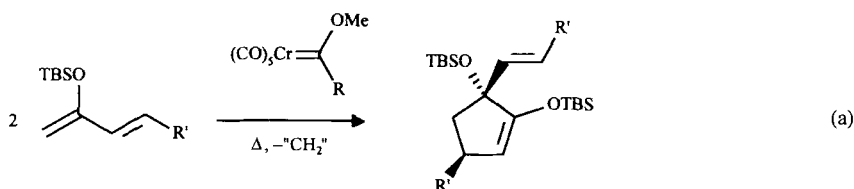
In an extremely complex sequence of roughly 15 reaction steps ethyldiisopropylamine (Hünig's base) reacts with disulfur dichloride to give thiazine **1** [Eq. (a)]. Remarkable features of this reaction are the selectivity (only the isopropyl groups are attacked), the mild conditions relative to those in other diol syntheses, and the overall yield of 40%.



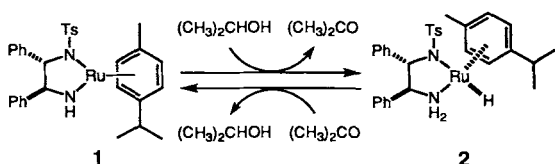
C. F. Marcos, C. Polo, O. A. Rakitin,
C. W. Rees,* T. Torroba* 281–283

From Hünig's Base to Bis([1,2]dithiolo)-[1,4]thiazines in One Pot: The Fast Route to Highly Sulfurated Heterocycles

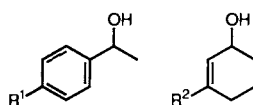
The metal-induced dimerization of dienes with expulsion of "CH₂" is a formal description of the reaction of Fischer carbene complexes with certain siloxydienes [Eq. (a)]. The key steps in the reaction are carbene ligand metathesis (the original carbene ligand is not incorporated in the product) and a highly diastereoselective [3+2]cycloaddition. TBS = *t*BuMe₂Si; R = Ph, Me; R' = CO₂Me, Ph.



New insight into the mechanism of catalysis. The purple 16-electron complex **1** and the yellow 18-electron complex **2** directly mediate the asymmetric, Ru^{II}-catalyzed hydrogen transfer between secondary alcohols and ketones. Both complexes were characterized by X-ray crystallography.



Acetone serves as the hydrogen acceptor in the kinetic resolution of racemic alcohols catalyzed by a chiral Ru^{II} complex. This method provides access to alcohols that are not available from the corresponding ketones by standard enantioselective reduction (examples of substrates are given on the right) and is particularly interesting for *meso* compounds. R¹ = (CH₃)₂N, R² = H, CH₃.



M. Hoffmann, M. Buchert,
H.-U. Reissig* 283–285

New Surprises with Fischer Carbene Complexes: Formal [3+2]Cycloadditions with and without Preceding Carbene–Ligand Metathesis

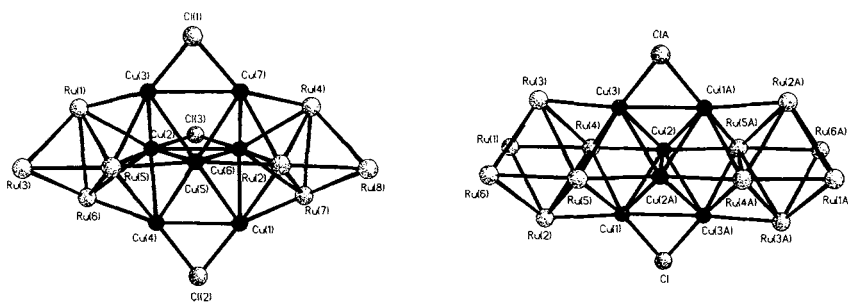
K.-J. Haack, S. Hashiguchi, A. Fujii,
T. Ikariya, R. Noyori* 285–288

The Catalyst Precursor, Catalyst, and Intermediate in the Ru^{II}-Promoted Asymmetric Hydrogen Transfer between Alcohols and Ketones

S. Hashiguchi, A. Fujii, K.-J. Haack,
K. Matsumura, T. Ikariya,
R. Noyori* 288–290

Kinetic Resolution of Racemic Secondary Alcohols by Ru^{II}-Catalyzed Hydrogen Transfer

A linear arrangement of condensed octahedra and fused square-based pyramids are present in the novel, high nuclearity, mixed-metal dianions of the title (**2** and **1**, respectively), which are formed in the reaction of [Ru₆H(CO)₁₈][−] with excess [Cu(MeCN)₄]⁺ in the presence of chloride ions in CH₂Cl₂ (**1**) and CH₃CN (**2**). In these dianions the metallic ruthenium cluster cores are fused together through a central copper cluster unit (metal cores of **1** (left) and **2** (right) are depicted below).



M. A. Beswick, J. Lewis, P. R. Raithby,*
M. C. Ramirez de Arellano 291–293

The High Nuclearity Mixed–Metal Cluster Dianions [Ru₈H₂Cu₇Cl₃(CO)₂₄]^{2−} and [Ru₁₂H₂Cu₆Cl₂(CO)₃₄]^{2−}

* Author to whom correspondence should be addressed

BOOKS

| | | |
|---|--|-----|
| Enough for One Lifetime. Wallace Carothers, Inventor of Nylon · M. E. Hermes | <i>B. Cornils</i> | 295 |
| To See the Obvious · A. J. Birch | <i>G. B. Kauffman and L. M. Kauffman</i> ... | 296 |
| The Natural Selection of the Chemical Elements · R. J. P. Williams, J. J. R. Frausto da Silva | <i>H. Strasdeit</i> | 298 |
| The Chemistry of Organophosphorous Compounds. Volume 4. Ter- and Quinquevalent Phosphorous Acids and their Derivatives · F. R. Hartley | <i>R. Schmutzler</i> | 298 |
| Electron Transfer and Radical Processes in Transition-Metal Chemistry · D. Astruc | <i>C. A. Mirkin</i> | 299 |

German versions of all reviews, communications, and highlights in this issue appear in the first February issue of *Angewandte Chemie*. The appropriate page numbers can be found at the end of each article and are also included in the Author Index on p. 301.

SERVICES

| | |
|----------------|-----|
| ● Keywords | 300 |
| ● Author Index | 301 |
| ● Preview | 302 |

All the Tables of Contents from 1995 onwards may be found on the WWW under <http://www.vchgroup.de/home/angewandte>

ANGEWANDTE CHEMIE

A Journal of the
Gesellschaft
Deutscher Chemiker

International Edition in English

1997/36
1/2

Pages 1–174

EDITORIAL

The same procedure as last year in the editorial office—at least as regards the increasing numbers of excellent papers received daily, the tight deadlines, and the battle against increasing costs; one exception, however, at the beginning of this year is the double issue of January that follows the double issue of December. And again, the old year foreshadows the new with epothilone! Epothilone? Only a few natural products succeed in rapidly attracting the attention of many chemists, to say nothing of the wider public. One such compound is “Taxol” (which should be referred to as “paclitaxel” because the original name has been registered as a trademark): it raised the hopes of many cancer patients because of its biological activity and stimulated chemical research in many directions (biosynthesis, total synthesis, toxicology, pharmacology, etc.). Since the name “Taxol” has been patented, we will find another molecule that can do the same! thought chemists—and discovered the epothilones. These compounds form a new class with a totally different structure, but a mode of action and range of activity that resembles that of paclitaxel (a rose by any other name. . .!). In the July issue of *Angewandte Chemie* last year G. Höfle et al. described the isolation and structure of epothilones A and B, and the race was on to complete the total synthesis of this potentially important compound.

Diverse forces drive chemists: The search for knowledge for knowledge' sake and commercial interests are perhaps two of the most important motivations supplemented by competitive spirit and the urge to create beauty in, for instance, molecules or solids with highly symmetric structures. Last year we were privileged to present many of the outstanding results of chemical research in *Angewandte Chemie*—and epothilone came again into the limelight in the December issue. The race to achieve the total synthesis, in which at least three groups worldwide competed (see the publications of Nicolaou et al. in number 20/1996 of *Angewandte Chemie*, of Schinzer et al. in number 11/1996 of *Chemistry—A European Journal*, and of Danishefsky et al. in number 23/1996 of the *Journal of Organic Chemistry*), was finally won by Danishefsky's group. Their description of the total synthesis was received by fax in the editorial office on October 17, 1996, evaluated by two referees within a day, accepted on October 18, 1996, and published in the December issue (p. 2801). On November 25 a manuscript of the Nicolaou group arrived, describing a totally different route to the target. It was also refereed rapidly and accepted within the same week, and can be found in this issue (p. 166). You can read more about the isolation, properties, structure, and synthesis of these new compounds in a Highlight in one of the next issues.

"Hot Papers" are not rare—they provide the excitement in the chemical literature. To facilitate further the readers' search for the raisins in the already rich "*Angewandte*" pudding and to direct their attention to particularly important papers as early as possible, we have offered abstracts of "Hot Papers" on the World-Wide Web (WWW) for some time on our home page:

(<http://www.vchgroup.de/home/angewandte>)

In addition you'll find there the Tables of Contents and Keywords. Even before the readers have the issue in their hands they can look at the Table of Contents and electronically search for authors, keywords, and parts of titles (using AND, OR, and NOT operators) in all Tables of Contents from 1995 onwards. Of course, we will expand our WWW program, which is already used extensively.

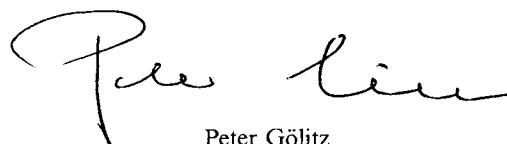
Short publication times are the aim of every journal, and indeed not only for "hot" papers. Of the articles in *Angewandte Chemie* the reviews naturally have the longest path from submission to print, whereas the Highlights are published on a fast track. A feature common to these two sections is that they can be planned by the editorial office, since many of the articles are invited. The difference between them and the communications is that the communications are generally submitted without prior consultation with the editorial office. Ever more chemists choose to offer *Angewandte* their communications: in 1986 we received 426, by 1991 already 738, and in 1996 the number rose to 1260; in last year alone the submissions increased by 16%! An expansion of the volume of the journal and an increase in the rejection rate were the consequences. In merely this and the December double issues, 91 communications were published, mostly four to six months after *initial* submission. The rejection rate at present is about 55%. The appeal of the journal for authors is reflected in the development in its Impact Factor (see Table 1), as well as, of course, in the fact that authors send

us manuscripts of the quality and interest of the epochal papers, for example. And that definitely also has something to do with the attractive presentation of scientific results in this journal.

A picture paints a thousand words—this is particularly valid in chemistry with its formulas and figures. The full-page pictures that were introduced last year at the front of each review and the communications section structure each issue. Even for a complicated subject they elicit a spontaneous "Gee Whiz" response—and spontaneous, positive feedback came from readers and authors.

The internationalization of the journal was the turning point in the development of the past years and as important as the inexorable striving for quality. Because of the German edition the visibility of *Angewandte* is particularly high in German-speaking countries with their important chemical industry, which is an advantage for all authors. The international success is crucial for the German edition, and the benefit to the German reader is immense. Not only are the technical terms for the latest developments also in German, but so much more can be absorbed in the mother tongue in a given amount of time. We also do not forget our international readers who do not speak English as their first language. The editors at *Angewandte* do their best to make the language as clear as possible to aid the understanding and speed of reading.

The same procedure as last year, but where is "Chemistry"? The journal has grown out of *Angewandte Chemie*! For twenty-one months "Chemistry" enriched "Angewandte"'s contents. But 2000 pages are projected for 1997, and that is far too many to continue to be offered as a bound-in supplement in 1997. What other new journal can boast such a successful development? *Angewandte Chemie* is proud of its "little sister" and sad at the parting, but you will find it nearby on the shelf or on your desk. A Table of Contents of "Chemistry" (without annotation) will still be found in *Angewandte Chemie*—and, of course, on the WWW!



Peter Göllitz

Table 1. Impact factors of some important chemistry journals that publish communications and/or full papers.

| Journal | Impact Factor | | | |
|--------------------------|---------------|--------|-------|-------|
| | 1995 | 1993 | 1989 | 1984 |
| <i>Angew. Chem.</i> | 6.983 | 6.168 | 5.049 | 4.007 |
| <i>J. Am. Chem. Soc.</i> | 5.263 | 5.365 | 4.415 | 4.43 |
| <i>Chem. Rev.</i> | 14.513 | 15.748 | 9.656 | 8.024 |
| <i>Acc. Chem. Res.</i> | 8.823 | 10.879 | 7.419 | 7.653 |
| <i>Chem. Commun.</i> | 2.652 | 2.54 | 2.223 | 2.437 |
| <i>Chem. Soc. Rev.</i> | 5.604 | 6.152 | 4.406 | 5.75 |

COVER PICTURE

The cover picture shows the formula of globo H-KLH in the center, which show the strongest immunological activity in the presence of the immunological adjuvant QS-21. Globo H-KLH is a conjugate of the hexasaccharide globo H and hemocyanin from *Megathura crenulata*. Antibodies against globo H-KLH—the syringe reminds us that their formation is induced in mice—recognize the globo H epitope on the surface of breast cancer cells and activate the complement system to initiate lysis of the tumor cells. The sugar epitope of globo H was synthesized from glycal units (shown schematically at the top of the picture) and linked with KLH. The transfer of the immunization strategy to humans is the next step in the project that Danishefsky, Livingston, et al. report on page 125ff (graphics: G. Schulz, Fussgönheim, Germany).



REVIEW

Contents

Minding the gates! Lipophilic xenobiotic compounds are potentially dangerous substances for the central nervous system. But the blood–brain barrier, which is an anatomical constraint with special morphological features, specific proteins, and transport systems, blocks passage of certain neurotoxic substances and serves as a site of active detoxication.

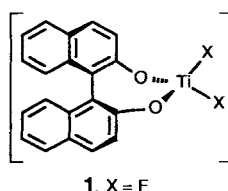
A. Aigner, S. Wolf,
H. G. Gassen* 24–41

Transport and Detoxication: Principles, Approaches, and Perspectives for Research on the Blood–Brain Barrier

HIGHLIGHTS

Contents

A breakthrough in enantioselective catalytic addition of allylsilanes to aldehydes was made by Gauthier and Carreira with a fluorotitanium catalyst (**1**) prepared in situ from TiF_4 and binaphthol. Only 10% of **1** gives 94% *ee* for the addition of allyltrimethylsilane to, for example, *tert*-butylcarbaldehyde! The extreme polarity of the Ti–F bond is responsible for the special properties of catalyst **1**.



R. O. Duthaler,* A. Hafner 43–45

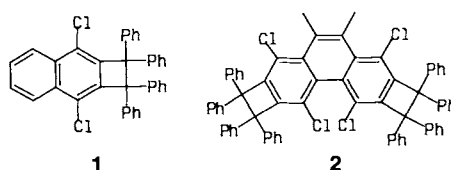
Fluorotitanium Compounds—Novel Catalysts for the Addition of Nucleophiles to Aldehydes

Multiple scattering of electrons in a crystal and the resulting interference problems make electron crystallography of inorganic substances a problematic undertaking. A recent publication by T. E. Weirich et al. now shows that electron crystallography could be the method of choice, for example, to determine the structure of small crystals. Providing that one has access to a high-resolution electron microscope, the other requirements of this method are relatively small.

W. Mertin* 46–47

Electron Crystallography—Now a Handy Method

What is the maximum length of a single bond between carbon atoms? Certainly, this question cannot be answered by quantum mechanical calculations alone—reliably interpreted physical measurements on real molecules are crucial. The longest unequivocally determined C–C single bonds (1.72 Å) have recently been found in tetraphenyldihydrocyclobutarenes **1** and **2**.

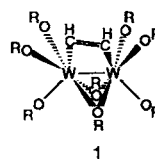


G. Kaupp,* J. Boy 48–49

Overlong C–C Single Bonds

COMMUNICATIONS

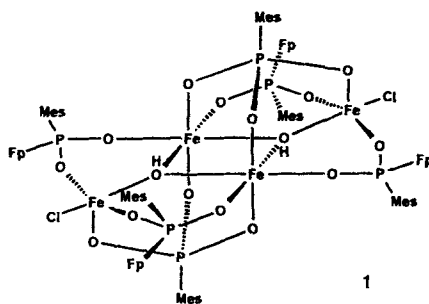
An unusual orientation of the bond is shown by the bridging ethyne ligand in complex **1**, which is prepared from $[\text{W}_2(\text{OCH}_2t\text{Bu})_8]$ and ethyne: the crystal structure analysis of **1** revealed that the C–C bond of this ligand is neither parallel nor perpendicular to the W–W bond, but at an angle of 67° to it. Furthermore, the reactivity studies of $[\text{W}_2(\text{OCH}_2t\text{Bu})_8]$ with CO, ethene, allene, benzophenone, and thiobenzophenone have provided several tungsten complexes with remarkable structures.



M. H. Chisholm,* K. Folting,
M. A. Lynn, W. E. Streib,
D. B. Tiedtke 52–54

Organometallic Chemistry of $[\text{W}_2(\text{OCH}_2t\text{Bu})_8]$

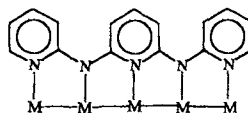
Aerial oxidation with drastic consequences: The dinuclear building block $[\text{Fp}_2(\text{Mes})\text{PH}]\text{Cl}$ ($\text{Fp} = \text{CpFe}(\text{CO})_2$, $\text{Mes} = \text{mesityl}$) is converted into the polynuclear, antiferromagnetic cage compound **1**. In addition to retention and elimination of the Fp units at the phosphorus atoms, four iron(III) centers, four μ_2 -phosphinato, and two μ_3 -phosphonato ligands are formed, which are connected through O bridges.



I.-P. Lorenz,* W. Pohl,
H. Nöth 55–56

Molecular Self-Assembly to Give the Antiferromagnetic Cage Compound
 $[\{\text{CpFe}(\text{CO})_2(\text{Mes})\text{PO}_2\}_4\text{MesPO}_3\text{Fe}_2(\text{OH})\text{Cl}\}_2]$

Both anti-anti-anti-anti and syn-syn-syn-syn conformations of the bound metal ions are possible with the new ligand N,N' -bis(α -pyridyl)-2,6-diaminopyridine (H_2tpda). Pentanuclear Co^{II} and Ni^{II} complexes are accessible with this ligand (see sketch on the right). The metal chain is helically wrapped by four all-syn tpda ligands.



S.-J. Shieh, C.-C. Chou, G.-H. Lee,
C.-C. Wang, S.-M. Peng* 56–59

Linear Pentanuclear Complexes Containing a Chain of Metal Atoms: $[\text{Co}_5^{\text{II}}(\mu_5\text{-tpda})_4(\text{NCS})_2]$ und $[\text{Ni}_5^{\text{II}}(\mu_5\text{-tpda})_4\text{Cl}_2]$

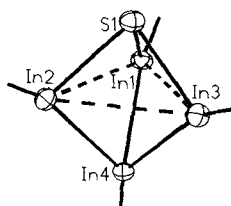
Hydrogen bonds and π - π stacking stabilize a supramolecular cage (depicted schematically on the right) constructed from five components, namely two trifurcated trisammonium cations and three ditopic crown ether molecules. This molecule is a remarkable example of a programmed supramolecular system: the information essential for the cage's assembly is stored in the covalent frameworks of the two building blocks.



P. R. Ashton, A. N. Collins,
M. C. T. Fyfe, P. T. Glink,
S. Menzer, J. F. Stoddart,*
D. J. Williams 59–62

An Interwoven Supramolecular Cage

A trigonal-bipyramidal In_4S central framework, which in terms of its electron count resembles a *closo*-cluster, is present in the title compound (structure on the right; $\text{C}(\text{SiMe}_3)_3$ substituents on the In atoms are omitted). This was prepared by treatment of $\text{In}_4[\text{C}(\text{SiMe}_3)_3]_4$ with the sulfur donor propylene sulfide and is the first organoindium analog of the *closo*-borates.



W. Uhl,* R. Graupner, W. Hiller,
M. Neumayer 62–64

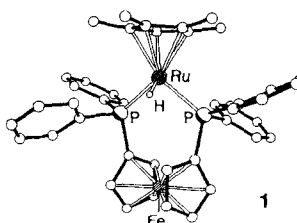
$\text{In}_4\text{S}[\text{C}(\text{SiMe}_3)_3]_4$: An Organoindium Compound with an In_4S Core Isovalence Electronic to Pentahydro-*closo*-pentaborate(2–)

Weak thallium–thallium interactions are present in the thallium tetrahedron of the crystalline alkylthallium(I) compound $\text{Tl}[\text{C}(\text{SiMe}_3)_3]_3$, which is easily accessible from cyclopentadienylthallium(I) and tris(trimethylsilyl)methyl lithium. In solution, however, only the monomer of the extremely thermally sensitive compound can be detected.

W. Uhl,* S. U. Keimling,
K. W. Klinkhammer,
W. Schwarz 64–65

$\text{Tl}[\text{C}(\text{SiMe}_3)_3]_3$ —An Alkylthallium(I) Compound with a Distorted Tetrahedron of Tl Atoms in the Solid State

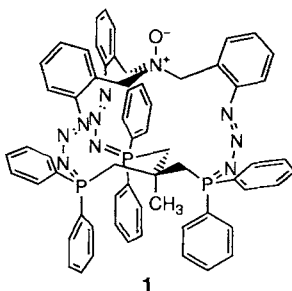
Different products are formed from the electron transfer reaction between the ruthenium hydride **1** and the trityl cation when **1** is employed as a “redox-switch” catalyst or as stoichiometric reducing agent. In the first case **1** converts H_2 into a one-electron reducing agent for C–C bond formation, thus yielding the product known as Gomberg's dimer. In contrast, only triphenylmethane is produced in the stoichiometric reactions, by an electron-transfer/hydride-transfer mechanism.



R. T. Hembre,* J. S. McQueen 65–67

“Redox-Switch” Catalysis of C–C Bond Formation with H_2 : One-Electron Reduction of the Trityl Cation

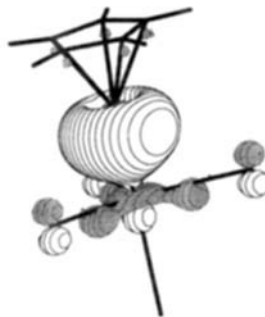
Highly unusual! Both the Z configuration of the intracyclic N=N bond and the conformation of the triphos group in **1** are novel. This chiral macrocycle, which is formed from the appropriate tripodal tris(azide) and triphos by self-assembly, has propellerlike, C_3 symmetry according to its X-ray crystal structure. triphos = $\text{CH}_3\text{C}(\text{CH}_2\text{PPh}_2)_3$.



M. Alajarín,* P. Molina,
A. López-Lázaro,
C. Foces-Foces* 67–70

New Cage Compounds: Preparation and Characterization of Chiral C_3 -Symmetric Macrobicyclic Tris(phosphazides)

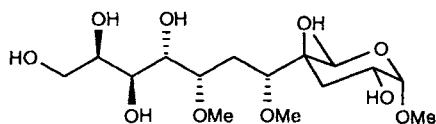
The bonding in the unprecedented complex $[\text{Cp}^*\text{Al}-\text{Fe}(\text{CO})_4]$ (depicted on the right) was investigated by quantum theoretical methods by using the model compound $[\text{CpAl}-\text{Fe}(\text{CO})_4]$. The strength of Al \rightarrow Fe donor–acceptor bond, which is characteristic for this complex, is estimated to be about 50 kcal mol^{-1} .



J. Weiss, D. Stetzkamp, B. Nuber,
R. A. Fischer,* C. Boehme,
G. Frenking* 70–72

$[(\eta^5\text{-C}_5\text{Me}_5)\text{Al}-\text{Fe}(\text{CO})_4]$ —
Synthesis, Structure, and Bonding

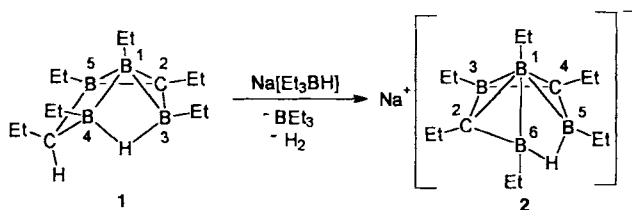
The total synthesis of four diastereomeric glycosides was necessary to determine the relative configuration of the epitope of a highly antigenic lipooligosaccharide isolated from *Mycobacterium gastri*. The correct diastereomer is shown below.



J. Longépé, J. Prandi,*
J.-M. Beau 72–75

Relative Configuration and Synthesis of a New C-4 Branched Sugar, a Component of the Lipooligosaccharide LOS-III from *Mycobacterium gastri*

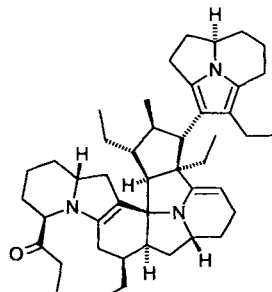
Integration of a carbon atom in the carborane cage is the key feature of the deprotonation of **1** with $\text{Na}[\text{Et}_3\text{BH}]$ to give the sodium salt **2**. The process is reversible: treatment of **2** with methanol leads to the reformation of **1**.



B. Wrackmeyer,* H.-J. Schanz,
W. Milius 75–77

The First 2-Carba-*nido*-pentaborane(8) Derivative; Structure of Sodium Hexaethyl-2,4-Dicarba-*nido*-hexaborate(1–)

Chemical warfare in insects: Ants have a vast arsenal of chemical weapons for defense or to catch prey. Here the isolation and identification of a highly sensitive alkaloid, myrmicarín 663, which has an entirely novel carbon skeleton, is reported.

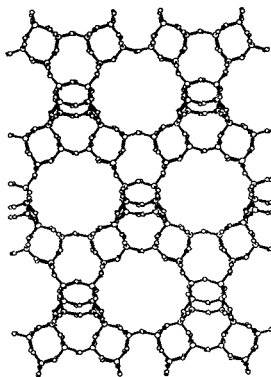


Myrmicarín 663

F. Schröder, V. Sinnwell, H. Baumann,
M. Kaib, W. Francke* 77–80

Myrmicarín 663: A New Decacyclic Alkaloid from Ants

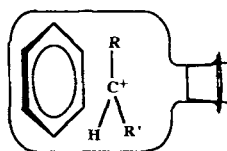
The design of inorganic solids and state-of-the-art microcrystallography at Europe's newest synchrotron facility go hand-in-hand in the synthesis and structure elucidation of STA-1, a low-density member (projection shown on the right) of the family of large-pore aluminophosphates.



G. W. Noble, P. A. Wright,* P. Lightfoot,
R. E. Morris, K. J. Hudson, Å. Kvik,
H. Graafsma 81–83

Microporous Magnesium Aluminophosphate STA-1: Synthesis with a Rationally Designed Template and Structure Elucidation by Microcrystal Diffraction

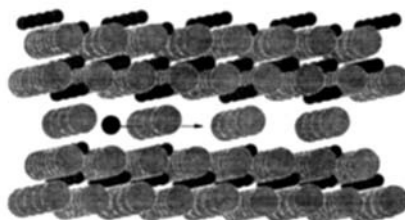
Enantiomerically pure, gaseous reagents can be used to probe the chemical identity and the spatial arrangement of reaction partners confined within ion–molecule complexes (schematically represented on the right). The addition of gaseous arenium ions to (*R*)-(–)-*s*-C₄H₉Cl affords complexes within which aromatic alkylation proceeds with complete racemization. This suggests that the components of the complex undergo mutual rotation and that the *s*-butyl cation is the electrophile.



M. Aschi, F. Cacace,*
A. Troiani 83–85

Probing Gaseous Ion–Molecule Complexes with Chiral Agents: The Reaction of Arenium Ions with (*R*)-(–)-*s*-Butyl Chloride

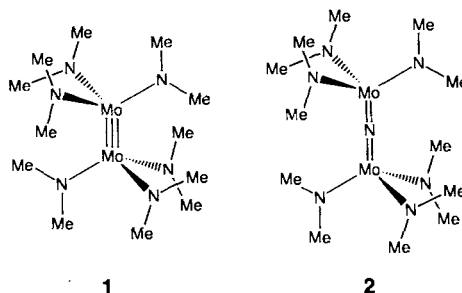
Mobile trivalent cations in solids? The results of temperature-dependent, single-crystal X-ray structure investigations of a Pr³⁺-β''-Al₂O₃ crystal (see structure on the right, Pr³⁺ as black sphere) indicate just such an unusual ionic current transport mechanism.



J. Köhler, W. Urland* 85–87

On the Mobility of Trivalent Ions: Pr³⁺ in Pr³⁺-β''-Al₂O₃

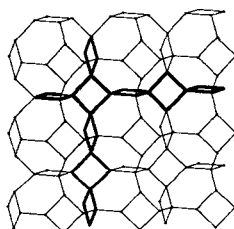
Formal N-atom insertion into the metal–metal triple bond of the diamagnetic compound **1**, which has been known for over twenty years, results in the paramagnetic, nitrido-bridged molecule **2**. The characterization of three such N- and P-atom bridged species is described, and their role as intermediates in three-electron atom transfer reactions is highlighted.



M. J. A. Johnson, P. M. Lee,
A. L. Odom, W. M. Davis,
C. C. Cummins* 87–91

Atom-Bridged Intermediates in N- and P-Atom Transfer Reactions

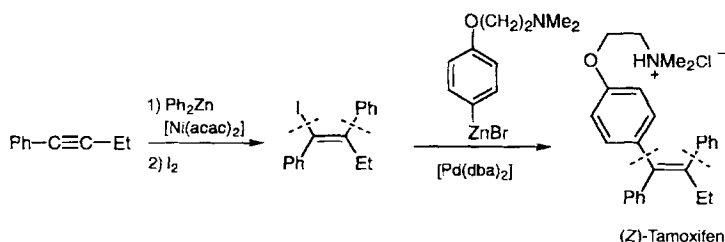
Large pores and reactive centers characterize the novel, more open vanadium phosphates. The three-dimensional nets on which they are based differ from those of classical microporous materials such as aluminosilicate zeolites; however, they have interesting topological relationships to some of them (see, for example, the framework of the sodalite type depicted on the right). Based on these relationships, microporous materials can be envisaged that contain arbitrary functional groups.



M. Schindler,* W. H. Baur* 91–93

Insertion of Functional Groups into Square-Planar Units: A New Construction Principle for Open Microporous Framework Structures

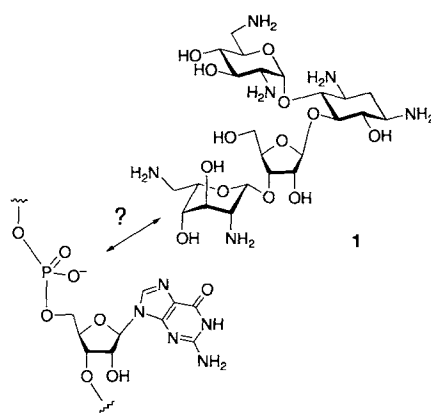
A new highlight in the repertoire of carbometalation reactions is the highly stereo- and regioselective nickel-catalyzed carbzincation of internal alkynes. This is exemplified by a short and effective synthesis of the anti-breast-cancer drug (Z)-tamoxifen (see below; *Z:E* > 99:1; acac = acetylacetonate, dba = dibenzylideneacetone). This reaction also allows the stereoselective synthesis of various tri- and tetrasubstituted olefins in good yield.



T. Stüdemann, P. Knochel* 93–95

New Nickel-Catalyzed Carbzincation of Alkynes: A Short Synthesis of (Z)-Tamoxifen

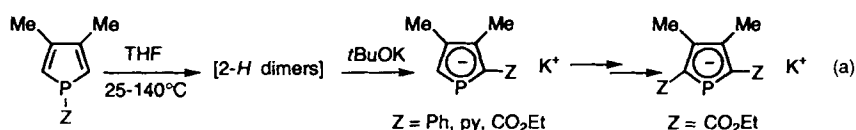
Particularly stable complexes with bidentate binding are formed between 1,3-hydroxyamines and dimethylphosphate, which serve as models of the complexes formed by aminoglycoside antibiotics such as neomycin B (**1**) and RNA phosphodiester. This recognition motif involving a hydrogen bond with the hydroxyl group is also found in the complexation of anions by simple aminoglycosides in aqueous solution.



M. Hendrix, P. B. Alper, E. S. Priestley, C.-H. Wong* 95–98

Hydroxyamines as a New Motif for the Molecular Recognition of Phosphodiester: Implications for Aminoglycoside–RNA Interactions

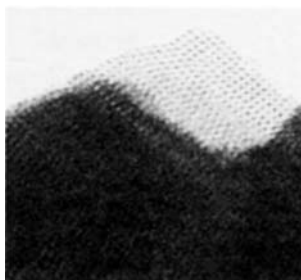
The synthesis of porphyrin-like arrays based on the phosphole ring has moved a step closer with the simple and general route to α -functional phospholide ions presented here [Eq. (a)]. py = 2-pyridyl.



S. Holand, M. Jeanjean, F. Mathey* 98–100

A Straightforward Access to α -Functional Phospholide Ions

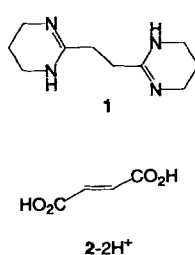
A structure similar to that of microporous titanosilicate ETS-10 is reported for the first large-pore vanadosilicate framework containing stoichiometric amounts of hexacoordinated vanadium. A section of the high-resolution electron micrograph of the vanadosilicate is shown on the right.



J. Rocha,* P. Brandão, Z. Lin, M. W. Anderson, V. Alfredsson, O. Terasaki 100–102

The First Large-Pore Vanadosilicate Framework Containing Hexacoordinated Vanadium

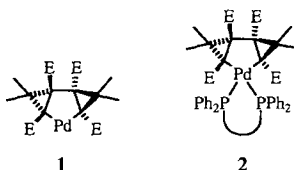
Fourfold hydrogen donors or acceptors for hydrogen bonding, the diprotonated bisamidinium **1-2H²⁺** and the deprotonated fumaric acid **2²⁻**, cocrystallize to form one-dimensional α -networks when the ratio of **1-2H²⁺** to **2²⁻** is 1:1 and two-dimensional β -networks when the ratio is 1:2.



O. Felix, M. W. Hosseini,* A. De Cian, J. Fischer 102–104

The Simultaneous Use of H-Bonding and Coulomb Interactions for the Self-Assembly of Fumaric Acid and Cyclic Bisamidinium into One- and Two-Dimensional Molecular Networks

A dramatic deviation from square-planar coordination for Pd^{II} complexes: the C-Pd-C and P-Pd-P planes in the helical chiral complexes **2** ($\cup = 1,1'$ -ferrocenediyl) are unexpectedly tipped toward each other by as much as 30°. These complexes are prepared from the appropriate bidentate phosphane ligands and the bishomopalladole **1**, which is remarkably stable and available in enantiomerically pure form in good yields. E = CO₂Me.



A. S. K. Hashmi,* F. Naumann,
R. Probst, J. W. Bats 104–106

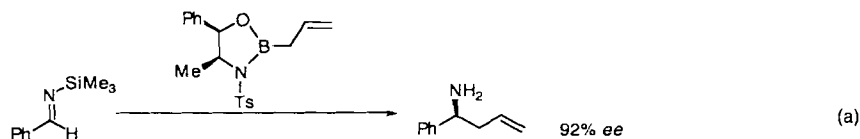
Preparation of Enantiomerically Pure 5-Palladatricyclo[4.1.0.0^{2,4}]heptanes and Conversion into Enantiomerically Pure Complexes with Helical Chirality at Palladium

What are the thermodynamic prerequisites of the Berkessel–Thauer mechanism of action of the first metal-free hydrogenase? Model reactions of planar and bent amidinium ions with H₂ in the absence and presence of H₂O and NH₃ as bases demonstrate the significance of a proton acceptor in these reactions; the bending of the amidinium ion provides the necessary fine-tuning.

J. Cioslowski,* G. Boche* 107–109

Geometry-Tunable Lewis Acidity of Amidinium Cations and Its Relevance to Redox Reactions of the Thauer Metal-Free Hydrogenase: A Theoretical Study

N-silylated imines are well-suited for reaction with chirally modified allylboron reagents to give enantiomerically enriched primary homoallylamines in high yields [Eq. (a)]. The chiral ligand, here *N*-tosyl-(–)-norephedrin, can be recovered after the reaction and used again to generate the chiral allylboron reagent. Ts = *p*-toluenesulfonyl.



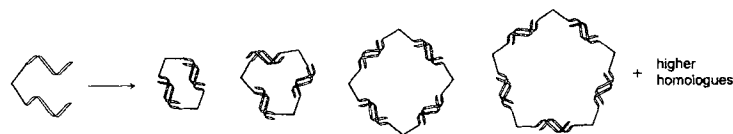
S. Itsuno,* K. Watanabe, K. Ito,
A. A. El-Shehawy,
A. A. Sarhan 109–110

Enantioselective Synthesis of Homoallylamines by Nucleophilic Addition of Chirally Modified Allylboron Reagents to Imines

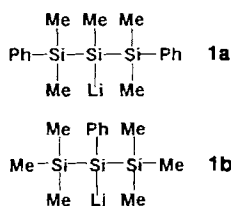
Rigid vertices are essential for the formation of supramolecular rings with DNA sequences. Two *p*-(2-hydroxyethyl)phenylethynylphenyl spacers attached to a central sp³ C atom are extended with oligonucleotide chains (single-stranded DNA). The conjugates that form (see below) self-assemble into a series of cyclic homologues, which can be separated by gel electrophoresis.

J. Shi, D. E. Bergstrom* 111–113

Assembly of Novel DNA Cycles with Rigid Tetrahedral Linkers



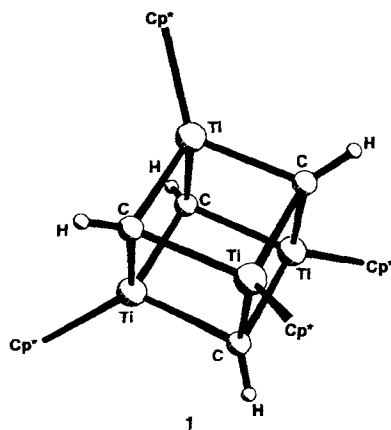
Lithium–mercury exchange of the appropriate precursors in toluene yielded the first unsolvated, dimeric lithiosilanes **1**. X-ray crystallographic data and NMR spectra of both compounds provide evidence of intramolecular lithium–phenyl interactions.



A. Sekiguchi,* M. Nanjo, C. Kabuto,
H. Sakurai* 113–115

[Me(PhMe₂Si)₂SiLi] and [Ph(Me₃Si)₂SiLi]: Preparation, Characterization, and Evidence for an Intramolecular Li–Ph Interaction

An almost perfect Ti₄C₄ cube is present in compound **1**, which is formed by methane elimination from [Cp*TiMe₃] at 95 °C. Compound **1** is a dark brown crystalline solid that is stable in solution in toluene at 200 °C for several days. Cp* = C₅Me₅.



R. Andrés, P. Gómez-Sal, E. de Jesús,
A. Martín, M. Mena,*
C. Yélamos 115–117

Thermal Decomposition of [(η⁵-C₅Me₅)-TiMe₃]: Synthesis and Structure of the Methylidyne Cubane [(η⁵-C₅Me₅)Ti]₄-(μ₃-CH)₄]

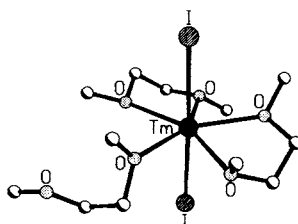
Ligand-induced perturbation of structure and function of a copper–dioxygen complex is revealed by structural characterization and reactivity studies of the complex shown on the right. In addition to preventing formation of a (μ -peroxo)dicopper isomer, notable effects arising from the ethylene linker between the capping ligands include discernible puckering of the $[\text{Cu}_2(\mu\text{-O})_2]^{2+}$ unit, lengthened Cu–O distances, and slowed intramolecular monooxygenase reactivity compared to planar analogs lacking the tether.



S. Mahapatra, V. G. Young Jr.,
S. Kaderli, A. D. Zuberbühler,*
W. B. Tolman* 130–133

Tuning the Structure and Reactivity of the $[\text{Cu}_2(\mu\text{-O})_2]^{2+}$ Core: Characterization of a New Bis(μ -oxo)dicopper Complex Stabilized by a Sterically Hindered Dinucleating Bis(triazacyclononane) Ligand

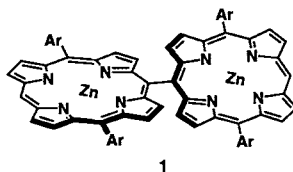
Divalent 4f element chemistry can now be expanded from Eu, Yb, and Sm to include Tm since a synthetic route to the first crystallographically characterizable molecular complex of Tm^{II} has been found. The intense green title complex was isolated from the reaction of TmI_3 and Tm in dimethoxyethane. The photosensitive complex has the pentagonal-bipyramidal structure shown on the right.



M. N. Bochkarev,* I. L. Fedushkin,
A. A. Fagin, T. V. Petrovskaya,
J. W. Ziller, R. N. R. Broomhall-Dillard,
W. J. Evans* 133–135

Synthesis and Structure of the First Molecular Thulium(II) Complex: $[\text{TmI}_2(\text{MeOCH}_2\text{CH}_2\text{OMe})_3]$

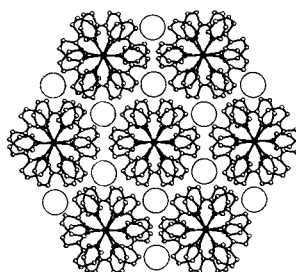
The perpendicular arrangement of porphyrin units in dimer 1 is reflected in a large excitonic coupling that leads to splitting of the Soret bands and only modest spectral changes in the Q-bands. Compound 1 and the analogous trimer and tetramer are prepared by oxidative coupling of the corresponding 5,15-diarylporphyrin and are the first examples of compounds having direct *meso,meso*-linked porphyrin chromophores. Ar = 3,5-*t*Bu₂C₆H₃.



A. Osuka,* H. Shimidzu 135–137

meso,meso-Linked Porphyrin Arrays

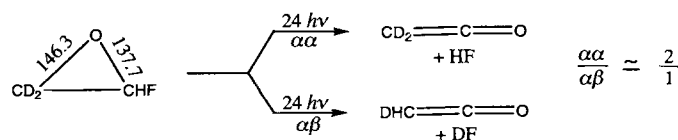
No counteranions or solvent molecules are found in single crystals of $[\text{Ru}(\text{bpy})_3]_3^0$, an air-sensitive but thermally stable new material. Analysis of the X-ray structural data reveals a relatively undistorted C_3 -symmetric system with empty lattice spaces, which are represented by empty circles in the picture on the right. This packing structure is reminiscent of those in electrides.



E. E. Pérez-Cordero, C. Campana,
L. Echegoyen* 137–140

X-ray Structure of $[\text{Ru}(\text{bpy})_3]_3^0$:
An Expanded Atom or a New Electride?

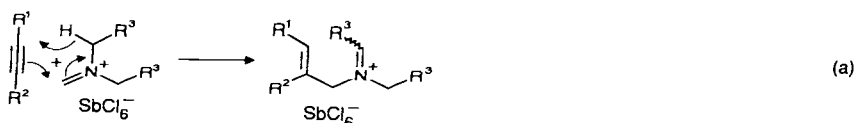
Formation of a CO double bond by elimination of HF is the reaction undergone by the newly prepared fluorooxiranes (shown below for the deuterated compound) on multiphoton excitation with a CO₂ laser: the difference in the CO bond lengths [pm] suggests ketene formation. The structural characterization was performed by high-resolution FTIR spectroscopy.



H. Hollenstein, D. Luckhaus, J. Pochert,
M. Quack,* G. Seyfang 140–143

Synthesis, Structure, High-Resolution Spectroscopy, and Laser Chemistry of Fluorooxirane and 2,2-[²H₂]-Fluorooxirane

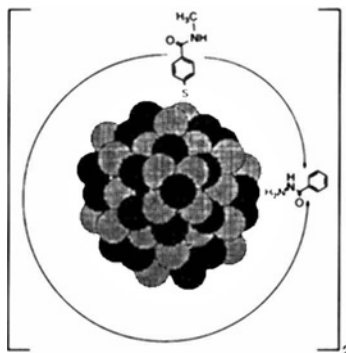
Counterion in control! When complex anions with low nucleophilicity are used, a previously unknown ene reaction of iminium ions and alkynes occurs [Eq. (a)], which provides straightforward stereo- and regioselective access to substituted allylamines.



A. R. Ofial, H. Mayr* 143–145

Ene Reactions of Alkynes for the Stereoselective Synthesis of Allylamines

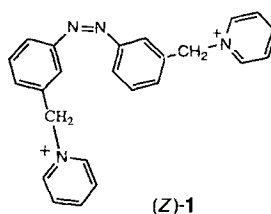
By size-selective precipitation homodimeric CdSe nanocrystals could be isolated from a mixture of oligomers formed when monodisperse CdSe nanocrystals (see right) were linked by the bifunctional organic ligand, bis(acyl hydrazide). TEM images revealed a reproducible separation between CdSe particles of approximately a quarter of the particle diameter. This distance is consistent with the physical dimensions of the linker.



X. Peng, T. E. Wilson, A. P. Alivisatos,*
P. G. Schultz* 145–147

Synthesis and Isolation of a Homodimer of Cadmium Selenide Nanocrystals

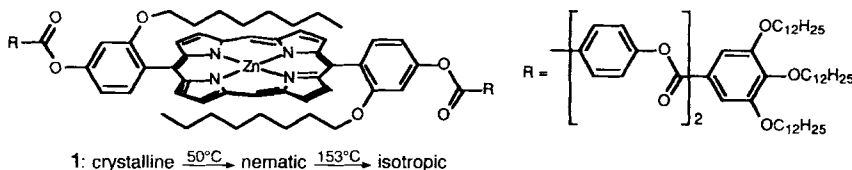
The formation and dissociation of complexes between eosin derivatives and the photoisomerizable azobenzene derivatives (*E*)-**1** and (*Z*)-**1** is reversibly switched light. An eosin monolayer assembled onto a quartz crystal is an active interface for the transduction of the photochemically induced formation of the complex with (*E*)-**1** and the dissociation of the complex upon photoisomerization to the *Z* isomer. Thus optical signals can be transduced into electronic signals.



K. T. Ranjit, S. Marx-Tibbon,
I. Ben-Dov, I. Willner* 147–150

Formation of Supramolecular Donor–Acceptor Complexes between Bis(pyridinium-methyl)azobenzenes and Eosin in Solutions and at Solid Interfaces: Transduction into Optical and Microgravimetric Signals

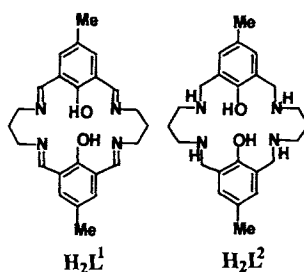
The type of mesophase can be controlled by the addition of side chains to porphyrins bearing several long terminal chains (see, for instance, **1**). Either columnar phases or those characteristic of rodlike molecules are formed, whose transition temperatures are lower than those found in the parent systems.



Q. M. Wang, D. W. Bruce* 150–152

Low-Melting, Liquid-Crystalline Metalloporphyrins

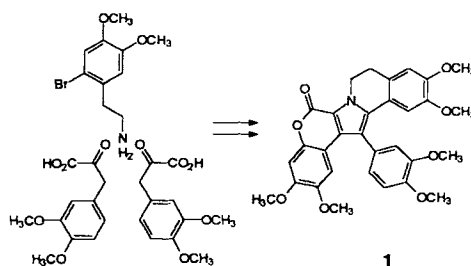
The two macrocyclic ligands H_2L^1 and H_2L^2 are not very different, but their $\text{Fe}^{\text{II}}\text{Fe}^{\text{III}}$ complexes are remarkably so. $[\text{L}^1\text{Fe}_2(\mu\text{-OAc})_2](\text{ClO}_4)_4$ is valence-delocalized on the Mössbauer time scale over the range 1.8–364 K, whereas $[\text{L}^2\text{Fe}_2(\mu\text{-OAc})(\text{OAc})(\text{H}_2\text{O})](\text{ClO}_4)_4 \cdot 2\text{H}_2\text{O}$ is valence-trapped even at room temperature. The difference in properties of these complexes is also reflected in their electronic spectra, in their electrochemical and magnetic behavior, and in their structures.



S. K. Dutta, J. Ensling, R. Werner,
U. Flörke, W. Haase, P. Gülich,
K. Nag* 152–155

Valence-Delocalized and Valence-Trapped $\text{Fe}^{\text{II}}\text{Fe}^{\text{III}}$ Complexes: Drastic Influence of the Ligands

Three steps to lamellarins—these marine alkaloids such as **1**, which show cytotoxic and immunomodulatory activity, are formed from two arylpyruvic acids and one (phenylethyl)amine building block. The key step in this reaction sequence is a Heck cyclization.

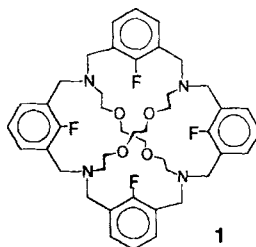


A. Heim, A. Terpin,
W. Steglich* 155–156

Biomimetic Synthesis of Lamellarin G Trimethyl Ether

Covalently bound fluorine atoms are effective donors!

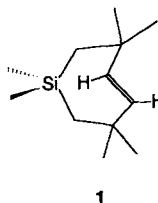
This is demonstrated by the $F_4O_3N_1$ coordination of the Cs^+ ion in the complex with the macropolycyclic ligand **1**. Three of the four shortest bonds to the metal ion are $Cs^+ - F$ bonds, and one of these is extremely short (284.2(3) pm).



H. Plenio,* R. Diodone,
D. Badura 156–158

Synthesis and Coordination Chemistry of
Fluorine-Containing Cages

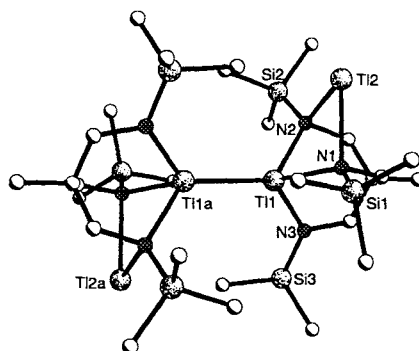
A strongly deformed C–C double bond is present in the chiral *trans*-cycloheptene derivative **1**. Nonetheless it is thermally quite stable and can be separated into enantiomers. Two effects are responsible for this: four methyl groups in the α -positions increase the barriers for the *trans*–*cis* isomerization and the dimerization, and the introduction of $Si(CH_3)_2$ in place of CH_2 in the *trans*-cycloheptene reduces the ring strain.



A. Krebs,* K.-I. Pforr, W. Raffay,
B. Thölke, W. A. König,* I. Hardt,
R. Boese* 159–160

A Stable Hetero-*trans*-cyclopentene

Aggregation through weak metal–metal contacts as well as redox disproportionations are the chemical characteristics of the metal exchange products of the tripodal tris(lithium amide)s $[H_3CC\{CH_2N(Li)SiMe_3\}_3]^- (L)_3]$ ($L = \text{dioxane, THF}$) with MCl ($M = \text{In, Tl}$). These reactions yield the first examples of mixed-valent M^I/M^{II} compounds like $[H_3CC-(CH_2NSiMe_3)_3Tl_2]_2$ (see structure on the right).



K. W. Hellmann, L. H. Gade,*
A. Steiner, D. Stalke,
F. Möller 160–163

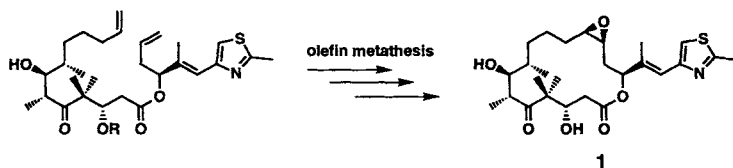
Aggregation and Redox-Disproportionation in Tripodal Indium and Thallium Amides: First Characterization of Mixed-Valent M^I/M^{II} Compounds ($M = \text{In, Tl}$)

Irradiation of aqueous suspensions of carbon black with a pulsed laser heats the carbon particles to high temperatures, initiating chemical reactions. In addition to H_2 , CO , and CO_2 , the usual products in the carbon–steam and shift reactions, CH_4 , C_2H_2 , C_2H_4 , and C_2H_6 are also produced as the carbon is consumed.

H. Chen, T. McGrath,
G. J. Diebold* 163–166

Laser Chemistry in Suspensions: New Products and Unique Reaction Conditions for the Carbon–Steam Reaction

A flexible alternative route to the total synthesis of the antitumor agent epothilone A (**1**, see below) has been achieved by a highly convergent strategy involving olefin metathesis as a key step. The strategy may allow the chemical synthesis of a library of designed epothilones for biological screening.



Z. Yang, Y. He, D. Vourloumis,
H. Vallberg, K. C. Nicolaou* 166–168

Total Synthesis of Epothilone A:
The Olefin Metathesis Approach

* Author to whom correspondence should be addressed

BOOKS

Spectacular Experiments and Inspired Quotes. Chemical Curiosities ·
H. W. Roesky, K. Möckel

W. N. Lipscomb 169

Qu'est-ce que l'alchimie? · P. Laszlo

C. Meinel 169

Dendritic Molecules · G. R. Newkome, C. N. Moorefield, F. Vögtle

B. Meijer 170

The Responsible Conduct of Research · D. Beach

R. Hoffmann 170

German versions of all reviews, communications, and highlights in this issue appear in the January issue of *Angewandte Chemie*. The appropriate page numbers can be found at the end of each article and are also included in the Author Index on p. 173.

SERVICES

| | |
|----------------|---------|
| ● Events | 42, 168 |
| ● Keywords | 172 |
| ● Author Index | 173 |
| ● Preview | 174 |

All the Tables of Contents from 1995 onwards may be found on the WWW under:
<http://www.vchgroup.de/home/angewandte>

Deposition of Data from X-Ray Structure Analyses

In order to make life easier for authors and referees the Cambridge Crystallographic Data Centre (CCDC) and the Fachinformationszentrum Karlsruhe (FIZ) have unified their procedures for the deposition of data from single-crystal X-ray structure analyses.

From now on prior to submitting your manuscripts please deposit the data for your compound(s) **electronically** at the appropriate data base, that is, at the CCDC for organic and organometallic compounds and at the FIZ for inorganic compounds. Both data bases will be pleased to provide help (see our *Notice to Authors* in the first issue of this year). In general, you will receive a depository number from the data base within two working days after electronic deposition; please include this number with the appropriate standard text (see our *Notice to Authors*) in your manuscript. This will enable the referees to retrieve the structure data quickly and efficiently if they need this information to reach their decision.

This is now the uniform procedure for manuscripts submitted to the journals *Angewandte Chemie*, *Chemische Berichte*, *Chemistry—A European Journal*, and *Liebigs Annalen*.